TUM SCHOOL OF LIFE SCIENCES

TECHNICAL UNIVERSITY OF MUNICH

Dissertation

Nitrogen controls on plant carbon-use efficiency

Melanie Alexandra Kern

TUM SCHOOL OF LIFE SCIENCES

TECHNISCHE UNIVERSITÄT MÜNCHEN

Nitrogen controls on plant carbon-use efficiency

M.Sc. Melanie Alexandra Kern

Vollständiger Abdruck der von der TUM School of Life Sciences der Technischen Universität München zur Erlangung des akademischen Grades eines *Doktors der Naturwissenschaften (Dr. rer. nat.)* genehmigten Dissertation.

Vorsitzende/-r: apl. Prof. Dr. Thomas Rötzer

Prüfende/-r der Dissertation:
1. Prof. Dr. Anja Rammig
2. Assoc. Prof. Dr. Karin Rebel

Die Dissertation wurde am 11.05.2020 bei der Technischen Universität München eingereicht und durch die Fakultät TUM School of Life Sciences am 16.10.2020 angenommen.

Ich versichere, dass ich die vorliegende Dissertation selbstständig verfasst und nur die angegebenen Quellen und Hilfsmittel verwendet habe.

Hamburg, 31.01.2021 Melanie Alexandra Kern

Vorwort

Die vorliegende Dissertation ist im Rahmen meiner Tätigkeit als Wissenschaftliche Mitarbeiterin am Max-Planck-Institut für Biogeochemie (MPI-BGC) in Jena von Oktober 2015 bis Oktober 2019 entstanden.

Neben der hier dokumentierten Arbeit habe ich an der Entwicklung des Terrestrischen Biosphärenmodels QUINCY (*Thum et al.* (2019)) mitgearbeitet und folgende Publikation miterstellt:

- Thum, T., Caldararu, S., Engel, J., **Kern, M.**, Pallandt, M., Schnur, R., Yu, L., Zaehle, S. (2019): A new terrestrial biosphere model with coupled carbon, nitrogen, and phosphorus cycles (QUINCY v1.0; revision 1772). Geoscientific Model Development.

Außerdem habe ich meine Arbeit bei internationalen Konferenzen und Workshops in Form von Vorträgen präsentiert und diskutiert:

- Kern, M. et al. (2019): Towards the integration of mycorrhizal processes into assessments of ecosystem carbon-nitrogen dynamics in forests under elevated CO_2.
  EGU General Assembly 2019 in Wien, AT.
- Kern, M. et al. (2018): A novel plant-mycorrhiza interaction model improves representation of plant responses to elevated CO_2.
  EGU General Assembly 2019 in Wien, AT.
- Kern, M. et al. (2017): Enhanced C investment into alternative N acquisition strategies under elevated CO_2.
  ClimMani Workshop *Global change effects on terrestrial ecosystems across spatial and temporal scales: gradients, experiments, remote sensing & models* in Doorn, NL.

Abstract

The terrestrial biosphere sequesters currently about 25% of anthropogenic CO_2 emissions, which reduces human-induced climate change. Models and observations suggest that this is largely caused by a CO_2 fertilization effect on plants, which may be reduced in the future due to progressively increasing N limitation. However, the extent to such so-called progressive N limitation (PNL) occurs is highly uncertain, and causes major disagreement among model projections of future land C uptake. Recent studies have shown that most terrestrial biosphere models (TBMs) have the tendency to overestimate PNL on plant growth under elevated CO_2 (eCO_2) by lacking a representation of the potential of plants to acclimate to environmental changes, particularly with regard to plant N nutrition and plant N acquisition. In this context, the present study focuses on two important plant N acquisition strategies, which rely on symbioses, i.e. symbiotic N fixation and mycorrhizal fungi, that are only insufficiently represented in TBMs yet to answer the questions if and to what extent nitrogen (N) controls plant growth under current conditions, as well as under rising atmospheric CO_2, to improve predictions of future land C uptake.
After implementing them into the novel TBM QUINCY (*Thum et al.* (2019)) I quantify effects of improved N nutrition by symbiotic N acquisition on plant growth by applying QUINCY and QUINCY with the newly implemented schemes of symbiotic N fixation (Q-BNF), plant-mycorrhiza symbiosis (Q-MYC), and a combination of both strategies (Q-MYFUN) and comparing simulation results. I analyze (i) changes in simulated leaf CN ratio and simulated plant carbon-use efficiency (CUE), which is defined as ratio of net primary production (NPP) to gross primary production (GPP) and therefore comprises the information, how efficient plants or ecosystems use assimilated C for biomass production, and (ii) differences in simulated responses to eCO_2 by comparing two simulations for each model variant, one with ambient CO_2 and one with a cCO_2 elevation of 200ppm CO_2 for 40 years.

I show that the use of any symbiotic N acquisition strategy improves simulated leaf CN ratio (Q-BNF: -1.4%, Q-MYC: -14.8%, Q-MYFUN: -19.1%) compared to the reference model QUINCY and lowers CUE (QUINCY: 0.50, Q-BNF: 0.46, Q-MYC: 0.49, Q-MYFUN: 0.47). Latter is rather caused by a strong increase in GPP (Q-BNF: +19.0%, Q-MYC: +20.6%, Q-MYFUN: +20.0%), which is caused by improved N nutrition, whereas NPP responds generally less (Q-BNF: +8.9%, Q-MYC: +14.0%, Q-MYFUN: +10.6%) due to also increased respiration costs by symbiotic N acquisition.
Under eCO_2 all model variants with symbiotic N acquisition strategies simulate a persistent positive NPP response to eCO_2 even after 40 years compared to the simulation

without enhanced cCO_2 (QUINCY: +5%, all others: +30%), which results in similar positive vegetation C responses (QUINCY: $\pm$0kgC/m^2, all others: +2.5kgC/m^2) by preventing plants from PNL, which occurs in QUINCY. This is a significant improvement of plant responses to eCO_2, as it fits to observations. However, soil C responses vary largely among model variants, since fixation of ecosystem-external N, which increases ecosystem N generally and thus increases C-storage potential, and mycorrhizal interaction with SOM, which accelerates decomposition and decreases SOM. This leads to different ecosystem C responses to eCO_2 (QUINCY: +2kgC/m^2, Q-BNF: +4.5kgC/m^2, Q-MYC: +3kgC/m^2, Q-MYFUN: +3kgC/m^2). Nevertheless, as all model variants with symbiotic N acquisition strategies improve simulations of plant responses to eCO_2, and agree on an increase in land C storage in response to eCO_2 compared to QUINCY, the implementation of such strategies into any TBM may reduce current model uncertainty of future land C sink in general.

Kurzfassung

Etwa 25% anthropogenen CO_2 Emissionen werden derzeit von der terrestrischen Biosphäre aufgenommen, was den menschen-induzierten Klimawandel reduziert. Modelle und Beobachtungen legen nahe, das die erhöhte Kohlenstoffaufnahme auf einem CO_2-Düngeeffekt auf Pflanzen beruht, welcher jedoch zukünftig durch progressiv ansteigende Stickstofflimitierung verringert werden könnte. Dabei ist jedoch das Ausmaß der sogenannten progressiven Stickstofflimitierung (PNL) äußerst unsicher, was zu großen Unterschieden in Modellsimulationen der zukünftigen Landkohlenstoffsenke führt. Aktuelle Studien haben gezeigt, dass die meisten Terrestrischen Biosphären Modelle (TBMs) den Effekt der PNL auf das durch erhöhtes CO_2 (eCO_2) stimulierte Pflanzenwachstum tendenziell überschätzen, da pflanzliche Anpassungsprozesse an sich ändernde Umweltbedingungen, insbesondere in Bezug auf Stickstoffaufnahme, nicht oder nur unzureichend dargestellt werden. In diesem Kontext beschäftigt sich die vorliegende Arbeit mit zwei wichtigen Stickstoffaufnahmestrategien, die auf Symbiosen mit stickstofffixierenden Bakterien und Mykorrhizen beruhen und bislang nicht in TBMs implementiert sind. Ziel ist die Beantwortung der Fragen, ob und in welchem Ausmaß Stickstoff (N) Pflanzenwachstum unter aktuellen und erhöhten atmosphärischen CO_2 Konzentrationen kontrolliert, um die modellbasierte Vorhersage der zukünftigen Landkohlenstoffsenke zu verbessern.
Hierzu implementiere ich beide Symbiosen in das neu entwickelte TBM QUINCY (*Thum et al.* (2019)) und quantifiziere den Effekt der symbiotisch unterstützen Stickstoffaufnahme, indem ich Simulationen des Referenzmodells (QUINCY) mit Simulationen vergleiche, die die symbiotische Stickstofffixierung (Q-BNF) oder Mykorrhizen (Q-MYC) berücksichtigen, oder den Pflanzen beide Symbiosen erlauben (Q-MYFUN). Ich analysiere (i) Änderungen im simulierten Blatt-Kohlenstoff-zu-Stickstoff (CN)-Verhältnis und der simulierten Kohlenstoffnutzungseffizienz (CUE) als relative Wachs-tumsrate zur absoluten Kohlenstoffaufnahme der Pflanzen und (ii) Unterschiede in den Reaktionen der Vegetation, des Bodenkohlenstoffs und des gesamten Ökosystems auf eCO_2 analysiert. Für letzteres wird ein 40-jähriges CO_2-Düngeexperiment mit um 200ppm erhöhtem CO_2 simuliert und die Simulationen mit Simulationen der ungestörten Ökosysteme verglichen.

Ich zeige, dass die Nutzung jeder symbiotischen Stickstoffaufnahmestrategie das Blatt-CN-Verhältnis positiv im Vergleich zum Referenzmodell beeinflusst (Q-BNF: -1.4%, Q-MYC: -14.8%, Q-MYFUN: -19.1%) und die simulierte CUE sinkt (QUINCY: 0.50, Q-BNF: 0.46, Q-MYC: 0.49, Q-MYFUN: 0.47). Grund dafür sind eine deutlich erhöhte Kohlenstoffassimilationsrate (Q-BNF: +19.0%, Q-MYC: +20.6%, Q-MYFUN: +20.0%) aufgrund der verbesserten N Verfügbarkeit, die das Pflanzenwachstum prozentual geringer ver-

stärkt (Q-BNF: 8.9%, Q-MYC: +14.0%, Q-MYFUN: +10.6%), da auch Atmungsraten durch symbiotische Stickstoffaufnahme erhöht werden.
Unter eCO_2 simulieren alle Modellvarianten mit symbiotischer Stickstoffaufnahme durch die Verhinderung von PNL ein dauerhaft verstärktes Pflanzenwachstum (Q-BNF, Q-MYC, Q-MYFUN: +30%; QUINCY: +5%) im Vergleich zu Simulationen ohne eCO_2, was zu einer deutlichen Zunahme der Pflanzenbiomasse (Q-BNF, Q-MYC, Q-MYFUN: +2.5kgC/m^2). Da die dauerhafte Erhöhung des Pflanzenwachstums durch Beobachtungen unterstützt wird, stellt dies deutliche Verbesserung der modellierten Reaktion der Vegetation auf eCO_2 dar. Die Reaktion des Bodenkohlenstoffs auf eCO_2 variiert jedoch stark in Abhängigkeit von der Art der simulierten Symbiose, da symbiotische Stickstofffixierung den Gesamtstickstoffgehalt des modellierten Ökosystems erhöht und damit ein größeres Kohlenstoffspeicherpotential schafft, wohingegen Mykorrhizen durch den Abbau von organischem Material im Boden zur Freisetzung von N die Bodenkohlenstoffmenge im Modell verringert. Insgesamt ergeben sich daher je nach simulierter Symbiose unterschiedliche Gesamtantworten des simulierten Ökosystems auf eCO_2 (QUINCY: +2kgC/m^2, Q-BNF: +4.5kgC/m^2, Q-MYC: +3kgC/m^2, Q-MYFUN: +3kgC/m^2), wobei jedoch alle Modellvarianten mit symbiotischen Stickstoffaufnahmestrategien eine Erhöhung des Kohlenstoffspeichers im Vergleich zum Referenzmodell simulieren. Zusammengenommen mit der deutlich verbesserten Simulation der Reaktion der Pflanzen auf eCO_2 deutet dies darauf hin, dass die Implementierung symbiotischer Stickstoffaufnahmestrategien auch in andere TBMs deren Vorhersage der zukünftiger Landkohlenstoffaufnahme verbessern und die Modellunsicherheiten und –abweichungen zwischen TBMs verringern könnte.

Contents

List of Figures

List of Tables

1. Introduction

1.1. Motivation

Atmospheric carbon dioxide (CO_2) concentrations (cCO_2) and levels of other greenhouse gases (GHGs), such as methane (CH_4) and nitrogen oxides (NO_X), are increasing strongly due to human activities such as the use of fossil fuels and land-use changes (*IPCC* (2013)). Compared to pre-industrial times, i.e. before around 1750 (*IPCC* (2013)), cCO_2 rose up from less than 280 ppm to more than 400 ppm, which is an increase of about 45% (*Hartmann et al.* (2013), *Friedlingstein et al.* (2019)). Simultaneously, the temperatures increased around 1 K globally, which is partly caused by the effect of GHGs on the global radiation budget (*Hartmann et al.* (2013)). Thus, rising cCO_2 influences climate on Earth intensively (*Arneth et al.* (2010), *Arora et al.* (2013), *Bonan* (2015)).
However, an increase in cCO_2 does not only affect climate, and atmospheric dynamics, but also all other compartments of the Earth system due to the constant exchange of mass, energy, and momentum between spheres (*Bonan* (2008), *Ciais et al.* (2014), *Bonan* (2015)). Changing cCO_2 therefore perturb carbon (C) cycling within the entire Earth system, and influences C stocks of all spheres, especially stocks of the land and ocean, since those two share a surface, i.e. a direct exchange area, with the atmosphere. C exchange between atmosphere and ocean is mainly driven by physical and chemical processes that balance concentration differences (*Rhein et al.* (2013)), whereas marine photosynthesis caused by marine biosphere plays a minor role as it is buffered by the carbonate-system (*Rhein et al.* (2013)). In contrast to that, C exchange between atmosphere and land is mainly caused by the terrestrial biosphere, i.e. by biological processes such as photosynthesis and respiration, which is further influenced by humans due to land-use change (*Friedlingstein et al.* (2014), *Schimel et al.* (2015), *Friedlingstein et al.* (2019)). Since most biological processes involve also nutrients, such as nitrogen (N) or phosphorus (P), C cycle fluxes between atmosphere and the terrestrial biosphere are tightly linked to nutrient cycles within the biosphere (*Vitousek and Howarth* (1991), *Hungate et al.* (2003), *Bonan and Doney* (2018)).

This tight coupling complicates predictions of future development, (long-term) feedbacks between human activities and climate, as well as anthropogenic impacts on the Earth system, which are estimated by running Earth System models (ESMs, *Bonan and Doney* (2018)). Especially nutrient constraints on C cycling are only poorly understood on global scales, which complicates their representation in terrestrial biosphere models (TBMs) that are part of ESMs. It is therefore necessary to understand the system and its ex-

change processes, as well as C-nutrient coupling within the biosphere in order to better predict future conditions and implications, and reduce uncertainties of predictions (*IPCC* (2013)).

As N is the second most abundant biogeochemical compound within the biosphere (after C), the coupling of C and N within the terrestrial biosphere, and the representation of this coupling in a TBM is the major focus of the present study. In particular, I ask the question, if and to what extend N availability constrains C exchange between atmosphere and land by controlling plant growth, which determines C uptake of the terrestrial biosphere. For that, I focus on two important symbioses, i.e. with N-fixing microbes and mycorrhizal fungi, that are known to support plant N acquisition (*Gutschick* (1981), *Read* (1991)), but may be only insufficiently implemented into TBMs yet (*Brzostek et al.* (2017)), even though it is argued that neglecting such symbioses may underestimate the impact of terrestrial ecosystems on climate change (*Shi et al.* (2019)).

1.2. Background

This section provides the theoretical background for the study. It firstly reviews current knowledge about the global carbon (C) cycle with a special focus on vegetation and soil as components of the terrestrial C cycle (sec. 1.2.1), the terrestrial nitrogen (N) cycle (sec. 1.2.2), and shortly other terrestrial nutrient cycles, such as the P cycle (sec. 1.2.3). Thereby it particularly focuses on C-N interactions and (potential) effects of rising atmospheric CO_2.
Secondly, this section introduces terrestrial biosphere models (TBMs) that build the biogeochemical core, i.e. the (terrestrial) C- or CN-model, of Earth system models (ESMs), and presents recent uncertainties that are related to C-N coupling in general, before it focuses on the novel TBM QUINCY specifically and its representation of vegetation and soil dynamics as framework for the following study (sec. 1.2.4).

1.2.1. The global carbon cycle: stocks and fluxes

The global C cycle on Earth can be divided into two different cycles that act on different time scales: A slow C cycle, which is associated with inorganic C forms, that has a recycling time of millennia, and a fast C cycle, which acts on time scales from seconds to decades and is mainly associated with living matter. It principally connects the C reservoirs of atmosphere, land and ocean, whereas the slow cycle integrates the lithosphere into the global C cycle, which actually holds 99.95% of the global C. Exchange processes within the slow cycle are mainly driven by physical and chemical processes, such as rock weathering, sedimentation, mineralization, diffusion/outgassing at water surfaces, and volcanic activities, and integrate the lithosphere into the global C cycle, which actually holds 99.95% of the global C. The remaining 0.05% are exchanged between atmosphere and land via biological processes, i.e. photosynthesis and respiration (fig. 1.1, thin green arrows), and between atmosphere and ocean via physico-chemical processes that balance the C concentration between atmosphere and ocean (fig. 1.1, thin turquoise arrows, *Falkowski et al.* (2000), *Friedlingstein et al.* (2019)). Only very little amounts of C are exchanged by marine photosynthesis and respiration between atmosphere and ocean, since these fluxes are buffered by the carbonate-system (fig. 1.1, thin turquoise circled arrows). Marine photosynthesis is mainly driven by dissolved CO_2, which has already entered the ocean by physico-chemical processes, and not by atmospheric CO_2, and respires CO_2, which becomes dissolved within the ocean immediately, too (*Rhein et al.* (2013)).

With the beginning of industrialization in the middle of the 18^{th} century, humans started to emit C via fossil fuel combustion and cement production into the atmosphere (*IPCC* (2013)). The positive trend in atmospheric CO_2 concentrations (cCO_2) has been reported by various studies and long-term records (e.g. *Ayres et al.* (1994), *Falkowski et al.* (2000) or *Dlugokencky and Tans* (2019)).

Regarding the *slow and fast cycles*-system, human induced emissions from gas, oil and coal reservoirs (fig. 1.1: E_{FF}), constitute a transfer of C from the slow cycles to the fast cycle, as emitted C originates from the lithosphere and an increase of atmospheric C has to be buffered by other spheres due to the closeness of the entire system (*Keenan and Williams* (2018)). On short time scales, i.e. decades to centuries, which are the focus of this study, gained atmospheric C (fig. 1.1: G_{ATM}) can only be cached by land and ocean by enhanced sink fluxes from atmosphere to land or ocean, respectively (fig. 1.1: S_{LAND} and S_{OCEAN}), that increase the C reservoirs of land and ocean (*Keenan and Williams* (2018)).

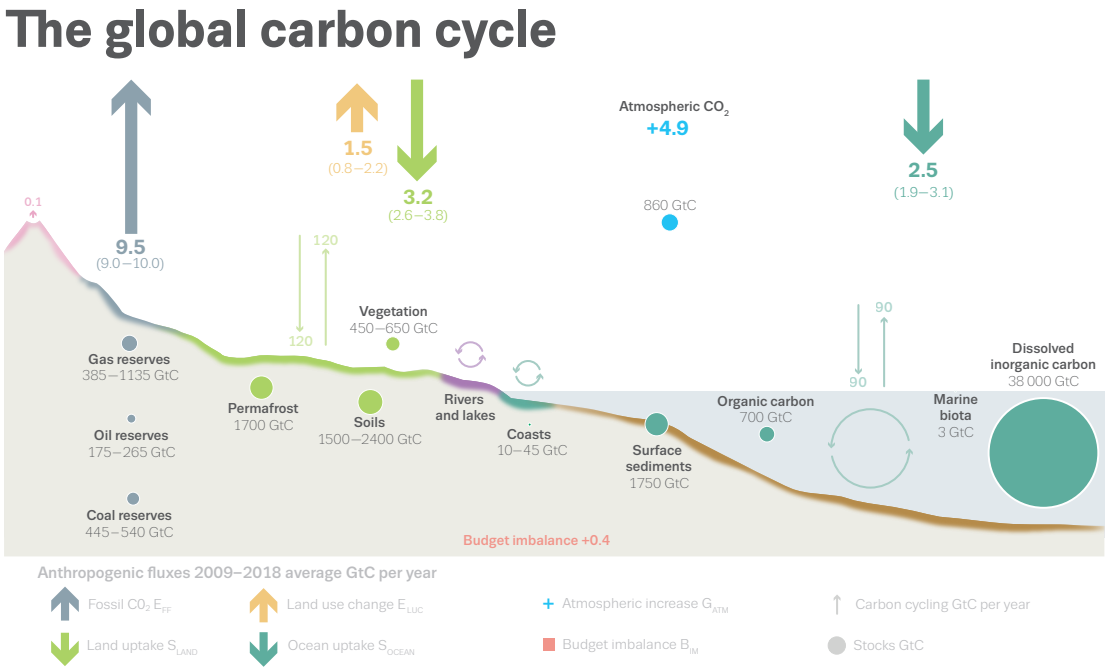

Figure 1.1.: Schematic representation of athropogenically induced global carbon cycle perturbations (thick arrows) and background fluxes (thin arrows), averaged globally for the decade 2009–2018. See legends for the corresponding arrows and units. Figure is taken from *Friedlingstein et al.* (2019).

Since atmosphere-ocean exchange is driven by a CO_2-concentration imbalance, fluxes are depending on the actual difference at the sea surface, which is buffered by C-redistribution due to diffusion and streams within both spheres. This leads to a rather smooth increase of the net C flux from atmosphere to ocean (fig. 1.2: turquoise). However, as C enters the ocean mainly in from of dissolved CO_2, it acidifies the ocean, which has large and long-lasting impacts to marine ecosystems (*Rhein et al.* (2013)).
In contrast to that, atmosphere-land exchange is driven by biological processes that react very quickly to changes. As first response to atmospheric CO_2 elevation, photosynthesis is enhanced (*Ainsworth and Rogers* (2007), *Ainsworth* (2008)), which increases vegetation biomass as part of the land C stock (*Ciais et al.* (2014)). By senescence

vegetation biomass enters soil, which then also increases C within this compartment of the land C reservoir. However, increased organic material, i.e. vegetation biomass or soil organic material (SOM), leads to an increase in respiration (*Sprugel et al.* (1995), *Amthor and Baldocchi* (2001), *Tedeschi* (2006)). This results in a complex system with many interfering feedbacks. Thus, a derivation of the net C flux from atmosphere to land in response to elevated atmospheric CO_2 (eCO_2) is highly uncertain and changes rapidly due to recent environmental conditions (fig. 1.2: green and blue), and is further influenced by humans by land-use change, which affects respiration (fig. 1.1: E_{LUC} and fig. 1.2: brown, *Ammann et al.* (2007), *Pongratz et al.* (2009), *Ciais et al.* (2014), *Friedlingstein et al.* (2014), *Friedlingstein et al.* (2019)). Besides, fluxes that are driven by the terrestrial biosphere are highly localized, which additionally complicates net flux estimations (*Beringer et al.* (2011)). Consequently, the so-called 'land C sink' is either derived as missing C in the global C budget that takes measurements and estimates of fossil fuel emissions (E_{FF}), atmospheric and marine C reservoir evolutions (G_{ATM} and S_{OCEAN}), and land-use chance effects (E_{LUC}) into account, but is only partly based on land C observations, or derived from models, i.e. Dynamical Global Vegetation Models (DGVMs, sec. 1.2.4), which often leads to a slight imbalance in the global C budget (fig. 1.1: B_{IM} and fig. 1.2 difference between pink line and sum of partitioning, *Friedlingstein et al.* (2014), *Bonan and Doney* (2018), *Friedlingstein et al.* (2019)). Figure 1.2 presents, how estimated global C fluxes developed over time.

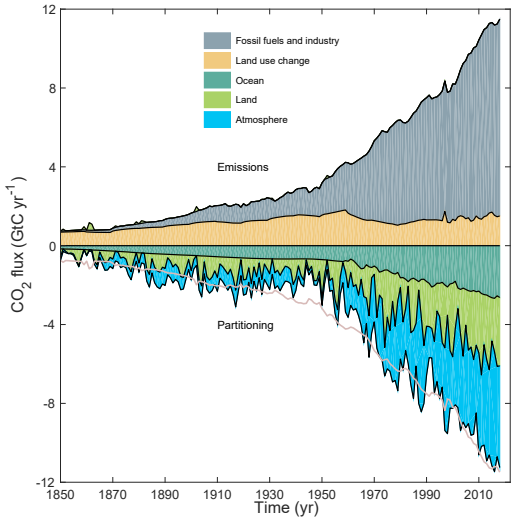

Figure 1.2.: Combined components of the global carbon budget (fig. 1.1) as a function of time, for fossil CO_2 emissions (grey) and emissions from land use change (brown), as well as their partitioning among the atmosphere (blue), ocean (turquoise), and land (green). The partitioning is based on estimates from observations for atmosphere and from process model ensembles for ocean and land constrained by data. The sum of partitioning does not exactly add up to the sum of the emissions, resulting in a budget imbalance, which is represented by the difference between the bottom pink line, which reflects total emissions, and the sum of the ocean, land, and atmosphere. Figure is taken from *Friedlingstein et al.* (2019).

However, to predict future development and estimate future C storage of the land, it is necessary to not only derive current C stock changes by closing the budget system, but to understand the mechanisms that drive fluxes between atmosphere and terrestrial biosphere, their limitations, and how they are constrained by (i) C stocks themselves, (ii) environmental conditions, such as temperature and water availability that may influence vegetation growth, SOM decomposition, respiration rates,..., and (iii) nutrient cycles, e.g. nitrogen (N) and phosphorus (P) cycles that are tightly coupled to the C cycle (sec. 1.2.2 and sec. 1.2.3).

In order to better understand the complex land C system and its underlying mechanisms, vegetation C balance, which is much easier to observe than SOM C balance, and vegetation C response to eCO_2 are a major focus of Earth system research for decades already. Several experimental studies, which range from chamber measurements to free-air CO_2 enrichment (FACE) experiments, where entire ecosystems were exposed to CO_2 enriched air, as well as long-term ecosystem observations provide evidence that eCO_2 fertilizes plant growth and that vegetation biomass is increased in response to eCO_2 (*Norby et al.* (2002), *Norby et al.* (2005), *Bonan* (2008)). During the last decade there is increasing evidence, e.g. from FACE studies, that soil C stocks, which actually build the major part of the land C reservoir (for numbers see fig. 1.1), are also responding to eCO_2 (*Lichter et al.* (2008), *Phillips et al.* (2012)).
The C balances of both land compartments, i.e. vegetation and SOM, and their responses to eCO_2 are explained in more detail in the following sections 1.2.1.1 and 1.2.1.2. All further relevant[1] fluxes described in this sections can be found in figure 1.3 (green arrows).

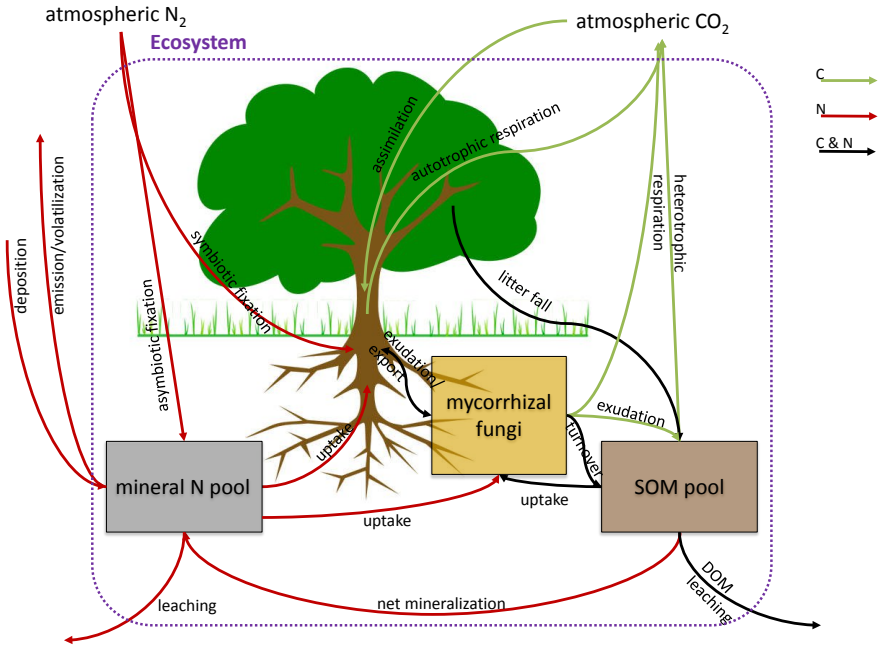

Figure 1.3.: Schematic overview over ecosystem carbon and nitrogen cycles, and exchange with ecosystem external sinks and sources. Tree represents vegetation (pools), boxes represent soil pools. SOM pool sums up all different stages of (decomposed) soil organic material, i.e. from fresh litter to old highly decomposed material. Green arrows: C fluxes, red arrows: N fluxes, black arrows: C and N fluxes.

[1] *further relevant* meaning further relevant for the present study

1.2.1.1. Vegetation carbon balance and its response to elevated CO_2

Plants assimilate atmospheric C via photosynthesis. The related flux is referred to as gross primary production (GPP) and is depending on the leaf-surrounding cCO_2 (*Farquhar et al.* (1982), *Amthor and Baldocchi* (2001)). In order to maintain and grow biomass and to acquire nutrients, plants also release C to the atmosphere by autotrophic respiration (R_a). The remaining net flux from atmosphere to vegetation is called net primary production (NPP):

$$NPP = GPP - R_a, \; with \tag{1.1a}$$

$$R_a = \sum_j R_j = R_g + R_m + R_X \tag{1.1b}$$

whereas R_j terms all kinds of plant respiration, i.e. maintenance respiration (R_m), growth respiration (R_g), and nutrient acquisition respiration (R_X). Maintenance respiration is respiration related to all processes that maintain existing cellular structures and intracellular ionic gradients, and is therefore always prioritized (*Thornley and Cannell* (2000)). Growth respiration is respiration related to processes that build new tissues (*Amthor* (2000)). Nutrient acquisition respiration is related to the transformation of acquired (mineral) nutrients to organic material, i.e. to amino acids (*Zerihun et al.* (1998)), or to C/energy investment into acquisition processes such as energy investment into nitrogen (N) fixation (*Gutschick* (1981)).

Since GPP is directly depending on cCO_2, eCO_2 enhances plant C assimilation, and also biomass production, i.e. eCO_2 has a fertilization effect on plants (*Norby et al.* (2002), *Norby et al.* (2005), *Ainsworth and Rogers* (2007), *Bonan* (2008)). But increased growth rates increase also growth respiration, and increased biomass increases progressively maintenance respiration as more biomass has to be maintained. Furthermore, nutrient acquisition respiration may respond positively to eCO_2 as well, due to (i) a higher demand of N that has to be acquired, since more biomass is produced, and (ii) progressive N limitation (sec. 1.2.2.2) that forces plants to acquire N from more C-cost intensive sources.

To quantify the net C exchange between atmosphere and vegetation, under ambient and changed conditions, such as eCO_2, the so-called C-use efficiency (CUE) is defined as ratio of remaining C in the system (NPP) to C that has entered the system (GPP):

$$CUE = \frac{NPP}{GPP} \tag{1.2}$$

By definition, a low CUE indicates that only minor C is converted to biomass and much C is released to atmosphere again due to high respiration rates. This further indicates a rather open biological C cycle, whereas a high CUE points to a rather closed C cycle, where much C is incorporated into biomass and remains in the biosphere (*Manzoni et al.*

(2018))[2]. However, there are limitations for the range within CUE can vary as plants have to ensure to incorporate enough freshly assimilated C to survive (lower bound) and minimum respiration rates (upper bound). *Waring et al.* (1998) suggested an universal CUE of 0.47±0.04 (mean±SD) among biomes, tree species and stand ages, which would simplify estimates of global C exchange between atmosphere and land. *Amthor* (2000) proposed a range of 0.2 to 0.65 for forest CUE on average, whereby young forests may have higher CUE ratios due to the fact that they invest less C into maintenance processes, since their biomass is lower. By comparing 200 studies, *Collalti and Prentice* (2019) confirmed the *Waring*-mean value for CUE (0.46), but they also reported a large spread among the data (0.22 - 0.79), which increased the standard deviation to ±0.12. They concluded, that even the *Waring*-mean value may be a good first guess, the deviation is too large to be ignored for global estimates.

Taking eCO_2 into account, it is expected that CUE is constant or decreases, because of the increase in GPP that may only initially lead to higher NPP (constant CUE). As enhanced biomass needs to be maintained, R_m may increase progressively, and potentially also R_X, since plants may be forced to acquire N from more C-cost intensive sources, which may lower NPP compared to GPP, and consequently may reduce CUE in long-term response to eCO_2.

1.2.1.2. Soil carbon balance and its response to elevated CO_2

Once C has entered the terrestrial biosphere and has become part of vegetation biomass, is partly transferred to soil by litter fall, or by plant C exudation to soil in order to stimulate the microbial community. Thus, soils, i.e. soil organic material (SOM), which is defined as sum of all dead organic compounds in soil, (plant, animal and microbial necromass) at all stages of decomposition, as well as microbes itself (*Trumbore* (1997), *Trumbore and Czimczik* (2008)), constitute a major part of the C stock of the terrestrial biosphere and determines largely, how long C remains in the system (*Trumbore* (2000)).
After C has entered soil in form of litter, the material is metabolized and transformed by decomposing microbes that incorporate litter C, release C by heterotrophic respiration (R_h), or convert it into soluble material. Incorporated C (microbial biomass) remains in the system, and is partly recycled by microbial turnover, whereas soluble material (dissolved organic material, DOM) moves through soil pores, transports C and nutrients and thus drives various biogeochemical processes, before it may be leached out (*Scott and Rothstein* (2014)). Fractions of SOM are stabilized for longer periods, i.e. protected

[2]There exists also other forms of CUE, such as the biomass-production efficiency (BPE) or the C-storage efficiency (CSE) of the entire ecosystem (*Manzoni et al.* (2018)). BPE is defined as the ratio of plant biomass production (BP), which is different from NPP in case exudation to root symbionts is taken into account, to GPP (see also *Vicca et al.* (2012) and *Collalti et al.* (2019) for differentiation of CUE and BPE). CSE is defined as ratio between net ecosystem exchange (NEE) and GPP, whereas NEE is calculated similar to NPP, but includes also heterotrophic respiration (R_h).

from microbial access and respiration, by several processes, such as physico-chemical stabilization (*von Lützow et al.* (2006)), which binds SOM chemically to mineral soil compartments, and physical protection by aggregation, whereby aggregates build a physical barrier between (stabilized) SOM and microbes (*Six et al.* (2002)).

By SOM decomposition, microbes are not only cycling C through soil, but also nutrients and release them, which is the reason, why plants exude C to stimulate microbes. Nutrients, such as N and P, are part of SOM, as they were incorporated into biomass during the life cycle of any organism, because all organisms have specific C:nutrient ratios to maintain their metabolism or grow. After death, organisms become part of SOM, which consequently contains nutrients that are then cycled and released by decomposition as well (*Scheffer and Schachtschnabel* (1998), *White* (2006)).

Under eCO_2 vegetation biomass, i.e. vegetation C, is enhanced (sec. 1.2.1.1), which increases litter fall, and consequently SOM. Additionally, plants may exude more C to soil to stimulate microbes further and accelerate SOM decomposition as their nutrient demand increases with increasing biomass. Thus, both pathways for C to enter soil may increase soil C in response to eCO_2.
Compared to vegetation C response, soil C response is potentially delayed, as C has primarily to pass vegetation, before it may become part of soil C. Nevertheless, an increase of soil C in response to eCO_2 is expected and observed at FACE sites (*Lichter et al.* (2008)). However, due to higher C input into soil, microbes decompose more SOM, which also enhances heterotrophic respiration. Consequently, soil C response may be very low and is highly uncertain due to (i) general difficulties to measure below-ground properties, and (ii) C:nutrient linkages that may in- or decrease decomposition and stabilization. Especially N as second most abundant biogeochemical compound within the biosphere (after C) plays an essential role, as its ratio compared to C influences soil processes largely. Since it is also vital for vegetation processes, the next section gives an overview about the terrestrial N cycle and its coupling to the C cycle.

1.2.2. The terrestrial nitrogen cycle

Nitrogen (N) is cycled through the Earth system, but the majority of N is stored in the lithosphere and therefore unavailable for (terrestrial) ecosystems. Only smallest fractions are released by physico-chemical processes, such as weathering, and become (plant) available (*Galloway et al.* (2004), *Fowler et al.* (2015)). This section focuses on the terrestrial N cycle that describes fluxes within the terrestrial biosphere, as well as exchange fluxes between atmosphere and the terrestrial biosphere[3], and its thigh coupling to the C cycle. All fluxes described in this section can be found in figure 1.3 (red arrows).

[3] Since the present study focuses only on *terrestrial* ecosystems and the *terrestrial* biosphere, and not on marine systems, I will use the terms *ecosystem* and *biosphere* from now on exclusively for terrestrial systems in case it is not indicated otherwise.

Generally, atmosphere is a practically infinite and ubiquitous available reservoir of N, because around 78% of its composition is dinitrogen (N_2), but gaseous N_2 is almost unreactive due to its molecular triple bonding. To enter the biosphere and become bioavailable, this bonding has to be broken (*Galloway et al.* (2004), *Galloway et al.* (2008)). The transformation of atmospheric N_2 into reactive forms of N in ecosystems therefore requires much energy.

Naturally, N enters the terrestrial biosphere mainly by biological N fixation (BNF), which terms the conversion of atmospheric N_2 by specific bacteria into bioavailable ammonium (NH_4) that can be taken up by plants (*Gutschick* (1981), *Gutschick* (1982)). Some of these bacteria live in symbiosis with specific plants, others are free-living and fix N everywhere, in case they need it for their own metabolism. Both, symbiotic and free-living bacteria, require energy to break up the triple bonding and anaerobic conditions, which limits the amount of N that is fixed naturally. In case of symbiotic fixers, energy in form of sugars, and anaerobic conditions are provided by plants that build nodules to host bacteria, but still rates are low (*Gutschick* (1981), *Gutschick* (1982)). The low rates, and the general high abundance of N_2, impede exact fixation rate measurements, but it is assumed that 100-150 TgN yr^{-1} are fixed globally (*Galloway et al.* (2004), *Vitousek et al.* (2013), *Wieder et al.* (2015), *Meyerholt et al.* (2016)), and it is assumed that the rate increases due to human agriculture, because cultivated crops are usually able to host N fixers (*Galloway et al.* (2004)). Additionally up to 10 TgN yr^{-1} are globally fixed by abiotic processes that release a lot of energy, such as volcanic eruptions and lightning (*Galloway et al.* (2004)).
Besides these natural pathways for N to enter terrestrial ecosystems, there are two human induced pathways: deposition of reactive N that was anthropogenically emitted by fossil fuel burning (mainly nitrogen oxides: NO_X) or agricultural emissions (mainly ammonia: NH_3), and the entry of fertilizer, since chemical N fixation ('Haber-Bosch process') was invented in the early 20^{th} century. In total human induced N entries are assumed to double natural N entries globally (*Ayres et al.* (1994), *Galloway et al.* (2008), *Gu et al.* (2013)).

Once, N has entered a terrestrial ecosystem in bioavailable form (mainly NH_4 or NO_3) it is taken up by plants or soil microbes and incorporated into their biomass in forms of amino acids, which are either used as structural material, or to build enzymes that catalyze all kinds of biochemical processes that are vital for life. Through senescence organic N enters soil, where it is decomposed by microbes that finally mineralize organic N again and release plant available NH_4. NH_4 is partly further transformed by soil bacteria via nitrification into plant available nitrate (NO_3). This microbial-driven part of the ecosystem internal N cycle is sometimes referred to as 'microbial bottleneck' (*Knops et al.* (2002)), since it potentially limits plant growth by not providing enough available N to meet plant N requirements for growth. *Chapman et al.* (2006) introduced mycorrhizal fungi to *Knops'* microbial loop, which are known to support plant N nutrition (*Read* (1991), *Marschner*

and Dell (1994)). Within this framework, mycorrhizal fungi access organic N in soils as nutrient source and provide it to plants as strategy to 'uncork' the bottleneck, since this pathway builds a short-cut within the internal ecosystem N cycle.

N leaves the ecosystem by gaseous emissions due to nitrification and denitrification, volatilization of NH_3, and leaching of NH_4 and NO_3 under specific circumstances. Nitrification oxidizes NH_4 to dinitrogen oxide (N_2O) and NO_3, whereby the intermediate products nitrogen oxide and nitrogen dioxide (NO and NO_2, respectively; summed up as NO_X) are emitted to atmosphere. Since N_2O is a strong GHG itself, and NO_X is a precursor of ozone, which is another GHG, this process is highly climate relevant. Denitrification terms the sequential reduction of NO_3 to N_2 that is emitted to atmosphere again. However, during the process, NO_X is emitted as well. Volatilization of NH_3 happens in case it cannot be reduced to NH_4 due to (i) already high concentrations of NH_4, which can be found in agricultural systems, (ii) alkaline conditions, or (iii) high soil temperatures. NH_4 is leached out of the system, when it is adsorbed to soil particles that are leached out, whereas NO_3 is only leached out in case of high concentration, or precipitation/irrigation, since its negative charge inhibits adsorption to soil particles (*Galloway et al.* (2004)).

1.2.2.1. Vegetation nitrogen balance and nitrogen limitation on plant growth

Plants need N, because N is vital to maintain all kinds of metabolic processes, and to grow tissue. Metabolic processes are driven by enzymes that catalyze biochemical reactions, and new tissue is build up by structural material. Both, enzymes and structural material contain N. Thus a sufficient amount of available N is needed to ensure plant fitness and growth.

This amount is defined by stoichiometric ratios that depend on plant tissue and vary among plant types. Foliar tissues are measured to have CN ratios between 22 and 42 (*White et al.* (2000), *Kattge et al.* (2011)), whereas fine root CN ratios vary between 48 and 90 (*Kattge et al.* (2011)). Woody tissues reach CN ratios of more than 400 (*Kattge et al.* (2011)), since wood is mainly dead cell and cell walls, which are generally nutrient poor due to nutrient retranslocation to save them before cells die. For the same reason litter CN ratio varies between 45 and 120, which is significantly higher than foliar CN ratio. Generally, living and productive tissues have a lower CN ratio than death tissues, because nutrients are more valuable for plants than C, which they can assimilate themselves easier.

Various studies have shown that plant growth is often limited by N, because plants are not able to meet stoichiometric requirements and consequently cannot build as much new biomass as they may be able to, in case of sufficient N availability (*Vicca et al.* (2012), *Wright et al.* (2018)). Thus, agricultural systems are often fertilized to produce

products more efficiently, but also forests are observed to produce biomass more efficiently, in case they are fertilized (*Vicca et al.* (2012), *Wright et al.* (2018)).

To quantify vegetation N balance and its coupling to vegetation C balance, the so-called N-use efficiency (NUE, eq. 1.3) is defined similar to the CUE (eq. 1.2) as ratio between net primary production (NPP) and total N acquisition (A_N). Since NPP is a C flux, this ratio is also an indicator for N limitation on growth, or for plant strategy to cope with limitation, because plants could either adjust NUE, or N acquisition.
An adjustment of NUE in response to N availability would result in either a change in CN ratios of specific tissues, which is possible within specific ranges, e.g. leaf CN ratio is shown to decrease under N fertilization (*Magill et al.* (2004)), or in a change of biomass allocation by growing tissues with a higher CN ratio under N limitation and lower CN ratio under N fertilization. However, this strategy is rather passive, as it implies that plants simply grow less productive tissues (or less tissues at all, as they still have to maintain existing tissues) under N limitation, whereas an adjustment of N acquisition by changing N acquisition strategies to environmental conditions is a rather active strategy.

$$NUE = \frac{NPP}{A_N} \tag{1.3}$$

whereby A_N is defined as total N that plants acquire by all N acquisition strategies, namely direct root uptake (U_N; sec. 1.2.4.3) of mineral N (NH_4 and NO_3), export from hosted mycorrhizal fungi (ΔE_N; cf. chapter 3), and fixation by symbiotic bacteria (F; cf. chapter 2).

$$A_N = U_N + \Delta E_N + F \tag{1.4}$$

1.2.2.2. Progressive nitrogen limitation

A special case of N limitation occurs under elevated atmospheric CO_2 (eCO_2), when plants are expected to assimilate more C (sec. 1.2.1.1), which increases their N growth requirements (sec. 1.2.2.1, *Comins and McMurtrie* (1993)). This has to result in higher N acquisition rates in order to build biomass and maintain tissue CN rations, and sequesters additional N in vegetation biomass. Since the entire N cycle is likely not accelerated as much as the C cycle, soils may become N depleted in long-term response to eCO_2 (*Reich et al.* (2006)). *Luo et al.* (2004) tested this setting by running models and came up with the the term of *progressive N limitation* (PNL) to describe N limitation on plant growth that results from increased biomass production as response to eCO_2. Thus, long-term plant growth response to eCO_2 and land C sink may depend strongly on plant available N and/or plant strategy to acquire N (*Field* (1999), *Oren et al.* (2001), *Norby* (2010)).

1.2.3. Other terrestrial nutrient cycles

Other nutrients, such as phosphorus, sulfur, or potassium, are also cycled through the Earth system, and their cycles are tightly coupled to the C cycle as well as among each other. Since stoichiometric requirements to build biomass are highest for N, most ecosystems are rather N limited, but plants rely also on other nutrients as they need them for specific cellular structures, or for specific processes within their metabolism (*von Liebig* (1863), *Fisher et al.* (2012), *Gill and Finzi* (2016)).
Especially tropical ecosystems are shown to be phosphorus (P) limited, due to heavily weathered soils, that do not to provide enough P to fulfill stoichiometric requirements for P (*Reed et al.* (2011)). In contrast to N, P availability is mainly driven physically, because it enters the ecosystems mostly by rock weathering, and incidental by deposition (*Walker and Syers* (1976), *Hou et al.* (2018)). Weathering acts on geological time scales, i.e. similar to the slow C cycle (sec. 1.2.1), and may limit fast growing ecosystems, or ecosystems that are N fertilized (*von Liebig* (1863), *Vitousek and Howarth* (1991)). Within the system, P is converted from organic to mineral, i.e. plant available, P by mineralization similar to N. It leaves the system by erosion and occasionally by leaching.
In contrast to N and P, nutrients like sulfur, potassium or iron, are often referred to as micro-nutrients, indicating minor demand to maintain and grow biomass. However, they are still needed, and therefore influencing plant growth, i.e. limiting plant growth in case of not meeting requirements (*von Liebig* (1863)).

1.2.4. Terrestrial biosphere models

Since ancient times, human beings have been interested into nature as their livelihood and into future. They have explored and described their environment, e.g. weather and climate, or vegetation, and combined observations to gain knowledge about dependencies and underlying processes, which allowed to estimate future development by building 'models' (*Prentice and Cowling* (2013), *Fisher et al.* (2014)).

The first vegetation 'models' were established in the early 20^{th} century by differentiation vegetation on Earth in several biomes (*Prentice et al.* (2007), *Fisher et al.* (2014)). Since that time a lot of research has been done and the knowledge about the biosphere and its interaction with other spheres was magnified. Since scientists became aware of the carbon-climate feedback (sec. 1.1), and the C uptake potential of the biosphere (sec. 1.2.1, *Moorcroft* (2006), *Tang and Bartlein* (2008)), vegetation models, and their integration into climate models became a major research focus, and several approaches to simulate land-C-dynamics were developed.
Model approaches can be divided into *Behavioral Ecological Models* (BEMs), *forest 'gap'* models, *Soil-Vegetation-Atmosphere* (SVA) models, and *Terrestrial Biosphere Models* (TBMs), which all try to simulate land ecosystem dynamics by slightly different concepts and aims (*Galbraith and Christoffersen* (2015)). BEMs originally focus on functional behavior of communities (here: specifically plant communities) and how they are influenced by their environment. Gap models are individual-based models that focus forest

succession by simulating forest structure, composition, and demography on fine spatial scale over time. Both model types provide unique insight into ecosystem development, but depend on many parameters, which are usually difficult to measure and quantify and lack of generality, i.e. parameters that are determines for a specific ecosystem or plant, are not necessarily usable for other ecosystems, or even other plant communities or plant types. Additionally, the large amount of parameters and processes requires too high computational resources to run such models globally and/or couple them to climate models. Thus, an application of such detailed models on the global scale is almost impossible, but one needs global models to simulate present and future C land uptake, since atmospheric CO_2 is rising everywhere due to atmospheric dynamics.
SVA models are originally developed as *land-surface models* by the atmospheric science community and are therefore usually based on rather physical principles by simulating exchange of mass, energy and momentum between soil, vegetation and atmosphere on broader scale. They were developed to be easily embedded into *General Circulation Models* (GCMs) that model the physically based circulations of atmosphere and ocean to predict climate. However, they usually lack of biogeochemical details that shape exchange fluxes. Biogeochemical cycles and interactions are the major focus of TBMs (*Arora* (2002), *Raupach et al.* (2005)). Both model types, i.e. SVAs and TBMs, are coarse enough to run globally and to be coupled to climate models with a reasonable amount of computational power. However, they lack the individual-based information by using prescribed and static plant functional types (PFTs) to describe the most important quantities of a particular plant stock interacting with other spheres (*Galbraith and Christoffersen* (2015)).
Dynamic Global Vegetation Models (DGVMs) build a bridge between these model approaches by using the biogeochemical cycles from TBMs, physical principles of SVA models, and dynamic community shifts based on BEMs and gap model approaches (*Galbraith and Christoffersen* (2015)). They are usually based on 10 to 15 PFTs, based on TBM/SVA approaches, but allow a community/PFT shift in response to environmental changes. This makes DGVMs the state-of-the-art models[4], which are used in Earth System Models (ESMs) that are applied to predict future climate change (*Prentice et al.* (2007), *Prentice and Cowling* (2013), *Fisher et al.* (2014)).

Until the late 20^{th} century the focus of DGVM development was the exchange of energy, water and C, but the rising awareness of nutrient limitation on plant growth, especially by PNL (sec. 1.2.2.2), introduced a new generation of DGVMs that incorporated the N cycle into its biogeochemical part, i.e. the TBM part. Often these model generations are distinguished by the suffix **-C** for the C-only version and **-CN** for the C-N coupled version (or only **-N** in case the original version does not have the **-C** suffix). Some models even have a P cycle coupling incorporated that is named with the suffix **-CNP**.

[4] One can also find the opposite definition that DGVMs build a sub-group of TBMs, which allow dynamic ecosystem adjustments to environmental changes (e.g. *Fisher et al.* (2014)).

However, increasing model complexity by the inclusion of nutrient cycles does not necessarily improve model performance and/or lower model uncertainties. The next sections therefore review general present-day model performance of DGVMs (or TBMs), and highlight potential missing links, which are related to the topic of the study, before the TBM QUINCY (*Thum et al.* (2019)) is introduced as framework for model development within this study.

1.2.4.1. Model-data (mis)matches and key uncertainties

Generally, state-of-the-art TBMs (or DGVMs) are able to meet large-scale patterns, such as vegetation distribution and seasonal dynamics, which reproduce present-day C cycle patterns mostly well. This is caused by a generally good representation of the land C cycle and its major processes, as well as a good understanding of biome distribution and climate-induced changes within plant communities, which determines the modelled plant functional type (PFT). Both, process representation and PFT distribution, are based on large data sets of observations that either indicate which plants grow where and under which conditions, or constrain C fluxes by vegetation (above-ground) biomass observations and/or atmosphere-vegetation exchange measurements. Thus, TBMs may differ in specific functions and used parameters, which are used to calculate fluxes, but generally they are based on the same key equations, e.g. the photosynthesis model after *Farquhar et al.* (1982), or respiration rates after *DeVries* (1972), and consequently simulate present-day C cycle patterns similarly and well. This is the case for C-only TBMs, but also for later generations that are extended by nutrient cycles, i.e. by the N cycle or even the P cycle additionally. The extension of C-models to CN-models (or CNP-models) rounds out the vegetation part of TBMs by a better representation of plant processes that further constrains modelled fluxes, but necessitates a better representation of soil processes, which determine nutrient availability. Unfortunately, the knowledge about below-ground processes is much weaker than about above-ground processes, which hinders soil-model development and leads to a very simplified process representation in the soil part compared to vegetation process representation (sec. 1.2.4.3).
Besides, fluxes that are constrained by past and present-day observations may be inappropriate in the future, especially with respect to extremely fast environmental changes, i.e. climate changes and rising atmospheric CO_2 concentrations.

Wieder et al. (2015) used 20 models from the Coupled Model Intercomparison Project (CMIP5, *IPCC* (2013)) and compared predicted NPP and resulting land C development within the 21^{st} century under the Representative Concentration Pathway 8.5 (RCP 8.5, *IPCC* (2013)). They found a CO_2 fertilization effect on global present-day and future NPP among all model variants, but the effect was significantly lower in simulations that were constrained by N (CN-models hereafter) or N and P (CNP-models hereafter) stoichiometry and allocation due to nutrient constraints on plant growth (fig. 1.4a). This may lower land C change in response to eCO_2 to that effect that the present-day land C sink may turn into a C source until 2100 (fig. 1.4b). Besides, the variance among

model predictions is lower within CN- and CNP-models than among the original, C-only CMIP5 models, which is caused by tighter constraints on (future) C fluxes by nutrient interactions.

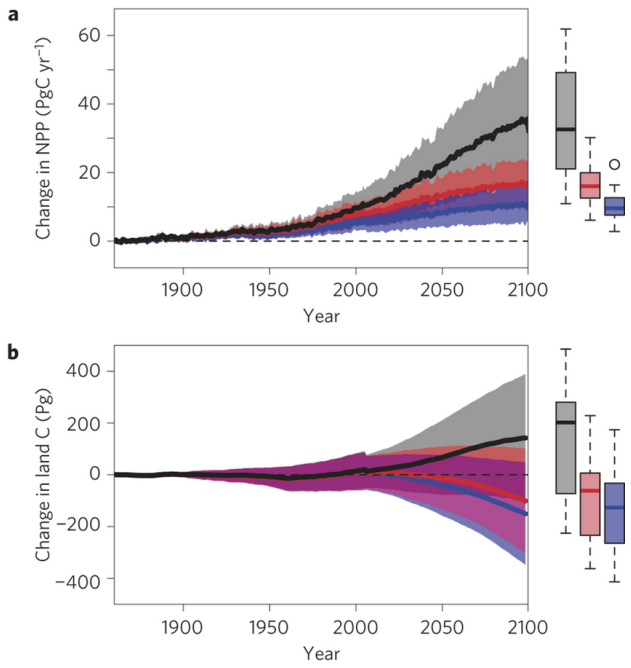

Figure 1.4.: Change in global NPP and land C storage from CMIP5 model projections. Difference in global NPP (a) and land C storage (b) from initial CMIP5 model values with prescribed CO_2 forcings over the historical period (1860–2004) and RCP 8.5 (2005–2100). C-only CMIP5 ensemble mean ($\pm$1SD; black), N-constrained CMIP5 ensemble mean (red), and NP-constrained CMIP5 ensemble mean (blue). Boxplots indicate the median, quartile range, extreme values, and outliers for the end of the twenty-first century (2090–2099). Figure is taken from *Wieder et al.* (2015).

Different responses of C-models compared to CN-models (or CNP-models) are caused by simulated strong progressive nutrient/N limitation (PNL, sec. 1.2.2.2) in response to eCO_2 by CN-models (*Thornton et al.* (2007), *Sokolov et al.* (2008), *Thornton et al.* (2009), *Zaehle et al.* (2010), *Fleischer et al.* (2019)), but the actual decrease in C sequestration is highly uncertain (fig. 1.4b: boxplots, *Friedlingstein et al.* (2014)), which is mainly due to knowledge gaps about general processes that drive ecosystem CN coupling (*Zaehle and Dalmonech* (2011)), and specifically soil processes, which determine N supply (*Bradford et al.* (2016)), which are both poorly represented in TBMs.
Missing process understanding lead to several different model approaches in currently used TBMs, ranging from fixed to flexible CN ratios, over N uptake adjustments, and soil N cycling variations, to additional N inputs to ecosystem, that lead to different sensitivities to eCO_2 and various levels of PNL occurrence (*Zaehle and Dalmonech* (2011), *Thomas et al.* (2013), *Thomas and Williams* (2014), *Meyerholt and Zaehle* (2018), *Davies-Barnard et al.* (2020)).

An extensive FACE experiment modelling study, where 11 state-of-the-art TBMs were run for two specific FACE experiments, finally pointed to major concerns regarding plant N acquisition (*Zaehle et al.* (2014)). *Zaehle et al.* (2014) reported, that modelled PNL was much more intensive than observed N limitation on growth by showing that observed NPP response to eCO_2 was higher than simulated NPP response during the

experiments. They particularly found a major mismatch in simulated to observed plant N acquisition. Observed N acquisition responded positively to eCO_2, indicating that plants have mechanisms to increase N acquisition in accordance to growing N demand. This feature was not captured by TBMs at all, and simulated N acquisition responded rather negatively to eCO_2, indicating PNL (sec. 1.2.2.2). Even worse, some TBMs simulated an increasing N-use efficiency (eq. 1.3) in response to eCO_2, meaning either a shift in tissue CN ratios, or a shift in tissue growth by prioritizing tissue with higher CN ratios, that was not observed at all (*Finzi et al.* (2007)). Consequently, even TBMs that simulated NPP response to eCO_2 better, did that mainly due to wrong reasons.
This points to major knowledge gaps in plant N acquisition, as well as plant N availability, or at least a very poor representation of relevant processes, and requests a revision modelled plant N acquisition strategies, and plant N availability in order to improve model predictions with respect to eCO_2.

1.2.4.2. Potential missing links

State-of-the-art TBMs usually model plant N acquisition as direct root uptake of mineral N (either only as mineral/plant available N, or divided into NH_4 and NO_3), but do not take symbiotic N fixation as plant controlled N acquisition strategy into account, or consider symbiotic mycorrhizal fungi at all. Nevertheless, there is evidence that both symbionts, i.e. fixing bacteria and mycorrhizal fungi, are largely used by plants to support their N acquisition (cf. chapter 2 and *Gutschick* (1981), *Vitousek and Howarth* (1991), *Ayres et al.* (1994); and *Vitousek et al.* (2013) for N fixation and chapter 3 and *Read* (1991), *Marschner and Dell* (1994), *Hodge et al.* (2001); and *Göransson et al.* (2006) for the importance of mycorrhizal fungi for plant N acquisition), and that the inclusion of biological N fixation or mycorrhizal fungi into stand- or ecosystem models improves plant N acquisition (*Meyer et al.* (2010), *Meyer et al.* (2012), *Meyerholt and Zaehle* (2015), *Wieder et al.* (2015), *Meyerholt et al.* (2016)). Furthermore, most TBMs consider leaf-to-root ratios as constant, whereas various studies show that plants allocate C into tissue growth depending on their actual demand, i.e. in case of (progressive) nutrient demand they enhance root growth (*Matamala and Schlesinger* (2000), *King et al.* (2001), *Norby et al.* (2002)).
This leads to a strong N availability control on plant growth, whereas N availability is controlled by soil processes, mainly by decomposition processes that are driven by microbial activity. These processes are again only weakly understood and thus only simplified represented as first-order decay in state-of-the-art TBMs, even if there is again wide evidence that (plant controlled) rhizosphere processes are a key component of terrestrial ecosystems (*Knops et al.* (2002), *Chapman et al.* (2006), *Finzi et al.* (2015)) and neglecting them may largely underestimate the impact of the terrestrial biosphere to (future) climate (*Shi et al.* (2019)).

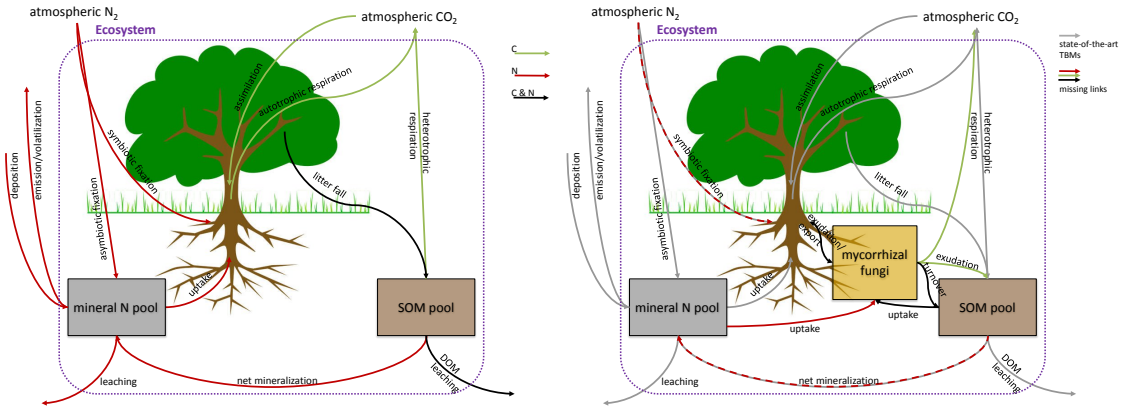

(a) Ecosystem N balance and cycle in state-of-the art TBMs

(b) Missing fluxes in ecosystem N balance and cycle in state-of-the art TBMs

Figure 1.5.: Schematic figures of ecosystem N cycle with driving C fluxes in state-of-the-art TBMs (a), and highlighted missing fluxes (b), derived from figure 1.3. Ecosystem with included internal N cycle (inside violet frame), and external N sink and source. Tree represents vegetation (pools), boxes represent soil pools. Green arrows: C fluxes, red arrows: N fluxes, black arrows: C and N fluxes. Grey arrows in (b) depict fluxes shown in (a) to highlight additional fluxes.

These various ways how plants **actively** interact with soil and soil microbes in order to gain N that range from interacting with mycorrhizal fungi to hosting N fixing bacteria, which were presented in section 1.2.2, and their representation (missing representation) are shown in figure 1.5. Figure 1.5 stripes down the C and N fluxes that were presented in figure 1.3 into fluxes that are represented in state-of-the-art TBMs yet (a, sec. 1.2.4.3), and highlights potentially missing fluxes (b).
These missing fluxes, and plant control on those, may be the key missing processes to improve model performance primarily with respect to plant N acquisition, but consequently also in plant response to eCO_2.

1.2.4.3. Carbon-nutrient cycling within terrestrial biosphere models by the example of QUINCY[5]

The novel TBM QUINCY (QUantifying Interactions between terrestrial Nutrient CYcles and the climate system, *Thum et al.* (2019)) simulates the cycling of carbon (C), nitrogen (N), and phosphorus (P) within the entire ecosystem by taking the water and energy requirements into account (fig. 1.6).

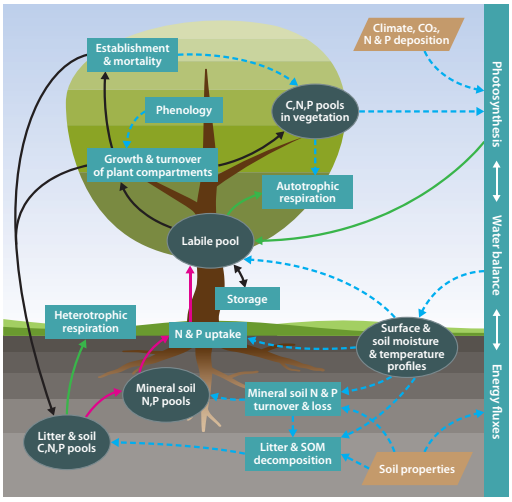

Figure 1.6.: Overview about QUINCY model pools (dark ovals) and fluxes (black arrows: C, N and P; green arrows: C; pink arrows: N and P) that are linked by processes (turquoise boxes), where dependencies follow blue dashed arrows. Brown boxes present forcing data. Figure taken from *Thum et al.* (2019).

QUINCY, as most TBMs, consists of a vegetation, and a soil model/part, which are described in the upcoming parts (parameters can be found in appendix A in tab. A.1), and simulates all processes on an half-hourly time step (denoted as dt) to account for vegetation processes that respond very quickly to environmental changes. Associated fluxes are considered to have a process-specific time lag or process memory, which is represented by a running mean with a time-average filter:

$$\Phi^{process}_{mavg,new} = \Phi^{process}_{mavg,old} \times (1-\omega) + \Phi_{current} \times \omega, where \tag{1.5a}$$

$$\omega = \frac{dt}{\tau^{process}_{mavg}} \tag{1.5b}$$

where $\Phi_{current}$ is the instantaneous pool or flux, whereas $\Phi^{process}_{mavg,old}$, and $\Phi^{process}_{mavg,new}$ are the averaged values of the previous and current time step. ω weights the instantaneous pool or flux with respect to the process-specific memory time $\tau^{process}_{mavg}$.

Vegetation

QUINCY simulates vegetation dynamics based on eight plant functional types (PFTs) that distinguish climate (tropical, temperate, or boreal), growth form (trees, shrubs, or grasses), leaf type (needle-leaved or broad-leaved), leaf habit (evergreen or deciduous, i.e. rain green or summer green), and photosynthetic pathway (C3 or C4), on grid cells,

[5] If not indicated otherwise, section 1.2.4.3 refers to *Thum et al.* (2019).

whereas one grid cell can be inhabited by different PFTs. Vegetation is then modelled as average representative of a specific PFT, and consists of six structural tissue pools, from which three are fast-living (leaves, fine roots, and fruits), and three are long-living, i.e. woody (sapwood, heartwood, and coarse roots), as well as of two non-structural pools (labile, storage). The labile pool is a fast over turning, respiring pool that allows the decoupling of resource input, and resource usage, whereas the storage pool buffers seasonal changes, and ensures resource supply for yearly off-spring for example (cf. *Thum et al.* (2019), A3).

Plant biomass production is determined by the input of resources, and its partitioning to different processes, such as maintenance and growth, and in the case of C, to (associated) respiration fluxes. To decouple those plant-internal processes from the instantaneous C assimilation by photosynthesis, and N uptake by roots, resources are added to the labile pool at first, from where they are allocated based on the turnover of the labile pool. Thus the specific turnover time of the labile pool, which is five days, is used as memory time for the following fluxes (eq. 1.5). Plants generally prioritize maintenance of existing tissues, and thus maintenance respiration, over growth. The storage pool is used either as resource source, and as resource sink, based on current conditions such as resource uptake and demand, season of the year, and successional state.

$$\frac{dC_{labile}}{dt} = U_C + \Delta S_C - G_C - R_g - R_m - R_{U_N} \tag{1.6a}$$

$$\frac{dN_{labile}}{dt} = U_N + \Delta S_N - G_N \tag{1.6b}$$

where U_X are uptake rates, given by gross photosynthesis for C, and uptake by roots for N. ΔS_X is the net exchange between the labile and storage pool, G_X are the growth rates to build new tissues, and R indicates respiration rates that is separated into respiration associated with growth (R_g), maintenance (R_m), and N uptake (R_{U_N}).

C uptake rate (U_C) is given by gross photosynthesis that is calculated after *Kull and Kruijt* (1998) with an extension of C4 photosynthesis based on *Friend et al.* (2009). C3 photosynthesis is either light limited, or calculated as minimum of carboxylation, which is limited by electron-transport capacity, and Rubisco-limited photosynthesis. C4 photosynthesis can be further limited by bundle-sheath transport.

N uptake rate (U_N) is a sum of the uptake rates of NH_4, and NO_3. Both are calculated similarly following an extend Michaelis-Menten saturation function:

$$U_{N,j}^{pot} = v_{max,j}(T_s, \phi) \times N_j \times (K_{m1,j}(T_s, \Theta) + \frac{1}{K_{m2,j}(T_s, \Theta) + N_j}) \times \zeta_N(\chi_{labile}^{CN}) \times C_{fr} \tag{1.7}$$

where j as index refers to either NH_4, or NO_3, and N_j denotes NH_4, or NO_3 concentration in soil. $v_{max,j}$ is the PFT-specific maximum uptake rate per unit root biomass (C_{fr}) that is adjusted by soil temperature (T_s), and the current root zone moisture potential (ϕ),

which takes limited nutrient transport in dry soils into account. K_m are nutrient sensitivity parameters of the low and high affinity transporters. These affinities are also adjusted to soil temperature, and soil moisture (Θ). Latter accounts for the difference between mass-based and soil solution concentrations *Ahrens et al.* (2015). Plants can down-regulate the potential uptake of N_j, if their demand (ζ_N) is low. ζ_N is calculated based on C, and N availability, given by the current CN ratio of the labile pool (χ^{CN}_{labile}), and C, and N requirements for growth.
Actual N_j uptake rates are calculated based on all potential out fluxes for N_j, considering leaching and competition with microbes for example, and the current size of N_j. If out-fluxes would exceed available N_j, all out flux rates are recalculated based on their fraction of the total out flux (cf. *Thum et al.* (2019), A4.5).

The exchange of C, and N with the storage pool (ΔS) varies seasonally and in accordance to stress. Plants target to fill their reserve pool to ensure the annual growth of leaves and fine roots throughout the entire years, but if resources are needed to maintain or grow tissue the storage is used.
The growth rates G_X are calculated based on available C, and N, CN ratios of the tissue pools that should grow, and current allocation ratio, such as leaf-to-root ratio.

Respiration is divided into growth respiration, maintenance respiration, and N uptake respiration. Growth respiration is estimated as constant fraction of growth rate G_C:

$$R_g = f_{resp,growth} \times G_C \tag{1.8}$$

Maintenance respiration is determined for every structural tissue pool (i) individually by using its N content (N_i) as proxy for living cells and considering an instantaneous temperature response:

$$R_{m,i} = g(T) \times f^i_{resp,maint} \times N_i \tag{1.9}$$

where g(T) is the temperature response function after *Lloyd and Taylor* (1994) with T being current air or soil temperature for above- and below-ground tissues, respectively, and $f^i_{resp,maint}$ is the maintenance respiration per unit N.

N uptake respiration is based on the assumption that plants have to invest C into the transformation of N from mineral sources into organic material. It is calculated by specific costs (R_j, *Zerihun et al.* (1998)) for each mineral form N_j, and the actual plant uptake $U_{N,j}$.

$$R_{U_{N,j}} = r_j \times U_{N,j} \tag{1.10}$$

where j refers to either NH_4, or NO_3.

Soil Biogeochemistry
The soil part of QUINCY (cf. *Thum et al.* (2019), A4) follows the CENTURY approach of *Parton et al.* (1993) and consists of five organic pools with prescribed CNP ratios that are three litter pools (metabolic litter, structural litter, and woody litter) and two soil organic matter (SOM) pools (fast SOM, and slow SOM), and three mineral pools (NH_4, NO_3, and PO_4).

Organic material enters soil by litter fall that is partitioned to the litter pools accordingly to its source: Litter from plant labile and reserve pools enter metabolic litter, litter from woody pools enter woody litter pool, and litter from all other tissue pools is allocated into metabolic and structural litter.
Litter decomposition is calculated based on turnover times for each litter pool, which is adjusted by soil temperature and soil moisture, and decomposed material enters SOM pools. SOM is again decomposed based on specific turnover times and soil conditions until material is mineralized and thus enters the mineral pools, from where it can be taken up by plants again, or leached out (*Davidson et al.* (2012)). Decomposition (or losses) of all organic soil pools (i) therefore follow the following first-order decay equation:

$$L_i = \frac{1}{\tau_i^*} \times X_i, \; with \tag{1.11a}$$

$$\tau_i^* = \tau_i \times f(T_s) \times g(\Theta) \tag{1.11b}$$

where L is the fraction of the specific organic pool i with pool size X (C, N, or P) that is decomposed/lost and allocated to other pools. τ_i^* is the actual turnover time of pool i that is derived from base turnover time of pool i (τ_i), which is adjusted to current soil conditions by soil temperature (T_s) and soil moisture (Θ). i denotes metabolic, structural, and woody litter, as well as fast and slow SOM.

Since organic soil pools have prescribed CNP ratios, material has to change its CNP ratio accordingly during decomposition process. And as further decomposed pools have a smaller CNP ratio, surplus C is respired as heterotrophic respiration to fulfill the CNP ratio requirements of the entered pool. Only the fast SOM pool, which represents microbial community, can change its CNP ratio in accordance to NH_4 availability following *Parton et al.* (1993).

1.3. Research questions and thesis outline

The necessity to revise plant N acquisition strategies in in state-of-the-art TBMs (sec. 1.2.4.1) is the basis for the present study. By revising currently represented plant N acquisition, i.e. direct root uptake of mineral N from soil, and incorporating potentially important symbioses to support plant N acquisition, i.e. with N-fixing bacteria and mycorrhizal fungi, I aim for the development of a plant controlled N acquisition model. This model may allow plants to adjust to rising atmospheric CO_2, and may lead to a better model-data match and/or narrow uncertainty by an improved representation of underlying processes.
However, especially under ambient conditions in a steady-state ecosystem, I do not expect a major influence of such strategies on absolute plant growth, as TBMs are rather well constrained with respect to the global C cycle. Consequently, plant biomass and NPP should not change much, but I expect an effect on GPP, and respiration, which determine NPP (eq. 1.1). GPP may increase due to a better N nutrition, which allows plants to assimilate more C, but respiration may increase as well due to C investment into N acquisition. To disentangle such effects, I use not only absolute fluxes, i.e. GPP and NPP, but rather CUE to quantify effects of additional plant controlled N acquisition strategies on plant growth.

Apart from the different structure of both symbioses, i.e. almost all terrestrial plants host mycorrhizal fungi, whereas only some host N-fixers, they differ also in the accessed N source. N-fixing bacteria fix ecosystem external N. Mycorrhizal fungi take up only ecosystem internal N, but contrary to plants, they may also access organic N in addition to mineral N. Consequently, I separate the development of the final dynamic plant N acquisition model into the evaluation of simulated symbiotic N fixation in chapter 2 (fig. 1.7, purple frame: BNF model), where I implement two existing models into the TBM QUINCY, and the development and evaluation of an explicit plant-mycorrhiza interaction model within the QUINCY framework in chapter 3 (fig. 1.7, blue frame: MYC model). Both chapters/studies are independent from each other an have slightly different main points. Chapter 2 focuses on existing C-cost based fixation models and their suitability for QUINCY in particular. Chapter 3 develops a plant-mycorrhiza interaction model and assesses different proposed mycorrhizal functionalities for forest ecosystems.
Both models, i.e. the BNF model and the MYC model, are coupled in chapter 4 to accomplish a fully plant controlled N acquisition model (fig. 1.7, violet frame: MYFUN model) that takes ecosystem internal and external N sources into account. As the MYFUN model allows plants to control ecosystem N gain by fixation, and ecosystem N cycling by utilizing mycorrhizal fungi, chapter 4 especially assesses the question, if and to what extend plant control on ecosystem N dynamics may be reasonable.

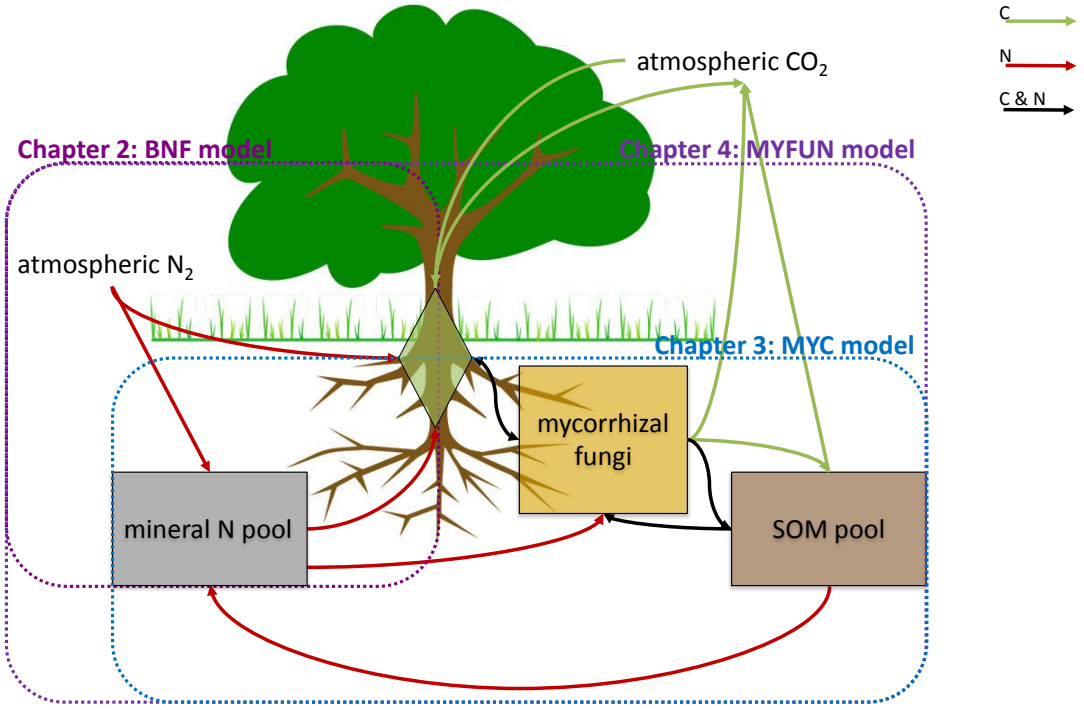

Figure 1.7.: Overview over thesis structure and model parts.
Diamond represents plant (labile) pool, boxes represent soil pools. Green arrows: C fluxes, red arrows: N fluxes, black arrows: C and N fluxes. For flux terms see figure 1.5.

To build a frame, the entire study is additionally guided by the following questions:

1. What does the implementation of plant controlled N acquisition by symbiotic N fixation and/or mycorrhizal fungi into a TBM imply for simulated (i) plant N nutrition, (ii) plant CUE, and (iii) ecosystem CN budgets and dynamics?
2. What drives ecosystem dynamics? Does N availability control plant growth/CUE, or do plants control N availability by investing C into N acquisition?

These questions will be discussed and (potentially) answered in chapter 5.

2. Testing carbon cost based symbiotic nitrogen fixation as strategy to overcome progressive nitrogen limitation under elevated CO_2

2.1. Introduction

Increasing atmospheric carbon dioxide (CO_2) concentrations (cCO_2) caused by human activities rose the question of the carbon (C) storage potential of ecosystems, which is expected to increase under elevated cCO_2 (eCO_2) conditions (*Ciais et al.* (2014), *Friedlingstein et al.* (2014), *LeQuéré et al.* (2018)). Long-term ecosystem C balance is driven by input and output fluxes, which are mainly C gain by plant photosynthesis, and C loss by autotrophic and heterothrophic respiration, as well as minor losses by leaching. The influence of eCO_2 on C input and output fluxes was explored, whereby photosynthesis increased stronger than output fluxes, which leads to a shift in ecosystem C balance towards higher C sequestration (*Norby et al.* (2002), *Norby et al.* (2005), *Bonan* (2008)). However, ecosystem C balance and C cycling though the ecosystem are tightly linked to ecosystem nitrogen (N) cycling and ecosystem N balance (*Vitousek and Howarth* (1991)). N is a major component of proteins, which are the basis of all living biomass, and also the basis of the Rubisco enzyme that drives plant photosynthetic capacity (*Lorimer* (1981)). Consequently, N availability constrains plants' ability to assimilate C, as well as plants' ability to produce biomass and thus fix freshly assimilated C. Both, assimilation and fixation of C in plant biomass, and thus in ecosystems, are reduced in case there is not enough N available for building proteins that are necessary to activate enzymes or produce biomass (*Vitousek and Howarth* (1991), *Gruber and Galloway* (2008)). Moreover, N stress increases (maintenance) respiration, and consequently ecosystem C losses (*Amthor* (1994), *Amthor* (1995)). By influencing both, ecosystem C gain and losses, ecosystem N balance strongly affect ecosystem C balance, which constrains ecosystem C storage in response to eCO_2 (*Luo et al.* (2004), *Bonan and Doney* (2018)).

2.1.1. Biological nitrogen fixation as nitrogen source for ecosystems

Similar to ecosystem C balance, long-term ecosystem N balance is driven by input fluxes, i.e. deposition and fixation, and output fluxes, i.e. gaseous losses and leaching (fig. 2.1). Naturally, N deposition, which terms the input of reactive N species from atmosphere to biosphere, is rather low, but rates are increasing due to higher input of such species by human activity (*Vitousek et al.* (2010), *Peñuelas et al.* (2013), *Ciais et al.* (2014)). Without anthropogenic influence, ecosystems gain N mainly by fixation of inert atmospheric dinitrogen (N_2, *Ayres et al.* (1994)), which happens either abiotic by processes that release a lot of energy, such as lightning or volcanic eruptions, or biotic by microorganisms that are able to fix N. N-fixing bacteria are either free-living, like *Cyanobacter* and *Azotobacter*, or live in symbiosis with plants. Since especially Cyanobacter are almost everywhere, biological N fixation (BNF) is by far more important as ecosystem N input than occasional abiotic events (*Gutschick* (1981)).

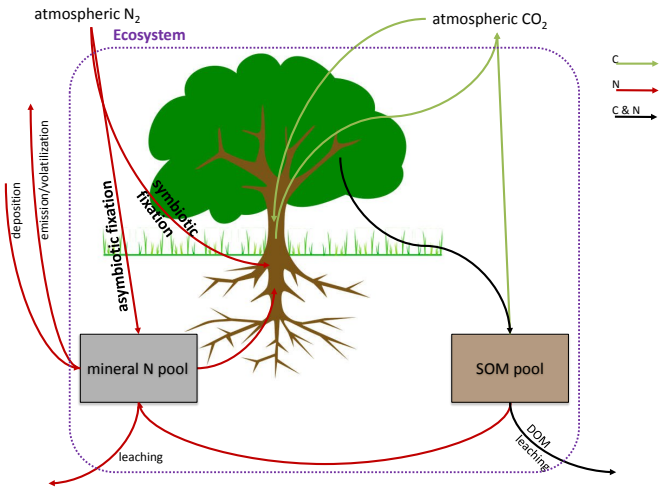

Figure 2.1.: Schematic figure of ecosystem C and N cycles and exchange with external sinks and sources with focus on N exchange fluxes. Ecosystem internal CN and N cycles are simplified presented to complete C and N cycling (for additional information and flux terms see figure 1.3). Tree represents vegetation (pools), boxes represent soil pools. Red arrows: N fluxes, green arrows: related C fluxes, black arrows: related CN fluxes.

However, because of the high energy requirements to split the molecular triple bonding of N_2, BNF is strongly regulated by energy limitation, and tightly coupled to the microorganisms' needs in case of asymbiotic BNF (aBNF) by free-living bacteria (*Gutschick* (1981), *Vitousek and Howarth* (1991)). Thus, this ecosystem N influx may not respond strongly to a higher ecosystem C influx, which is driven by plants in response to eCO_2, but I expect the opposite for symbiotic BNF, which is done by bacteria that are hosted by plants. Symbiotic living microorganisms live in plant root nodules and fix N accordingly to

plant N demand, because plants provide carbohydrates for microbial growth, and as energy source for N fixation (*Gutschick* (1981)). Under eCO_2, I expect plants to assimilate more C than they can use for own biomass growth due to growth limitation by N. They may invest this surplus C into BNF to gain additional N that will allow further biomass production (*Rastetter et al.* (2001), *Fisher et al.* (2010)).
And even though increased fixation rates are observed in response to eCO_2 (*Zanetti and Hartwig* (1997), *Lam et al.* (2012), *Nasto et al.* (2019)), *plant controlled* symbiotic fixation is hardly considered in terrestrial biosphere models (TBMs) that are used to explore ecosystem C balance and predict its future development in order to assess the question of future ecosystem C storage. This may lead to an underestimation of the impact of terrestrial ecosystems on the global C balance under eCO_2 and consequently on climate change (*Shi et al.* (2019)).

2.1.2. Previous approaches to simulate nitrogen fixation in terrestrial biosphere models

Most terrestrial biosphere models (TBMs) simulate both, aBNF and BNF, whereby aBNF is usually calculated as function of climate conditions, such as (soil) temperature, moisture, and shading, which are used as proxy for energy limitation for microbial activity. BNF is largely considered as empirical function either of actual evapotranspiration (ET, *Cleveland et al.* (1999)), or of net primary production (NPP, *Thornton et al.* (2007), *Goll et al.* (2012)). Both approaches are based on *Cleveland et al.* (1999) estimations. Similar to *Wieder et al.* (2015), it could be argued that both, ET and NPP, are plant growth controlled and thus react to climate changes, but none of this functions is actually process-based, or take plant N demand, or soil N availability and thus, plant ability to take up N into account.

During the last decade, more process-based fixation models were developed and coupled to existing TBMs, such as the N cycle extension of LM3V (*Gerber et al.* (2010)), which is the land component of the Geophysical Fluid Dynamics Laboratory (GFDL) model (*Shevliakova et al.* (2009)), or the Fixation and Uptake of Nitrogen (FUN) model (*Fisher et al.* (2010), *Brzostek et al.* (2014)) that was coupled to the Community Land Model (CLM, *Lawrence et al.* (2011)). The extension by *Gerber et al.* (2010) derives BNF rates from plant N demand, soil N availability, and light availability as proxy for energy, which allows to account for observed successional effects, i.e. very high fixation rates in early (secondary) succession, but low rates in an evolved ecosystem, that were reported by *Gorham et al.* (1979), *Sprent* (1987), and *Batterman et al.* (2013). However, this model still does not consider C investment into BNF that may change plant C balance, and ecosystem C balance in response to eCO_2. To my knowledge only the C cost based models of *Rastetter et al.* (2001) and the FUN model (*Fisher et al.* (2010), *Brzostek et al.* (2014)) consider C investment into BNF, and compare it to (potential) root N uptake costs, which (i) allows plants to actively choose for the C cheapest N acquisition strategy in order to maximize growth by investing as little C into N acquisition as

possible while satisfying N demand, and (ii) changes plant C balance by increasing respiration under N limitation accordingly.
However, in the context of rising atmospheric CO_2, and increasing progressive N limitation (PNL) on plant growth (sec. 1.2.2.2), C cost based N fixation approaches that take C investment in form of respiration into account are necessary to (i) allow plants to adapt to changing conditions, and (ii) improve C balance predictions.

2.1.3. Study scope and hypotheses

The aim of this study is to investigate the importance of symbiotic, i.e. plant controlled, N fixation on plant and ecosystem C balance by the implementation of C cost based symbiotic N fixation into the TBM QUINCY (*Thum et al.* (2019), sec. 1.2.4.3). I expect, that plants will actively invest C into fixation in case of N limitation. This will change plant C balance and following ecosystem C balance especially in response to rising atmospheric CO_2 concentrations that are expected to increase ecosystem C storage (*Ciais et al.* (2014), *Friedlingstein et al.* (2014), *LeQuéré et al.* (2018)), which may lead to progressive N limitation (PNL, sec. 1.2.2.2).
I choose the two C cost based models,i.e. the *optimal* model by *Rastetter et al.* (2001) and the *resistance* approach that was used by FUN (*Fisher et al.* (2010), *Brzostek et al.* (2014)), and implement them into the QUINCY model as they are based on the same principle of comparing C investment into different N acquisition strategy, but the differ in the resulting fixation flux. The implementation of both models allows me to *test*, how much control plants may have on actual BNF rates, because the two chosen models constrain BNF rates differently. *Rastetter et al.* (2001) treats BNF as additional N acquisition strategy only on top of N uptake by roots that is limited by plant root biomass to account for potential nodules to host fixing bacteria. FUN scales all N acquisition strategies with actual plant N demand, which allow plants to satisfy N needs entirely.
Plant controlled BNF will improve plant N nutrition, which will likely increase GPP as photosynthesis may be more efficient, because it relays on N-rich proteins such as Rubisco (sec. 1.2.2.1). Similarly, active C investment into BNF will increase plant respiration and thus lower NPP compared to GPP, i.e the carbon-use efficieny (CUE, eq. 1.2). In combination, I expect that the implementation of C cost based N fixation will lower modelled plant CUE, but not to the cost of NPP due to higher GPP (H2.1).
As N fixation accesses an ecosystem-external source for N, I hypothesize further that the effect of a plant controlled N fixation scheme is low in an ecosystem in equilibrium, because there is enough N in the system to meet plan demands by internal N cycling, but the effect is high in evolving ecosystems, and/or under changing conditions (H2.2). Latter is especially important with respect to rising atmospheric CO_2 concentrations that lead to PNL on plant growth. Adaptive C investment into N fixation will prevent plants from PNL, and enhance growth under eCO_2 (H2.3).

2.2. Materials and methods

2.2.1. Carbon cost based biological nitrogen fixation approaches

Generally, QUINCY (sec. 1.2.4.3) takes biological N fixation as asymbiotic process into account (*Thum et al.* (2019), A4.6). N is fixed during an enzymatic process, which is temperature depending, and added to the NH_4 pool in soil. It is suppressed, if N in soil exceeds a critical threshold (N^F_{limit}, tab. A.1), which is described by *Zaehle et al.* (2010).

$$F^{asym} = v_{max,F^a} \times f(T_s) \tag{2.1}$$

where $v_{max,F}$ is a parameter that represents the base rate of fixation (tab. A.1) and $f(T_s)$ is the temperature response of nitrogenase.
I will use this *standard* scheme as baseline for comparisons in section 2.3 to section 2.5.

To implement schemes for biological nitrogen (N) fixation (BNF), which allows plants to adapt to their N demand, I start with a modified version of equation 1.6. In contrast to the standard fixation scheme of QUINCY (sec. 1.2.4.3), I add symbiotically fixed N directly to plant labile N pool, because I assume that plants invest C to host N-fixing bacteria that fix N exclusively for them in a usable form (*Gutschick* (1981)). Nevertheless the standard fixation, which is added to NH_4 in soil (*Thum et al.* (2019)), is not set to zero, but to 10% of its original value to account for asymbiotic BNF (aBNF) by free-living fixers and for abiotic fixation by lightning. I subtract carbon (C) that plants invest into symbiotic bacteria to stimulate N fixation as fixation respiration (R_F) from plant labile pool.

$$\frac{dC_{labile}}{dt} = U_C + \Delta S_C - G_C - R_g - R_m - R_{U_N} - R_F \tag{2.2a}$$

$$\frac{dN_{labile}}{dt} = U_N + \Delta S_N - G_N + F \tag{2.2b}$$

where U_X are uptake rates, ΔS_X net exchange with the storage pools, G_X growth rates, and R_g, R_m, and R_{U_N} respiration rates, which are related to growth, maintenance or N uptake processes (eq. 1.6). R_F is respiration associated with symbiotic N fixation, and F is the symbiotic fixation rate.

I calculate fixation respiration analog to N uptake respiration (eq. 1.10), based on C cost per unit N that is fixed, and the fixation rate:

$$R_F = r_F \times F \tag{2.3}$$

where r_F is the actual fixation cost, which depends on nitrogenase activity (eq. 2.9, *Houlton et al.* (2008), *Fisher et al.* (2010)), and F is the actual symbiotic N fixation rate (eq. 2.10 or eq. 2.11, respectively).

I assume that plants target maximal growth, and since biomass contains C, and N, they need a sufficient influx of both to grow (*Mäkelä et al.* (2008), *Caldararu et al.* (2020)). So N fixation as C cost intensive N acquisition strategy will only happen in case of *surplus* C availability, which cannot be used for biomass production, as N demand is not met by N uptake from soil due to limited soil N availability[1]. N-fixing bacteria have the ability to fix ubiquitous N_2, which they to either as free-living ones or in symbiosis. Latter are more beneficial for plants in case of N limitation, since they fix exclusively for their host plant, which grow nodules to establish anaerobic conditions that facilitate fixation and supply C as energy source for nitrogenase.
I apply an economical approach, where plants spend C into the cheapest N acquisition strategy, or the cheapest combination of N acquisition strategies, which leads to the question of *C costs for N acquisition strategies* such as root uptake and symbiotic N fixation (fig. 2.2). After estimating potential costs that depend on current environmental conditions, plants 'decide' for the C cost cheapest strategy to acquire enough N to meet growth requirements.
As plants will not change their strategy instantaneously, I assume a memory of a week, which is the memory of plant C allocation from labile pool, that I use as average time in the following code (eq. 1.5, *Thum et al.* (2019)), if not indicated otherwise. It allows plants to adapt quickly in case of increasing N demand that is not met by root uptake solely, but buffers immediate changes, for example caused by the daily temperature cycle.

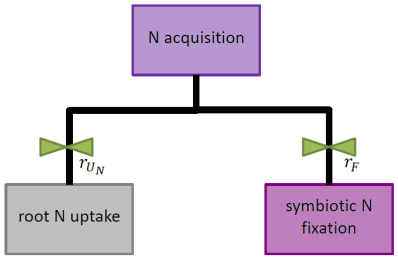

Figure 2.2.: Conceptual idea of symbiotic BNF schemes, which adds symbiotically fixed N to plant N acquisition by adding it directly to plant labile pool, similar to plant root uptake (eq. 2.2). Fixation schemes, i.e. optimal scheme and resistance scheme, calculate (potential) C costs (green locks) for root uptake (r_{U_N}, eq. 2.4) and N fixation (r_F, eq. 2.9), and use C costs to derive optimal C investment into fixation, which determines fixation rates (eq. 2.10 and eq. 2.11 respectively).

[1] Surplus C that cannot be incorporated into biomass, is often problematic for TBMs, which is why some models introduced an additional wastage respiration in order to maintain plant CN ratios (*Zaehle and Friend* (2010)). As C wastage is ineffective from plants' view, I assume that plants invest surplus C into N acquisition to maximize growth either by growing more roots to access further distant soil N, or by hosting N-fixing bacteria.

I calculate C costs for N uptake (eq. 2.4a) by roots as a sum of so-called opportunity costs, and transformation respiration (eq. 2.7).
Opportunity costs take the efficiency of root uptake into account (eq. 2.4b), which I estimate by calculating the current gain of N that is the forthcoming N uptake based on C investment into roots (eq. 2.5), and compare it with gain of C, which is the forthcoming C uptake based on C investment into leaves, respectively (eq. 2.6). Opportunity costs will therefore go to zero, in case root uptake is very efficient and N gain is very high, because N availability in soil is sufficient. But they reach extremely high values, in case soil is N limited and root uptake is very inefficient, which reduces gain of N. As neither soil N, nor root biomass changes much under stable conditions, gain of N is rather constant throughout the entire year compared to gain of C that varies with among seasons. This is caused by plants' phenological cycle, which is determined by climatic and meteorological conditions, such as temperature, and sun light. They constrain photosynthesis, i.e. plants' uptake capacity per leaf, and, in case of deciduous trees, also the general availability of trees. Besides, also C availability for growth, as well as investment into fixation is limited by photosynthesis.
Thus, the estimation of opportunity costs is based on the question, whether it is more beneficial to grow leaves or roots under current environmental conditions, and given that both, leaves and fine roots will take up C or N during their whole lifespan, but will also need to be maintained, which leads to further C losses due to maintenance respiration. To account for that, I use fine root turnover time as process memory for opportunity costs (eq. 1.5, *Thum et al.* (2019)).

$$r_{U_N} = r_{opp} + R^{pot}_{U_N},\ with \tag{2.4a}$$

$$r_{opp} = \frac{g_C}{g_N} \tag{2.4b}$$

where r_{opp} refers to opportunity costs, given by g_X, which denotes the gain of C, and N respectively, and $R^{pot}_{U_N}$ is the potential respiration rate for N uptake by roots.

For current C and N gain estimations, I follow *Rastetter et al.* (2001), who assumed C investment into leaves or fine roots to achieve a marginal increase of leaf biomass, or fine root biomass, and calculate resulting increased net uptake of C, and N.

$$g_N = \frac{dU_N}{C^{invest}_{fr}} \tag{2.5a}$$

$$\approx \frac{U_N \times \frac{dC_{fr}}{C_{fr}}}{(1 + R^{fr}) \times dC_{fr}} \tag{2.5b}$$

$$= \frac{U_N}{C_{fr} \times (1 + R^{fr})} \tag{2.5c}$$

$$g_C = \frac{dNPP}{C_{leaf}^{invest}} \tag{2.6a}$$

$$\approx \frac{NPP \times \frac{dC_{leaf}}{C_{leaf}}}{(1 + R^{leaf}) \times dC_{leaf}} \tag{2.6b}$$

$$= \frac{NPP}{C_{leaf} \times (1 + R^{leaf})} \tag{2.6c}$$

where dU_N the marginal increased uptake rate of N, and dNPP is the marginal increased net uptake rate of C. I calculate both based on current uptake rates per existing leaf or fine root biomass. C_i^{invest} denotes C investment into either leaves or fine roots, given by the targeted marginal increase of biomass dC_i and associated respiration rates R^i. R^i are sums of growth respiration to gain biomass, and (potential) maintenance respiration to obtain it over its lifespan, which I estimate by current maintenance respiration for existing biomass. i is either $leaf$, or fr, which denotes leaf or fine root pools and linked fluxes, respectively.

I calculate the potential transformation respiration rates for N uptake simply by using current fractions of N uptake from NH_4 and NO_3, and multiply those fractions with associated transformation costs (*Zerihun et al.* (1998)).

$$R_{U_N}^{pot} = \sum_j \frac{U_{N,j}}{U_N} \times r_j \tag{2.7}$$

where $U_{N,j}$ are current uptake rates of j, and U_N is the total uptake rate as sum of all $U_{N,j}$. r_j are associated transformation costs. j is NH_4, or NO_3 (tab. A.1).

I estimate C costs for symbiotic N fixation based on nitrogenase activity, and constrain them with minimal and maximal costs due to measurements by *Gutschick* (1981) and *Gutschick* (1982). Since nitrogenase is an enzyme, its activity is temperature dependent (sec. 2.1.1), which is described by equation 2.8 (*Houlton et al.* (2008)).

$$\phi_F = c_\phi \times exp[a_\phi + b_\phi T_s \times (1 - \frac{T_s}{2T_0})] \tag{2.8}$$

where c_ϕ is a scaling factor to constrain nitrogenase activity (ϕ_F) to 1 at the optimal temperature T_0, and a_ϕ and b_ϕ are empirical parameters (tab. 2.1). T_s describes the actual (soil) temperature.

With this normalized nitrogenase activity, I derive C costs for N fixation that are lowest at the optimal temperature, and higher, if the actual temperature is lower than the optimal temperature to account for a higher demand of energy for nitrogenase activity, or if the temperature if higher to account for degenerating enzymes.

$$r_F = r_{F,max} - (r_{F,max} - r_{F,min}) \times \phi_F \tag{2.9}$$

where $r_{F,max}$ and $r_{F,min}$ are maximal and minimal costs for symbiotic N fixation (tab. 2.1) and ϕ_F is the normalized temperature function for nitrogenase activity.

After estimating (potential) C costs for N uptake by roots and actual C costs for N fixation, I use two different approaches to calculate resulting fixation rates, namely the optimal approach that is based on *Rastetter et al.* (2001) (eq. 2.10a), and the resistor approach that is used in the Fixation and Uptake of Nitrogen (FUN) model by *Brzostek et al.* (2014) (eq. 2.11a).

The *optimal approach* (opt) was introduced by *Rastetter et al.* (2001) and implemented into the O-CN model (*Zaehle and Friend* (2010)) by *Meyerholt and Zaehle* (2015). It basically assumes that N fixation only happens, if C costs for root uptake exceed C costs for fixation (eq. 2.10b), and that the amount of nodules that host fixing bacteria is limited by plant fine root biomass. Resulting fixation rates are calculated by a saturation function, which I scale by a temperature dependent factor to account for the temperature depending efficiency of nitrogenase, as I assume that N fixation is not only cheaper, but also more efficient at optimal temperature (eq. 2.10c). I calculate the scaling factor by using *Houlton's* temperature function again (eq. 2.8), but as I do not want to reduce fixation to zero in case of too low/high temperatures, I lower it only to half of its current potential maximum. An assessment of this modification can be found in appendix B.1.2.

$$F_{opt} = C_{fr} \times v_{max,F} \times \frac{\Delta r}{k_F + \Delta r} \times f_{\phi_F}, with \tag{2.10a}$$

$$\Delta r = r_{U_N} - r_F \tag{2.10b}$$

$$f_{\phi_F} = \frac{1 + \phi_F}{2} \tag{2.10c}$$

where C_{fr} is plant fine root biomass, as the amount of hosted bacteria scale with nodules which is depending on the amount of fine roots, $v_{max,F}$, and k_F are empirical parameters (tab. 2.1), Δr is the C cost difference between root uptake costs (r_{U_N}) and fixation costs (r_F), and f_{ϕ_F} is a temperature dependent scaling factor that takes *Houlton's* temperature function (ϕ_F) into account.

The *resistance approach* (res) is based on the idea of *Fisher's* Fixation and Uptake of Nitrogen (FUN, *Fisher et al.* (2010)), and further developed by *Brzostek et al.* (2014). It treats C costs for root uptake and fixation as parallel resistors in an electric circuit, and calculates resulting fixation and uptake rates likewise electric fluxes would pass the circuit. This results in an optimal allocation of C into both N acquisition strategies, i.e. root uptake and N fixation (eq. 2.11b). Both strategies are always available to use, but with very low costs for N uptake, N fixation rate will become low, whereas N fixation will be the main strategy to acquire N, in case root uptake costs are high. I adjust this approach by an offset parameter to outbalance the transformation costs that I added to root uptake costs. They were not considered in the original approach, but they would lead to notable

fixation rates, even if root uptake would full fill plant N demand entirely. An assessment of this modification can be found in appendix B.1.3.
The optimal share of N acquisition that should be taken from N fixation is finally scaled with N demand (eq. 2.11c) to calculate actual fixation:

$$F_{res} = \alpha_F \times \zeta_N, \qquad with \tag{2.11a}$$

$$\alpha_F = \frac{r_{U_N} - \alpha_0}{r_{U_N} + r_F}, \qquad and \tag{2.11b}$$

$$\zeta_N = C_{labile} \times \psi_N^{growth} - N_{labile} \tag{2.11c}$$

where α_F is the share of N acquisition that should complied by fixation under current conditions, given by C costs for root uptake (r_{U_N}), and BNF costs (r_F), and the empirical offset parameter α_0 (tab. 2.1), and ζ_N is plant N demand, averaged over τ_{labile} as memory time (tab. A.1). Plant N demand is calculated by N that is required for growth, given C available for growth (C_{labile}), and according N requirements (ψ_N^{growth}), and N that is already available for growth (N_{labile}).

2.2.2. Model setup

QUINCY requires a half-hourly meteorological forcing that contains air temperature, precipitation (rain and snow), longwave and shortwave radiation, atmospheric CO_2 concentration as well as N and P deposition rates. Meteorological data are derived from the CRUNCEP dataset, version 7 (*Viovy* (2016)), which provides daily data from 1901 to 2015. Data are disaggregated using the statistical weather generator (*Zaehle and Friend* (2010)) to the half-hourly model time step. Time series for atmospheric CO_2 concentration are taken from *LeQuéré et al.* (2018), and N deposition rates from *Lamarque et al.* (2010) and *Lamarque et al.* (2011).
Additionally, QUINCY requires information about vegetation, given as plant functional type (PFT), and soil, such as texture, bulk density, and rooting and soil depth, for each site. As my later study aims for N controls on plant growth, I also use information about inorganic P content that is kept constant to avoid influence by P limitation.

If not indicated otherwise, QUINCY pools (vegetation and soil) are brought to quasi equilibrium by a defined spin-up period that uses repeatingly meteorological data from 1901 to 1930 to drive simulations, before the actual simulation period (1901-2015) starts with transient climate and CO_2 concentrations as described above. If harvest year is reported in literature (*Luyssaert et al.* (2007)) after 1901, vegetation tissue pools are set to zero, but harvested biomass persists in the system by adding it to litter, except from woody biomass, from which a fraction of 80% is removed.

Table 2.1.: BNF model parameter

symbol	**description**	BNF scheme	**value & unit**	**reference**
a_ϕ	parameter to estimate nitrogenase activity	opt, res	-3.62	*Houlton et al.* (2008)
b_ϕ	parameter to estimate nitrogenase activity	opt, res	0.27 $1/^\circ$C	*Houlton et al.* (2008)
c_ϕ	normalizing factor for nitrogenase activity	opt, res	1.25	*Houlton et al.* (2008)
k_F	half-saturation parameter for N fixation	opt	5.0 gC/gN	this study[a]
$r_{F,max}$	maximal C costs per unit N that is fixed	opt, res	17.5 gC/gN	this study[a]
$r_{F,min}$	minimal C costs per unit N that is fixed	opt, res	8.0 gC/gN	*Gutschick* (1981)
r_{NH_4}	specific C cost per unit uptake of NH_4	opt, res	1.7 gC/gN	*Zerihun et al.* (1998)
r_{NO_3}	specific C cost per unit uptake of NO_3	opt, res	2.3 gC/gN	*Zerihun et al.* (1998)
T_0	optimal temperature for nitrogenase	opt, res	25.15 $^\circ$C	*Houlton et al.* (2008)
v_{max_F}	max. N fixation capacity per unit biomass	opt	22.5 mgN/(gC m^2 yr)	*Meyerholt et al.* (2016)
α_0	offset parameter for N fixation	res	3.91 gC/gN	this study[a]

[a]For parameter assessment see appendix B.1.

2.2.3. Observational Data

Observational data to evaluate the BNF schemes are taken from the Global Forest Data Base (GFDB) or from *Cleveland et al.* (1999), who provides N fixation estimations for 23 ecosystems.

2.2.3.1. Global Forest Data Base

The Global Forest Data Base (GFDB), which I use as source for observational GPP and NPP data to evaluate the BNF schemes is originally compiled by *Luyssaert et al.* (2007). It contains forest site information and ecosystem properties such as geographical location, tree species composition and site management, as well as information on C fluxes, such as GPP, NPP, which is further hierarchically subdivided into NPP components, such as above-ground NPP and below-ground NPP, and different respiration fluxes. Sites were chosen by referential integrity, methodological criteria, consistency of NPP data, and uncertainty in accordance to the length of time series and methodological approach to ensure the quality of the data base.
In total, the GFDB has information about 513 forest stands, but I use only 61 that have independent measurements of GPP and NPP. (Ecosystem) C fluxes are usually measured by eddy covariance stations. They monitor instantaneous, i.e. every 10 seconds, atmospheric CO_2 concentration and 3-dimensional wind directions above a certain area, i.e. a forest. The resulting C flux is estimated by calculating covariances of both measurements over a period of 30 minutes. The total net flux per time interval, e.g. a day or a year, is defined at net ecosystem production (NEP), which is the net flux from GPP and respiration. By assuming that GPP is zero at night, since plants need sunlight for photosynthesis, night-time fluxes are used to determin ecosystem respiration (R_e), which is the sum of autotrophic (plant) respiration (R_a) and heterotropic (soil) respiration (R_h). NEP and R_e are used to derive GPP. GFDB-NPP information are based on direct measurements of main NPP components, such as annual litter production and litter fall, and branch and stem increment. Total plant biomass production, i.e. NPP, is then estimated by using species-specific allometric dependencies. Further information about the GFDB, e.g. measurements methods, data organization, uncertainties, can be found in *Luyssaert et al.* (2007), *Vicca et al.* (2012), and *Campioli et al.* (2015).
The location of the 61 chosen sites, as well as the QUINCY PFT classification for each site, which is based on climate (tropical, temperate, boreal), and leaf habit (evergreen, deciduous), can be found in figure 2.3.

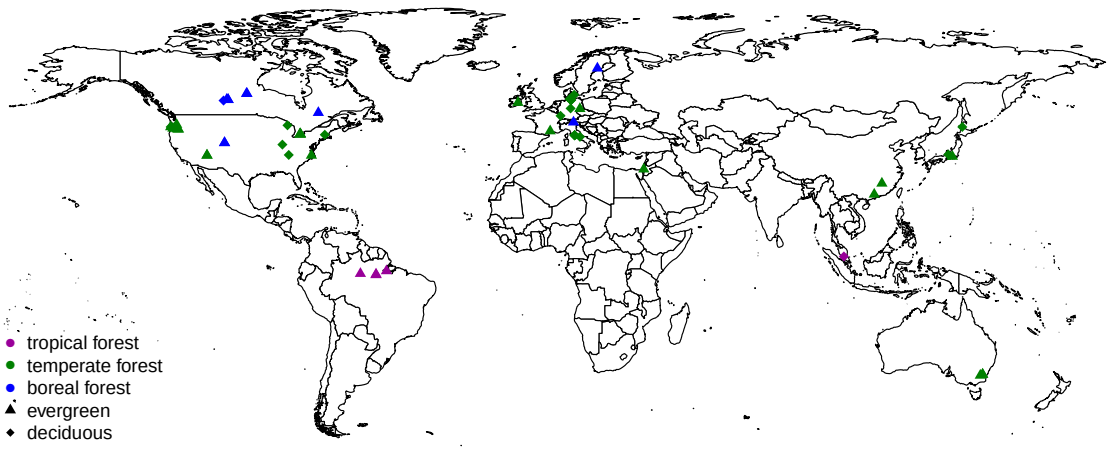

Figure 2.3.: Location and QUINCY PFT characterization of GFDB sites.

2.2.3.2. Site descriptions

I evaluate the N fixation schemes on an annual scale among all sites of the GFDB, where I have independent GPP and NPP observations (sec. 2.2.3.1), and on an sub-yearly scale for specific sites (fig. 2.4) that are chosen from the GFDB to represent different climate zones, leaf habits, and stand ages.

I expect that

- climate influences C costs for fixation and fixation rates that calculated by the optimal scheme caused by the underlying temperature function for nitrogenase activity (eq. 2.8, *Houlton et al.* (2008)),
- leaf habit influences C costs for root uptake by changing (i) opportunity costs (eq. 2.4), since the C gain is different for evergreen and deciduous trees, caused by seasonality and phenology, and (ii) N demand, as they have different CN ratios (*Kattge et al.* (2011)), and
- stand age affects N demand and N availability, since *young* ecosystems may have lower N availability than mature ecosystems, but a greater N demand due to their fast growing behavior. This may result in higher fixation rates in early succession as observed by *Gorham et al.* (1979), *Sprent* (1987), and *Batterman et al.* (2013).

Tapajos National Forest (2.90°S, 55.00°W; fig. 2.4: purple dot) was established as part of the Brazilian National Forest System in 1974 in the area of Amazon rain forest. The site is about 50km south of Santarem, Para, Brasil, and covers approximately 60km^2 between the Rio Tapajos, the Cupari River, and the Santarem-Cuiba Highway. Mean temperature is 26°C, whereas the temperature varies between 21°C and 31°C, and the annual rainfall can reach 2.000mm, which is why parts of the forest are seasonally flooded. Besides this alluvial rain forest, TAP has a dense rain forest with emergent trees, open tropical forest, and secondary forest along the borders and routs (*Harvard University (web presence)* (2002)).
GPP and NPP data are taken from GFDB (*Luyssaert et al.* (2007)) that refers to *Goulden et al.* (2004). N fixation estimates are taken from *Cleveland et al.* (1999) for tropical forests. QUINCY applys the PFT **Tropical humid Broadleaved Evergreen** (TrBE) for TAP.

Cascade Head Experimental Forest (45.20°N, 123.58°W; fig. 2.4: green dot) was established in 1934 and became an nature conservancy in 1966. CAS can be described as coastal temperate rain forest, because the climate is mostly driven by its location on the central Oregon Cost (US). Mean temperature is 10°C with low seasonal fluctuations, and the annual rainfall can reach 2.500mm. Even if CAS was established to represent a typical Stika-spruce forest, one could also find Douglas-fir, and even areas that are dominated by red alder (*U.S. Forest Service (web presence)* (2019)).
As both leaf habit types are measured and reported by GFDB, QUINCY runs CAS either as CAS_01 as **Temperate humid Needle-leaved Evergreen** (TeNE) site, or as CAS_02 as **Temperate humid Broadleaved Summergreen** (TeBS) site.
GPP and NPP data are taken from GFDB (*Luyssaert et al.* (2007)) that refers to *Law et al.* (2004). N fixation estimates are taken from *Cleveland et al.* (1999) for temperate forests, which do not distinguish between leaf habits.

Metolius Forest Site (fig. 2.4: orange dot) was established as conservation area within the Deschutes National Forest in 1990. It has ten management areas included that allows me to get data from a mature forest (44.43°N, 121.67°W, stand age more the 250 years), as well as from a young forest (44.42°N, 121.57°W), which was planted in 1985. Metolius is a pine forest located in central Oregon, US, so QUINCY runs it as **Temperate semi-arid Needle-leaved Evergreen** (TeNE) site with two different harvest dates (*Friends of the Metolius (web presence)* (2019)).
GPP and NPP data are taken from GFDB (*Luyssaert et al.* (2007)) that refers to *Law et al.* (2001) and *Law et al.* (2004).

Thompson Forest Site (55.53°N, 98.20°W; fig. 2.4: blue dot) is located next to Thompson, Manitoba, Canada. The climate is boreal/sub-arctic, where the temperature ranges from -23°C to 16.2°C. Mean temperature is -2.9°C. Annual precipitation is around 500mm, whereas around 200mm fall as snow. Dominant spices are spruce, pine, and fir (*Government of Canada (web presence)* (2019)).
GPP and NPP data are taken from GFDB (*Luyssaert et al.* (2007)) that refers to *Bond-Lamberty et al.* (2004). N fixation estimates are taken from *Cleveland et al.* (1999) for boreal forests. QUINCY uses **Boreal semi-arid Needle-leaved Evergreen** (BNE) as PFT to describe THO.

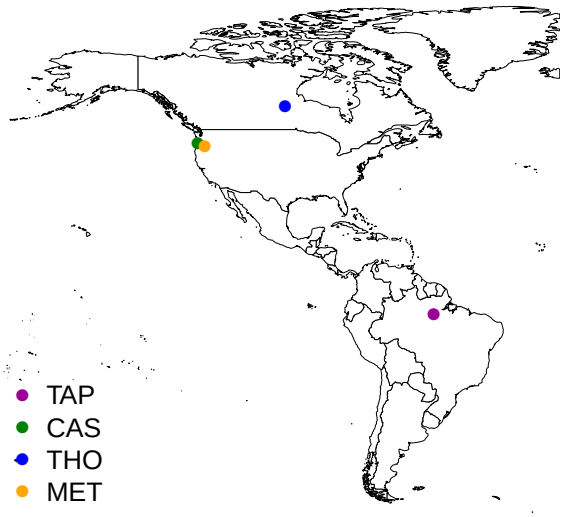

Figure 2.4.: Location of specific sites that are analyzed in section 2.3.

2.3. Results I: Nitrogen fixation scheme evaluation

As I aim to understand, where and why the two C cost based N fixation schemes differ, and how this may influence plant growth under elevated CO_2 and/or N limitation, I compare simulations by QUINCY with resistance and optimal scheme to simulations by QUINCY with standard scheme, and to observations, if available (sec. 2.2.3).

I start my evaluation with QUINCY (revision 1878) simulations with the same model protocol and input data as described in section 2.2.2 and a spin-up period of 300 years, and compare model output among all sites of the GFDB (sec. 2.2.3.1), before I examine the influence of climate and temperature, which drive fixation costs and fixation efficiency (eq. 2.8 - 2.10), leaf habit, which affects plant N demand and C costs for root uptake, and stand age and ecosystem history, which determine ecosystem N availability, to modelled N fixation for specific sites.
If not indicated otherwise all model results are averaged over 30 years from 1986 to 2015 in order to eliminate inter-annual climate variations.

2.3.1. Global assessment of nitrogen fixation schemes

In general I find lowest annual fixation rates in boreal forests, and highest in tropical forests (tab. 2.2, and fig. 2.5), which I expected due to fixation being an enzymatic process that is most efficient in a warm environment (sec. 2.1). The only exclusion within this pattern is N fixation at temperate forests simulated by resistance scheme that is extremely high. Observed fixation, which is estimated for each biome by *Cleveland et al.* (1999), is generally higher than modelled fixation, whereas the resistance scheme captures observed fixation rates best, as it simulates highest fixation rates. Optimal scheme simulates lowest fixation rates (tab. 2.2, and fig. 2.5).

Table 2.2.: Annual N fixation rates among climate zones. Observations from *Cleveland et al.* (1999), simulations from QUINCY with standard, resistance, and optimal fixation schemes, presented as mean $\pm$ 1SD for the years 1986 - 2015. Values are given in gN $m^{-2}year^{-1}$.

ecosystem	Cleveland	standard	resistance	optimal
boreal forest	0.46 $\pm$ 0.41	0.36 $\pm$ 0.09	0.46 $\pm$ 0.36	0.30 $\pm$ 0.32
temperate forest	1.77 $\pm$ 5.00	0.44 $\pm$ 0.22	1.59 $\pm$ 1.82	0.47 $\pm$ 0.44
tropical forest	1.85 $\pm$ 2.09	1.07 $\pm$ 0.18	1.04 $\pm$ 0.43	0.48 $\pm$ 0.17

Standard deviation is highest in temperate forests ($\sim$50% in QUINCY with standard scheme, $\sim$100% in QUINCY with optimal scheme, and >100% in QUINCY with resistance scheme and observations), which is caused by leaf habit, i.e. evergreen or deciduous, that is more diverse in temperate forests. Especially by resistance scheme simulations, deciduous forest sites have much higher annual fixation rates than evergreen forests (+265% on average compared to evergreen trees), but optimal (+5%) and standard scheme (+12%) also show this behavior.

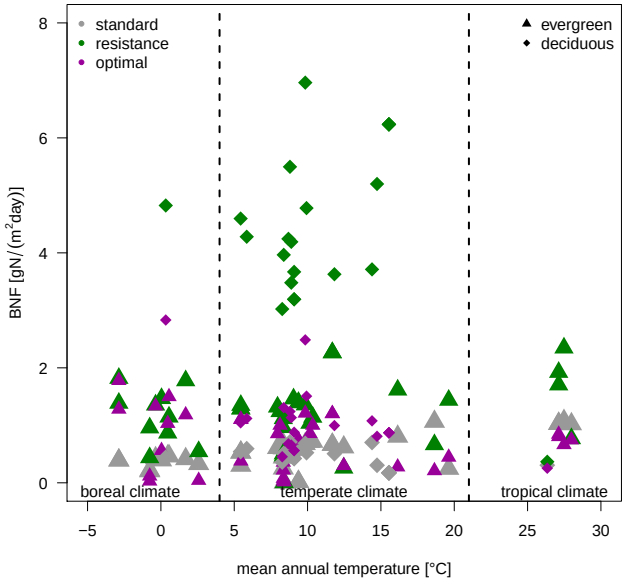

Figure 2.5.: Annual N fixation rates against mean annual temperature. Grey: standard scheme, green: resistance scheme, purple: optimal scheme. Triangles: evergreen forest sites, diamonds: deciduous forest sites. Dashed lines present climate zone ranges accordingly to QUINCY PFT classification.

Since deciduous forest sites are more present in temperate regions (20 from 42), than in boreal (1 from 10) and tropical regions (1 from 4), I find stronger influence of leaf habit to mean N fixation there. In general, the resistance scheme simulates higher annual fixation rates for most sites (44 from 56, +204% on average) compared to standard scheme, and for all sites compared to optimal scheme (+198% on average).
This pattern can is consistent not only for all deciduous forest sites (maximal annual fixation: 6.69 gN $m^{-2}year^{-1}$) at Cascade Head Experimental Forest, US), but also for most evergreens (maximal annual fixation: 2.58 gN $m^{-2}year^{-1}$) at Tumbara, Australia).
To assess the influences of both, climate zone/temperature and leaf habit, i.e. deciduous and evergreen, in more detail, and separate the effects on fixation rates, I will analyze on sites the represent different climate zones in section 2.3.2.1, and a specific site, where both leaf habits can be found, in section 2.3.2.2. But first, I will further focus on general differences between the standard scheme and both adaptive schemes.

Averaged annual N fixation rate over all sites for the optimal scheme does not differ from standard scheme (-1.5$\pm$78%), but standard deviation is high due to the fact that annual fixation rates are either enhanced, or diminished, but not equal (fig. 2.6).
I find a remarkable number of sites lying on or even below the 1:0.1 line that represents the maximal asymbiotic fixation that is possible in QUINCY with adaptive fixation schemes, i.e. 10% of standard scheme fixation (sec. 2.2.1). This emphasizes sites that

do not simulate symbiotic N fixation during my period to analyze. Most of these sites are harvested during the simulation period from 1960 on. Low or non-existing fixation rates indicate either no or a very low plant N demand, which is questionable especially for young forests that have a notable growth rate, or a sufficient (or too high) amount of available N in soil, which may be caused by harvest simulation by QUINCY. I will analyze this further in section 2.3.2.3.

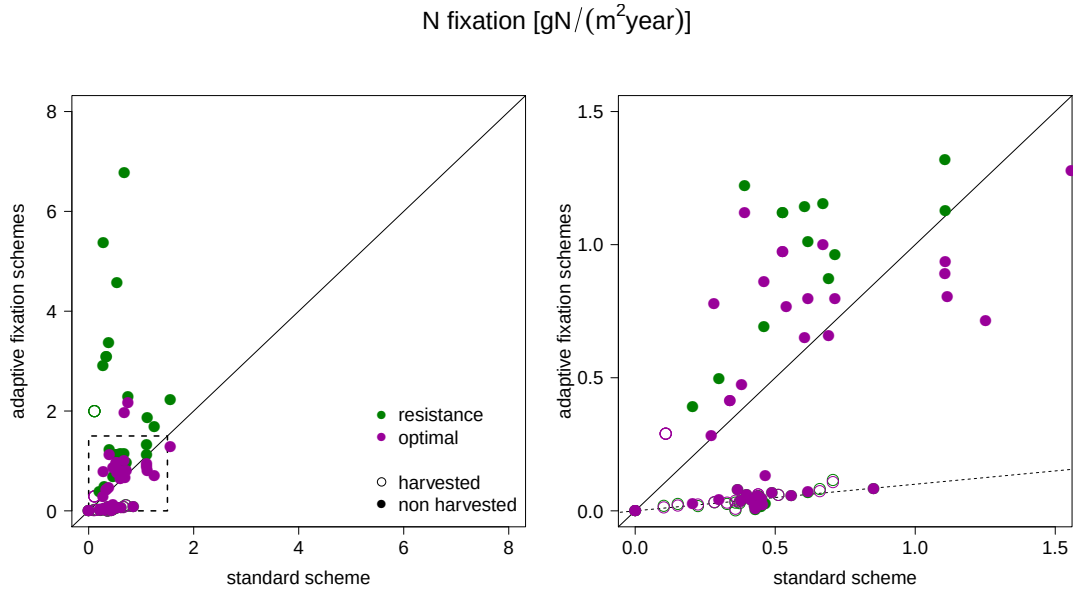

Figure 2.6.: Annual N fixation simulated by resistance (green) and optimal scheme (purple) against annual N fixation simulated by standard scheme. Solid line presents the 1:1 line.
Left: Full range of annual N fixation. Dashed box indicates cut out, which is shown on the right site. Right: Cut out, indicated on the left. Dashed line marks 1:0.1 line as measure for maximal asymbiotic fixation. Open circles present sites that are harvested during simulation period from 1960, filled circles present mature forests.

2.3.2. Site evaluation of nitrogen fixation schemes

I found differences in modelled annual N fixation among all fixation schemes caused by temperature/climate, leaf habit, and ecosystem N dynamics that are influenced by ecosystem history. I choose sites that have a temperature gradient/different climate, different leaf habits, or different stand ages to explore model performance in more detail.

2.3.2.1. Nitrogen fixation across climate zones

To evaluate how climate, especially temperature and its seasonal cycle, influences N fixation rates, I analyze the behavior of forests across climate zones on a sub-annual scale for all three fixation schemes within QUINCY for representative sites for different climate zones. I choose three evergreen and mature sites, namely the Tapajos National

Forest (hereafter TAP) as example for a tropical forest, the Cascade Head Experimental Forest (hereafter CAS) as example for a temperate forest, and the Thompson Forest Site (hereafter THO) as example for a boreal forest[2].

Table 2.3.: Annual N flux rates among climate zones. Observations from *Cleveland et al.* (1999), simulations from QUINCY with standard, resistance, and optimal fixation schemes, presented as mean ± 1SD for the years 1986 - 2015. Values are given in gN $m^{-2}year^{-1}$.

site		observation	standard	resistance	optimal
TAP	root uptake	NA	17.42 ± 1.82	16.81 ± 1.84	14.72 ± 1.33
	symbiotic fixation	1.07 ± 0.53	NA	1.74 ± 2.01	0.64 ± 0.22
	asymb. fixation	0.78 ± 1.56	1.03 ± 0.22	0.18 ± 0.20	0.16 ± 0.09
CAS	root uptake	NA	6.91 ± 0.64	9.27 ± 0.95	6.96 ± 0.72
	symbiotic fixation	1.60 ± 4.66	NA	1.30 ± 0.30	1.14 ± 0.31
	asymb. fixation	0.17 ± 0.34	0.68 ± 0.02	0.06 ± 0.01	0.07 ± 0.02
THO	root uptake	NA	4.52 ± 0.55	6.30 ± 0.30	4.92 ± 0.46
	symbiotic fixation	0.34 ± 0.31	NA	1.38 ± 0.46	1.24 ± 0.42
	asymb. fixation	0.12 ± 0.10	0.39 ± 0.02	0.01 ± 0.01	0.04 ± 0.02

Total simulated fixation, as sum of symbiotic and asymbiotic fixation, is generally lowest by standard scheme and highest by resistance scheme. Compared to observations, which are given for climate zones and not for the specific sites (*Cleveland et al.* (1999)), standard scheme tends to underestimate total fixation, whereas both adaptive schemes tend to overestimate fixation.

Since the standard scheme does not simulate a symbiotic fixation flux, asymbiotic fixation is the only simulated fixation flux by this scheme. Consequently, it is much higher than asymbiotic fixation fluxes by any other scheme, and also compared to data. Contrary to that, adaptive fixation schemes generally tend to underestimate asymbiotic fixation compared to observations. Differences between both adaptive schemes with regard to asymbiotic fixation are minor, because both simulate asymbiotic fixation based on standard fixation simulation and are limited to 10% of maximum standard fixation flux.
In general, asymbiotic N fixation decreases from TAP to THO for all simulations and generally for observations, whereby observed standard deviation is extremely high for temperate sites due to the mixing of evergreen and deciduous forests (tab. 2.3). This decrease is expected due to the underlying temperature function that takes energy limitation on nitrogenase activity due to colder temperatures into account (eq. 2.1).
In contrast to this clear trend, symbiotic fixation simulated by optimal and resistance scheme does not show such a clear relation to climate, but may be rather governed by site specifics. Compared to data, both schemes tend to overestimate symbiotic fixation.

[2] An assessment of the representative abilities of each site to their related climate zone, i.e. how they generally behave compared to all sites among their represented climate zone, can be found in appendix B.2.

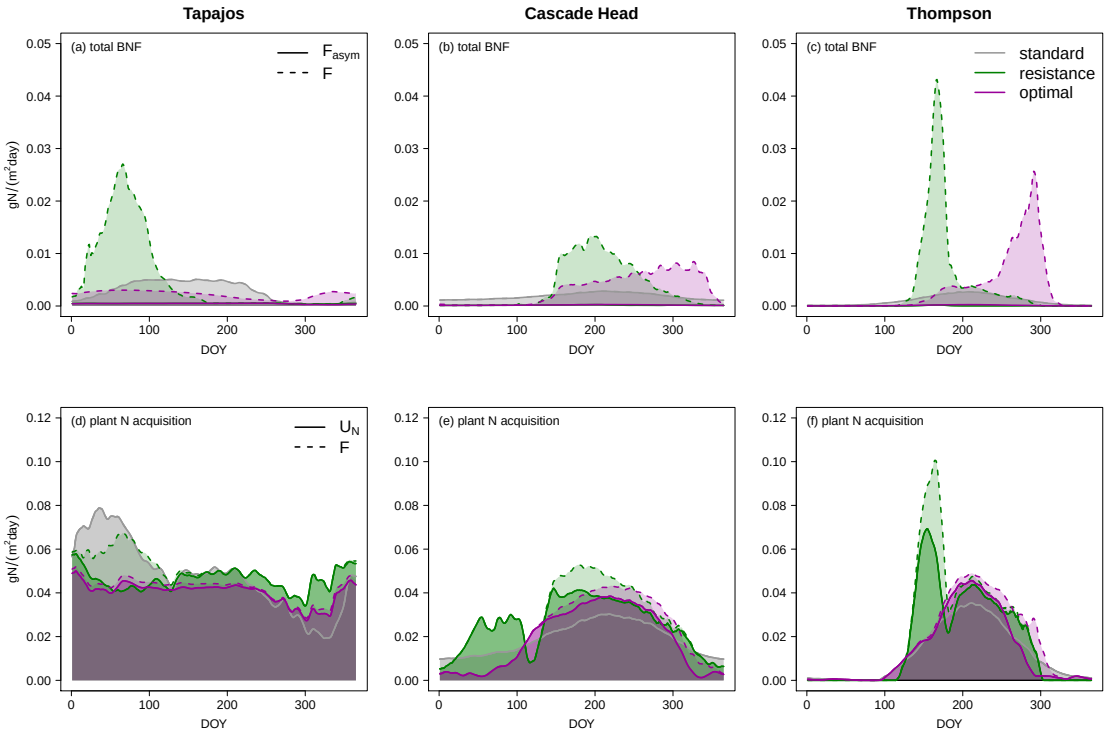

Figure 2.7.: N Fixation (a, b, c) and plant N acquisition (d, e, f) for the tropical forest site Tapajos (a, d), the temperate forest site Cascade Head (b, e), and the boreal forest site Thompson (c, f).
N fixation is divided into asymbiotic BNF (F^{asym}, solid line), and additional symbiotic BNF (F, dashed line) for adaptive schemes, N acquisition is divided into plant root uptake (U_N, solid line), and additional symbiotic BNF (F, dashed line) for adaptive schemes. Grey: standard scheme, green: resistance scheme, purple: optimal scheme.

TAP as tropical sites does not have a distinct temperature-related seasonal cycle, and a (simulated) medium temperature of 27.1°C, which is close to the optimal temperature for nitrogenase activity (T_0, tab. 2.1), but also for decomposition processes, which recycle N within the soil (*Thum et al.* (2019)).
For standard scheme simulations, this means that soil N is comparably high, which is shown by high root uptake rates, in combination with comparably low (asymbiotic) fixation rates, i.e. compared to asymbiotic fixation simulated by optimal and resistance scheme. Asymbiotic fixation by both adaptive schemes is around 15% of actual standard fixation, but limited to 10% of the maximum possible fixation by standard scheme. This means that QUINCY with standard fixation scheme does not simulate the maximal possible fixation flux, because soil N does not fall below the threshold that controls (asymbiotic) fixation (N^F_{limit}, tab. A.1, *Zaehle et al.* (2010)) as often as simulated by adaptive schemes. This may indicate that growth is limited by other constrains in standard fixation simulation such as P limitation, which is usual for tropical sites (*Vitousek* (1984), *Vitousek et al.* (2010), *Fleischer et al.* (2019)), or that soil decomposition processes already provide enough N for optimal growth.

For adaptive fixation schemes, tropical climate leads to rather low and stable fixation costs (9.86±0.25 gC/gN) that lead to high symbiotic fixation rates, whereby seasonal pattern differ among adaptive schemes (fig. 2.7a). As expected from minor temperature variations, symbiotic fixation by optimal scheme does support plant N acquisition throughout the entire year (1.7±0.7 mgN day^{-1}m^{-2}), whereas resistance scheme does show a seasonal behavior that is not (only) related to climate, but driven by plant N demand. This leads to symbiotic fixation rates up to 26.6 mgN day^{-1}m^{-2} within the first half of the year, and to almost no fixation within the second half of the year. That this behavior is caused by plant N demand, is confirmed by the comparison with plant N acquisition by standard scheme, which is highest at the same period. N acquisition simulated by standard scheme is only plant root uptake, which is controlled by soil N availability and by plant N demand. As soil N availability may not be the limiting factor at TAP, as shown previously for asymbiotic fixation, plant N demand controls plant N acquisition in standard scheme simulation for TAP, and thus allows conclusions for periods of high/low plant N demand within the year. Besides this direct effect of plant N demand on resistance scheme fixation calculation (eq. 2.11), high symbiotic N fixation rates increase general N input to the ecosystem, which increases N availability in soil. High soil N availability lower opportunity costs for root uptake (eq. 2.4), so that resistance scheme fixation costs fall below root uptake costs only parts of the year and allow symbiotic fixation by this scheme.

CAS and THO have a clear temperature-related seasonal cycle and lower mean temperatures than TAP, which affects not only fixation costs directly by influencing nitrogenase activity (eq. 2.8), but also plant growing season, which has several effects on symbiotic N fixation. Plant growing season drives C availability for fixation, and plant N demand, which are both related to plant C assimilation, and influences fixation costs indirectly by affecting C gain (eq. 2.6).
In combination, this leads to higher and more variable fixation costs compared to TAP (CAS: 16.71±1.88 gC/gN, THO: 18.3±2.5 gC/gN), and to much clearer seasonal patterns for symbiotic fixation and total plant N acquisition (fig. 2.7). In general, plant N acquisition is driven by root uptake, but plant N demand leads to notable symbiotic fixation rates during the growing season, especially at THO, where growth is strongly limited by N in QUINCY with standard scheme (tab. 2.4).
Interestingly, both adaptive fixation scheme show opposite fixation pattern throughout the year, but patterns are consistent across both sites, which indicates an entirely different behavior of both fixation scheme. Resistance scheme fixation happens mainly during the first two thirds of the growing season, which is driven by high N demand that forces plants to invest into fixation without any limits to fulfill plant N requirements (eq. 2.11). This leads to daily fixation rates up to 18.3 mgN day^{-1}m^{-2} (DOY 195) at CAS, and 44.8 mgN day^{-1}m^{-2} (DOY 165) at THO. Those high fixation rates lead to high N availability in soil later in the year, because of (i) high N input into the ecosystem by symbiotic N fixation, and (ii) less use of N sources in soil. This lowers root uptake costs

and consequently shifts plant N acquisition strategy from fixation towards root uptake, which explains the increase in root uptake on annual basis compared to QUINCY with standard scheme (+34% at CAS, + 39% at THO, tab. 2.3). In contrast to that, symbiotic fixation simulated by optimal scheme increases during the entire growing season and has its maximum in the end or even after the growing season (maximum rate at CAS 9.7 mgN day^{-1}m^{-2} (DOY 333), maximum rate at THO 27.6 mgN day^{-1}m^{-2} (DOY 298)), when root uptake is low because of limited soil N and low soil organic material (SOM) mineralization activity due to coldness. However, as N fixation is also temperature dependent and rather ineffective in winter, this seasonal pattern is unexpected. One would rather expect highest N fixation rates in spring, as resistance scheme does, due to high N demand, high C availability, and open canopy. This delay is caused by the combination of fixation rate limitation by a maximum rate ($v_{max_{BNF}}$), and the averaging period for both, plant N demand and C allocation from plant labile pool, which hinders an immediate C investment into fixation in case of limitation.
On annual basis, both adaptive model schemes simulate less symbiotic fixation at CAS than observed in temperate forests (resistance: -19%, optimal: -29%), which is caused by the influence of deciduous forests that shifts observations towards higher values and results in a high standard deviation that both fixation schemes meet. In contrast to that, both adaptive schemes simulate more fixation at THO than observed in the boreal zone (resistance: +305%, optimal: +265%) indicating a strong N limitation on growth at THO. However, total N acquisition is only enhanced by about 20% for both adaptive schemes compared to QUINCY with standard scheme at THO, which points again to N limitation in QUINCY with standard scheme that plants try to avoid by active investment into fixation, but emphasizes also that fixation rates are very small, so that even a small absolute increase in fixation leads to high relative changes.

A reduction of N limitation on growth by symbiotic fixation at THO is indicated by an increase of NPP of 50% by both adaptive schemes compared to standard scheme (tab. 2.4). Concurrently, the C investment into symbiotic fixation to lower or avoid N limitation on growth leads to a decrease in CUE of 14% in QUINCY with resistance scheme compared to QUINCY with standard scheme, and of 4% in QUINCY with optimal scheme, which is caused by major enhancements of GPP rates (resistance: +74%, optimal: +56%). This confirms hypothesis H2.1, i.e. that the use of symbiotic fixation schemes lowers CUE, but rather due to strongly enhanced GPP than caused by lower NPP, at THO, where plant growth is clearly N limited in QUINCY with standard scheme. However, standard scheme simulations are closer to observations, which indicates that real-world plants are actually not able to overcome N limitation on growth at this site as easy as QUINCY with both adaptive fixation schemes predicts.
I find similar, but less significant results for CAS, because CAS is less N limited than THO. Consequently, NPP is only increased by 20%. As GPP is increased stronger, CUE is again decreased compared to standard scheme simulations (resistance: -16%, optimal: -4%), which is also in line with H2.1. Notably, NPP enhancement is similar for QUINCY

with both adaptive schemes at both sites, but CUE decrease varies almost 10% caused by a stronger GPP increase with resistance scheme, which indicates other limitations on growth, such as P, water, or light.
Growth limitation by other factors than N availability, such as P limitation that usually occurs at tropical forest sites (*LeBauer and Treseder* (2008), *Vitousek et al.* (2010)), is obvious at TAP, too, where simulations by QUINCY with adaptive fixation schemes do not differ much from QUINCY simulations with standard scheme on annual basis. C investment into fixation does not lead to a much higher N availability, as I found previously, and consequently does not enhance growth rates or change annual C allocation significantly (tab. 2.4).

Table 2.4.: Annual C allocation among climate zones. Observations from GFDB (sec. 2.2.3.1), simulations from QUINCY with standard, resistance, and optimal fixation schemes, presented as mean ± 1SD for the years 1986 - 2015. GPP and NPP are given in kgC $m^{-2}year^{-1}$, fixation respiration (R_F) is given in gC $m^{-2}year^{-1}$, and CUE is given in gC/gC.

site		GFDB	standard	resistance	optimal
TAP	GPP	3.00 ± 0.29	3.64 ± 0.26	3.66 ± 0.22	3.49 ± 0.22
	NPP	0.87 ± 0.35	1.00 ± 0.10	1.01 ± 0.26	1.04 ± 0.11
	R_F	NA	NA	15.10 ± 1.60	5.40 ± 0.80
	CUE	0.29	0.27	0.28	0.30
CAS	GPP	2.04 ± 0.77	1.39 ± 0.15	1.98 ± 0.14	1.77 ± 0.13
	NPP	0.70 ± 0.26	0.71 ± 0.05	0.86 ± 0.06	0.86 ± 0.07
	R_F	NA	NA	12.92 ± 3.12	16.76 ± 1.96
	CUE	0.34	0.51	0.43	0.49
THO	GPP	0.67 ± 0.09	0.62 ± 0.05	1.08 ± 0.10	0.97 ± 0.10
	NPP	0.23 ± 0.12	0.36 ± 0.04	0.54 ± 0.05	0.54 ± 0.06
	R_F	NA	NA	16.10 ± 3.50	19.90 ± 2.23
	CUE	0.34	0.58	0.50	0.56

2.3.2.2. Nitrogen fixation differences among leaf habits

I found a large spread among annual fixation rates within temperate forest that is caused by leaf habit, i.e. evergreen or deciduous (sec. 2.3.1, fig. 2.5). Leaf habit does not only influence the plant phenological cycle, but also plant N demand, since deciduous trees have a much higher N demand than evergreens. This is mainly caused by the necessity to build new leaves every year and loosing N with senescence, even if N is partly re-translocated from leaves into plants' storage before, as well as by different leaf CN ratios. Mean leaf CN ratio is approximately 25 gC/gN for deciduous trees, and around 42 gC/gN for evergreen trees (*Kattge et al.* (2011)). Besides, deciduous trees have much higher C assimilation rates than evergreen trees, as soon and as long as they have leaves, which affects gain C (eq. 2.6) that determines opportunity costs for root N uptake (eq. 2.4). Freshly assimilated C demands N for growth, as well as provides C

for investment into symbiotic fixation. Thus a strong influence of leaf habit on symbiotic fixation appears reasonable.
Since both adaptive fixation schemes use similar C cost calculations for fixation and root uptake (eq. 2.4 and eq. 2.9), but treat plant N demand differently in following fixation rate calculations (eq. 2.10 and eq. 2.11), I analyze the influence of leaf habit on symbiotic N fixation at the same forest site, the Cascade Head Experimental Forest, in this section to decouple climate and environmental effects from specific plant N demand and resulting N acquisition strategies. QUINCY simulations and GFDB observations for the evergreen stand are referred to as CAS-E, whereas CAS-D refers to simulations and observations of the deciduous stand hereafter.

Annual N acquisition rates, i.e. the sum of root uptake and symbiotic fixation, if existing, for deciduous trees are much higher than N acquisition rates for evergreen trees among all fixation schemes (standard: +63%, resistance: +96%, optimal: +111%, tab. 2.5), which is caused by the expected higher N demand of deciduous trees. Both adaptive schemes acquire almost twice as much N as standard scheme at CAS-D, which indicates a growth limitation by N at CAS-D in QUINCY with standard scheme. However the strategy to overcome N limitation on growth is different among both schemes.

Table 2.5.: Annual N flux rates among leaf habits at CAS. Observations from *Cleveland et al.* (1999), simulations from QUINCY with standard, resistance, and optimal fixation schemes, presented as mean $\pm$ 1SD for the years 1986 - 2015. Values are given in gN $m^{-2}year^{-1}$.

leaf habit		observation	standard	resistance	optimal
deciduous	root uptake	NA	11.26 $\pm$ 1.56	13.80 $\pm$ 1.63	20.59 $\pm$ 2.38
	symbiotic fixation	1.60 $\pm$ 4.66	NA	6.69 $\pm$ 1.08	2.30 $\pm$ 0.72
evergreen	root uptake	NA	6.91 $\pm$ 0.64	9.27 $\pm$ 0.95	6.96 $\pm$ 0.72
	symbiotic fixation	1.60 $\pm$ 4.66	NA	1.30 $\pm$ 0.30	1.14 $\pm$ 0.31

Optimal scheme mainly increases root uptake, which indicates either almost sufficient soil N availability to meet plant N requirements via root uptake due to previous N influx into the ecosystem, or the limitation of symbiotic fixation by the maximum fixation capacity ($v_{max_{BNF}}$, eq. 2.10, tab. 2.1, *Rastetter et al.* (2001)). Since root uptake costs are always higher than fixation costs at CAS-D (fig. 2.9, right), it is actually the maximum fixation capacity that determines actual symbiotic fixation rates, and forces plants to still use root uptake as main N acquisition strategy throughout the entire year, whereas symbiotic fixation is only a supportive strategy. On annual basis, symbiotic fixation covers 11% of annual plant N acquisition at CAS-D with optimal scheme.
Symbiotic fixation simulated by resistance scheme are almost three times as much as symbiotic fixation simulated by optimal scheme at CAS-D, and cover almost a third of annual plant N acquisition. This is caused by the intensive use of symbiotic fixation to meet N demand as soon as fixation costs fall below the threshold (eq. 2.11) and without any limitations. This demand based N fixation calculation results in extremely high fixation rates from more than 25 mgN $day^{-1}m^{-2}$ from April to September (maximum

value: 55.4 mgN $day^{-1}m^{-2}$, DOY 145), and almost no fixation from January to April, which indicates no N demand at all, because root uptake is also zero (fig. 2.8). Full satisfaction of any N requirements over months is caused by the very high fixation rates in spring and summer that overfill plant labile N pool. This is unreasonable, since most 'real world' trees in natural ecosystems respond to N fertilization, which implies that their growth is limited by N (*Wright et al.* (2018)). Besides, daily fixation rates that cover more than a third of observed annual fixation are certainly too high, which points out that the resistance scheme misses a limitation factor in case of severe N demand, or a different cost-calculation average-period, which could be either longer (e.g. the entire year) to down-regulate fixation rates accordingly to annual plant N requirements, or shorter (e.g. half-hourly) to stop fixation as soon as plant N demand is met. An average-time between both in combination with no fixation limitation leads to too high fixation rates over a too long period. However, longer or shorter averaging periods lead to other problems, i.e. plants are prevent from adjusting to current environmental conditions by too long averaging periods, which are actually the reason for including symbiotic fixation into a TBM, or lead to very spiky rates in case plants are able to fix as much as they want as soon as they want.

Nevertheless, also N seasonal behavior by N fixation with optimal scheme is questionable, because plants use N fixation as main strategy for N acquisition in winter, when fixation is rather ineffective due to coldness. Cold temperatures lowers soil dynamics and consequently N availability, which causes low root uptake rates, too, but an entire shift towards N fixation is unreasonable and indicates that plants are not able to meet their N demand by N acquisition throughout the year especially at CAS-D with optimal scheme. As result, they need to fix in winter, even if fixation is expensive and ineffective, to refill their internal storage.[3]

Generally, differences in fixation rates among fixation schemes as well as among leaf habits are not only caused by different ways to calculate resulting fixation rates by given root uptake and fixation costs, but also by different root uptake costs itself that result from variations in opportunity costs (eq. 2.10b). Opportunity costs differ because of seasonal variations in C gain per leaf (g_C, eq. 2.6), which is most pronounced in spring at CAS-D, when trees gain a lot more C by every new leaf, and by differences in N gain per root that is mainly driven by available N in soil, which is higher in simulations with resistance scheme due to (prior) higher N input into ecosystem by symbiotic fixation (sec. 2.3.2.3).

[3] I observed the same unexpected seasonal pattern at Thompson Forest (sec. 2.3.2.1), which indicates a general problem of delayed response to plant N demand by optimal scheme that results from (i) my chosen memory period that was not considered by *Rastetter et al.* (2001), and (ii) the annual fixation limitation by $v_{max_{BNF}}$ that is not adjusted to QUINCY.

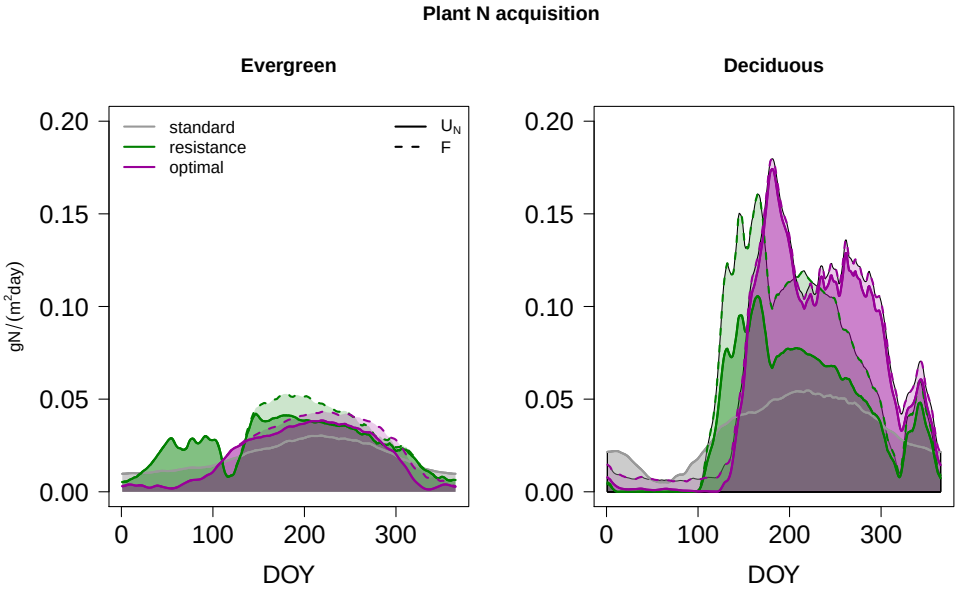

Figure 2.8.: Plant N acquisition for the evergreen, and the deciduous forest site at Cascade Head as sum from root uptake (U_N, solid line), and additional symbiotic fixation (F, dashed line). Grey: standard scheme, green: resistance scheme, purple: optimal scheme.

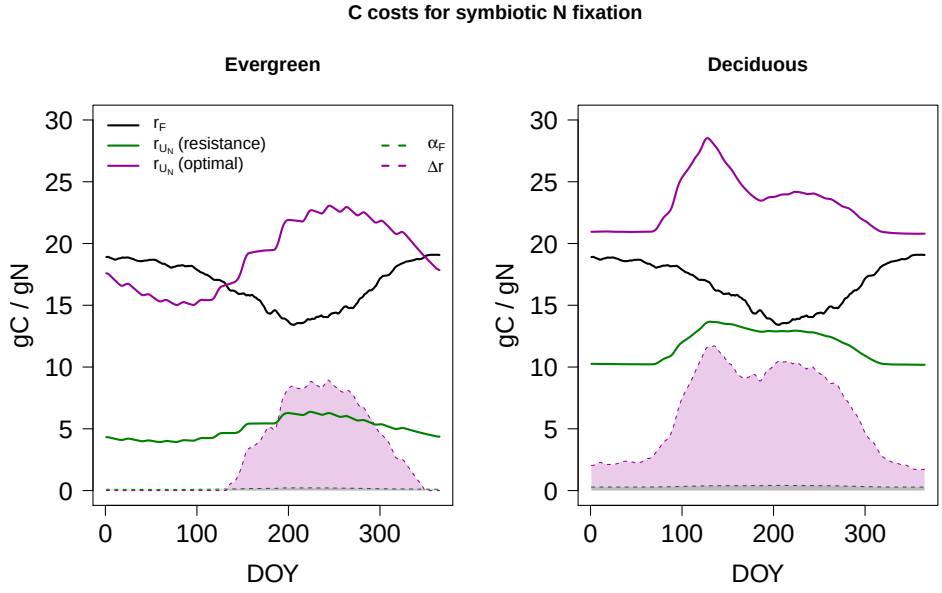

Figure 2.9.: C costs (solid lines) for N fixation (black) and root N uptake calculated by both adaptive schemes (green: resistance scheme, purple: optimal scheme) for the evergreen, and the deciduous forest site at Cascade Head. Dashed lines and shaded areas refer to cost related BNF scaling factor, which is Δr in case of optimal scheme (purple, eq. 2.10), and α_F in case of resistance scheme (green, eq. 2.11).

Table 2.6.: Annual C allocation among leaf habits at CAS. Observations from GFDB (sec. 2.2.3.1), simulations from QUINCY with standard, resistance, and optimal fixation schemes, presented as mean ± 1SD for the years 1986 - 2015. GPP and NPP are given in kgC $m^{-2}year^{-1}$, fixation respiration (R_F) is given in gC $m^{-2}year^{-1}$, and CUE is given in gC/gC.

leaf habit		observation	standard	resistance	optimal
deciduous	GPP	1.83 ± 0.76	1.13 ± 0.12	2.16 ± 0.24	2.25 ± 0.24
	NPP	0.84 ± 0.25	0.60 ± 0.07	0.98 ± 0.13	1.01 ± 0.13
	R_F	NA	NA	72.23 ± 11.66	35.43 ± 11.09
	CUE	0.46	0.53	0.45	0.45
evergreen	GPP	2.04 ± 0.77	1.39 ± 0.15	1.98 ± 0.14	1.77 ± 0.13
	NPP	0.70 ± 0.26	0.71 ± 0.05	0.86 ± 0.06	0.86 ± 0.07
	R_F	NA	NA	12.92 ± 3.12	16.76 ± 1.96
	CUE	0.34	0.51	0.43	0.49

Since root uptake costs calculated by optimal scheme exceeds fixation costs at CAS-D throughout the entire year (Δr = 6.42±4.06 gC/gN, fig. 2.9), symbiotic fixation happens at any time, whereas they fall below fixation costs at CAS-E from December to May, which stops fixation during that period. However, since fixation rates are limited by $v_{max_{BNF}}$ daily rates do not differ much between CAS-D and CAS-E, and annual differences are mostly caused by different fixation periods. Differences in root uptake costs, which are always lower than fixation costs, among leaf habits calculated by resistance scheme do not influence resulting fixation rates that much, because root uptake costs are only used as scaling factor for fixation, and surpassed by plant N demand.

Resulting high fixation rates in combination with moderate (but not cheap) fixation costs (16.71±1.88 gC/gN) lead to a notable investment of up to 3.3% of annual GPP into symbiotic fixation at CAS-D (resistance scheme, optimal scheme: 1.6%, tab 2.6), which is significantly higher than C investment into fixation at CAS-E (resistance scheme: 0.7% of annual GPP, optimal scheme: 0.9%). This lowers CUE for both adaptive schemes among both leaf habits compared to QUINCY simulations with standard scheme, but still results in higher annual NPP rates, caused by strongly increase GPP rates, which is again in line with hypothesis H2.1 (sec. 2.1.3).
The enhancement of both, NPP and GPP, indicates N limitation on growth, which is more pronounced at CAS-D, where adaptive schemes lead to an NPP increase of more than 60%. Even if simulated NPP rates, as well as GPP rates, by QUINCY with adaptive schemes therefore exceed observed rates, they meet within 1SD, whereas QUINCY with standard fixation scheme underestimates NPP and GPP significantly.

2.3.2.3. Nitrogen fixation evolution during forest succession

Since I hypothesized that plant controlled N fixation has a higher effect on forest growth in evolving ecosystems and/or under changing conditions (H2.2), but is less necessary in steady-state ecosystems, and because of my findings that most forests that were harvested during the simulation period behave differently from mature forests (fig. 2.6), I analyze the three N fixation schemes for QUINCY simulations at Metolious Forest site (sec. 2.3.2). I focus on primary forest succession first by analyzing simulations during the spin-up period, and afterwards on secondary forest succession, i.e. after harvest. The main difference between both successions is the stage of soil and soil processes that evolve during spin-up, which is why I assume this to be similar to a primary succession, and that already have evolved in a secondary succession after harvest.

N fixation evolution during spin-up period

Annual N fixation rates increase strongly during the first years of simulation, but resulting rates and actual fixation-onset years differ among fixation schemes (fig. 2.10). Symbiotic fixation rates simulated by QUINCY with resistance scheme are existent from simulation start on, because they are linked to plant N demand directly, but strong enhancement starts from simulation year 10 on. This is caused by inorganic N availability in soil, which is high at the beginning of QUINCY simulations and rises until simulation year 8, but then drops quickly, which causes N limitation on plant growth soon. This is not the typical evolution that I expected for primary succession, but a model artefact to start the simulation. Without a certain N availability in soil, the entire system would not survive the first years, since a lot N is lost then due to leaching without existing vegetation and evolved soil. N soil falls below the threshold of 0.7 gN m^2 in simulation year 18, which causes the onset of asymbiotic N fixation by QUINCY with standard scheme and by QUINCY with optimal scheme. Since asymbiotic fixation in QUINCY with standard scheme is limited to around 0.5 gN $m^{-2}year^{-1}$, annual fixation rates increase only until simulation year 21, when this value is reached. This causes limited growth, i.e. a minor increase in vegetation C, from simulation year 21 on in QUINCY with standard scheme, compared to QUINCY with both adaptive schemes. That is the time, when symbiotic fixation simulated by optimal scheme starts to increase, because plants start active investment into N fixation to overcome growth limitation.

Annual fixation rates peak in simulation year 28 in QUINCY with resistance scheme (4.9 gN $m^{-2}year^{-1}$), and in simulation year 35 in QUINCY with optimal scheme (3.0 gN $m^{-2}year^{-1}$), which indicates the time, when forest growth rates decline, because it turns into a mature forest with a closed canopy (LAI $\approx$4). This finding is in line with observations that report extremely high fixation rates at the beginning of forest succession, either caused by pioneer species that are able to fix and that are driven out as soon as there is enough N in the evolving system, but also by comparably high root nodulation, which indicates N demand that plants try to overcome by hosting N fixers, and moderate to low fixation rates after canopy closure, which is caused by either light-limitation for fixing bacteria, and a sufficient amount of N in the ecosystem (*Gorham et al.* (1979), *Sprent* (1987), *Batterman et al.* (2013)).

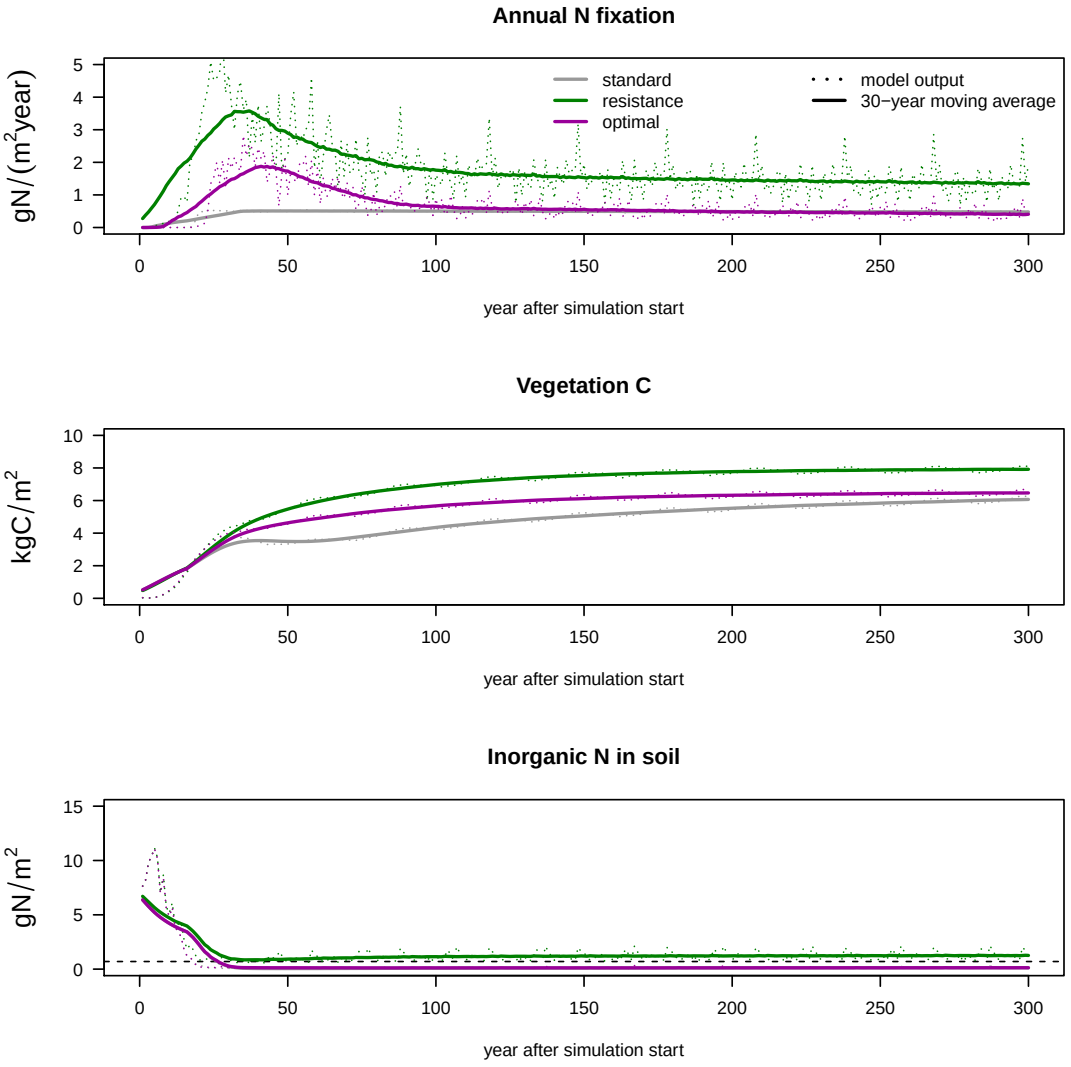

Figure 2.10.: N fixation during ecosystem evolution. Annual N fixation (a), vegetation biomass (b), and inorganic N in soil (c, with shown threshold for fixation as black dashed line) during QUINCY spin-up period. Grey: standard scheme, green: resistance scheme, purple: optimal scheme. Dotted lines show actual model output, solid lines a 30-year moving average.

Actually, QUINCY does not represent species or a vegetation community shift during succession, but (forest) ecosystems, where I assume that mainly understory hosts fixing bacteria. This understory may change over time, even this is not modelled explicitly, but represented by less strong fixation in later succession.

After canopy closure, fixation rates for both adaptive schemes decline, which is in line with my hypothesis that plant controlled N fixation is important in an evolving ecosystem, but less necessary in equilibrium. Fixation rates simulated by optimal scheme are almost equal to fixation rates in QUINCY with standard scheme from simulation year 103 on, but fall further slowly, because the ecosystem simulated by QUINCY with optimal scheme is already equibrilated, whereas the ecosystem simulated by QUINCY with standard scheme still evolves, what is shown by further growing vegetation, since growth is slower due to N limitation. Fixation rates that are simulated by QUINCY with resistance scheme saturate, too, but remain more than twice as much as fixation rates by both other schemes, which is caused by the direct coupling of fixation rates to plant N demand. Plants invest into fixation, before they try to satisfy their demand by root uptake, which leads to 10 times higher N availability in soil after the spin-up period.

N fixation evolution after harvest

Metolious Forest was partly harvested and replanted in 1985, which allows to compare the influence of harvest, as abrupt unsettling of the ecosystem, to N fixation, and N fixation during secondary succession, which is naturally more often observed than primary succession. I compare simulations for the remaining old forest (MET-old hereafter), and the harvested[4] and reestablished young forest (MET-young hereafter) to evaluate the behavior of N fixation schemes in a sudden unbalanced ecosystem.

Annual N fixation rates are almost constant previous to harvest in 1985. Inter-annual variations of fixation rates simulated by adaptive schemes are caused by climate variability that influences plant growth rates and consequently N demand that is satisfied by symbiotic fixation. Annual fixation rates simulated by QUINCY with standard scheme is constant, because it is not linked to plant N demand, but to soil N content, and limited by a maximal annual N fixation rate. Annual fixation rates simulated by QUINCY with resistance scheme are twice as high as fixation rates simulated by QUINCY with optimal or standard scheme (fig. 2.11).
Harvest reduces N fixation to zero due to either an increase in soil N, which is caused by decomposition of harvested litter, that exceeds the threshold in case of asymbiotic fixation (tab. A.1) or missing plants in case of symbiotic fixation. As soon as plants start growing again, resistance scheme simulates fixation, which is similar to first succession behavior of this scheme and causes an higher increase in soil N availability compared to MET-young simulations with both other fixation schemes. Due to the high soil N content, asymbiotic N fixation stays off during the first 10 years after harvest at MET-young, but reaches comparable rates to MET-old after 15 years in QUINCY with standard and op-

[4] Harvest, from the modelling site, means that vegetation biomass is added to the respective litter pools, except of woody biomass, which is mainly removed from the system (sec. 2.2.2).

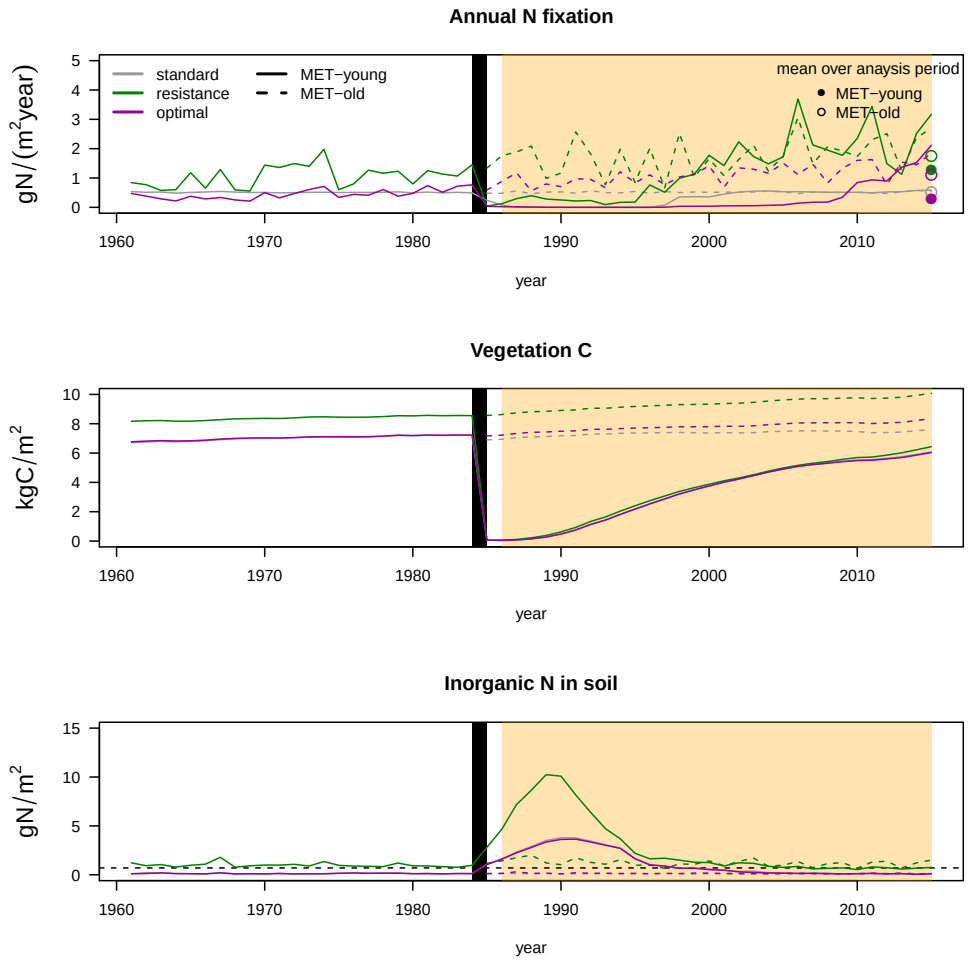

Figure 2.11.: Influence of harvest to N fixation rates. Annual N fixation (a), vegetation biomass (b), and inorganic N in soil (c, with shown threshold for fixation as black dashed line) from 1961 to 2015, which includes harvest in 1985 (black bar) for MET-young (solid line). Dashed line presents MET-old for comparison. Grey: standard scheme, green: resistance scheme, purple: optimal scheme. Orange shading represents analysis period for section 2.4, and circles represent averaged N fixation over analysis period.

timal scheme. However, symbiotic fixation simulated by QUINCY with optimal scheme is almost zero during the first 20 years after harvest at MET-young, but then quickly increased to higher rates than fixation rates at MET-old, which indicates increasing N limitation on plant growth due to then again low soil N availability in combination with a young, fast growing forest.

Generally the behavior of all three fixation schemes after harvest is similar to their behavior during first succession, and therefore in line with observations by *Gorham et al.* (1979), *Sprent* (1987), and *Batterman et al.* (2013) for adaptive fixation schemes, as reported for primary succession already, but periods are shorter and fixation rates are lower. This is caused by a less intensive increase of soil N by litter decomposition after harvest in an evolved ecosystem compared to the evolving ecosystem during spin-up. Latter is a model artefact, because soil N is strongly enhanced at the beginning of the spin-up period intentionally to allow plants to grow knowing that the ecosystem will loose much of this starting N and equibrilates itself after a while.
Although all fixation schemes show an expected behavior, and adaptive fixation schemes agree with observational behavior in general, they need too long to react, because of the very high soil N availability. The high soil N content prevent standard and optimal scheme from simulating any fixation during the first years, and only resistance scheme simulates fixation, caused by existing plant N demand as soon as plants grow. Low or nonexistent fixation during the first years of succession is contradictory to observations, which report an almost immediate increase of fixation activity after harvest either by pioneer species, and by increased nodulation growth, since harvest usually leads to a strong N loss in ecosystem by leaching, which is likely not enough represented by QUINCY, and delays fixation responses to harvest by 10 to 20 years. This is not an issue during spin-up, because general model performance agrees with observations, and spin-up length should always be chosen, so that the analyzed ecosystem has reached its steady-state, which is usually the case only after 300 to 500 years, but it becomes problematic, if comparing real measurements after harvest with model simulations, and it propagates to too low fixation rates, when the analyzed period is too short after harvest, and too high fixation rates, when the analyzed period is around 30 to 50 years after harvest.
Therefore annual N fixation rates at MET-young, which are averaged over 30 years, starting in 1986, only one year after harvest, are lower than averaged fixation rates at MET-old for QUINCY with all fixation schemes, even if I would expect higher fixation rates in a new established forest. This causes issues for the 30-year averaged analysis that I used in section 2.3.1, and explains the variable behavior of young forests that I found in figure 2.6. It further leads to an indifferent assessment of H2.2, because symbiotic fixation is less important in steady-state ecosystems than in evolving or disturbed ecosystems (confirming H2.2), but its effect on secondary succession is delayed (partly rejecting H2.2).

2.4. Results II: Assessments of symbiotic nitrogen fixation influence on plant carbon-use efficiency

I assess now the importance of symbiotic N fixation on plant C-use efficiency (CUE) under ambient, and elevated atmospheric CO_2 concentrations (aCO_2 and eCO_2, respectively), because I hypothesized that active C investment into N fixation lowers plant CUE, but not to the cost of plant growth (H2.1), and that this effect is stronger under changing environmental conditions (H2.2), which will prevent plants from progressive N limitation (PNL, sec. 1.2.2.2) in response to rising atmospheric CO_2 concentrations (H2.3).
To address this, I run QUINCY (revision 1878, 300-year spin-up) with all N fixation schemes for 42[5] forest sites of the GFDB (sec. 2.2.3.1), either with transient climate as described by the standard model protocol and input data (sec. 2.2.2), and with CO_2 fertilization, where I add 200 ppm CO_2 to ambient atmospheric concentrations starting 1976. Model results averaged for 1986 to 2015 to avoid effects of climatic inter-annual variability.
Since the 42 analyzed forests are only monitored under ambient conditions, I compare only ambient runs to observtions, and focus on relative flux responses to CO_2 fertilization later that are calculated as following:

$$\delta Y = \frac{Y_{ele} - Y_{amb}}{Y_{amb}} \tag{2.12}$$

where δY is the relative response to eCO_2 of the regarded flux Y. Y_{ele} depicts flux Y under elevated CO_2 condition, whereas Y_{amb} depicts flux Y under ambient CO_2 condition.

2.4.1. Plant carbon-use efficiency under ambient conditions

Generally QUINCY tends to underestimate annual GPP rates for boreal and temperate forests and overestimates annual GPP rates for tropical forests among all fixation schemes. Only QUINCY with resistance scheme simulates more annual GPP on average for temperate forests sites (tab. 2.7). This fits well to my previous findings about annual GPP rates at THO, CAS, and TAP as representative sites for forests across climate zones (sec. 2.3.2.1, tab. 2.4).
Simulated NPP rates are higher for boreal sites and lower for temperate and tropical sites among all schemes compared to observations, which differs from my findings about CAS and TAP as representative sites for temperate and tropical forests. This is caused by the general lower modelled NPP at tropical sites (sec. 2.2.3.1), and the high variability within NPP of temperate forests due to leaf habit (sec. 2.3.2.2).
Resulting from GPP and NPP pattern modelled CUE is slightly higher at boreal and temperate sites, and lower at tropical sites than observed CUE, which fits again my previous findings in section 2.3.2.1.

[5] I exclude 19 of 61 sites that were harvested after 1960, since harvest strongly influence plant growth rates as well as N availability in soil, which causes issues for all fixation schemes (sec. 2.3.2.3).

If I compare only simulated C fluxes among fixation schemes, I find the hypothesized pattern of decreased CUE in case of adaptive N fixation schemes compared to standard fixation scheme that is rather caused by increased GPP, than by decreased NPP (H2.1, tab. 2.7 and fig.2.14 aCO_2-simulations). However, changes in GPP and CUE are not significant, which reasonable in a steady-state ecosystem, where also standard fixation is able to meet ecosystem N requirements by balancing ecosystem N losses.

Table 2.7.: Annual C allocation among all sites of GFDB. Observations from GFDB (sec. 2.2.3.1), simulations from QUINCY with standard, resistance, and optimal fixation schemes, presented as mean ± 1SD for the years 1986 - 2015. GPP and NPP are given in kgC $m^{-2}year^{-1}$, and CUE is given in gC/gC.

	ecosystem	observation	standard	resistance	optimal
GPP	boreal forest	0.86 ± 0.24	0.75 ± 0.15	0.91 ± 0.28	0.84 ± 0.27
	temperate forest	1.67 ± 0.87	1.51 ± 0.56	1.59 ± 0.54	1.52 ± 0.54
	tropical forest	3.25 ± 0.33	3.80 ± 0.33	3.79 ± 0.22	3.42 ± 0.19
NPP	boreal forest	0.40 ± 0.21	0.41 ± 0.08	0.48 ± 0.13	0.45 ± 0.13
	temperate forest	0.75 ± 0.45	0.66 ± 0.20	0.70 ± 0.21	0.69 ± 0.21
	tropical forest	1.26 ± 0.32	0.86 ± 0.20	0.85 ± 0.14	0.90 ± 0.19
CUE	boreal forest	0.46 ± 0.14	0.55 ± 0.02	0.53 ± 0.03	0.55 ± 0.03
	temperate forest	0.45 ± 0.10	0.46 ± 0.06	0.45 ± 0.04	0.46 ± 0.05
	tropical forest	0.39 ± 0.10	0.23 ± 0.07	0.23 ± 0.04	0.26 ± 0.05

Under ambient CO_2 conditions, none of the adaptive schemes is able to improve C flux simulations compared to standard fixation schemes, when comparing simulated GPP, NPP, and CUE to observations per site (fig. 2.12). Coefficients of determination (R^2) between observations and QUINCY with standard scheme are slightly higher than coefficients of determination between observations and QUINCY with both adaptive schemes. Actually QUINCY with optimal scheme shows weakest agreement, but differences are minor.

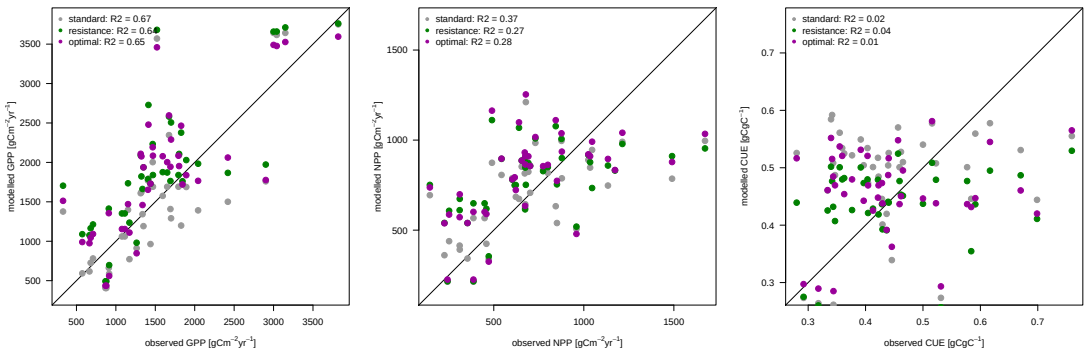

Figure 2.12.: Modelled versus observed GPP, NPP, and CUE among 42 mature forest sites from GFDB (sec. 2.2.3.1). Grey: QUINCY with standard fixation scheme, green: QUINCY with resistance fixation scheme, purple: QUINCY with optimal fixation scheme.

The general decrease in agreement between observations and simulations at each site from GPP to NPP, and consequently CUE as ratio of both is caused by measurement and model issues. GPP is mostly driven by current climate, which is a large scale driver compared to usual plot sizes. Thus, a point-specific GPP measurement is likely representative for the entire ecosystem. And modelled GPP is mainly depending on provided meteorological forcing, which is usually well reported on simulated scales. In contrast to that, respiration rates, are much more variable as they depend on site-specifics, such as plant community, soil microbial community and soil properties in general. These parameters may change within meters, which is clearly below the site size, and usually not well observed and constrained. This high spatial variability weakens the representativeness of measured fluxes for the entire site, in case NPP is estimated by measuring GPP and respiration rates. In case NPP is estimated by measuring the annual growth increment and collecting litter, measurements are even more uncertain. Again, the measured trees may not represent the stand, but the estimation is also based on empirical allometric functions, which may over- or underestimate actual NPP (*Luyssaert et al.* (2007), *Vicca et al.* (2012)). The spatial variability also complicates NPP simulations, as soil properties are not as well reported as climate and may change within small distances. Changing soil properties, such as N content, pH, pore sizes, affect N availability and consequently de- or increase plant C investment into N acquisition by root uptake (R_{U_N}). Simulated NPP is therefore rather a mean rate for the ecosystem and may not actually represent the actual measured trees. Consequently, model-data agreement is much lower for NPP than for GPP for all model variants. This low agreement is propagated, and by that amplified into CUE.

2.4.2. The influence of adaptive nitrogen fixation on plant responses to elevated CO_2

Relative flux responses to eCO2 differ among time scales. Initial responses are solely driven by CO_2 elevation that increases C uptake by plants directly, but long-term responses are influenced by plants' ability to continuously increase growth in response to eCO_2, which is likely hindered by progressive N limitation (PNL). Thus I analyze both, initial and long-term responses to eCO_2, whereby I define initial responses as responses within the first year of fertilization experiment, and long-term responses as responses after at least 10 years of experiment. Latter are therefore averaged over a time period from 1986 to 2015 to compensate other environmental or climate changes besides CO_2 elevation.

Initial GPP and NPP responses are high in all QUINCY simulations, because plants increase C uptake in accordance to higher C availability, which fertilizes plant growth (fig. 2.13a and b). However, QUINCY with standard scheme shows a wider spread among NPP responses already in the first year of fertilization, which is caused by a weaker response in N acquisition compared to QUINCY with adaptive N fixation schemes indicating N limitation. Adaptive schemes increase symbiotic fixation by more than 100%

initially, which enhances N acquisition response by around 10% compared to standard scheme (fig. 2.13c and d), and thus prevent plants from N limitation, which confirms H2.3 on short time scales.

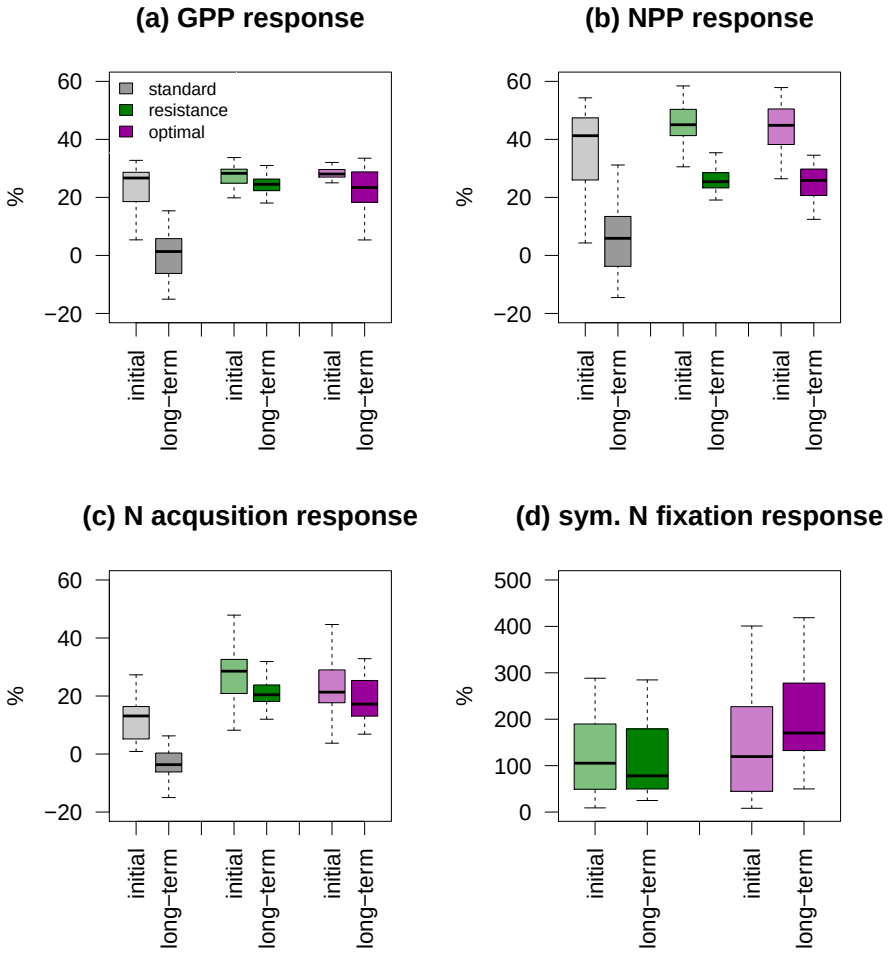

Figure 2.13.: Relative initial and long-term responses to eCO_2 of annual GPP (a), NPP (b), N acquisition (c), and symbiotic N fixation (d) among 42 mature forest sites from GFDB (sec. 2.2.3.1). Boxes represent the inner-quartile range, which is divided by the median. Whisker show 10% and 90%-quantile. Grey: QUINCY with standard fixation scheme, green: QUINCY with resistance fixation scheme, purple: QUINCY with optimal fixation scheme.

Long-term responses to eCO_2 show a different pattern, as most of them decrease compared to initial responses. Decline is strongest in QUINCY simulations with standard scheme, because of severe PNL, which is indicated by a rather negative N acquisition response to eCO_2. PNL reduces NPP, because even in case of enhanced C uptake, plants cannot grow biomass due to too little N. In the long-term, this also decreases GPP

response. Simply because of less biomass that leads to less leaves, which would assimilate C (fig. 2.13a - c). However, NPP responses, as well as N acquisition responses to eCO_2 are also decreased in the long-term in QUINCY with adaptive fixation schemes, even if GPP responses persist high. Since decline is stronger in NPP response, this is rather caused by intensive C investment into N fixation, than by PNL itself. Intensive C investment into fixation in response to eCO_2 is confirmed by still high symbiotic fixation rates in response to eCO_2 in the long-term. Even if symbiotic N fixation response is slightly reduced in QUINCY with resistance scheme, symbiotic fixation is still almost doubled in response to eCO_2, whereas symbiotic fixation response in QUINCY with optimal scheme is actually further increased to more than 150% enhancement on average (fig. 2.13d) indicating increasing PNL that plants try to overcome by N fixation. Differences in the direction of long-term response compared to initial response for symbiotic fixation are caused by (i) the faster reaction by resistance scheme to environmental changes (sec 2.3.2.3), and (ii) the higher ambient symbiotic fixation rates that are simulated by resistance scheme compared to optimal scheme and lower relative responses.

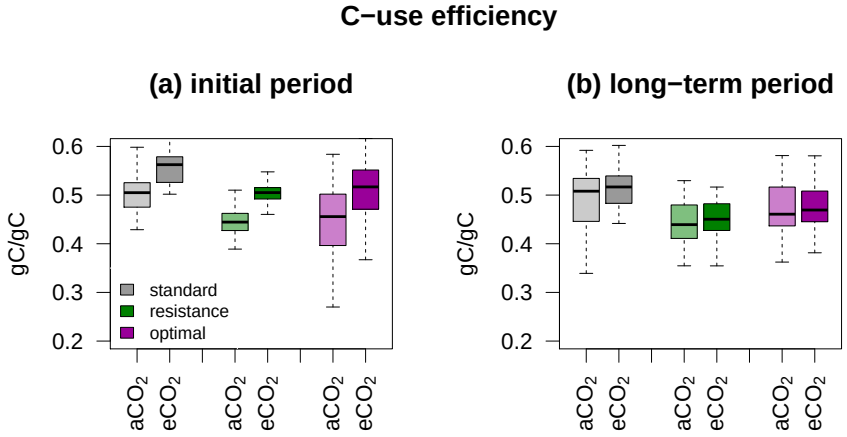

Figure 2.14.: C-use efficiency for ambient CO_2 (aCO_2), and elevated CO_2 (eCO_2) simulations among 42 mature forest sites from GFDB (sec. 2.2.3.1) for (a) initial CO_2 fertilization period, and (b) long-term period. Boxes represent the inner-quartile range, which is divided by the median. Whisker show 10% and 90%-quantile. Grey: QUINCY with standard fixation scheme, green: QUINCY with resistance fixation scheme, purple: QUINCY with optimal fixation scheme.

As I found in section 2.4.1, ambient CUE estimated from QUINCY simulations with standard fixation scheme is higher than CUE estimated from QUINCY simulations with both adaptive fixation schemes, caused by C investment into N fixation. This pattern does not change for eCO_2 simulations at any time-scale, but plants increase CUE initially in response to eCO_2, because of higher C uptake that is used for growth enhancement. However, long-term CUE is almost equal among CO_2 treatments, indicating that plants have an emergent equilibrium CUE for each N fixation scheme (fig. 2.14). This confirms H2.3 also in the long-term, because declining NPP and N acquisition responses to eCO_2 are linked to this optimal CUE that plants return to, after initial increase.

2.5. Summary and Discussion

I implemented two carbon (C) cost based biological nitrogen (N) fixation (BNF) models into the terrestrial biosphere model (TBM) QUINCY to either test the level of freedom that plants have to control BNF, and to assess the importance of active C investment into N fixation for plant, especially in the context of rising atmospheric carbon dioxide (CO_2) concentrations, which are expected to fertilize plant C uptake, but may be hindered by progressively increasing N limitation.

2.5.1. Discussion of hypotheses

H2.1: Active C investment into symbiotic N fixation decreases plant CUE, but not NPP through an increase in GPP.
Modelled vegetation by QUINCY with both adaptive fixation schemes invest C actively into symbiotic N fixation, which leads to a decrease of plant CUE of approximately 10% compared to averaged plant CUE simulated by QUINCY with standard scheme among all sites. Specific sites as the boreal forest site at Thompson even show a stronger decline in CUE, which is caused by strong N limitation on growth without symbiotic fixation. However, NPP rates were not affected, or actually slightly increased in case of using adaptive N fixation schemes, due to much higher GPP rates (+15% on average) either on average among 42 mature forest sites of the GFDB (sec. 2.2.3.1), and for specific sites. I.e. at Cascade Head and Thompson, where plants could enhance growth caused by the immediate N supply, if needed (sec. 2.3.2.1 and sec. 2.4.1). Thus, I can confirm H2.1 for both C cost based N fixation schemes.

H2.2: Adaptive N fixation schemes are important under changing environmental conditions, but rather unimportant in a steady-state ecosystem.
During the first 100 years of primary succession both adaptive fixation schemes increase N inflow into ecosystem by symbiotic fixation intensively, whereas this development is stronger in QUINCY with resistance scheme, because this scheme is not limited by a saturation function. After sufficient N accumulation in forest ecosystems, both adaptive schemes reduce symbiotic fixation, which is in line with observations by *Batterman et al.* (2013) for example (sec. 2.3.2.3). Total fixation that includes both, symbiotic and asymbiotic fixation modelled by resistance scheme persists higher than annual total fixation rates modelled by standard scheme. In contrast to that, total fixation by optimal scheme is lower than fixation by standard scheme at almost half of the sites in equilibrium, or resulting from harvest (sec. 2.3.1).
This temporal evolution and differences in long-term fixation are in line with previous evaluations of both model approaches. Both models, i.e. the optimal approach, which has been developed by *Rastetter et al.* (2001), and the resistance approach, which has been developed by *Fisher et al.* (2010), have been tested for early succession by *Rastetter et al.* (2001) and *Fisher et al.* (2016), respectively, and were shown to successfully reproduce high fixation rates within early succession, and lower rates after canopy-closure.

Especially low fixation rates by optimality-based fixation calculation, i.e. by a *Rastetter*-based scheme, have also been reported by *Meyerholt and Zaehle* (2015), who compared the performance of six different BNF models on global scale.
Harvest that introduces a secondary succession causes issues for all fixation schemes, because (i) enhanced litter increases N availability in soil strongly, which decreases N fixation rates, and (ii) low root biomass, which is linked to fixation rates by optimal scheme, since root biomass limits the amount of potential nodules, where plants host fixing bacteria. Consequently, the expected increase in symbiotic fixation rates that was found during primary succession is smoother and delayed. This smoother increase of fixation during secondary succession compared to primary succession is also reported by *Rastetter et al.* (2001). (i) actually indicates that litter from harvest may be too much in QUINCY, because neither increased N soil availability during primary succession/at the beginning of spin-up period, nor low root biomass, influenced N fixation there that much (sec 2.3.2.3).
From primary succession analysis, I can confirm the importance of adaptive fixation for non steady-state ecosystems, which declines when ecosystems become mature. However, from secondary succession analysis, I cannot clearly derive that adaptive fixation is more important under (abrupt) changing environmental conditions, but have to record unintentional issues among all fixation schemes. Issues are caused by simulated harvest, which adds much litter to soil that is decomposed and increases soil N greatly. Actually, adding harvested tissues to litter, is reasonable, as well as increased nutrient availability afterwards, but maybe the litter amount is too large or decomposition is too fast. Possibly, one has to account for leaves and light twigs that are further distributed, or thick above-ground litter layers that are decomposed over a longer period, instead of simply adding all harvested plant tissues to related litter pools that have a prescribed turnover time that drives simulated decomposition. Delayed decomposition may smooth the increase in soil N, but may also last over a longer period, and potentially lead to more reasonable results.

H2.3: Plant controlled symbiotic N fixation prevent plants from progressive N limitation under eCO_2 by continuously providing N that is needed for enhanced growth.
Symbiotic N fixation simulated by both C cost based fixation schemes supports plant N acquisition under elevated CO_2 (eCO_2) concentrations at any time scale, which prevents plants from progressive N limitation (PNL). Mild PNL occurs in QUINCY simulations with standard fixation schemes already at the beginning of the modelled fertilization experiment, which is reported by a lower N acquisition response that reduces NPP response in comparison to QUINCY simulations with adaptive fixation schemes, and becomes more intense in the long-term. This leads to zero or negative responses of N acquisition, NPP and GPP to eCO_2 in QUINCY with standard scheme, which is contrary to observed NPP and N acquisition responses to eCO_2 (*Finzi et al.* (2007), *Zaehle et al.* (2014)). In contrast to that, adaptive fixation schemes increase symbiotic fixation in response to eCO_2

by approximately 100% over the entire analyzed fertilization period. This enhancement is rather high, compared to previous studies. *Fisher et al.* (2010) reported an increase of fixation under eCO_2 by FUN, i.e. a resistance approach, that was not high enough to explain observed N acquisition enhancement at the evaluation site. The better performance of the resistance approach as part of QUINCY may be caused be the dynamic inclusion into the model framework operating on a very short time step, i.e. half-hourly, whereas FUN was originally only plugged in into an existing TBM and run more or less independently on a yearly time step. This may hamper an appropriate response of the scheme to eCO_2. Later versions of FUN (e.g. *Brzostek et al.* (2014), *Shi et al.* (2016)) did respond to eCO_2, but as they already included further N acquisition strategies, such as mycorrhizal fungi, a comparison with QUINCY with only symbiotic fixation is unreasonable. The optimal approach has already been shown to respond positively to eCO_2 (*Rastetter et al.* (2001)), but fixation enhancement was less than 30% in long-term simulations by *Meyerholt and Zaehle* (2015), which is much lower than observed here. This may be caused by site specifics, as *Meyerholt and Zaehle* (2015) applied the optimal approach globally, or by minor adjustments of the scheme to QUINCY. Possibly, also the short time-step of QUINCY plays a role. However, fixation enhancement leads to a positive response of N acquisition to eCO_2 initially and in the long-term, and enhances NPP continuously reproducing observed plant behavior. Nevertheless, NPP responses are decreasing slightly in the long-term compared to initial responses, also with adaptive schemes. This is less caused by occurring PNL, but more by an optimal plant C allocation that takes growth, as well as C investment into fixation into account. This optimal allocation may be rather constant, as CUE is only affected initially by eCO_2, but falls back to its prior-to-eCO_2 value thereafter (sec. 2.4.2). Therefore, I can confirm H2.3 from modelling site. However, from observational site, the effect of eCO_2 to symbiotic fixation is highly uncertain. This may be caused by difficulties to measure N fixation due to its low rates and the high abundance of atmospheric N_2, but actually both is reported: an increase of symbiotic fixation in response to eCO_2, mainly when observing individual species (*Zanetti and Hartwig* (1997), *Lam et al.* (2012), *Nasto et al.* (2019)), as well as no response at a forest ecosystem (*Hoosbeek et al.* (2010)). This impedes a clear assessment of symbiotic N fixation as strategy to overcome PNL in reality, but it clearly improves simulated plant growth responses to eCO_2.

2.5.2. Assessment of different carbon cost based nitrogen fixation schemes

I implemented two different C cost based N fixation schemes, to assess not only the importance of plant controlled N fixation, especially with respect to plant growth, which I quantified by using CUE, but also the degree of freedom that plants have to decide on N fixation.

Both schemes are shown to not increase model-data agreement for CUE (and also not for GPP and NPP) compared to the standard scheme, when comparing them site wise

to observations from the GFDB (sec. 2.4.1). This is caused by several reasons, which are not only based on simulation issues, but also arise from measurement uncertainty, which then propagates into CUE estimations.
Model-data agreement (based on R^2 values) is generally better for GPP, since both, modelled and measured data are more reliable and representative for the entire stand. This is, because GPP is mainly driven by current climate, which is (i) well observed and reported, which allows a good forcing for the model, and (ii) a large scale process, which increases the representative ability of measured and modelled fluxes itself. In contrast to that, NPP rates are much more uncertain, since actual growth depends additionally on soil properties, which determine nutrient availability for example. Soil properties are spatially very variable, which complicates the estimation of actual growth rates, i.e. NPP, and only weakly reported compared to weather data. Consequently, models lack reasonable constrains for NPP with regard to soil properties (*Vicca et al.* (2018)), and observed NPP may not be representative for the entire stand, because soil properties may change and affect NPP. Additionally, NPP estimates are based on direct measurements of main NPP components, such as annual litter production and litter fall, and stem and branch increments, which are then upscaled to total NPP. This includes potentially high observation errors, in case of missing litter and not measuring exactly the same tree-high to derive growth increments, as well as further assumptions on allometric dependencies, which also increase the uncertainty of observed NPP fluxes.
However, the slight decrease of model-data agreement by applying adaptive fixation schemes indicates that (i) models need better site information, especially for soil properties, which may affect growth largely, and (ii) there may be other processes and dependencies, besides nutrient availability that needs to be implemented into models to improve growth simulation.
Independently from those general issue when applying adaptive fixation schemes, I will now assess strengths and weaknesses for both schemes, and potential solutions.

Symbiotic N fixation by resistance scheme
Symbiotic N fixation calculated by resistance scheme (*Fisher et al.* (2010), *Brzostek et al.* (2014)) is directly linked to plant N demand, which allows plants to acquire N by fixation as soon as they need it, but it is also hardly set off, because plant N demand is almost never satisfied entirely as long as they assimilate C that could be used for growth. Consequently, this scheme gives a lot of freedom to plants to meet their requirements, but also forces plants to fix N almost always, which leads to unrealistic high fixation rates on short-term basis (e.g. daily), and annually. High short-term rates are responses to increasing plant N demand for example in the beginning of the growing season that lead to high annual rates, because of the force to fix N on top, even if there would be enough N in the ecosystem already. Thus plants fix N, instead of acquiring N by root uptake from soil N that is further increased (sec: 2.3.1 and sec. 2.3.2.2).
This performance is unrealistic, and caused by applying a fixation scheme that was developed for a model with an annual time step to a model with a much shorter time step.

Averaging plant N demand as well as all other used variables, such as temperature and soil N availability over the entire year, would potentially solve this problem, but it would inhibit plant short-term responses and adjustments to environmental changes, which are possible within the QUINCY framework. Thus, in its presented structure, the resistance scheme is not applicable by models with a sub-annual or even a sub-seasonal time step.

Symbiotic N fixation by optimal scheme
Symbiotic N fixation calculated by optimal scheme (*Rastetter et al.* (2001)) is limited by existing fine root biomass to account for a maximum amount of nodules that a plant can build to host fixing bacteria, and saturates at a maximum fixation rate. This limits symbiotic N fixation in case of sever N limitation and delays fixation in case of high N demand, but leads to a smooth annual cycle, where plants are able to almost meet N requirements most of the time, so that growth is not or only mildly limited by N. Plants especially fix N in the later growing season to support N acquisition by root uptake, and during winter to refill their pools, if temperatures are not too low, and fixation during warmer periods did not satisfy their demand entirely (sec. 2.3.2.1 and sec: 2.3.2.2).
This seasonal behavior is partly unexpected, as one would rather expect highest N fixation rates early in the growing season, when canopy is not closed so that fixers are not light limited, and plants assimilate a lot fresh C that demands N for growth and is available for investment into fixation. Again, this issue is caused by my chosen average period, which prevent plants from immediate investment into fixation in case they demand N. In combination with N fixation limitation by a time step maximum that is derived from an annual maximum, this leads to a delayed response of symbiotic fixation to plant N demand. Another possibility to solve this issue could be to increase the time step maximum, as I could assume that higher N fixation rates in spring and summer would be balanced out by lower rates in winter, so that the annual total would not exceed the previous maximum. From my perspective, this would be the better strategy.

2.5.3. Conclusion and Outlook

The implementation of adaptive N fixation schemes that allow plants to invest C into symbiotic N fixation fulfilled all hypotheses. Plants invest actively C, which lowers their CUE, but grow better due to satisfying their N requirements better and sooner. This enhances GPP and increases growth rates especially with respect to rising atmospheric CO_2 concentrations.
However, QUINCY with standard fixation that does not allow symbiotic fixation meets ambient observations better, which indicates that adaptive fixation is not necessarily needed for ambient model simulations or slow changing environmental conditions, since model parameters are well estimated to meet annual rates. But I likely have to take it into account, if CO_2 levels increase quicker or exceed a potential threshold, after which N deposition and asymbiotic N fixation cannot meet ecosystem N requirements anymore.

Harvest as an example for a rapid ecosystem change, causes issues for all fixation schemes due to strongly enhanced N availability in soil. As this was not the case when modelling primary succession, this may rather indicate that simulated litter input from harvest is too high in QUINCY, instead of support an assessment of fixation scheme responses to rapid ecosystem changes.
Long-term CO_2 fertilization simulations show a stronger growth with adaptive fixation schemes, which proves the importance of plant controlled N fixation for future climate predictions with respect to plant responses to eCO_2.
As I found issues for both adaptive fixation schemes that were caused by average period, which is too short for resistance scheme, and too long for optimal scheme, in combination with no fixation rate limitation in resistance scheme, or a too strong limitation in optimal scheme, one could test parameters and adjust them to QUINCY.
Resistance scheme may likely produce lower fixation rates, if (i) averaging period is longer, especially for plant N demand, and if (ii) symbiotic N fixation is limited to a maximum rate, which has to be estimated and tested for the model specific time step. Optimal scheme performance may be improved, by (i) shortening the averaging period, and by (ii) by adjusting maximum rate to model specific time step, which both may lead to higher fixation rates and faster responses of this scheme to environmental changes.

Prospective steps would therefore the adjustment of parameters in both fixation schemes specifically to QUINCY and potentially the revision of the amount of litter after harvest or at least an assessment of litter amount.
Thinking in the direction of plant controlled N acquisition, which could potentially prevent plants from progressive N limitation (PNL) under eCO_2, one has also to take internal N cycling into account, since the efficiency of plant root uptake strongly depends on soil dynamics. Soil N dynamics in QUINCY and most other TBMs are rather simple, as they are described by a first order decay from pool to pool until litter introduced N enters mineral N finally. This pathway is too slow to react on short-term to eCO_2, which limits simulated plant growth. However, instead of acquiring N ecosystem externally by fixation, plants could also try to accelerate decomposition or access SOM pools as nutrient source to short-cut ecosystem internal N cycling. Recently, mediation of mycorrhizal fungi between plants and soil is discussed, and their implementation into TBMs could prevent plants from PNL, if their interactions are controlled by plants, so that they also can be used as N acquisition strategy by plants.

3. Assessments of forest ecosystem carbon-nitrogen dynamics with integrated mycorrhizal processes under elevated CO_2

3.1. Introduction

Mycorrhizal fungi are ubiquitous and form symbioses with almost 95% of all terrestrial plant species (*Read* (1991)). Their importance for the carbon (C) and nutrient cycling within ecosystems is commonly assumed, as they support plant nutrient acquisition in exchange for carbohydrates (*Read* (1991), *Marschner and Dell* (1994)). However, they are hardly implemented in current terrestrial biosphere models (TBMs, *Johnson et al.* (2006)), likely leading to incorrect predictions of plant and ecosystem responses to elevated atmospheric CO_2 concentrations (eCO_2, *Brzostek et al.* (2017)) and to uncertain estimates of ecosystems' impact on climate change (*Shi et al.* (2019)). The occurring model-data mismatch is reported by *Zaehle et al.* (2014), who compared 11 TBMs at two free-air CO_2 enrichment (FACE) sites, and found that the observed nitrogen (N) limitation effect on CO_2-fertilized growth was much lower than modeled. This mismatch is mainly caused by the inability of models to simulate plant N acquisition response to eCO_2 appropriately. Most models predict no change in plant N acquisition, or even a negative response, whereas observations show that plants increase N acquisition in response to eCO_2. Instead of increasing N acquisition, which was not possible due to limited N availability in soil, models change plant N-use efficiency (NUE, eq. 1.3) by changing CN ratios in response to eCO_2, unlike to observations, which do not show a strong response of NUE to eCO_2 (*Finzi et al.* (2007)).
Consequently, even TBMs that succeeded in predicting NPP response to eCO_2 matched observations mainly due to wrong reasons. These findings point out, the need to revise N acquisition strategies that are used in TBMs, and consider the inclusion of mycorrhizal fungi and their ecosystem functioning into them. This may not only change modelled plant response to eCO_2 and vegetation C (C_{Veg}) storage, but else influence soil dynamics, which may change simulated soil organic C (C_{SOM}) content and response to eCO_2.

3.1.1. Mycorrhizae in terrestrial ecosystems

During evolution different forms of mycorrhizae developed (*Read* (1991)). It is assumed that the mutualistic relationship between host plants and mycorrhizal fungi is an adaptation to nutrient-poor conditions, where plants benefit from mycorrhizal supply of several nutrients, such as N, P, K, Ca, S, Cu, Fe, and Zn (*Ames et al.* (1983), *Read* (1991), *Marschner and Dell* (1994), *Ek et al.* (1997)). In return, plants export carbohydrates to hosted fungi, which covers most of fungal C demand, despite the fact that some mycorrhizal fungi are potentially able to gain C by accessing soil organic matter (SOM) (*Treseder et al.* (2007), *Malcolm et al.* (2008), *Nehls* (2008)). However, their saprotrophic abilities are largely discussed, since it is also argued that mycorrhizal fungi actually lack the genetic capacity to act as saprotrophs (*Frey* (2019)).
Mycorrhizal fungi are usually distinguished by their morphology and their preferred host plants. The two main types are ectomycorrhizae (EMs) and arbuscular mycorrhizae (AMs) (*Read* (1991)). AMs live in symbiosis with more than 80% of all plant families, in particular with crop and grass species, but also with most tropical trees (*Read* (1991)). They enter into plant cells and build arbuscules (or vesicles) to exchange sugar and nutrients. Most of the time AMs are considered to support especially P-nutrition, but they also provide N to the plants, which they take up from inorganic and organic sources in soil (*Hodge et al.* (2001), *Pérez-Tienda* (2012), *Hodge and Storer* (2015)). Furthermore, there is experimental evidence that AMs accelerate decomposition by exuding C to soil, which enhances mineralization of SOM (*Hodge et al.* (2001)). That speeds up ecosystem-internal N recycling, since mineral N can be taken up by plants and mycorrhizae again (*Paterson et al.* (2016)). In contrast to that, EMs build symbiotic associations with only 10% of plant species, but these species include most temperate and boreal tree species. They are mainly regarded as N providers, but can also export P to host plants (*Read* (1991)). EMs do not enter plant cells, but they cover the root tips of their host plants in a glove-like structure (hyphal mantle) that protect roots against other infections, works as a storage and exchange area for carbohydrates and nutrients, but also hinders plants from own nutrient uptake (*Jordy et al.* (1998), *Laczko et al.* (2004), *Pritsch et al.* (2004), *Finlay* (2008)). Outside the mantle, EMs build large networks that consist of fine hyphae to access mineral and organic nutrient sources (*Wu et al.* (2005)) or exude C to enhance decomposition of organic material (*Cheng et al.* (2012), *Lindahl and Tunlid* (2015)), and rhizomorphs, which are thicker hyphae, to transport carbohydrates and nutrients over long distances from distant nutrient sources to host plants (*Read and Perez-Moreno* (2003)).
Generally, estimates of the fraction of plant N acquisition via mycorrhizal fungi range from 5-20% in grasslands to up to 80% in forest ecosystems (*Van Der Heijden et al.* (2008)). Plants transfer 1-25% of freshly assimilated C to hosted mycorrhizae (*Jakobsen and Rosendahl* (1990), *Ek et al.* (1997), *Staddon et al.* (2003), *Hobbie* (2006)).
Besides its key role in plant N nutrition, plant-mycorrhiza interactions are important for C sequestration into soil either by allocating C into below-ground tissues such as root or mycorrhizal biomass, or by exuding C into soil, which influences ecosystem C (C_{Eco}) allocation, and consequently C_{Eco} storage (*Godbold et al.* (2006), *Frey* (2019)).

3.1.2. Previous approaches to include mycorrhizae into terrestrial biosphere models

Despite the knowledge about the significance of mycorrhizal fungi for plant N nutrition and soil dynamics, they are hardly represented in state-of-the-art TBMs. N acquisition in TBMs is usually represented only by root uptake, where plant roots directly access available N in soil that is given by mineral sources (*Phillips et al.* (2013), *Brzostek et al.* (2017)). This obviously lacks the representation of rhizosphere-SOM interactions by mycorrhizal fungi, which may improve plant N nutrition, especially in the context of eCO_2. However, during the last decade, some plant-mycorrhiza interaction models have been developed or included into existing TBMs in order to either explore C-nutrient exchange between host plant and fungi in more detail, or to improve the representation of nutrient acquisition in TBMs.

Approaches range from (i) the development of independent plant-mycorrhizal interaction models that explicitly simulate CN exchange between host plant and fungi and can be incorporated into other modelling frameworks (e.g. MYCOFON, *Meyer et al.* (2010)), over (ii) the revision and further development of fully coupled soil modules as part of ecosystem models or TBMs (e.g. ANAFORE, *Deckmyn et al.* (2011); MySCaN, *Orwin et al.* (2011)), to (iii) the inclusion of mycorrhizal influence on plant N acquisition into N acquisition modules that are already coupled to TBMs (e.g. FUN and FUN-CORPSE, *Brzostek et al.* (2014), *Sulman et al.* (2017)).

MYCOFON simulates the growth of mycorrhizal biomass and the exchange of C and N between fungi and plant roots based on current environmental conditions, such as temperature, C availability, derived from photosynthesis, and N availability in soil. It is developed exclusively for EMs and neglect AMs, since the aim was to model boreal and temperate forest sites. MYCOFON takes saprotrophic behavior, i.e. N uptake from SOM, of mycorrhizae into account, and has been coupled to the Modular Biosphere simuLation Environment (MoBiLE, *Grote et al.* (2008), *Grote et al.* (2009)) framework (*Meyer et al.* (2012)), as well as to the Coupled heat and mass transfer model for soil–plant–atmosphere systems Model (CoupModel, *Jansson* (2012)), to simulate ecosystem dynamics (*He et al.* (2018)). However, MYCOFON was only applied on ecosystem scale for specific sites, but neither the MoBiLE framework, nor the CoupModel run at global scale, which is necessary to potentially apply the model for global C simulations and predictions.

The Mycorrhizal Status, Carbon, and Nutrient cycling (MySCaN, *Orwin et al.* (2011)) model model and the ANAlysing FORest Ecosystems (ANAFORE, *Deckmyn et al.* (2008)) model are extensions of the CENTURY Soil Organic Matter model (*Parton* (1996)). MySCaN replaces the former 'active' biotic pool by specific pools for bacteria, (saprotrophic) fungi, mycorrhizal fungi, and below-ground grazers. This may run globally, but lacks a link between plant and soil fauna. ANAFORE directly focuses on the interaction of individual trees with their environment (*Deckmyn et al.* (2011)), but is similar to MYCOFON limited to ecosystem scale simulations.

The Fixation and Uptake of Nitrogen (FUN) model (*Fisher et al.* (2010)) was previously developed to explore C investment into N acquisition by several plant controlled mechanisms, i.e. root uptake, symbiotic N fixation, and N retranslocation before senescence,

and then coupled to the Community Land Model as TBM (CLM, *Lawrence et al.* (2011)). *Brzostek et al.* (2014) extended FUN by the inclusion of mycorrhizal N uptake, whereby mycorrhizae are distinguished between AMs and EMs based on the host plant, which is given by the plant functional type (PFT) in the coupled TBM. This approach improves the representation of N acquisition by plants on ecosystem scale, and allows to simulate mycorrhizal N support on global scale. To also account for mycorrhizal influence on C_{SOM} FUN was coupled to the Carbon, Organisms, Rhizosphere, and Protection in the Soil Environment (CORPSE) model (*Sulman et al.* (2014)), which simulates C_{SOM} dynamics. Recently FUN-CORPSE (or CORPSE-N, *Sulman et al.* (2017)) was run with CLM (*Sulman et al.* (2019)). This is, to my knowledge, the only model that is recently applied and still under development, considers mycorrhizal influence on vegetation and soil C and N dynamics, and runs on global scale. However, mycorrhizal fungi are still only considered as process, i.e. their functionality depend on their type, which is prescribed by the host plant, i.e. by the PFT given by the used TBM. This neglects mycorrhizal biomass, which is part of SOM and thus may change total soil C, and resulting mycorrhizal N demand, which may turn mycorrhizae into competitors in case of N limitation (*Franklin et al.* (2014)).

3.1.3. Study scope and hypotheses

Given this previous work, the modelling community still lacks an explicit dynamic plant-mycorrhiza interaction model as part of a globally running TBM that allows mycorrhizae to actively influence plant N nutrition and SOM dynamics (*Brzostek et al.* (2017), *Frey* (2019)). Additionally it remains unclear, how active mycorrhizal fungi decompose SOM, despite the question, whether I focus on AMs and EMs, because both are shown to either actively use SOM as N source by a direct enzymatic breakdown of material, or accelerate SOM decomposition passively by providing C for microbes. I will therefore neglect the question of mycorrhizal morphology, and follow the idea of *Phillips et al.* (2013), who developed the mycorrhizal-associated nutrient economy (MANE) framework, which actually distinguishes AMs and EMs, but links them to plant nutrient economic strategies, i.e. an organic and inorganic economic strategy. By concentrating on plant strategies, i.e. mycorrhizal functionalities, I develop an explicit plant-mycorrhiza interaction model as part of the QUINCY model (sec. 1.2.4.3) that allows me to test both observed mycorrhizal functionalities and their potential influence on ecosystem CN dynamics and allocation.

I hypothesize that the explicit formulation of mycorrhizal fungi in QUINCY as representative of TBMs accelerates internal N cycling within the ecosystem (H3.1). This prevents plants from PNL under eCO_2 conditions and explains observed growth responses (H3.2). Plant-mycorrhiza interactions support plant growth and increase C storage in vegetation under eCO_2, but mycorrhiza-soil dynamics enhance heterotrophic respiration and reduce modelled soil organic C stocks (H3.3) concurrently. This actually results in a reduction of simulated C storage within the entire ecosystem, in case mycorrhiza dynamics are explicitly modelled (H3.4).

I will explore H3.1 - H3.4 by testing two different mycorrhizal types: **saprotrophs** that actively mine SOM, and **decomposers** that passively prime SOM.

3.2. Material and Methods

3.2.1. MYC model description

Since there is evidence, that either ectomycorrhizal fungi, and arbuscular mycorrhizae can actively mine soil organic material (SOM) as nutrient source, or passively prime SOM, I will focus on these functionalities, following the suggestions of *Phillips et al.* (2013), and neglect morphological differences. I incorporate the mycorrhiza model, which includes plant-mycorrhiza dynamics, and mycorrhiza-soil interactions, into the QUINCY model (sec.: 1.2.4.3). QUINCY fluxes, as well as MYC model fluxes for both functionalities are presented in figure 3.1.

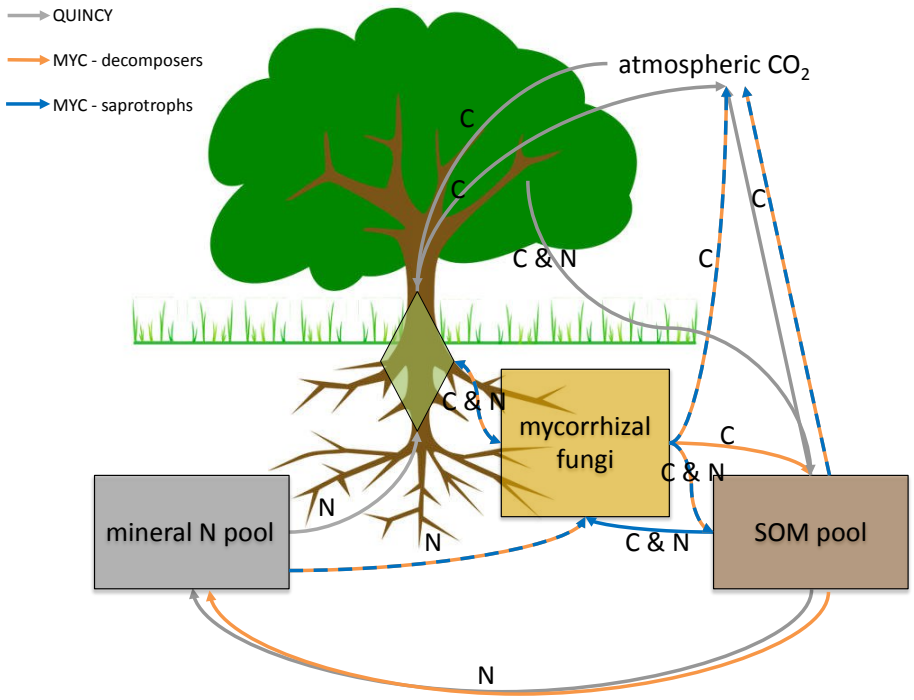

Figure 3.1.: Schematic figure of MYC model fluxes within QUINCY framework. Diamond represents plant labile pool, boxes represent soil pools. Grey arrows: QUINCY, orange arrows: MYC model with decomposing mycorrhizae, blue arrows: MYC model with saprotrophic mycorrhizae, dashed arrows belong to both functionalities. See figure 1.3 for flux terms.

First in this model description, I focus on the vegetation part of plant-mycorrhiza dynamics. This includes the carbon (C) flux from host plant to mycorrhizal fungi, as well as the influence of mycorrhizae to nitrogen (N) uptake by plant root system. Secondly, I focus on the mycorrhizal part that includes again fluxes between mycorrhizal fungi and host plant, but also mycorrhizal dynamics like respiration, and turnover, and mycorrhiza-soil interactions. Latter covers inorganic N uptake, as well as saprotrophic[1] and decomposing behavior.
All MYC model parameters and references can be found in table 3.1. However, due to the lack of below-ground measurement, all parameters have high uncertainties, and only about half are backed up with observational data. The rest are entirely hypothetical and fitted to the QUINCY model framework.

To simulate plant-mycorrhiza interactions, I start with the C and N budget of plant labile pool (eq. 1.6)[2], where I add exchange fluxes for both, C and N, and modify direct N uptake by roots, because I assume that the previous uptake includes mycorrhizal fungi implicitly. Consequently I have to reduce plants root uptake, if I model mycorrhizae explicitly, in order to maintain the total uptake flux.

$$\frac{dC^p_{labile}}{dt} = U^p_C + \Delta S^p_C - G^p_C + \Delta E_C - R^p_g - R^p_m - R^p_{U_N} \tag{3.1a}$$

$$\frac{dN^p_{labile}}{dt} = U^{p,*}_N + \Delta S^p_N - G^p_N + \Delta E_N \tag{3.1b}$$

where U^p_X are uptake rates, whereas * indicates the modification of plant root uptake by mycorrhizal fungi (eq. 3.2). ΔS^p_X are net exchange with the storage pools, G^p_X growth rates, and R^p respiration rates (eq. 1.6). ΔE_X are (net) exchange rates between host plant and mycorrhizal fungi (eq. 3.3). The subscript X denotes C, or N respectively.

Since plant N uptake via their own roots in minor in reality, I assume that the root uptake, calculated in QUINCY (eq. 1.7), to be rhizosphere uptake that plants benefit from. If I model mycorrhizal fungi as part of the rhizosphere explicitly, I have to modify plant fine root uptake accordingly to maintain the total N uptake. Therefore I adopt the idea of ectomycorrhizal morphology that cover fine root tips and disconnect roots from soil (*Read* (1991)). Consequently, I adjust the potential N uptake by a root coverage parameter that is sensitive to the current presence of mycorrhizae, as well as to their ability to take up N.

[1] Saprotrophic behavior by mycorrhizal fungi is largely discussed (*Frey* (2019)), but I decided to use this term anyway, because I need to consider C uptake, i.e. actual saprotrophic behavior, instead of the only active breakdown of SOM to acquire N for modelling reasons (eq. 3.8).

[2] In this model description the superscript ^{p} refers to plant pools and fluxes, whereas the superscript ^{m} refers to mycorrhizal pools and fluxes.

$$U_{N,j}^{p,pot,*} = v_{max,j}^{*} \times N_j \times (K_{m1,j} + \frac{1}{K_{m2,j} + N_j}) \times \zeta_N^p \times C_{fr}^{p,*} \quad , \textit{where} \tag{3.2a}$$

$$v_{max,j}^{*} = v_{max,j} \times f_{v_{max,j}} \tag{3.2b}$$

$$f_{v_{max,j}} = \frac{1}{1 - f_{cover,max} + f_{cover,max} \times f_{U_N^{eff}}^{m}} \tag{3.2c}$$

$$C_{fr}^{p,*} = C_{fr}^{p} \times f_{cover} \quad , \textit{where} \tag{3.2d}$$

$$f_{cover} = MIN(f_{cover,max}, \frac{C^m}{C_{fr}^{p}}) \tag{3.2e}$$

where j as index refers to either NH_4, or NO_3, and N_j denotes NH_4, or NO_3 concentration in soil. The modification of the maximum uptake rate per unit biomass ($v_{max,j}^{*}$) maintains the overall maximum uptake capacity of the rhizosphere by taking the relative presence of mycorrhizae ($f_{cover,max}$) and their higher uptake efficiency ($f_{U_N^{eff}}^{m}$) compared to plants into account, while the adjustment of root biomass considers the disconnection of root tips from soil by mycorrhizal fungi. This coverage is given by the current ratio of fine root biomass ($C_f^p r$) and mycorrhizal biomass (C^m), but constrained by a maximum coverage to account for a shift in mycorrhizal community to more exploitative species, if plants are under severe N limitation. I derive the actual N uptake by plants from potential uptake as described in section 1.2.4.3.

The main part of the plant-mycorrhiza model is the exchange of C and N between the host plant and attached mycorrhizal fungi, which is based on the explicit formulation of MYCOFON (*Meyer et al.* (2010)), but adapted to the QUINCY framework. For budget equations (eq. 3.1 and eq. 3.7), I simplified the exchange rates to net exchange rates, but they consist of an exudation flux from plants to mycorrhizae, and an export flux from mycorrhizae to plants.

$$\Delta E_C = -E_C^{p2m} + E_C^{m2p} \tag{3.3a}$$

$$\Delta E_N = -E_N^{p2m} + E_N^{m2p} \tag{3.3b}$$

where E_X^{p2m} are exudation fluxes from host plant to mycorrhiza (eq. 3.4), and E_X^{m2p} are export fluxes from mycorrhiza to host plant (eq. 3.12). Since there is no N exudation, E_N^{p2m} is zero and I neglect this possible flux from now on.

I constrain exudation, which is the C flux from plant to mycorrhiza, by

- a minimum and maximum amount of mycorrhizae compared to plant fine roots, to avoid mycorrhizal extinction, and to prevent that plants allocate C only into mycorrhizae in order to get N instead of building own roots (tab. 3.1)
- the amount of available C (eq. 3.5)
- plant N demand to force mycorrhizal growth in N limited conditions (eq. 3.6a)
- mycorrhizal support in order to decrease exudation, if plants do not benefit from them, which could happen either in case of satisfied demand by plants, or in case of severe N limitation, which turns mycorrhizal fungi into competitors that do not deliver any N to host plants (eq. 3.6b)

following the ideas of MYCOFON (*Meyer et al.* (2010)).

$$E_C^{p2m} = MIN(f_{m2r,min} \times C_{fr}^p - C^m, E_{C_{max}}^{p2m}) \tag{3.4}$$

where $f_{m2r,min}$ is a parameter for the minimal amount of mycorrhizae compared to plant fine roots, C_{fr}^p is plant fine root biomass C^m is mycorrhizal biomass, and $E_{C_{max}}^{p2m}$ is the maximum exudation.

I determine the maximum exudation rate by available C, and the optimal ratio between mycorrhizae and fine roots under current conditions.

$$E_{C_{max}}^{p2m} = MIN(f_{E_{C_{max}}^{p2m}} \times C_{labile}^p \times \tau_{labile}, f_{m2r,opt} \times C_{fr}^p - C^m) \tag{3.5}$$

where $f_{E_{C_{max}^{p2m}}}$ is the maximum share of available C that plants can allocate to mycorrhizal fungi, $C_{labile}^p \times \tau_{labile}$ describes the available C, and $f_{m2r,opt}$ is the optimal ratio between mycorrhizal biomass and plant fine root biomass.

I restrict the optimal ratio between mycorrhizal biomass and fine root biomass by a minimal and a maximal ratio, and scale it by plant N demand and mycorrhizal N support, which are averaged by eq. 1.5 over τ_{labile} as all other plant controlled fluxes in this sub-model. Plant N demand, as well as mycorrhizal N support are used to represent current environmental conditions, which drive plant-mycorrhiza interactions, because plant N demand in depending on plant C uptake by photosynthesis that links to stand related conditions, such as plant type, successional stage, growing season, and atmospheric conditions, and on N availability that links to soil properties and that is also depicted by mycorrhizal N support.

$$f_{m2r,opt} = f_{m2r,min} + (f_{m2r,max} - f_{m2r,min}) \times \zeta_N^p \times \eta_N, \; with \tag{3.6a}$$

$$\eta_N = \frac{E_N^{m2p}}{E_N^{m2p} + \epsilon} \tag{3.6b}$$

where $f_{m2r,min}$ and $f_{m2r,max}$ are parameters, describing the minimal and maximal ratio between mycorrhizal biomass and plant fine root biomass. ζ_N^p, and η_N are scaling factor between zero and one to describe plant N demand (eq. 1.7f), and N support by mycorrhizae that is derived from mycorrhizal N export (E_N^{m2p}), and an infinitesimal small number (ϵ) to stop C exudation, if plants do not benefit from mycorrhizae over a time period of a month.

To describe mycorrhizal dynamics, I set up similar budget equations for mycorrhizal C, and N balance as for plants (eq. 3.1), but I characterize mycorrhizae by only one pool. This simplifies growth and maintenance respiration to a total respiration rate, makes specific growth rates redundant, but necessitates the consideration of a turnover rate.

$$\frac{dC^m}{dt} = U_C^m - \Delta E_C - T_C^m - R_{m,g}^m - R_{U_N}^m - D_{SOM}^m \tag{3.7a}$$

$$\frac{dN^m}{dt} = U_N^m - \Delta E_N - T_N^m \tag{3.7b}$$

where U_X^m are uptake rates, ΔE_X are (net) exchange rates between host plant and mycorrhizal fungi, T_X^m are turnover rates, and R^m are respiration rates, whereas $R_{m,g}^m$ is a total respiration rate that combines maintenance and growth respiration, and $R_{U_N}^m$ is N uptake respiration. D_{SOM}^m is C that mycorrhizal fungi exude to soil in order to enhance the decomposition of organic material.

Mycorrhizal fungi are not able to assimilate C independently, but for saprotrophic behavior I assume that they take up organic forms of N, which leads to a potential uptake of C[3].

$$U_C^m = U_{N_{SOM}}^m \times \chi_{CN}^{SOM} \times CUE^m \tag{3.8}$$

where $U_{N_{SOM}}^m$ is the uptake of N from organic material, and χ_{CN}^{SOM} its CN ratio. CUE^m is the C-use efficiency of mycorrhizal fungi, and describes the share of C from SOM that mycorrhizae can incorporate. The rest is respired as heterotrophic respiration to maintain χ_{CN}^{SOM}.
Mycorrhizae take up N either from mineral sources (NH_4 and NO_3), and from organic material, if I consider saprotrophic fungi.

$$U_N^m = U_{N_j}^m + U_{N_{SOM}}^m \tag{3.9}$$

[3]This C uptake is contradictory to the fact the (most) mycorrhizal fungi lack the genetic capacity to act as saprotrophs (*Frey* (2019)), but saprotrophic behavior is necessary to hold C in the modelled ecosystem. Since QUINCY (as most TBMs) has a fixed CN ratio of SOM, it does not allow C accumulation, and N uptake from SOM would require large C losses by respiration to maintain SOM-CN ratio. To lower this C decrease I decided for saprotrophic behavior, i.e. the uptake of C from SOM, in case it is attached to N, to remain C in the ecosystem.

I calculate N uptake from mineral sources similar to plant N uptake (eq. 3.2), but I down-regulate N uptake rates, if potential C investment into N transformation costs (eq. 1.10) exceeds a certain threshold:

$$U_{N_j}^{m,pot} = v^*_{max,N_j} \times f^m_{U_N^{eff}} \times N_j \times (K_{m1,N_j} + \frac{1}{K_{m2,N_j} + N_j}) \times C^m \times f_{invest}, \; where \tag{3.10a}$$

$$f_{invest} = \frac{f_{resp,max} \times C^m}{R^{m,pot}_{U_{N_j}}}, \tag{3.10b}$$

where v^*_{max,N_j} is the modified maximum uptake rate per unit biomass (eq. 3.2), C^m is mycorrhizal biomass, $f^m_{U_N^{eff}}$ is a parameter that takes the higher uptake efficiency of mycorrhizal fungi compared to plants caused by their smaller diameter into account. The smaller diameter allows mycorrhizae to reach N_j, which cannot be found by coarser fine roots, and gives a higher surface-to-mass ratio, which makes uptake itself more efficient. f_{invest} is a scaling factor that down-regulates mycorrhizal uptake of N_j, if transformation costs are too high to maintain mycorrhizal biomass, whereas $f_{resp,max}$ is an empirical threshold for that.
Similar to plants uptake, I adjust the potential uptake for N from mineral sources accordingly to available NH_4 and NO_3, and to other loss rates, such as plant N uptake or leaching, to account for competition.

Saprotrophic mycorrhizae mine organic material in soil (SOM) as source for N. I assume that they access only older SOM (X_{slow}, sec. 1.2.4.3), because they have to compete with microbes, and I assume that microbes are more efficient in mining SOM, and more attracted by fresh SOM, which has a higher CN ratio, as they depend on SOM as C source. Since mycorrhizal fungi get C from their host plants, they are independent from SOM-C content, and can digest older, C depleted SOM with lower CN ratio.
I assume further that mycorrhizae are only potential saprotrophs, and that they decrease N uptake from SOM stepwise, if not needed by them or host plant, which is tested by current CN ratio of mycorrhizae.

$$U^m_{N_{SOM}} = v_{max,N_{SOM}} \frac{N_{SOM}}{K_{m,N_{SOM}} + N_{SOM}} \times C^m \times f_{limit}, \; where \tag{3.11a}$$

$$f_{limit} = \begin{cases} 1, & if \frac{C^m}{N^m} > \chi^m_{CN,\frac{min}{2}} \\ 0.5, & if \chi^m_{CN,\frac{min}{2}} > \frac{C^m}{N^m} > \chi^m_{CN,min}, \; with \quad \chi^m_{CN,\frac{min}{2}} = \frac{1}{2} \times (\chi^m_{CN} + \chi^m_{CN,min}) \\ 0, & if \frac{C^m}{N^m} < \chi^m_{CN,min} \end{cases} \tag{3.11b}$$

where $v_{max,N_{SOM}}$ is the maximum uptake rate per unit mycorrhizal biomass (C^m), $K_{m,N_{SOM}}$ is the N sensitivity parameter, and f_{limit} is the down-regulation function for N uptake from SOM, which is derived from target CN ratio of mycorrhizal fungi (χ^m_{CN}), a minimum CN ratio ($\chi^m_{CN,min}$), and the current CN ratio.

I assume that mycorrhizae will first maintain their own CN ratio, before they export surplus N to plants, and I calculate surplus N by current N uptake, and mycorrhizal N demand, which I estimate based on mycorrhizal CN ratio, and mycorrhizal C. Plants, on the downside, can suppress mycorrhizal export, if they do not need further N.
Since mycorrhizal fungi export N in form of amino acids, they also export C to plants. This export C is simply given by a constant CN ratio of amino acids.

$$E_N^{m2p} = (U_N^m - \zeta_N^m) \times \zeta_N^p, \; with \tag{3.12a}$$

$$\zeta_N^m = \frac{C^m}{\chi_{CN}^m} - N^m \tag{3.12b}$$

$$E_C^{m2p} = \chi_{CN}^{m2p} \times E_N^{m2p} \tag{3.12c}$$

where U_N^m is mycorrhizal N uptake, and ζ_N^m mycorrhizal N demand. ζ_N^p is plant N demand, respectively as given in equation 1.7f. This works as a down regulator for mycorrhizal activities, because mycorrhizae stop all interactions with soil, if they cannot export N to plants, so that their CN ratio falls below a critical value. C^m and N^m are mycorrhizal pools, and χ_{CN}^m and χ_{CN}^{m2p} are parameters, describing the CN ratios of mycorrhizae, and amino acids respectively.

I calculate the death of mycorrhizal fungi (T_X^m) based on the life span of mycorrhizae, calculated with turnover time (τ_{myc}), and pool sizes (X^m).

$$T_X^m = \frac{1}{\tau_{myc}} \times X^m \tag{3.13}$$

where X is either C, and N.

I estimate mycorrhizal respiration analog to plant growth respiration (eq. 1.8) by a constant mycorrhizal C-use efficiency (CUE), but I assume that this respiration rate also contains maintenance respiration.

$$R_{mg}^m = (1 - CUE^m) \times (U_C^m + E_C^{p2m}) \tag{3.14}$$

where CUE^m is the mycorrhizal C-use efficiency that is a constant fraction of recently gained C by mycorrhizae, which mycorrhizae are able to incorporate as biomass. Recently gained C is either C uptake caused by the uptake of organic N, and exudation C by plants.

I calculate N uptake respiration, where C has to be invested to transform mineral N into amino acids similar to plant N uptake respiration (eq. 1.10):

$$R_{U_{N_j}}^m = r_j \times U_{N_j}^m \tag{3.15}$$

where N_j is either NH_4, or NO_3, $U_{N_j}^m$ is the current uptake rate of N_j, and r_j specific C costs per unit N_j that is taken up.

Mycorrhizae do not only interact actively with SOM by mining as N source, but they have the ability to exude C to soil to accelerate decomposition. This C provides energy for microbes to decompose older SOM faster (X_{slow}, see sec. 1.2.4.3). This enhances the net mineralization flux, and fills soil mineral pools faster, from where mycorrhizal fungi, as well as plants, and microbes take up N.

$$D^m_{SOM} = f_{D_{SOM}} \times C^m \tag{3.16}$$

where $f_{D_{SOM}}$ is an empirical parameter to account for C exudation to accelerate SOM decomposition.

I estimate the decomposition acceleration itself by the presence of mycorrhizae that lowers the turnover time of SOM.

$$\tau^{*+}_{SOM} = \tau^*_{SOM} \times \frac{K_{m,\tau_{SOM}} + C^m}{v_{max,\tau_{SOM}} \times C^m} \tag{3.17}$$

where τ^*_{SOM} denotes the turnover time of the SOM without influence of decomposers, but in mycorrhizal presence (eq. 3.18), $K_{m,\tau_{SOM}}$, and $v_{max,\tau_{SOM}}$ are empirical parameters, and C^m is mycorrhizal biomass.

In order to maintain overall ecosystem dynamics, I have to adjust the turnover of slow-SOM in QUINCY (sec. 3.3.2.1).

$$\tau^*_{SOM} = \tau_{SOM} \times f_{\tau_{SOM}} \tag{3.18}$$

where τ_{SOM} is the turnover time of the slow-SOM pool in QUINCY, and $f_{\tau_{SOM}}$ is a hypothetical turnover adjustment parameter.

3.2.2. Duke Forest FACE experiment

I test the MYC model at the Duke Forest free-air CO_2 enrichment (FACE) site (hereafter Duke). The Duke FACE experiment (*McCarthy et al.* (2007)) was set up in a loblolly pine (*Pinus taeda*) plantation (35.9°N, 79.08°W, North Carolina, US) that was established in 1983 after a clear-cut. A prototype experiment started in June 1994, which contained only one plot with ambient and elevated (+200ppm) CO_2 concentrations. In August 1996 the main experiment begun with additional three plots each, whereby the plots were paired accordingly to soil N availability. In 1998 the prototype plots were shifted to a CO_2 x soil nutrient enrichment experiment, which is why I exclude those plots from my analysis in section 3.4.
Duke provides annual data for ambient and elevated treatments for net primary production (NPP) and plant N acquisition (A_N). Used data are averaged per each CO_2 treatment.

Table 3.1.: MYC model parameter

symbol	description	value	LHS interval	unit	reference
CUE^m	mycorrhizal C-use efficiency	0.7	0.5 - 0.8	gC/gC	this study
ϵ	sensitivity parameter for plant C exudation	0.005	0.0 - 0.01	μmol/(m^2 day)	this study
$f_{cover,max}$	maximal covered root surface by mycorrhizal fungi	0.3	0.1 - 0.5	m^2/m^2	*Meyer et al.* (2010)
$f_{D_{SOM}}$	mycorrhizal C exudation to SOM per unit biomass	0.05	0.01 - 0.1	gC/(gC day)	this study
$f_{E_{C^{p2m}_{max}}}$	maximal share of available C for exudation	0.3	0.1 - 0.5	gC/gC	*Meyer et al.* (2010)
$f_{m2r,max}$	maximum ratio of mycorrhizae to plant fine roots	0.5	0.3 - 0.7	gC/gC	*Marschner and Dell* (1994) *Göransson et al.* (2006)
$f_{m2r,min}$	minimum ratio of mycorrhizae to plant fine roots	0.1	0.01 - 0.3	gC/gC	*Marschner and Dell* (1994) *Göransson et al.* (2006)
$f_{resp,max}$	maximum C investment into N uptake	0.5	0.4 - 0.6	gC/(gC day)	this study
$f_{\tau_{SOM}}$	SOM turnover adjustment	5	1 - 10		this study
$f^m_{U^{eff}_N}$	surface ratio between plant fine roots and mycorrhizae	40	10 - 100	m^2/m^2	*Marschner and Dell* (1994)
$K_{m,N_{SOM}}$	half-saturation parameter for N_j uptake	400	300 - 500	m^3/mol	this study
$K_{m,\tau_{SOM}}$	half-saturation parameter to τ_{SOM} reduction	1.0	0.5 - 3.0	gC/m^3	this study
τ_{myc}	turnover time of mycorrhizae	0.3	0.2 - 0.7	years	*Smith and Read* (2010)
$v_{max,N_{SOM}}$	maximum N_{SOM} uptake capacity per unit biomass	0.3	0.1 - 0.5	μmol/(mol year)	this study
$v_{max,\tau_{SOM}}$					this study
χ^m_{CN}	CN ratio of mycorrhizal fungi	10.0	10.0 - 30.0	gC/gN	*Allen et al.* (2003) *Wallander et al.* (2003)
$\chi^m_{CN,min}$	minimal CN ratio of mycorrhizal fungi	0.8 $\times\chi^m_{CN}$	0.7 - 0.9 $\times\chi^m_{CN}$	gC/gN	this study
χ^{m2p}_{CN}	CN ratio of amino acids	3.0	0.0 - 5.0	gC/gN	*Hauptmann* (1985)
K_{m1,NH_4}	low affinity half-saturation parameter for NH_4 uptake	0.0416		m^3/mol	
K_{m1,NO_3}	low affinity half-saturation parameter for NO_3 uptake	0.0416	QUINCY	m^3/mol	*Thum et al.* (2019)
K_{m2,NH_4}	high affinity half-saturation parameter for NH_4 uptake	1.0	parameters	m^3/mol	cf. tab. A.1
K_{m2,NHO_3}	high affinity half-saturation parameter for NO_3 uptake	1.0	are not included	m^3/mol	for references
r_{NH_4}	uptake respiration per unit NH_4	1.8	into LHS	gC/gN	
r_{NO_3}	uptake respiration per unit NO_3	2.3		gC/gN	
τ_{labile}	turnover time of plant labile pool	7		days	
τ_{SOM}	turnover time of slow SOM pool	100		years	
$v_{max,j}$	maximum N_j uptake capacity per unit biomass	0.42		μmol/(mol s)	
χ^{SOM}_{CN}	CN ratio of SOM	9.0		gC/gN	

3.3. Results I: MYC model evaluation

In order to assess the general MYC model behavior based on its structure and both mycorrhizal functionalities, namely saprotrophic and decomposing behavior, as well as parameter uncertainty, I analyze model performance in comparison to QUINCY (revision 1878) without MYC and among both functionalities with a spin-up period of 500 years, and conduct a parameter sensitivity analysis.

Both analyses are done based on simulations with the same model protocol and input data as described in section 2.2.2 for the Duke Forest site (sec. 3.4.2). The analysis period from 1971 to 1980 is chosen previous to harvest to ensure a steady-state ecosystem for model evaluation, if not indicated otherwise. Simulation output is presented as daily or annual mean $\pm$ 1 standard deviation (SD).

3.3.1. MYC model behavior

I start the model evaluation by focusing on plant-mycorrhiza exchange fluxes, because C exudation from plant to mycorrhizal fungi drive the MYC model, and export fluxes from mycorrhizal fungi to host plant show the value of mycorrhizae for plants. I see a clear seasonal cycle that is governed by plants, since their C uptake by photosynthesis offers C for exudation, and demands N for growth, which should be supplied by mycorrhizae in return (fig. 3.2).

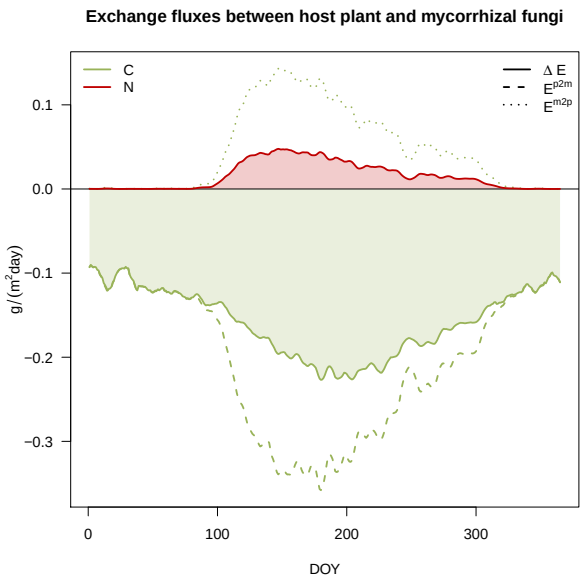

Figure 3.2.: Daily carbon and nitrogen exchange between plant and mycorrhizal fungi over one year. Daily exchange rates are averaged from 1971 to 1980. For simplification, the average over both functionalities is taken, since this exchange is the key process for the entire MYC model. As in equation 3.3 negative fluxes are defined as fluxes from plant to mycorrhizae, whereas positive fluxes are from mycorrhizae to plants. Net exchange (ΔE_C and ΔE_N) are shown as shaded areas with solid border lines, whereby the exudation flux from plants to mycorrhizae (E_C^{p2m}) is drawn as dashed line, and export from mycorrhizae to plants (E_C^{m2p} and E_N^{m2p}) is drawn in dotted lines.

In total, trees invest 57.57±2.75 gC $m^{-2}year^{-1}$ into mycorrhizae (E_C^{p2m}: -74.94±4.00 gC $m^{-2}year^{-1}$, E_C^{m2p}: 17.37±0.73 gC $m^{-2}year^{-1}$) and get 5.79±0.22 gN $m^{-2}year^{-1}$ in return, which is an investment-on-return ratio of 9.94±0.14 gC/gN, if I average fluxes over both mycorrhizal types. But this values strongly depend on mycorrhizal functionalities, ranging from 6.21±1.54 gC/gN in the presence of saprotrophic mycorrhizae to 13.78±2.26 gC/gN in the presence of decomposing mycorrhizae. This implies that N support by decomposers is almost twice as expensive in terms of C investment for plants than N support by saprotrophs (tab. 3.2 and tab. 3.3).
Despite these extreme investment differences for mycorrhizal N supply, annual N export from mycorrhizal fungi to host is only 3% lower in case of decomposing mycorrhizae, because plants need to fulfill their N requirements, and direct root uptake is decreased by 75-80% in the presence of mycorrhizal fungi, caused by (i) their higher N uptake efficiency, and (ii) their physical presence that covers plant roots on the other hand (eq. 3.2 and eq. 3.10). Consequently, total annual N acquisition by plants varies less than 10% among model variants, but is lower in the presence of both mycorrhizal fungi.

Table 3.2.: Annual N acquisition by plants (A_N^p) for QUINCY simulations, which is given by plant N uptake (U_N^p), and mycorrhizal export (ΔE_N). Values are presented as 10-year mean ± 1 standard deviation and given in gN $m^{-2}year^{-1}$.

	no mycorrhizae	decomposers	saprotrophs
A_N^p	8.22 ± 0.58	7.51 ± 0.43	7.81 ± 0.42
U_N^p	8.22 ± 0.58	1.81 ± 0.10	1.93 ± 0.11
ΔE_N	NA	5.71 ± 0.36	5.87 ± 0.31

Table 3.3.: Annual C allocation within plant-mycorrhiza symbiosis for QUINCY simulations. Values are presented as 10-year mean ± 1 standard deviation and given in gC $m^{-2}year^{-1}$. NPP is subdivided into plant biomass production (BP) and net C exchange with mycorrhizal fungi (ΔE_C)

	no mycorrhizae	decomposers	saprotrophs
GPP	1873 ± 72	1838 ± 69	1857 ± 71
NPP	663 ± 30	795 ± 39	729 ± 34
BP	663 ± 30	717 ± 31	693 ± 26
ΔE_C	NA	78 ± 8	36 ± 7

However, this does not lead to a limitation on growth, because both, annual NPP, including mycorrhizal biomass in model simulations with explicit mycorrhizal fungi, and annual plant biomass production (BP) are higher in QUINCY simulations with mycorrhizae (tab. 3.3). This seems surprising, because annual GPP varies less than 2% among model variants, which means that plants do not acquire more C, but have to invest C into mycorrhizal growth, and are still able to increase growth in the presence of mycorrhizae. Additionally, they acquire less N in total, which they need for biomass production. This is contradictory at first sight, but indicates a strong link to the timing, when mycorrhizae

support plants, which I cannot derive from annual fluxes, but which is visible in the steep increase of daily C exudation (E_C^{p2m}) that is followed by a fast increase of N export to plants (E_N^{m2p}, fig. 3.2). Caused by an increasing N demand for growth, plants invest up to 10% of daily GPP into mycorrhizae, which is in the middle of observed C exudation to mycorrhizal fungi that varies from 1-25% of freshly assimilated C (*Jakobsen and Rosendahl* (1990), *Ek et al.* (1997), *Staddon et al.* (2003), *Hobbie* (2006)). However, annually averaged C exudation to mycorrhizal fungi is only about 5% of GPP, which is at the lower end of observations. This is caused by the wide range of observations that reflect the high uncertainty of these measurements on the one hand, and by model parameterizations and simplifications on the other hand, which I will explore and discuss later.
For the moment, I continue the exploration of MYC model performance as introduced in section 3.2.1 to understand, how the MYC model influences QUINCY simulations in general, especially with respect to the two different mycorrhizal functionalities.

As I assume that it is not only the total N supply by mycorrhizae that supports plant growth, but rather the timing, I analyze daily total plant N acquisition now that is the sum of plant root uptake and N export by mycorrhizal fungi (fig. 3.3a).
Root uptake/N acquisition by plants in QUINCY without mycorrhizae has a clear seasonal cycle that is caused by plant phenological cycle, which drives plant N demand. Rates are highest at the beginning of plant growing season in spring, and lowest during winter. Since the seasonality of plant N demand is similar in QUINCY with mycorrhizae, N acquisition rates show similar behavior and rates, with highest N acquisition rates in spring and summer, and lowest rates in winter. However, root uptake is only minor, because of mycorrhizal ability to disconnect roots from soil by covering root tips, and N support by mycorrhizal fungi is major due to the higher N uptake efficiency of mycorrhizal fungi (eq. 3.2 and eq. 3.10). Nevertheless, root uptake and mycorrhizal support are positively correlated, i.e. higher plant root uptake rates correspond to higher mycorrhizal N support rates generally. This is caused by plant N demand, and was also simulated by MYCOFON (*Meyer et al.* (2010)) and FUN (*Shi et al.* (2016)).
Despite the overall similarity in N acquisition rates, there are differences not only between QUINCY without and with mycorrhizal fungi, but also among mycorrhizal types. Spring-time increase of N acquisition rates is delayed by approximately a week in QUINCY simulations with mycorrhizal fungi, because mycorrhizae maintain their own CN ratio first, before they deliver surplus N to host plants (eq. 3.12). As soon as mycorrhizae realize increasing plant N demand by enhanced C exudation, they grow and increase N uptake, but only after fulfilling own N requirements, mycorrhizal fungi export N as desired by plants. This is earlier the case for saproptrophs, since they take up N not only from mineral sources, but from SOM, too, which covers more than 70% of their N uptake in the first half of the year (fig. 3.3b). By accessing SOM as N source, saprotrophs are able to increase N export not only earlier than decomposers, but also much faster, which results in 20% higher daily plant N acquisition rates than rates by QUINCY without mycorrhizae

about week after they start increasing N export, and balances the previous delay out quickly. In contrast to that, decomposers rely on mineral N similar to plants, which is why they cannot increase their uptake as quickly as saprotrophs, because mineral N is a more limited source (fig. 3.3b). Consequently decomposers have to compete stronger with plants, which is why both, their uptake rates, as well as their export rates increase slower, but are higher in the second half of the year, when saprotrophs already decrease daily export and uptake rates, since their own N demand is fulfilled as well as plant N demand (fig. 3.3).

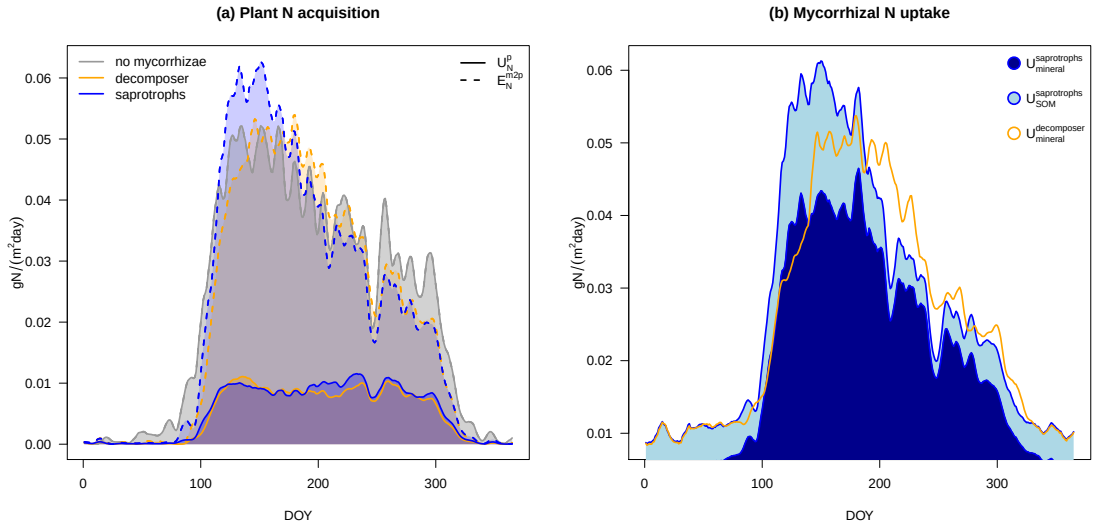

Figure 3.3.: Mycorrhizal N support. (a) Daily plant N acquisition as sum of direct root uptake (U_N^p, solid line around dark shaded area) and mycorrhizal N export (E_N^{m2p}, dashed line around light shaded area) for QUINCY without mycorrhizae (grey), QUINCY with decomposing mycorrhizae (orange), and QUINCY with saprotrophic mycorrhizae (blue). (b) Daily mycorrhizal N uptake. Uptake by saprotrophic fungi as sum of uptake from mineral N ($U_{N_{min}}^m$; darkblue area), and organic N ($U_{N_{SOM}}^m$; lightblue area), and uptake by decomposing fungi from mineral N (orange line).

Latter indicates plant control on mycorrhizal behavior, but the actual controlling is only visible, when I link mycorrhizae N export (E_N^{m2p}) directly to plant N demand (ζ_N^p, fig. 3.4). N export follows more or less a parabolic curve for both mycorrhizal types, because plant N demand scales N export directly (eq. 3.12), but also indirectly by scaling C exudation (eq. 3.6) that influences mycorrhizal growth. Increasing mycorrhizal biomass increases mycorrhizal N uptake rates (eq. 3.10 and eq. 3.11) that increases N availability for export, but also mycorrhizal N demand, which lowers N export, until mycorrhizal requirements are fulfilled. N export responses to plant N demand therefore follow a curve that is somewhere between a quadratic and a cubic parabola, whereby the saprotophic N export is closer to the X^3 curve, and the decomposing N export is closer to the X^2 curve.

The steeper increase and tighter width of the X^3 curve that may represent N export response to plant N demand by saprotrophs is linked to the higher N uptake capacity of saprotrophs by an additional N source. This surpasses the potential N export decrease by mycorrhizal N demand and therefore directly presents the stronger control of plants of saprotrophs, because even a medium demand result in high export. Contrary to that, the wider width and the slower increase of the X^2 curve that may represent N export response to plant N demand by decomposers, as well as the wider spread of data points around the curve indicates that decomposing fungi are not able to meet plant N requirements to such an extend as saprotrophs do, but act partly as competitors. This also explains the almost 30% higher plant N demand rates that are reached in QUINCY with decomposers.
This differences in plant control are expected due to the different influences of SOM dynamics that mycorrhizae exert. Saprotrophic behavior influences SOM directly by actively accessing SOM as N source. This allows a strong and direct plants to control on this N acquisition strategy, which is only shortly time-delayed due to the fact the mycorrhizea primarily maintain their own CN ratio, before the deliver N to host plants (eq. 3.12). Decomposing behavior, which is implemented as further C exudation to SOM to accelerate SOM decomposition, is an indirect way of influencing SOM dynamics, and a rather passive strategy to enhance N acquisition. Consequently, plant control on this strategy is weaker and potentially also more delayed. This is why I cannot recognize the performance of this mycorrhizal functionality properly by only accounting for plant N acquisition, but I have to take the overall N dynamics of the ecosystem into consideration.

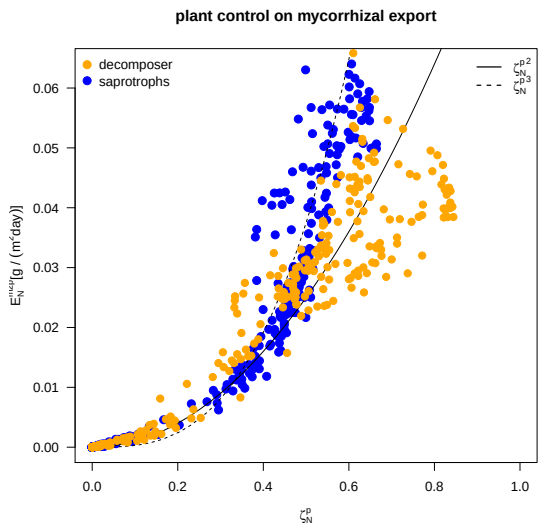

Figure 3.4.: Plant control on mycorrhizal N export, presented by daily mycorrhizal N export (E_N^{m2p}) from decomposing mycorrhizae (orange) and saprotrophic mycorrhizae (blue) as function of plant N demand (ζ_N^p). Curves show a quadratic (solid line) and cubic (dashed line) dependency from plant N demand.

For that aim, I compare annual N uptake rates from plants and mycorrhizae from different sources as proxy for N availability. I find an increase of 46% of total ammonium and of 26% of total nitrate uptake in the presence of decomposing mycorrhizae compared to

QUINCY without mycorrhizal fungi, which I cannot find in the presence of saprotrophic mycorrhizae (total ammonium uptake: -12%, total nitrate uptake: +12%[4]). Since uptake rates are tightly linked to the accessed pool size (eq. 3.2, eq. 3.10, eq. 3.11), I can derive that ecosystems that contain decomposing mycorrhizae provide a greater source of mineral N. This is caused by the ability of priming mycorrhizae to accelerate SOM decomposition, which they do by a decrease in SOM turnover time by almost 57% on annual basis that increases net mineralization by about 38%.

Table 3.4.: Annual N uptake by plants (U^p) and mycorrhizal fungi (U^m) from different sources (NH_4, NO_3, and SOM; indicated by subscript) for QUINCY simulations. Values are presented as 10-year mean $\pm$ 1 standard deviation, and given in gN $m^{-2}year^{-1}$.

	no mycorrhizae	decomposers	saprotrophs
$U^p_{NH_4}$	3.92 $\pm$ 0.35	0.89 $\pm$ 0.01	0.73 $\pm$ 0.04
$U^p_{NO_3}$	4.30 $\pm$ 0.23	0.92 $\pm$ 0.04	1.20 $\pm$ 0.02
$U^m_{NH_4}$	NA	4.85 $\pm$ 0.91	2.37 $\pm$ 0.34
$U^m_{NO_3}$	NA	4.50 $\pm$ 0.27	3.63 $\pm$ 0.29
$U^m_{N_{SOM}}$	NA	NA	3.75 $\pm$ 0.56

Overall, I find that both mycorrhizal types are able to increase N availability for plants in equilibrium, either by decomposing N that leads to higher N mineralization rates and increases mineral N availability, or by mining SOM directly (tab. 3.4). Both strategies therefore result in the hypothesized acceleration of the ecosystem internal N cycle (H3.1), but do not lead to higher N acquisition by plants on annual basis (tab. 3.2). However, since mycorrhizae provide N as soon as plants demand increases, plants increase their growth efficiency and resulting vegetation biomass is almost similar among all QUINCY simulations.

3.3.2. Parameter uncertainty

As observational data about mycorrhizal behavior for both, plant-mycorrhiza and mycorrhizal-soil interactions, are scarce and highly uncertain due to the difficulties to measure fluxes within the rhizosphere in an undisturbed (eco)system, most parameters of the MYC model are either completely hypothetical, or have a high uncertainty that can range over magnitudes (tab. 3.1). To address this issue, and test the robustness of my results, I assess the parameter uncertainty by two separate studies: the first one focuses only on the

[4]Decomposing mycorrhizae accelerate SOM decomposition, which mainly affects ammonium, as mineralized SOM N enters this pool. Contrary to that, saprotrophic mycorrhizae take up N from SOM directly, which reduces N that is mineralized from SOM to ammonium. Ammonium uptake is therefore strongly enhanced in the presence of decomposers, but reduced in the presence of saprotrophs. Nitrification, i.e. the oxidization of ammonium to nitrate, is less affected, which is why the increase of nitrate uptake is lower than the increase of ammonium uptake in the presence of decomposing mycorrhizae, but is slightly increased, even if ammonium uptake is decreased in the presence of saprotrophic mycorrhizae (sec. 1.2.2).

turnover adjustment parameter ($f_{\tau_{SOM}}$, eq. 3.18), because $f_{\tau_{SOM}}$ is an artificial parameter that does not directly influence MYC model behavior, but the entire ecosystem dynamics, whereas the second one test model behavior by changing all MYC model parameters simultaneous by a Latin Hypercube Sampling (LHS, *Saltelli et al.* (2000)), which allows me to test the robustness of model results, and to identify parameters that shape model performance most.

3.3.2.1. Influence of turnover adjustment on ecosystem dynamics

The turnover adjustment parameter ($f_{\tau_{SOM}}$) is an artificial parameter that changes SOM turnover by increasing the specific turnover time of the slow-SOM pool (τ_{SOM}) in QUINCY (sec. 1.2.4.3). Since τ_{SOM} is an empirical parameter itself that is determined to simulate reasonable ecosystem dynamics, it needs to be adjusted, if SOM dynamics are influenced by newly integrated processes, such as mycorrhizal interactions with SOM, in order to maintain previous SOM and ecosystem dynamics stable. As this adjustment is completely empirical, I need to check, if and how I influence simulated ecosystem dynamics. For that reason, $f_{\tau_{SOM}}$ is varied between 1 (no change of τ_{SOM} in the presence of mycorrhizae) to 10, whereas the default value in the MYC model is 5.
To assess the influence of $f_{\tau_{SOM}}$ to the entire ecosystem and its evolution, I extend my analysis period to 1966 to 2015. This extension allows me to compare a steady-state ecosystem prior to the harvest in 1982, and ecosystem evolution afterwards.

Because C pool sizes are rather constant in steady-state, I analyze solely simulation results for 1980 to account for general influence of mycorrhizal interaction on ecosystem C (C_{Eco}). C_{Eco} is highest in QUINCY without mycorrhizae, and lowest in simulations that includes decomposing mycorrhizae (-29%$\pm$10%, saprotrophic mycorrhizae: -11%$\pm$5%). Vegetation C (C_{Veg}), which includes mycorrhizal biomass (implicitly in QUINCY without mycorrhizae, and explicitly in QUINCY with mycorrhizae), differs less than 2% among model variants, and is robust against $f_{\tau_{SOM}}$ variations, but soil organic C (C_{SOM}) is decreased by 55% in QUINCY with decomposers, and by 23% in QUINCY with saprotrophs, which is induced by changes in slow-C_{SOM}, whereas litter-C and fast-C_{SOM} pools differ less than 10% among model variants (litter C content up to 9%, fast pool up to 3%) (tab. 3.5). Slow-C_{SOM} pool is reduced by almost 95% in the presence of decomposing mycorrhizal fungi, because of the acceleration of decomposition that enhances heterotrophic respiration and thus C losses, and by more than 60% in the presence of saprotrophic fungi, since QUINCY requires a fixed CN ratio for the slow-SOM pool, which leads to SOM-C losses, when mycorrhizae take up SOM-N, without $f_{\tau_{SOM}}$-adjustment compared to QUINCY without mycorrhizal fungi. Despite that the increase of heterotrophic respiration (decomposing mycorrhizae: +14$\pm$4%, saprotrophic mycorrhizae: +18$\pm$%) was foreseen as H3.3, this result is rather contradictory to observations that report C accumulation in ecosystems with mycorrhizal fungi (*Godbold et al.* (2006), *Averill et al.* (2014)) and therefore justifies the artificial turnover time adjustment by $f_{\tau_{SOM}}$. However, slow-C_{SOM} content saturates for QUINCY with saprotrophic mycorrhizae for

$f_{\tau_{SOM}} \geq 5$, whereas slow-C_{SOM} content in QUINCY with decomposers increases rather linearly even after $f_{\tau_{SOM}} = 10$ (fig. 3.5). In both cases slow-C_{SOM} pools are still smaller than slow-C_{SOM} pool in QUINCY without mycorrhizal fungi, which leads to lower C_{SOM} content and lower C_{Eco} content.

Table 3.5.: Ecosystem C budget in 1980. Values are given for default parameterization with $f_{\tau_{SOM}} = 5$, as well as for $f_{\tau_{SOM}} = 1$ and $f_{\tau_{SOM}} = 10$ in brackets as minimum and maximum values of parameter variations. Values are presented in kgC m^{-2}.

	no mycorrhizae	decomposers	saprotrophs
Ecosystem	22.05	15.70 (13.85 - 18.05)	19.51 (16.08 - 20.00)
Vegetation	10.50	10.31 (10.27 - 10.35)	10.57 (9.78 - 10.60)
Soil	11.55	5.39 (3.57 - 7.78)	8.94 (6.30 - 9.44)
- litter	2.04	1.89 (1.88 - 1.89)	1.98 (1.95 - 1.99)
- fast	1.15	1.18 (1.18 - 1.19)	1.17 (1.17 - 1.17)
- slow	8.35	2.32 (0.47 - 4.68)	5.78 (3.14 - 6.25)

The reduction of slow-C_{SOM} by 31% in QUINCY with saprotrophs and 72% in QUINCY with decomposers ($f_{\tau_{SOM}} = 5$) compared to QUINCY without mycorrhizal fungi lowers C_{SOM} by 22% (saprotrophs) and 53% (decomposers) respectively, and C_{Eco} by 11.5% (saprotrophs) and 29% (decomposers). Since C_{Veg} is hardly effected by mycorrhizae in equilibrium, C_{SOM} reduction shifts C allocation within the ecosystem from 48% of C_{Eco} in C_{Veg} in QUINCY without mycorrhizae, to 54% in QUINCY with saprotrophs and 66% in QUINCY with decomposers.

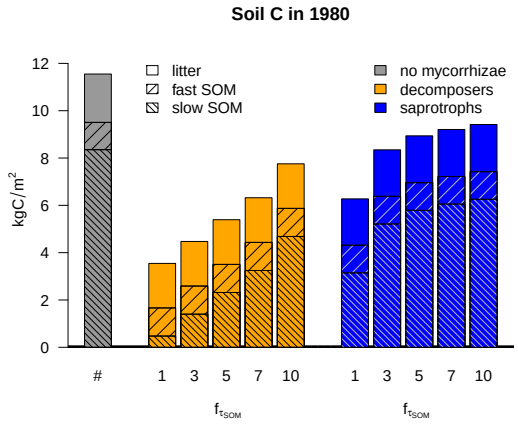

Figure 3.5.: Soil organic C stocks in 1980, divided into slow decomposing SOM-C (tightly striped), fast decomposing SOM-C (striped), and litter C (unfilled). Grey: QUINCY without mycorrhizae, orange: QUINCY with decomposing mycorrhizae, blue: QUINCY with saprotrophic mycorrhizae. X labels present $f_{\tau_{SOM}}$ that is used in QUINCY simulation with mycorrhizal fungi.

Harvest in 1982 takes ecosystem away from steady-state, but does not change C_{Eco} or C_{SOM} differences that are induced by mycorrhizal fungi. C_{Eco} in QUINCY without mycorrhizae remains highest, and C_{Eco} in QUINCY with decomposers remains lowest, which is caused by the fact the harvest primarily changes C_{Veg}, which was rather similar before harvest, and has only a lagged effect on SOM dynamics by higher litter input that is decomposed in the following years.

Notably, C_{Veg} in QUINCY with saprotrophs that was slightly higher then C_{Veg} in both other model variants before harvest, needs longest time for re-grow after harvest, and is still lower than C_{Veg} in QUINCY without mycorrhizae in the end of my simulation period. This indicates that saprotrophic mycorrhizae are rather competitors than supporters in the first years after harvest, and is caused by their ability to take up SOM-C, which ensures their survival, even if plants do not feed them, in combination with their higher N uptake efficiency. However, non of the model variants reaches its pre-harvest steady-state within the simulation period until 2015 (i.e. in 32 years), which includes the FACE experiment period from 1996 - 2006 that I analyze in section 3.4.1.

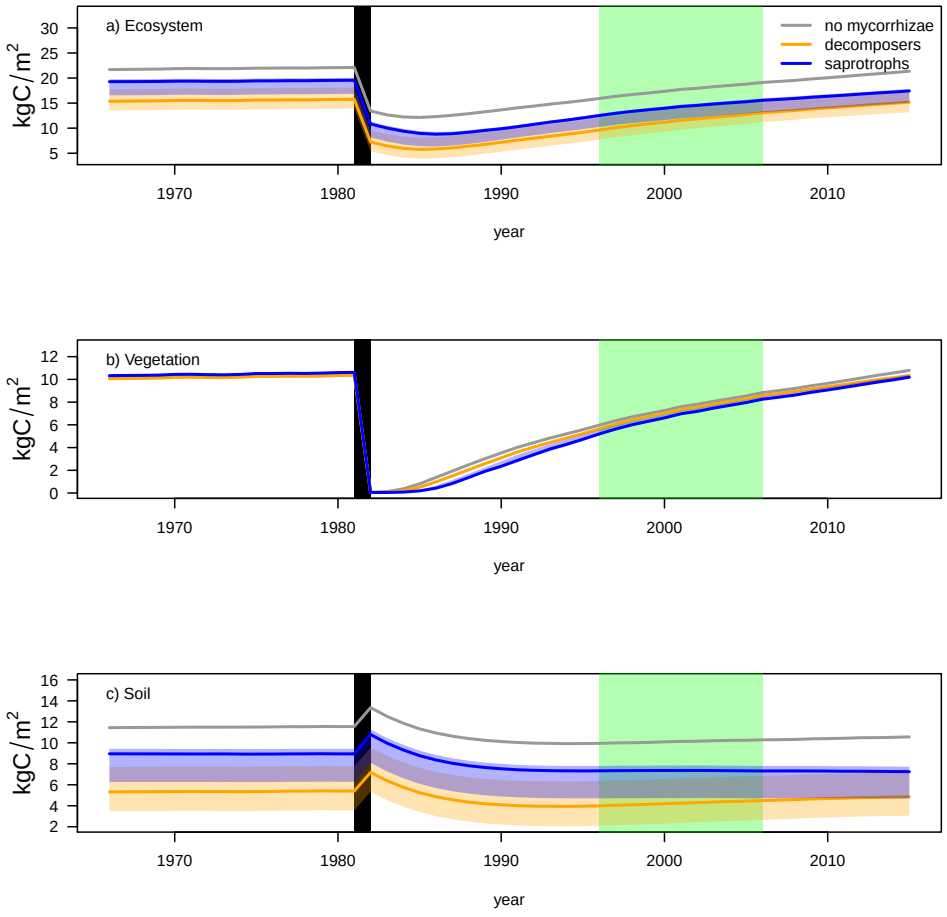

Figure 3.6.: (a) Ecosystem, (b) Vegetation, and (c) Soil organic C content from 1966 to 2015. Black line show harvest in 1982, and green shaded area FACE experiment period. Grey: QUINCY without mycorrhizae, orange: QUINCY with decomposing mycorrhizae, blue: QUINCY with saprotrophic mycorrhizae. Shaded ribbon represent range of simulation results depending on $f_{\tau_{SOM}}$ for QUINCY runs with mycorrhizal fungi.

3.3.2.2. Model sensitivity to MYC model parameterization

In order to test model sensitivity to all parameters that directly shape C and N fluxes between plant and mycorrhizae, mycorrhizae and soil, or plant and soil at the same time, I conduct a Latin Hypercube Sampling (LHS, *Saltelli et al.* (2000)) with 500 runs for each mycorrhizal type, where I vary parameters within ranges that are presented in table 3.1. I normalize the LHS results by results of reference runs using the standard parameterization, whereby both, LHS runs and reference runs, were averaged for 1971 to 1980 to eliminate climate variability.
Since LHS results were well centered around the results with standard parameterization, I did another sampling with only 200 runs each, where I varied parameters by $\pm$10% in order to treat all parameters similar. My further evaluations and studies are based on these second round of runs, but the interested reader can find the first sensitivity assessment with all 500 runs in appendix C.2.

I concentrate this analysis on some most substantial output variables, which are NPP, plant exudation mycorrhizal fungi (E_C^{p2m}), and N export from fungi to plant (E_N^{m2p}), as well as ecosystem C stocks. The inner-quartile range of model output for both, QUINCY with decomposers and QUINCY with saprotrophs, is well centered around the results of the standard parameterization (fig. 3.7 and fig. 3.8).
NPP varies less than 1% for 50% of all LHS runs (box-range), and less than 5% for 80% of all runs (whisker-range). However, the exudation flux from plant to mycorrhizae, which drives the entire MYC model, shows higher variations, especially with saprotrophs. This is mainly caused by uncertainties of $f_{m2r,min}$, CUE^m, and τ_{myc}. In a well established ecosystem, plants try to exude as little C as possible to hosted mycorrhizal fungi, as long as their N requirements are still met, which explains the huge influence of $f_{m2r,min}$ as measure of minimum mycorrhizal biomass, CUE^m as parameter that determines, how much of the exuded C is actually used for mycorrhizal growth, and τ_{myc} that defines mycorrhizal mortality rate. Meeting plants N requirements with the minimum amount of mycorrhizae, which is seen in the lower variation of N export from mycorrhizae to host plants, indicates too heavy influence of mycorrhizae to the entire N dynamics within the ecosystem. However, either exchange fluxes between host plants and mycorrhizae, and mycorrhizal influence on SOM dynamics, are hard to constrain, because data are rare, especially on ecosystem scale.
Despite this rather high uncertainty regarding mycorrhizal dynamics, ecosystem dynamics are rather robust. Since NPP does not vary much, vegetation biomass does not vary much either, among all LHS runs in relation to standard parameterization for both mycorrhizal functionalities. C_{SOM} is more sensitive, especially for saprotrophic mycorrhizae, which is expected due to the direct influence of saprotrophic mycorrhizae that is depending on the potential maximal N uptake rate from SOM ($v_{max,N_{SOM}}$). However, the inner-quartile range of LHS variations for C_{Eco} is less than 10%, and 80% of all LHS runs vary less than 30% from standard parameterization, even for saprotrophic mycorrhizae.

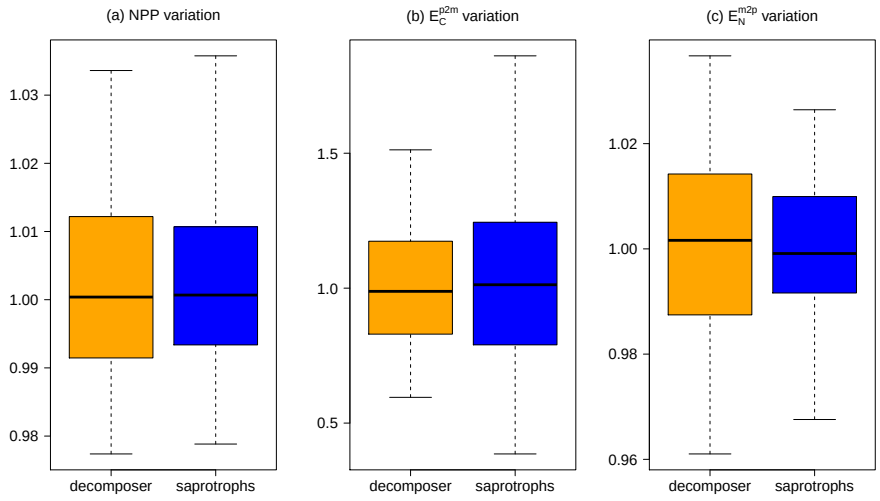

Figure 3.7.: Sensitivity of fluxes due to parameter uncertainty.
(a) NPP variations, (b) C exudation (E_C^{p2m}) variations, and (c) N export (E_N^{m2p}) variations caused by parameter uncertainty relative to standard parameterization. Boxes represent the inner-quartile range, which is divided by the median. Whisker show 10% and 90%-quantile.

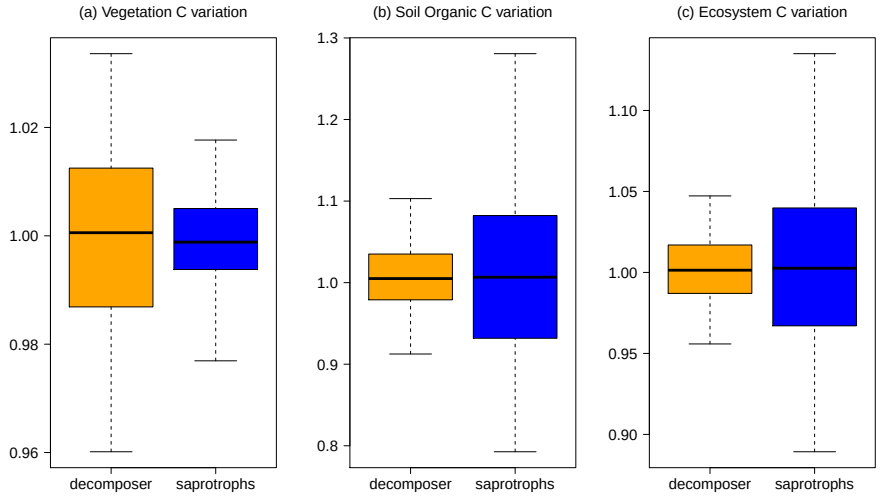

Figure 3.8.: Sensitivity of ecosystem C pools due to parameter uncertainty.
(a) Vegetation C variations, (b) soil organic C variations, and (c) total ecosystem C variations caused by parameter uncertainty relative to standard parameterization. Boxes represent the inner-quartile range, which is divided by the median. Whisker show 10% and 90%-quantile.

3.4. Results II: Assessments of ecosystem carbon-nitrogen dynamics at Duke Forest under elevated CO_2

Now I address H3.2 and H3.4, which hypothesized that (i) the confirmed acceleration of the internal N cycling within the ecosystem by explicitly modelled mycorrhizal fungi (H3.1, sec. 3.3.1) prevents plants from progressive N limitation (PNL) under elevated CO_2 (eCO_2) conditions (H3.2), but that (ii) the proven reduction in soil organic C (C_{SOM}) stocks by increased C losses due to enhanced heterotrophic respiration (H3.3, sec. 3.3.2.1) leads to a lower C storage under eCO_2 (H3.4). Therefore I run QUINCY (revision 1878) again with both mycorrhizal types and without mycorrhizae as reference with the same model protocol and input data as described in section 2.2.2 and with a 500-year spin-up period at the Duke Forest site. I carry out two runs for each case, one under ambient climate conditions, and one where atmospheric CO_2 concentrations are elevated by 200ppm from August 1996 on, as it was done in the FACE experiment. CRUNCEP data forcing and CO_2 concentration information (sec. 2.2.2 are replaced by local meteorological data and CO_2 concentration for the duration of the experiment, which are provided by *Walker et al.* (2014). To address model uncertainty, I use the same Latin Hypercube Sampling (LHS) for all MYC model parameters as in section 3.3.2.2.

Flux and flux ratio responses to eCO_2 are calculated as relative changes to ambient flux/flux ratio as following:

$$\delta Y = \frac{Y_{ele} - Y_{amb}}{Y_{amb}} \tag{3.19}$$

where δY is the relative response to elevated CO_2 of the regarded flux or flux ratio Y. Y_{ele} depicts flux or flux ratio Y under elevated CO_2 condition, whereas Y_{amb} depicts flux or flux ratio Y under ambient CO_2 condition.

Pool responses are presented as absolute response to eCO_2:

$$\Delta X = X_{ele} - X_{amb} \tag{3.20}$$

where ΔX is the absolute response to elevated CO_2 of the regarded pool X. X_{ele} depicts pool X under elevated CO_2 condition, whereas X_{amb} depicts pool X under ambient CO_2 condition.

3.4.1. Overall responses to elevated CO_2

During the first year of the FACE experiment, all standard parameterization model variants agree on an increase in GPP of 20-25% in response to eCO_2 (fig. 3.9a), which is caused by enhance C uptake per unit leaf area. However, they differ largely in long-term responses, where GPP is either further increased up to almost 30% compared to ambient CO_2 (aCO_2) simulations, or decreased to -14%. As GPP describes plant C assimilation, GPP responses build the basis for all other plant C flux responses. This causes only minor variations of initial plant biomass production responses among standard parameterization model variants, but large disagreements in long-term C flux responses, which vary in amplitude as well as in direction (fig. 3.9b). Exudation responses (fig. 3.9c) are almost zero for any period in QUINCY with decomposers, which indicates minor utility for plants, whereas initial exudation response to eCO_2 is negative in QUINCY with saprotrophs, caused by prioritizing own growth by plants, and end response is positive, because plants actively invest C into mycorrhizal growth to prevent N limitation (fig. 3.9, stars). Responses among LHS simulations (fig. 3.9, boxes) show a wider range, especially for initial responses in QUINCY simulations with saprotrophic mycorrhizae. However, this is only partly caused by a high uncertainty due to eCO_2 responses itself, but is more related to the slower vegetation re-grow after harvest that I found in section 3.3.2.1. Long-term responses show a less wide spread, which indicates robust model results with respect to eCO_2.

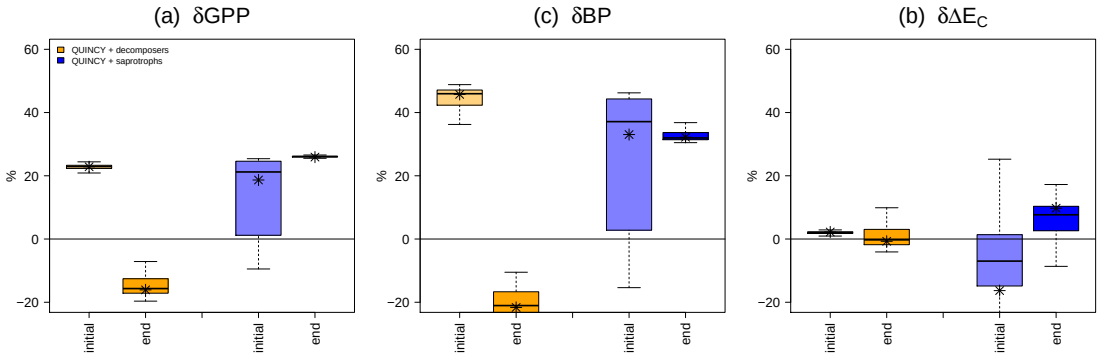

Figure 3.9.: Annual plant controlled C allocation response to elevated CO_2 within plant-mycorrhiza symbiosis during FACE experiment for first year (initial), and last year (end) for LSH simulations. C allocation response is presented by (a) GPP response (δGPP) to show changes in C inflow, (b) plant biomass production response (δBP), and (c) net exudation response (δ ΔE_C). Orange: QUINCY with decomposing mycorrhizae, blue: QUINCY with saprotrophic mycorrhizae. Stars mark values for simulations with default parameters.

Knowing this general model behavior in the beginning and end of the FACE experiment, I go from year-to-year comparisons to time series, because as Duke provides observations for NPP that includes both, plant and mycorrhizal biomass production, plant N acquisition (A_N^p), and plant N-use efficiency (NUE) for both CO_2 treatments at Duke (*Walker et al.* (2014)).

Modelled NPP for all model variants is lower than observed NPP (-21.4±5.7%), whereby QUINCY with saprotrophs shows a high range of simulated annual NPP among LHS simulations at the beginning of the analyzed period (322 - 886 gC $m^{-2}year^{-1}$), which decreases until 2002 (fig. 3.10a). This variety is caused by the stronger influence of harvest to ecosystems that have saprotrophic mycorrhizae (sec. 3.3.2.1). Thus, simulated responses to elevated CO_2 (eq.: 3.19) by QUINCY with saprotrophs have a huge range during the first years of the FACE experiment. NPP responses even change their sign in the beginning of the experiment, but in general this model variant meets observed responses best, especially in the long-term (fig. 3.10b and tab. 3.6).
All simulations capture initial observed NPP response well, but QUINCY without mycorrhizae and with decomposers increase NPP response to elevated CO_2 up to almost 50%, which is twice as much increase in NPP than observed. QUINCY without mycorrhizae stays on high levels of NPP response, whereas QUINCY with decomposers decrease NPP response after 4 years of experiment, so that long-term NPP response becomes negative. Only QUINCY with saprotrophs is able to capture both, initial and end NPP responses to elevated CO_2.
QUINCY without mycorrhizae and with saprotrophs meet observed N acquisition data within the boundaries of 1 standard error (SE) over the entire experiment, whereas QUINCY with decomposers underestimates N acquisition by 17% (fig. 3.10c). This underestimation causes the inability of this model variant to capture observed A_N^p responses initially, and in the long-term, and explains the strong decrease in NPP response after initial years due to strong progressive N limitation (PNL, fig. 3.10d and tab. 3.6). Decomposers cannot prevent plants from N limitation, since the increase in turnover is not strong enough to provide mineral N fast enough to meet both, plant and mycorrhizal, N requirements. Actually plants face a stronger limitation than in QUINCY without mycorrhizae, because decomposers compete in N uptake and hold it back from plants. QUINCY without mycorrhizae is able to meet observed initial A_N^p response, but decrease A_N^p response in the long-term due to PNL. This causes an increase of NUE response of 40%, which is 8 times higher than the observed NUE response in the end of the experiment (fig. 3.10f and tab. 3.6).
Only QUINCY with saprotrophs can meet initial, and long-term responses of A_N^p and NUE (fig. 3.10d and fig. 3.10f, and tab. 3.6), even if ambient NUE is underestimated by almost 20%, which is the same for QUINCY without mycorrhizae (fig. 3.10e). This indicates either too rigid N requirements for growth in QUINCY, since modelled plants require more N for biomass production (lower NUE) than observed (higher NUE), or an underestimation of actual A_N^p at Duke, which is actually derived as difference between total tissue N content of the actual to the previous year. Only QUINCY with decomposers meets observed ambient NUE, but this is only caused by an underestimation of both, NPP and A_N^p. These findings confirm the prevention of plants from PNL by explicitly modelled mycorrhizae that accelerate ecosystem N cycling (H3.2) only partly, since this is only shown for saprotrophic mycorrhizae. Decomposing mycorrhizae rather increase PNL for plants by competing in N uptake from mineral sources.

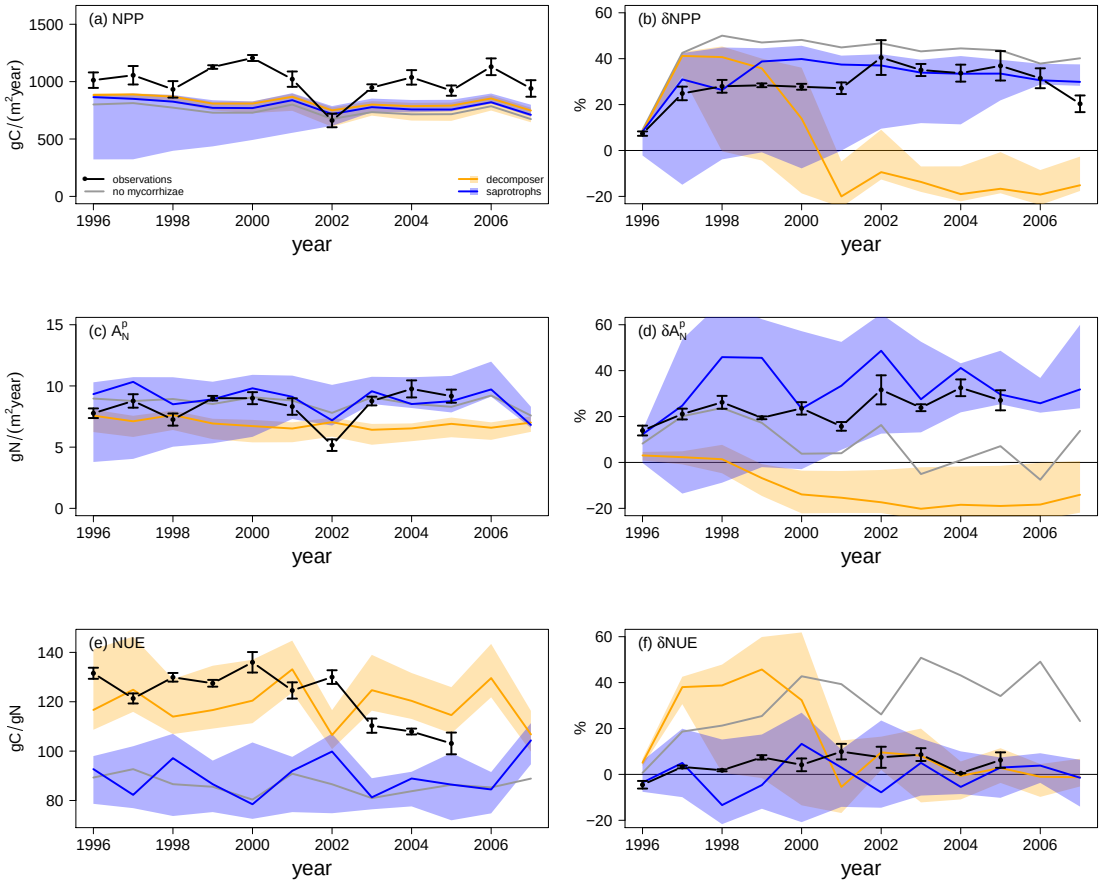

Figure 3.10.: Simulation-observation comparison for the Duke FACE experiment for net primary production (NPP; a, b), plant N acquisition (A_N^p; c, d), and N-use efficiency (NUE; e, f), from ambient CO_2 simulations and treatments (a, c, e), and in response to elevated CO_2 (b, d, f), which is calculated by eq. 3.19.
Grey: QUINCY without mycorrhizae, orange: QUINCY with decomposing mycorrhizae, blue: QUINCY with saprotrophic mycorrhizae, black: observations, averaged over treatments with error bars indication ± 1 SE. Shaded ribbons present min-max range of LHS simulations.

Table 3.6.: Initial and long-term/end responses of NPP (δNPP), plant N acquisition (δA_N^p) and plant N-use efficiency (δNUE) to elevated CO_2. Initial response is defined as 1^{st} year response, whereas end/long-term response is given by the mean $\pm$ 1 SD over the last 5 years of FACE experiment of standard parameterization simulations.

		observation	no mycorrhizae	decomposers	saprotrophs
δNPP [%]	initial	7.3	8.9	8.3	8.5
	end	31.4 $\pm$ 3.2	41.9 $\pm$ 1.3	-16.7 $\pm$ 1.5	32.3 $\pm$ 1.2
δA_N^p [%]	initial	13.9	8.2	3.0	12.2
	end	27.7 $\pm$ 3.3	1.8 $\pm$ 2.0	-18.0 $\pm$ 1.1	31.2 $\pm$ 3.2
δNUE [%]	initial	-4.5	0.6	5.1	-3.6
	end	5.1 $\pm$ 3.0	40.1 $\pm$ 11.3	1.6 $\pm$ 0.6	1.0 $\pm$ 1.1

3.4.2. Assessment of ecosystem carbon storage

Simulated ecosystem C content (C_{Eco}) changes in the presence of mycorrhizal fungi (fig. 3.11a), caused by their interaction with SOM to make N accessible, either by taking SOM-N up directly, or by enhancing SOM decomposition. Both strategies increase simulated heterotrophic respiration already under ambient conditions, which lowers simulated soil organic C content (C_{SOM}) by 22±10% (saprotrophs) and 53±12% (decomposers, sec. 3.3.2.1). Simulated vegetation-C content (C_{Veg}) is almost similar under ambient conditions, which is caused by similar NPP rates. Since NPP contains C for plant biomass production and exudation to mycorrhizal fungi, i.e. mycorrhizal biomass production, simulated mycorrhizal biomass is added to C_{Veg} for this analysis. Under elevated CO_2 concentrations, plants increase C uptake by photosynthesis, which is the only C inflow to ecosystem. This results in an increase of C_{Eco} among all model variants, but is significantly lowered by mycorrhizal presence (fig. 3.11b, tab. 3.7).
C_{Veg} allocation shift towards mycorrhizal biomass leads to a 2% stronger increase of below-ground biomass in the presence of mycorrhizal fungi for both mycorrhizal functionalities compared to the model variant without mycorrhizae (tab. 3.7). Besides, mycorrhizal interaction with SOM to make N accessible changes C_{Eco} allocation responses within the entire ecosystem (fig. 3.11, tab. 3.7).

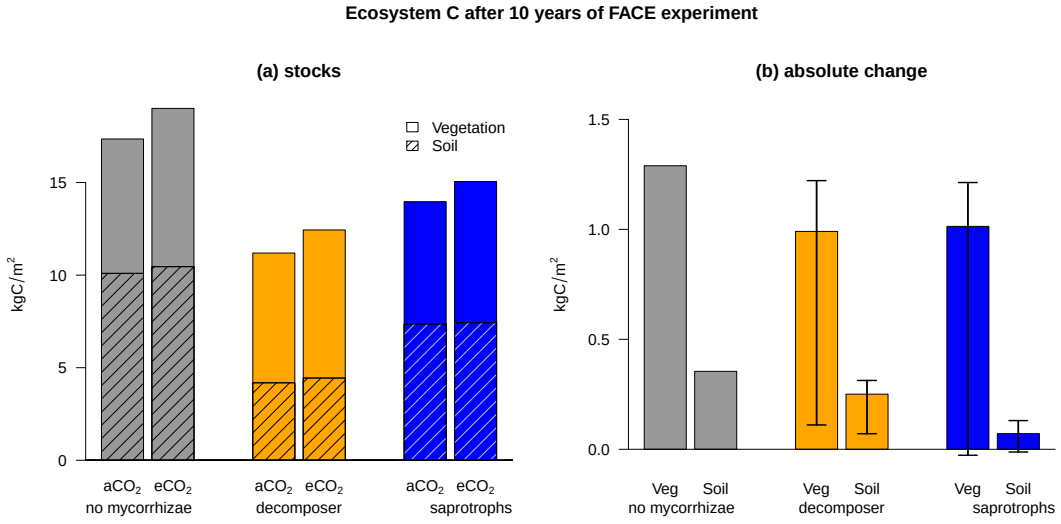

Figure 3.11.: Ecosystem C after 10 years of FACE experiment. (a) C storage of ambient and elevated treatments for soil (shaded) and vegetation, (b) absolute changes in C stocks (eq. 3.20) of vegetation and soil, whereby bars indicate simulations with default parameters (as shown in (a), values can be found in tab. 3.7), and error bars indicate range of LHS simulations. Grey: QUINCY without mycorrhizae, orange: QUINCY with decomposing mycorrhizae, blue: QUINCY with saprotrophic mycorrhizae.

Table 3.7.: Absolute ecosystem C storage response (eq. 3.20) after 10 years of FACE experiment for QUINCY without mycorrhizae and with mycorrhizae with standard parameterization. Values in brackets present min and max response among LHS runs. Values are given in kgC m^{-2}

	no mycorrhizae	decomposers	saprotrophs
Ecosystem	+1.65	+1.25 (+0.18 - +1.53)	+1.09 (-0.03 - +1.32)
Vegetation	+1.29	+0.99 (+0.11 - +1.22)	+1.01 (-0.03 - +1.21)
- above-ground	+1.17	+0.89 (+0.06 - +1.11)	+0.90 (+0.02 - +1.20)
- below-ground	+0.12	+0.10 (-0.01 - +0.21)	+0.11 (-0.03 - +0.19)
Soil	+0.36	+0.26 (+0.07 - +0.31)	+0.08 (-0.01 - +0.13)
- litter	+0.43	+0.28 (+0.04 - +0.41)	+0.17 (-0.01 - +0.40)
- fast	-0.07	-0.02 (-0.03 - +0.00)	+0.02 (-0.00 - +0.03)
- slow	-0.00	-0.00 (-0.01 - +0.02)	-0.11 (-0.15 - +0.00)

I find an increase of C_{Eco} as response to CO_2 fertilization over 10 years in all model variants. This is mainly driven by enhanced C_{Veg}, which is directly influenced by enhanced GPP. Plants allocate new biomass mainly above-ground (approximately 90%), but below-ground allocation response is enhanced by 1.5% in QUINCY simulations with mycorrhizal fungi.

Increase in C_{SOM} is much weaker, because GPP effect on C_{SOM} is indirect and lagged, since C has to enter ecosystem through plants first, that pass C into soil by litter subsequently. Thus, C_{SOM} enhancement is governed by increased litter, whereas both, fast and slow overturning C_{SOM} pools, are slightly decreased as response to eCO_2, caused by an increase of heterotrophic respiration by 3.0±5.5% and 11.3±10.7% in QUINCY simulations with either decomposing or saprotrophic mycorrhizal fungi respectively that show enhanced activity to overcome PNL. This leads to a lower C storage increase under eCO_2 in simulations that take mycorrhizal fungi explicitly into account. Actively mining of SOM as N source actually decreases slow-C_{SOM} content so much, that increased litter-C is almost balanced out.

Overall C_{Eco} storage increase under eCO_2 is 24.2% lower in QUINCY with decomposing mycorrhizae, and 33.9% lower in QUINCY with saprotrophic mycorrhizae compared to QUINCY without mycorrhizae after 10 years of CO_2 fertilization. This leads to a reduction in modelled C_{Eco} stocks after FACE experiment of 6.56 kgC m^{-2} in QUINCY with decomposers, and of 3.95 kgC m^{-2} in QUINCY with saprotrophic mycorrhizae due to already lower C stocks under ambient conditions (fig.: 3.11a). However, the actual C increase in both, vegetation and soil stocks, is highly uncertain, caused by (i) already lower C stocks under ambient conditions, which have a lower absolute response, even if relative response is equal or higher, (ii) mycorrhizal ability to prevent plants from PNL, which is necessary to increase C_{Veg}, and (iii) mycorrhizal interaction with SOM, which potentially decreases C_{SOM} (fig. 3.11b). The significantly lower response of C_{SOM} to eCO_2 in QUINCY with mycorrhizae is in line with observations of *Lichter et al.* (2008) and, who reported only minor C_{SOM} enhancement in response to eCO_2 after 9 years of fertilization at Duke.

3.5. Results III: Global assessment of forest ecosystem responses to elevated CO_2

I finally assess the importance of mycorrhizal processes and implications for future model developments and climate change predictions on the global scale. To address this, I run QUINCY (revision 1878) with both mycorrhizal functionalities, as well as QUINCY without mycorrhizae as reference for 42 forest sites[5] of the GFDB (sec. 2.2.3.1) with a 500-year spin-up period, either with the standard model protocol and input data (sec. 2.2.2), and with CO_2 fertilization, where I add 200 ppm CO_2 to transient climate starting from 1976. I average model results for 30 years, i.e. 1986 - 2015 to avoid effects of inter-annual climate variability.
Since the 42 analyzed forests are only monitored under ambient conditions, I calculate modelled N acquisition responses to eCO_2 in relation to C investment responses to eCO_2. This relation was investigated by *Terrer et al.* (2018) among 12 free-air CO_2 enrichment (FACE) experiments with 20 sites in total, and a comparison allows me to rate the performance of the MYC model on a broader scale, before I assess the question, how the MYC model generally affects ecosystem C (C_{Eco}) storage in response to eCO_2.

3.5.1. Nitrogen return on carbon investment responses to elevated CO_2

Terrer et al. (2018) defined a *return on investment* ratio (Ψ_N^{-1}, eq. 3.21) to describe the link between N acquisition response and below-ground C allocation response to eCO_2.

$$\Psi_N^{-1} = \frac{\delta A_N^p}{\delta C_{bg}^p} \,, \qquad with \tag{3.21a}$$

$$A_N^p = U_N^p + \Delta E_N \,, \qquad and \tag{3.21b}$$

$$C_{bg}^p = C_{fr} + \Delta E_C \tag{3.21c}$$

with Ψ_N^{-1} as *return on investment* ratio after *Terrer et al.* (2018), eq. 1, derived from plant N acquisition response (δA_N^p), and plant below-ground C allocation response (δC_{bg}^p) to eCO_2, calculated after equation 3.19. Plant N acquisition (A_N^p) is the sum from plant root uptake (U_N^p) and export from mycorrhizal fungi (ΔE_N) and plant below-ground C allocation (C_{bg}^p) is the sum of allocation to fine roots (C_{fr}) and to mycorrhizal fungi (ΔE_C)[6].

[5] I exclude 19 sites from the presented 61 that were harvested after 1960, since harvest strongly influence plant growth rates as well as N availability in soil (sec. 2.3.2.3 and sec. 3.3.2.1).

[6] Since below-ground data are scarce, *Terrer et al.* (2018) used widely fine root growth response to eCO_2 as proxy for total below-ground C allocation response to eCO_2 that contains also C transfer to mycorrhizal fungi (and N fixers). An assessment of potential mismatch to my simulations can be found in appendix C.3.

Modelled *return on investment* ratios are in a similar range to estimates by *Terrer et al.* (2018), which are derived from FACE observations. This supports modelled results and the assumption that the inclusion of mycorrhizal fungi may be the key to understand and predict ecosystem CN dynamics (sec. 3.1.1). It further justifies the global application of the MYC model that was only evaluated and tested on site-level at Duke (sec. 3.3 and sec. 3.4).

I find a strong positive relationship between the N acquisition response to eCO_2 and the below-ground C allocation response only for saprotrophic mycorrhizae, whereas the *return on investment* ratios estimated from QUINCY simulations without mycorrhizae or with decomposers tend to be zero or negative. This indicates again, that only saprotrophs are able to ensure sufficient N and prevent plants from progressive N limitation (sec. 3.4.1). *Terrer et al.* (2018) found a strong relationship between N acquisition and below-ground C allocation response to eCO_2 at sites that have ectomycorrhizae (EMs), whereas sites that contain arbuscular mycorrhizae (AMs) are found to show no or even a rather negative relationship between N acquisition and below-ground C allocation response to eCO_2.
Combining these findings suggests (i) that it may be the ability of EMs to act as potential saprotrophs and acquire N directly from organic sources that prevent plants from PNL, and (ii) that AMs may potentially relay on mineral uptake as plants (and mycorrhizae) do in QUINCY without mycorrhizae or with decomposers.

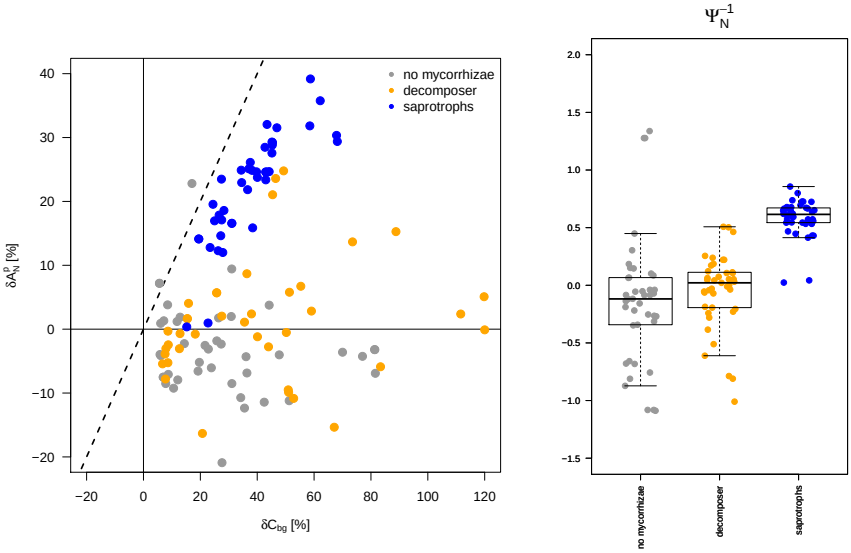

Figure 3.12.: Plant N return on C investment response to eCO_2. (a) Relationship between relative plant N acquisition ('N return') and below-ground C allocation ('C investment') responses to eCO_2 for 42 out of 61 forest sites of the GFDB (sec. 2.2.3.1) modelled by QUINCY without mycorrhizae (grey), QUINCY with decomposing mycorrhizae (orange), and QUINCY with saprotrophic mycorrhizae (blue). Black dashed line presents the 1:1 line. (b) Return on investment (Ψ_N^{-1}) among mycorrhizal types. Dots present individual site ratios, whereas boxes indicate inner-quartile range, divided by median. Whiskers show 10%- and 90%-quantile.

3.5.2. Global forest ecosystem responses to elevated CO_2

Absolute vegetation C (C_{Veg}) response to eCO_2 (eq. 3.20) is highest in QUINCY with saprotrophs (+2.41$\pm$1.07 kgC m^{-2}), and lowest in QUINCY without mycorrhizae (+0.88 $\pm$1.31 kgC m^{-2}, fig. 3.13a). This is caused by increasing progressive N limitation (PNL), which is more sever in this study than in the previous Duke FACE study, because of the much longer fertilization duration. Even QUINCY with decomposers simulate a higher C_{Veg} response (+0.97$\pm$1.22 kgC m^{-2}) indicating that the decomposing functionality is supporting plant N acquisition in response to eCO_2 only on longer time scales, but not within the previously analyzed rather short period of 10 years at Duke (sec. 3.4.2). This suggests that the confirmation or rejection of H3.2 that mycorrhizal fungi will increase internal N cycling and thus prevent plants from PNL is a question of the analyzed period. I can confirm H3.2 for saprotrophic mycorrhizae at any time-scale. But since the the acceleration of internal N cycling by an increased decomposition rate acts slower than the direct access of SOM as N source, H3.2 fails on shorter time scales with decomposing, but could be proven true on longer time scales.
In contrast to C_{Veg} responses, long-term C_{SOM} responses among GFDB forests are similar to short-term C_{SOM} responses at Duke due to the persistent increase of heterotrophic respiration under eCO_2. This reduces C_{SOM} response especially in the presence of mycorrhizae, which enhance heterotrophic respiration by both functionalities. However, mycorrhizal activities do not only lower C_{SOM} response, but also reduce the spread among sites (fig. 3.13b).
Consequently, the spread in simulated C_{Eco} response to eCO_2 is lower in QUINCY with mycorrhizal fungi than in QUINCY without mycorrhizae, and values are still highest for forest simulations by QUINCY with saprotrophs (+20.3% on average compared to QUINCY without mycorrhizae), caused by strongly enhanced C_{Veg} (fig. 3.13c). Since C_{Veg} enhancement under eCO_2 is weaker in QUINCY with decomposers than in QUINCY with saprotrophs due to the delayed prevention of PNL, and C_{SOM} responses are generally lower in QUINCY with any mycorrhizae, C_{Eco} response in QUINCY simulations with decomposers is lower than in QUINCY without mycorrhizae (-31% on average). Thus, I can neither confirm or reject H3.4, i.e. that modelling mycorrhizal fungi explicitly generally decreases simulated C_{Eco} response to eCO_2. Current results suggest, that the strong positive response of C_{Veg} leads to a slightly stronger positive response of C_{Eco} to eCO_2 in QUINCY with saprotrophic mycorrhizae compared to QUINCY with no mycorrhizae and that the weaker response in C_{Veg} in QUINCY with decomposers results in smaller C_{Eco} response. However, as I found that C_{Veg} response in QUINCY with decomposers is strongly dependent on the analyzed time-scale, this may actually change for even longer periods. Nevertheless, these shifts in C_{Veg}, C_{SOM}, and C_{Eco} responses to eCO_2 are not significant, particularly because of the high spread among QUINCY simulations without mycorrhizae.
But the general reduction of the spread among sites by the inclusion of any mycorrhizae suggests that the inclusion of mycorrhizal fungi into TBMs has the ability to reduce climate-change prediction uncertainty and current model disagreement in future land

C uptake predictions (sec. 1.2.4.1) by reducing the spread that is caused by an inappropriate simulation of plant N acquisition and its dynamic response to eCO_2.

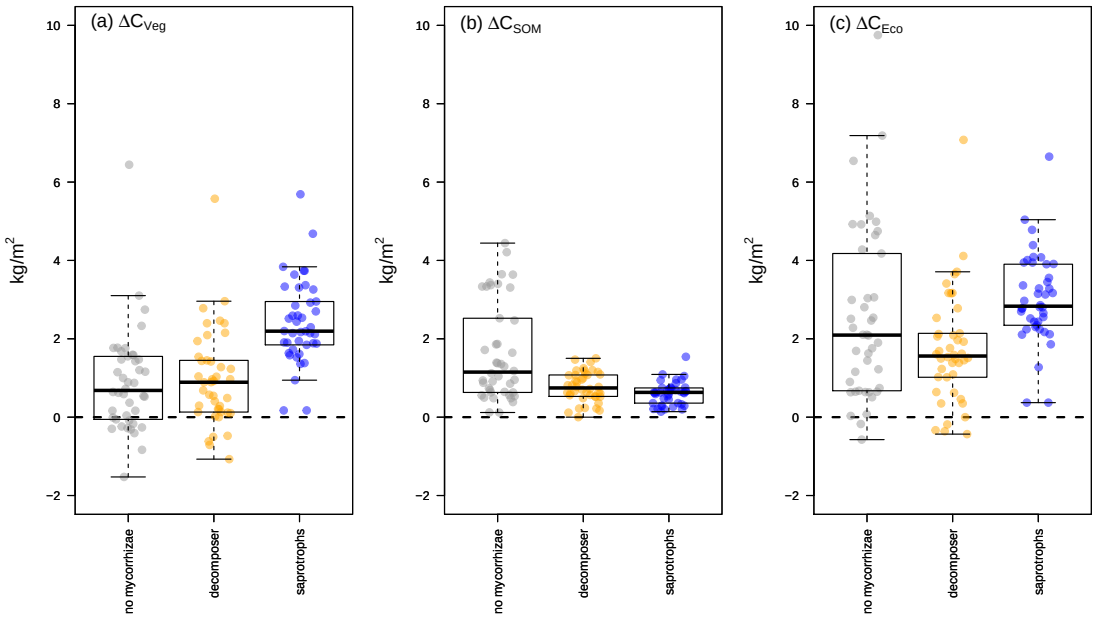

Figure 3.13.: Absolute ecosystem C storage response to eCO_2 (eq. 3.20) among 42 mature forest sites from GFDB (sec. 2.2.3.1). (a) Vegetation C response, (b) SOM C response, and (c) ecosystem C response, modelled by QUINCY without mycorrhizal fungi (grey), QUINCY with decomposing mycorrhizae (orange), and QUINCY with saprotrophic mycorrhizae (blue). Dots present individual sites, whereas boxes indicate inner-quartile range, divided by median. Whiskers show 10%- and 90%-quantile.

3.6. Summary and Discussion

I integrated a dynamical plant-mycorrhiza interaction (MYC) model in the terrestrial biosphere model (TBM) QUINCY (*Thum et al.* (2019)) to assess the importance of mycorrhizal fungi for TBM predictions by testing hypotheses for mycorrhizal functionalities based on observational findings. Based on this, I estimated implications for model predictions and uncertainty regarding soil and vegetation C storage in response to elevated atmospheric CO_2 concentration (eCO_2).

3.6.1. Discussion of MYC model simplifications and assumptions

The presented MYC model is developed to build a bridge between explicit individual based mycorrhizal models, and implicit mycorrhizal effects in TBMs (sec. 3.1.2). The development was limited by several constraints that either evolve from QUINCY framework or study setup, or from limited observations.

MYC model limitations due to model constraints
At its current state, the MYC model neglects P and water supply by mycorrhizal fungi, which is an issue, because vegetation represented by QUINCY is sensitive to both. Consequently, QUINCY-plants grow roots in order to fulfill their P and water demand, which also take up N, and make mycorrhizae potentially redundant for plant N acquisition, which is why plants exude only the minimum amount of C to hosted fungi to avoid mycorrhizal extinction. Besides, other studies have shown that rhizosphere priming, i.e. all processes within plant root system that influence SOM degradation, is potentially not only driven by plants and soil nutrient availability, but also directly influenced by soil properties, such as texture or chemistry, and climate variables, such as temperature and precipitation (*Cheng et al.* (2014)). Thus, a link between water availability and plant-mycorrhiza interactions is highly desirable. Plant leaf-to-root ratio also neglects mycorrhizal biomass, which again forces plants to grow more roots than they need in the presence of mycorrhizal fungi to ensure nutrient and water supplies, as well as physical stability. The inclusion of mycorrhizal fungi to P and water supply, and plant leaf-to-root ratio would therefore potentially intensify the meaning of mycorrhizal fungi for host plants and probably reduce uncertainty, especially under changing environmental conditions.
The fixed CN ratio of the slow decomposing SOM pool in QUINCY that is accessed as N source by SOM mining mycorrhizae causes issues. Since the CN ratio of slow-SOM has to be maintained, uptake of SOM-N requires a loss of SOM-C. I decided therefore to enable SOM-C uptake by mycorrhizae, i.e. turning them into actual saprotrophs, in case this C is attached to SOM-N to avoid unrealistic high C losses. Even if saprotrophic behavior is occasionally observed (*Wu et al.* (2005), *Treseder et al.* (2007)), mycorrhizae usually rely on plant C supply solely and are considered to lack saprotrophic abilities (*Frey* (2019)). A probably better solution would therefor be to allow C accumulation by mineralization or immobilization in the presence of (saprotrophic) mycorrhizae by a revision of the fixed CN ratio of slow-SOM in QUINCY.

MYC model limitations due to observational constraints
The MYC model contains 17 parameters in total (13 belong to both functionalities, two are specifically for each functionality), from which I found data or estimates for only seven parameters. Two out of these seven are based on former modelling studies, and the other five observation-based parameters vary partly over magnitudes (tab. 3.1). This is caused by large difficulties to measure within the rhizosphere without destructing plant-mycorrhizae symbiosis. This obviously limits the ability to constrain the MYC model and forced me to estimate many parameters hypothetically. Fluxes within the MYC model, which describe mycorrhizal C and N exchange with host plants and soil, are therefore highly uncertain and sensitive to parameter variations, whereas plants related or plant demand controlled fluxes are better constrained due to a much higher amount of plant measurements, such as GPP or NPP (sec. 3.3.2.2). This justifies to some extend the use of plant root measurements, such as fine-root biomass or plant C allocation into fine-root growth, as proxy for mycorrhizal biomass or C transfer from host plant to fungi, but the resulting systematic underestimation of flux responses to eCO_2 clearly points out the need of observational data about mycorrhizae (sec. 3.5.1 and app. C.3).
Besides, I decided to develop the MYC model based on proposed mycorrhizal functionalities within the soil, and not based on mycorrhizal types, owing to very limited knowledge about the actual functional differences between mycorrhizal types (sec. 3.1.1). However, an increasing amount of studies show that mycorrhizal types are an important factor for understanding vegetation-soil interactions and soil dynamics (*Phillips et al.* (2013) *Brzostek et al.* (2014), *Sulman et al.* (2014), *Brzostek et al.* (2015)) and predicting plant response to elevated CO_2 (*Terrer et al.* (2016), *Sulman et al.* (2017), *Terrer et al.* (2018)). This also necessitates further measurement-based research on their functions to allow a proper inclusion of mycorrhizal fungi into TBMs in order to reduce current uncertainty of modelled future land C uptake.

3.6.2. Confirmation/Rejection of hypotheses

H3.1: The explicit formulation of mycorrhizal fungi speeds up internal N cycling within the ecosystem.
Model variants with mycorrhizal fungi enhance plant N acquisition compared to the model variant without mycorrhizal fungi. This confirms H3.1, as general soil N or ecosystem N are not increased significantly. Increased plant N acquisition therefore indicates that the internal N cycling is accelerated, because N, which has entered soil by litter fall, becomes again plant-available sooner. This is due to (i) saprotrophic mycorrhizae that build a short-cut within the ecosystem N cycle by mining the slow decomposing SOM pool as N source or (ii) decomposing mycorrhizae that accelerate SOM decomposition and mineralization by exuding C to SOM (sec. 3.3.1 and sec. 3.5.2).
The general influence on ecosystem (C and) N cycling by modelling mycorrhizal fungi explicitly, was also found by *Meyer et al.* (2010), *Meyer et al.* (2012) and *He et al.* (2018), whereby they reported great variations among specific stands, even though they only simulated ectomycorrhizae (EMs), which were allowed to access SOM for N uptake, i.e.

were modelled as saprotrophs. *Phillips et al.* (2013), *Brzostek et al.* (2015) and *Sulman et al.* (2017) further observed different effects of modelling arbuscular mycorrhizae (AMs) and EMs. However, all agreed on an general effect of modelling mycorrhizal fungi on ecosystem N dynamics as hypothesized (H3.1) and found within this study.

H3.2: The explicit formulation of mycorrhizal fungi prevent plants from progressive N limitation under eCO_2 by the acceleration of N cycling (H3.1).
Simulated NPP response to eCO_2 agrees with observations from the Duke FACE experiment (*Finzi et al.* (2007), *Zaehle et al.* (2014)) for QUINCY without mycorrhizae and with saprotrophic mycorrhizae. In contrast to that, NPP response with decomposers is negative, which is contradictory to observations. This behavior is caused by the inability of the ecosystem to provide enough N for growth over the observed and analyzed period of 10 years, which causes progressive N limitation (PNL), confirmed by N acquisition rate under eCO_2. Modelled response of plant N acquisition rates to eCO_2 with decomposers is almost zero during the first years of experiment, and negative afterwards, which implies that PNL is actually more severe with decomposers than without mycorrhizae, because of competition of mineral N with mycorrhizal fungi. They take up N from soil more efficiently, but hold it back to maintain their own CN ratio instead of supporting their host plants, which is why plants with decomposers are not able to increase N acquisition rates under eCO_2 at all and run into PNL very soon. The tested decomposing functionality is obviously not working here, because (i) the effect on N mineralization is too small to provide sufficient N for plants and mycorrhizae on this time scale, and (ii) plants do not recognize that mycorrhizae are fulfilling their functionality, but feel competition, which is why they only host the minimum amount of mycorrhizal fungi. This even leads to less mycorrhizal interaction with SOM and intensifies the N limitation in ecosystem compared to QUINCY without mycorrhizae. One could solve this problem with a stronger acceleration of decomposition rates in the presence of decomposers, but because of already very low SOM stocks caused by this functionality, this is an unrealistic solution. This indicates that the decomposing functionality is too implicit and passive via mycorrhizal fungi to be actively used by plants to avoid PNL on the short term. However, my modelling CO_2 fertilization experiment that persists over 40 years showed that the decomposing functionality is working in forest ecosystems on longer time periods (sec. 3.4.1 and sec. 3.5.2). However, this competitive behavior of decomposers may link this functionality to AMs, as they are hypothesized to act strong competitive than EMs (*Brzostek et al.* (2015)).
In contrast to that, plants in QUINCY with saprotrophs are able to increase N acquisition rates under eCO_2 immediately and this effect persists also over longer time periods (sec. 3.4.1, sec. 3.5.1, and sec. 3.5.2). In comparison to plants in QUINCY without mycorrhizae, I see that plants in QUINCY with saprotrophs are able to avoid PNL by increasing plant N acquisition in response to eCO_2 instead of changing N-use efficiency. This may link this behavior to EMs, as Duke forest is reported to have EMs (*Finzi et al.* (2006), *Finzi et al.* (2007), *Lichter et al.* (2008)).

Regarding discussed hypothesis H3.2 that the explicit formulation of mycorrhizal fungi prevent plants from progressive N limitation under eCO_2, I can only confirm this for saprotrophic mycorrhizae that are actively used by plants to avoid PNL at any time scale, but have to reject it for decomposing mycorrhizae on shorter periods.

H3.3: The explicit formulation of mycorrhizal fungi increases heterotrophic respiration, which decreases soil organic C stocks.
QUINCY without mycorrhizae simulates an ecosystem that contains significantly more C than QUINCY with both mycorrhizal types. Both mycorrhizal strategies increase heterotrophic respiration, either by speeding up decomposition, or by uptake of SOM-N that requires loss of SOM-C, because the CN ratio of the slow-SOM pool of QUINCY is fixed. Both mycorrhizal types therefore increase heterotrophic respiration and consequently decrease soil organic C (C_{SOM}) content, which confirms H3.3, even if this effect is rather contradictory to observations that report C accumulation in ecosystems with mycorrhizal fungi (sec. 3.3.2.1).
However, as almost all ecosystems contain mycorrhizal fungi (*Read* (1991)), even if TBMs usually do not simulate them explicitly, the follow-up questions that need to be addressed by experiments are: Where does freshly assimilated C go and when does it enter the rhizosphere? How long does it stay within the ecosystem? Is this depending on plant N/nutrient demand? I therefore need experiments that measure at least over one growing season, preferably longer, and track C by isotopic signature throughout the entire ecosystem. Only long-term observations will reveal, whether and under which conditions mycorrhizae cause C is accumulation in ecosystems.

H3.4: The explicit formulation of mycorrhizal fungi supports plant growth (H3.2) and increases vegetation C, but reduces soil organic C stocks (H3.3), which reduces ecosystem C storage under eCO_2.
Both mycorrhizal types influence not only plant C allocation, but also C allocation and storage within the entire ecosystem. This has implications for C storage under eCO_2. Generally, C storage is lower in ecosystems that are modelled by QUINCY with mycorrhizal fungi, because of higher heterotrophic respiration rates (H3.3), which increase further by more than 20% in response to eCO_2. Consequently, C_{SOM} response to eCO_2 is almost zero, and C_{Eco} response is only driven by increased C_{Veg}. This lowers C_{Eco} storage response by a quarter (QUINCY with decomposers) to a third (QUINCY with saprotrophs) compared to QUINCY without mycorrhizal fungi over a time period of 10 years (sec. 3.4.2). This finding is in line with H3.4, and also supported by observations of *Lichter et al.* (2008), who reported only minor effects of eCO_2 on soil C.
However, the long-term modelling CO_2 fertilization experiment showed that the prevention of PNL may increase C_{Veg} response to eCO_2 to an extend that it offset the decrease in C_{SOM} response to eCO_2 in QUINCY simulations with mycorrhizae and leads to a higher C_{Eco} response under eCO_2 (sec. 3.5.2). This implies that I have to reject H3.4 at least for saprotrophic mycorrhizae in the case of long-term experiments, and over even longer time scales likely also for decomposers.

3.6.3. Conclusion and Outlook

Given the lack of data, it is hard to build and constrain an explicit mycorrhiza model, and therefore an implicit model that accounts for mycorrhizal functionalities within the ecosystem may be sufficient and more applicable on the global scale at current state (e.g. FUN-CORPSE, *Sulman et al.* (2019)). However, to *explore* dependencies within a plant-mycorrhiza symbiosis, *define* missing data, and *test* different hypotheses, such as different mycorrhizal functionalities, make such an explicit model both, useful and necessary, to build a bridge between explicit individual plant based models to ecosystem or global scale models. I need a tool to investigate, which fluxes and controlling mechanisms from individual-based observations are important on ecosystem scale to include those into TBMs, or to specify, which experiments are needed to improve model development.

For that aim, I will further develop the MYC model within QUINCY by (i) the addition of biological N fixation as active N acquisition strategy by plants, (ii) the inclusion of P and water support by mycorrhizal fungi, (iii) the consideration of mycorrhizal biomass in plant leaf-to-root ratio, and (iv) the revision of the fixed CN ratio of SOM.
The extension of the MYC model by symbiotic biological N fixation will add another active N acquisition strategy, and result in a fully plant controlled N acquisition model, where plants can decide, whether they accelerate internal N cycling by growing mycorrhizal fungi, or if they increase ecosystem N by enhancing the influx with investment into fixation of atmospheric N_2.
P and water supply, and the addition of mycorrhizal biomass to plant allometry calculations will intensify plant C allocation into mycorrhizal growth, because they will need much less own roots to fulfil either nutrient and water demand, and allometry requirements. However, I have to ensure that plants still grow enough roots to guarantee physical stability, and to provide connections to fungi. This will likely necessitate the revision of most MYC model parameters, because most are fitted to the current model in order to meet plant or ecosystem measurements, but not based on mycorrhiza observations.
Additionally the revision of the fixed SOM-CN ratio in QUINCY is necessary to account for soil C accumulation in the presence of mycorrhizal fungi. This is not a direct effect of mycorrhizae, but the vital interaction of mycorrhizal fungi with SOM to build a short-cut within the ecosystem internal N cycle by either take up SOM-N or accelerate SOM decomposition, requires high C losses, if SOM-CN is fixed. This is partly acceptable, as higher decomposition leads to higher heterotrophic respiration, but the amount of C loss caused by accessing SOM as N source is too high, and has to be lowered by allowing C remains in soil.

Finally, my results suggest that a link between proposed mycorrhizal functionalities and mycorrhizal types is likely possible, because of (i) textbook knowledge, which plant hosts which mycorrhizal type, and (ii) my findings about mycorrhizal functionalities that are important for specific ecosystems. However, at the current state, this link is only implicated

by a similar observed eCO_2 response of forests that contain EMs and modelled response by QUINCY with saprotrophs. This does neither provide any evidence that *all* EMs act saprotrophically, nor that they act *only* saprotrophically, which could justify the implementation of saprotrophic EMs into TBMs. And it does not say anything about AMs that could justify the implementation of non-saprotrophic, or even decomposing AMs into TBMs. Nevertheless a clear link between mycorrhizal type and their functioning on ecosystem scale would enable the use of data that focus on mycorrhizal type, which are largely available, for model development, and is therefore an important direction for further research for both, experimental and modelling approaches.

4. Plant control on forest ecosystem carbon-nitrogen dynamics by variable nitrogen acquisition strategies

4.1. Introduction

Ecosystem carbon (C) balance is tightly coupled to ecosystem nitrogen (N) balance, whereby the C balance is strongly controlled by plants' activity, since C assimilation by plant photosynthesis is the only way for C to enter ecosystems (sec. 1.2.1). Plant C uptake capacity is linked to their ability to also acquire N to meet growth requirements and maintain metabolic processes that also include photosynthesis (sec. 1.2.2.1), and links plant (and ecosystem) C balance to ecosystem N availability (*Vitousek and Howarth* (1991), *Hungate et al.* (2003), *Bonan and Doney* (2018)).
Ecosystem N balance is driven by N gains by deposition and fixation, and losses by gaseous emissions and leaching of SOM and mineral N (sec. 1.2.2, *Galloway et al.* (2004)). These fluxes de- or increase soil N, but only fixation also affects vegetation N content directly, which indicates a strong dependency of plant N acquisition (and following plant C uptake and ecosystem C uptake) by soil processes. Only N losses, i.e. leaching, and nitrification and dinitrification, which drive gaseous losses (sec. 1.2.2), depend on mineral N concentration in soil, and are affected by plants' activity due to uptake of mineral N (*Galloway et al.* (2004)). However, this effect is rather indirect and does not surpass soil control on N provision for plant N acquisition, as internal recycling of N, i.e. N cycling within the ecosystem by decomposition of soil organic material (SOM), covers almost 80% of plant N uptake (*Whittaker et al.* (1979), *Schlesinger and Bernhardt* (2013)). Thus soil processes constrain plant growth and consequently ecosystem C uptake largely, and there may be an emergent reciprocal control on ecosystem balances and dynamics, which are shaped by plants with regard to C and by soil with regard to N. Al least, this is, what most state-of-the-art terrestrial biosphere models (TBMs) simulate, as they have usually very advanced vegetation models, but comparable simple soil models, which are based on first-order decomposition kinetics (sec. 1.2.4, *Parton et al.* (1993)). This may not be an issue when simulating a steady-state ecosystem, where C and N gains are equal to C and N losses, and enough N is recycled within the ecosystem to meet plant N requirements, but may lead to problems under changing environmental conditions. Changing conditions, such as rising atmospheric CO_2 concentrations (cCO_2),

unbalance ecosystem dynamics and may cause shifts in ecosystem balances and adjustments of ecosystem dynamics, i.e. an increased C uptake by plants (and ecosystem) caused by higher cCO_2 requires a similar increase in plant N acquisition. This claims either an increase of ecosystem N in general by increased input fluxes or decreased losses, or an acceleration of N cycling within the ecosystem.
However, since vegetation and soil processes act mostly on different time scales that lead to different response times, and are affected differently by such changes, neither vegetation, nor soil can adjust processes persistently in models, since the fellow part hinders long-term adjustments. This leads to model failures in the prediction of long-term responses to elevated cCO_2 (eCO_2, *Zaehle et al.* (2014)).

Contrary to this modelled reciprocal control of vegetation and soil, there is observational evidence that plants may control soil processes that reveal N, if needed. *Knops et al.* (2002) and *Chapman et al.* (2006) reviewed observational studies and common assumptions, and suggest a stronger plant control on ecosystem N dynamics that is not incorporated into TBMs yet. *Knops et al.* (2002) discuss mechanisms that potentially allow plants to impact ecosystem N cycling in order to increase growth in response to ecosystem changes such as eCO_2, whereby they distinguish between (i) adjustment of plant NUE (*Vitousek* (1982), *D'Antonio and Vitousek* (1992)), (ii) plant control on ecosystem N dynamics by influence microbial activity via litter input (*Schmidt et al.* (1997), or (iii) plant control on ecosystem N gains/losses (*Vitousek et al.* (1987), *Wedin and Tilman* (1990), *Lovett and Lindberg* (1993)). They summarize that an adjustment of plant NUE cannot explain long-term responses to ecosystem changes, and that plant control on microbial community may rather lead to a negative feedback, since stronger microbial activity actually lead to a stronger control of microbes on ecosystem N. This may be caused by a so-called *microbial N loop*, in which microbes exchange N with SOM, but do not mineralize it, so that plants cannot use it. They conclude that plants may control ecosystem N mainly by an indirect control of N gains and losses by interactions with herbivores, soil microbial decomposers, and N fixing bacteria (*Stock et al.* (1995), *De Mazancourt et al.* (1998)). *Chapman et al.* (2006) follow the idea of a plant controlled N cycling within the ecosystem, but they revise the strong control by the microbial community by adding mycorrhizal fungi into the loop, which are stronger plant controlled, and allow plants to *uncork the microbial bottleneck* (*Cornelissen et al.* (2001)). They distinguish between N-conservative plants that strongly control ecosystem N dynamics by utilizing mycorrhizal fungi and N-extravagant plants (*Aerts and Chapin III* (1999)). N-conservative plants are likely to persist in N poor systems, since they access organic N directly, or supported by mycorrhizal fungi (*Chapin III* (1995)). N-extravagant plants produce high-quality, N-rich litter in order to influence microbial activity, but then rely on the speed of the microbial loop as suggested by *Knops et al.* (2002). *Chapman et al.* (2006) conclude that a strong control on ecosystem N is therefore more likely in ecosystems that are N limited and may force plants to act N-conservative, whereas plants may have a weaker control in not N limited systems that allow a N-extravagant strategy.

Further evidence for plant control on at least N acquisition is provided by long-term free-air CO_2 enrichment (FACE) experiments, where plants increased not only C assimilation, but also N acquisition in response to eCO_2. This allows a growth enhancement (*Finzi et al.* (2007)) and a greater C storage within the ecosystem than simulated by TBMs (*Zaehle et al.* (2014)). Actually most TBMs simulate rather an adjustment of NUE that was not shown at three out of four FACE sites (*Finzi et al.* (2007)), instead of an increase of N acquisition (*Zaehle et al.* (2014)).

This points again to a plant control on ecosystem/soil N provision that is not incorporated into TBMs yet, and refers to three questions:
Q1: Where does additional N come from?
Q2: How do plants control processes that supply N?
Q3: To which extent can plants control ecosystem/soil processes?

To address these questions, I have to go deeper into the N balance of ecosystems, ecosystem N sinks and sources, as well as internal N recycling processes, and may potentially have to revise state-of-the-art TBM processes.

4.1.1. Modelled ecosystem nitrogen balance and dynamics: State-of-the-art and potentially missing links

Ecosystem N balance is driven by its sources, i.e. deposition and fixation, and its sinks, i.e. emissions and leaching (fig. 4.1, violet frame).

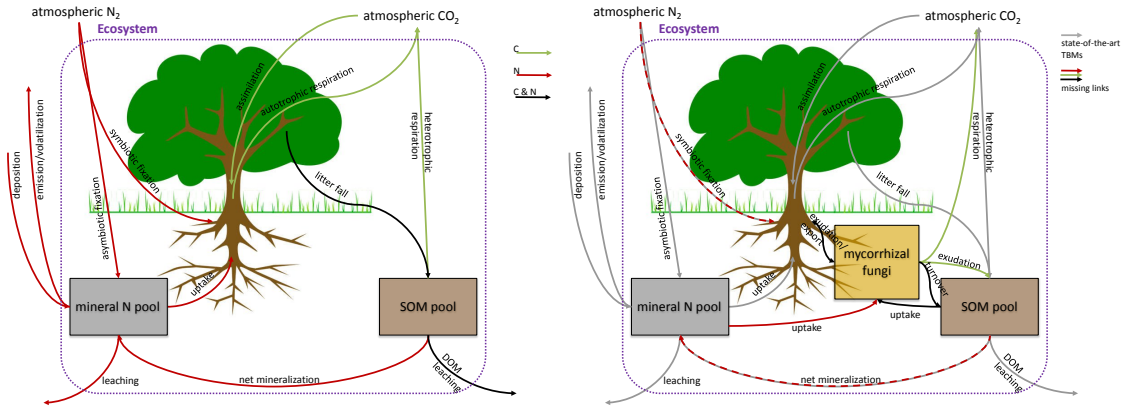

(a) Ecosystem N balance and cycle in state-of-the art TBMs.

(b) Missing fluxes in ecosystem N balance and cycle in state-of-the art TBMs.

Figure 4.1.: Schematic figures of ecosystem N cycle with driving C fluxes in state-of-the-art TBMs (a), and with missing fluxes (b). Ecosystem with included internal N cycle (inside violet frame), and external N sink and source. Tree represents vegetation (pools), boxes represent soil pools. Green arrows: C fluxes, red arrows: N fluxes, black arrows: C and N fluxes. Grey arrows in (b) depict fluxes shown in (a) to highlight additional fluxes.

At first sight, these fluxes are resulting from physical unbalances, chemical reactions, and soil processes, but are not controlled by plants in such am manner that they would increase upon plant demand (fig. 4.1a). However, fixation as symbiotic fixation is actually controlled by plants, which provide anaerobe conditions and carbohydrates to stimulate symbiotic N fixers (sec. 2.1.1). Thus, plants can control parts of ecosystem N influx, and may increase C investment into fixation in response to eCO_2 in order to satisfy their growth requirements (fig. 4.1b).
Recent TBM development therefore tested different approaches of how to include plant controlled symbiotic fixation that range from simple evapotranspiration (ET, e.g. *Cleveland et al.* (1999)) or net primary production (NPP, e.g. *Thornton et al.* (2007)) functions, which are used to describe plant activity as proxy for plant N demand, to more advanced ideas that take plant N demand, soil N availability and/or plant C availability as investment resource directly into account (e.g. *Gerber et al.* (2010), *Fisher et al.* (2010), *Brzostek et al.* (2014)). *Meyerholt et al.* (2016) showed that such approaches are necessary to reduce uncertainties for both, ecosystem C and N responses to eCO_2.

Once N has entered the ecosystem, it is cycled internally (fig. 4.1, violet frame). TBMs simulate mineral N uptake by plants, its incorporation into vegetation biomass, and its turnover into the soil compartment by litter fall. Organic N forms, i.e. litter-N or SOM-N, are inaccessible to plants and need to become plant-available again by decomposition of SOM. Most TBMs follow the CENTURY soil model approach of *Parton et al.* (1993) (fig. 4.1a), which is very simplified and assumes that plants do not affect decomposition. Despite that it is known that plant exudation of C into the rhizosphere accelerates decomposition (*Hodge et al.* (2001)), and that their symbiosis with mycorrhizal fungi short-cuts ecosystem N recycling, since some fungi are able to digest SOM (*Treseder et al.* (2007), *Malcolm et al.* (2008)). By digesting SOM, organic N becomes available for mycorrhizae, and since they deliver N in return to plants N supply, mycorrhizae are an implicit opportunity for plants to access SOM as additional N source (fig. 4.1b, sec. 3.1.1).
Recently, many models are developed that try to simulate plant-mycorrhiza interactions, and/or mycorrhiza-soil interactions, or plant-soil interactions at different levels of detail. They range from individual plant based models with explicit interaction with mycorrhizal fungi (e.g. *Meyer et al.* (2010)), over models that revise the simple first-order decay decomposition of the CENTURY approach (e.g. *Deckmyn et al.* (2011), *Ahrens et al.* (2015)), to models that take mycorrhizae rather implicit into account by calculating their N return on plant C investment without considering their effect on SOM (e.g. *Brzostek et al.* (2014)). However, these model approaches, especially the more explicit ones, are mostly only applied on ecosystem scale, whereas the rather implicit approach of *Brzostek et al.* (2014) runs globally and *Shi et al.* (2016) and *Brzostek et al.* (2017) further point out the necessity to consider plant mycorrhizal support of plant N acquisition on the global scale. The coupling of plant controlled N acquisition that accounts for mycorrhizal fungi to a C explicit soil model was then done by *Sulman et al.* (2017) and extended to a CN version (*Sulman et al.* (2019)).

Latter is, to my knowledge, the only existing model that (i) runs globally, (ii) takes both, plant controlled symbiotic N fixation and mycorrhizal support of plant N demand, into account, and (iii) simulates explicitly vegetation and soil C and N balances to address changes of ecosystem C and N balances in response to eCO_2. Nevertheless, the CENTURY approach is still state-of-the-art in most TBMs, even if results of *Sulman et al.* (2019) emphasize the need of plant controlled N acquisition in order to meet observed plant and ecosystem responses to eCO_2 by TBMs and therefore improve future predictions by reducing uncertainties that are caused by N limits on plant growth under eCO_2. This may also improve estimations of ecosystem impacts to climate change (*Shi et al.* (2019)).

4.1.2. Study scope and hypotheses

In the previous chapters, I implemented two C cost based symbiotic Biological N Fixation (BNF) schemes into the QUINCY model to account for plant control on ecosystem N influx (chapter 2), and developed a plant-MYCorrhiza interaction (MYC) model that covers two different proposed mycorrhizal functionalities within the ecosystem to account for plant control on ecosystem internal N cycling (chapter 3).

The scope of this chapter is to couple both sub-models, i.e. the BNF and the MYC model, to allow plants to actively adjust N acquisition to environmental conditions by either accelerating internal N cycling with the support of mycorrhizal fungi that interact with soil organic matter (SOM), or by fixing atmospheric N_2, which is an ecosystem external source.
I hypothesize that plants generally, i.e. independently from plant type and ecosystem, favor mycorrhizal N support over symbiotic N fixation, as they rather supply their needs by internal ecosystem N acquisition than by accessing ecosystem external N (H4.1, *Whittaker et al.* (1979), *Schlesinger and Bernhardt* (2013)) for economical reasons, i.e. support by mycorrhizal fungi may be cheaper in terms of C investment per unit N than N fixation. But plants invest C into symbiotic fixation, in case they are N limited (H4.2, *Gutschick* (1981)), as atmospheric N_2 represents an unlimited source of N. This may happen either seasonally due to high N demand, or less available N (H4.2a), or in a N-stressed ecosystem (H4.2b), or under elevated CO_2 (eCO_2) that leads to progressive N limitation (PNL, sec. 1.2.2.2, H4.2c). Thus, under specific circumstances (H4.2a - H4.2c), fixation may become the more favorable strategy, because internal N recycling does not fulfill plant N needs, but the C-cost intensive fixation accesses an unlimited N source, i.e. atmospheric N_2. Furthermore, I hypothesize that the use of any additional symbiotic N acquisition strategy to plant root uptake prevent plants from occurring PNL under eCO_2 and enhances growth in short-term response, as well as in long-term response to eCO_2 (H4.3). The persistent positive response of vegetation to eCO_2 leads to a stronger positive ecosystem response to eCO_2 than simulated with the model variant without any symbiotic N acquisition strategy (H4.4).
Besides, the access of ecosystem internal and external N sources stabilize ecosystem N against both, external and internal changes, because plants will balance changes out by changing N acquisition strategy (H4.5).

4.2. Materials and methods

4.2.1. MYFUN model description

The MYcorrhizal export, symbiotic Fixation and plant Uptake of Nitrogen (MYFUN) model (fig. 4.2) is the coupled version of the Biological Nitrogen Fixation (BNF) model (chapter 2, sec.: 2.2.1) and the plant-MYCorrhiza interaction (MYC) model (chapter 3, sec.: 3.2.1), where I combine the C cost based approach of the BNF model, but take plant-mycorrhiza exchange of C and N into account[1].
I start with an extended version of the budget equations of plant labile C and N pool (eq. 1.6) that contains fluxes from the BNF, and the MYC model budget equations (eq. 2.2, and eq. 3.1):

$$\frac{dC_{labile}}{dt} = U_C + \Delta S_C - G_C + \Delta E_C - R_g - R_m - R_{U_N} - R_F \tag{4.1a}$$

$$\frac{dN_{labile}}{dt} = U_N^* + \Delta S_N - G_N + \Delta E_N + F \tag{4.1b}$$

where U_X are uptake rates, * indicates the modification of U_N caused by mycorrhizae (eq. 3.2), ΔS_X net exchange with the storage pools, G_X growth rates. ΔE_X denotes the net exchange fluxes between plants and mycorrhizal fungi, and R respiration rates, whereas R_F is respiration associated with BNF, and F is the fixation rate.

4.2.1.1. The inclusion of mycorrhizal fungi into the fixation scheme carbon cost calculation

To include mycorrhizal fungi into the fixation scheme framework, I implement them in the C cost calculation that is the basis for symbiotic N fixation calculation (sec. 2.2.1, eq. 2.10 and eq. 2.11).

One of the fundamentals of the MYC model is that plants have to exude C to hosted fungi to avoid their extinction, even if plants do not need mycorrhizal N support, or do not benefit from mycorrhizal fungi (sec. 3.2.1, eq. 3.6). Consequently, I cannot treat them similarly to symbiotic fixation, which can be entirely eliminated by plants in the model, in case they do not need N support. Besides, almost all terrestrial plant spices host mycorrhizal fungi (*Read* (1991)), whereas only some host N fixers (*Gutschick* (1981)).
Therefore I consider mycorrhizal fungi as part of plant root system and modify root uptake costs to rhizosphere uptake costs that are compared to fixation costs to determine symbiotic N fixation rates (fig. 4.3). This idea is in contrast to the approach of *Brzostek et al.* (2014) and *Sulman et al.* (2019), which calculates the C allocation into all N acquisition strategies only based on the relative C costs for each N acquisition strategy individually.

[1] For both sub-model parts, i.e. the BNF model and the MYC model, I do not change any previously determined parameters. Parameters can be found in table 2.1 for the BNF model and table 3.1 for the MYC model.

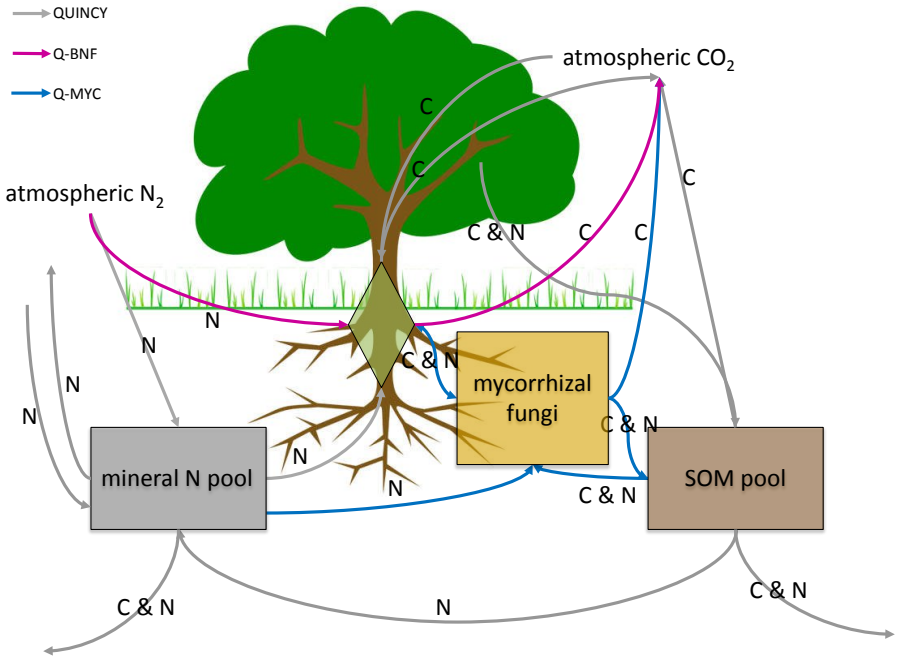

Figure 4.2.: Schematic figure of MYFUN model fluxes within QUINCY framework. Diamond represents plant labile pool, boxes represent soil pools. Grey arrows: QUINCY (section 1.2.4.3), purple arrows: BNF model (chapter 2), blue arrows: MYC model (chapter 3). See figure 4.1 for flux terms.

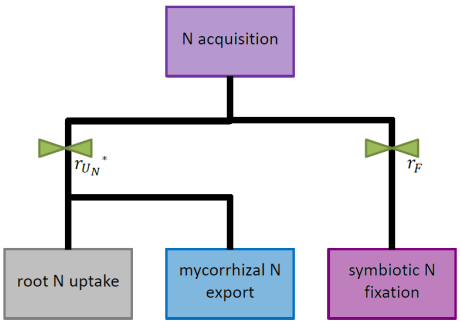

Figure 4.3.: Conceptual idea of MYFUN model hierarchy based on BNF scheme concept (fig. 2.2). Hosting mycorrhizal fungi is assumed to be mandatory, which is why their effect on plant N acquisition is added to plant N uptake, *before* N fixation is calculated on the basis of C costs. Comparative C costs, which are used to calculate fixation rates, therefore represent rhizosphere N acquisition ($r^*_{U_N}$), including N gain by plant roots and mycorrhizal fungi and the C investment into both, and symbiotic N fixation (r_F).

I estimate a gain by mycorrhizae (g_{myc}) that I add to N gain by roots (g_N) to modify equation 2.5. By adding g_{myc} resulting r_{opp} becomes lower, which lowers rhizosphere uptake costs in the presence of mycorrhizal fungi. g_{myc} is derived from net C investment into mycorrhizal fungi (ΔE_C) and N export from mycorrhizal fungi (ΔE_C, eq. 3.3) and averaged over the life span of mycorrhizae (τ_{myc}) to account for their on-going support once plants invested C into their growth.

$$r^*_{opp} = \frac{g_C}{g_N + g_{myc}}, \; with \tag{4.2a}$$

$$g_{myc} = \frac{\Delta E_N}{\Delta E_C} \tag{4.2b}$$

where r^*_{opp} are modified opportunity costs (eq. 2.4b) for rhizosphere N acquisition that include mycorrhizal influence by mycorrhizal gain (g_{myc}) for plants.

Finally, I replace opportunity costs for root uptake by opportunity costs for rhizosphere N acquisition in root uptake cost calculation (eq. 2.4a) that is used for N fixation calculations by both N fixation schemes (eq. 2.10 and eq. 2.11).

4.2.1.2. Coupling choices

Having included two different C cost based symbiotic N fixation schemes, i.e. the optimal scheme and the resistance scheme (sec. 2.2.1), and having implemented two different mycorrhizal functionalities, i.e. saprotrophic mycorrhizae and decomposing mycorrhizae (sec. 3.2.1), into QUINCY (sec. 1.2.4.3) would allow to run QUINCY with four different combinations. Considering the standard fixation, which is part of the QUINCY model, and the option of 'no mycorrhizae' increases the number of potential combinations to nine (tab. 4.1).

Table 4.1.: Potential and chosen BNF-MYC combinations for MYFUN.
Chosen combinations are marked by an X. For model variant names see table 4.2.

		BNF		
		standard	optimal	resistance
MYC	no	X	X	
	saprotrophs	X	X	
	decomposer			

However, I decided to couple only the optimal N fixation scheme and saprotrophic mycorrhizae, and neglect the resistance N fixation scheme and decomposing mycorrhizae for this study for the following reasons:

BNF scheme testing has shown issues for both fixation schemes, but unrealistic high fixation rates that are simulated by resistance scheme are much more problematic than the delayed seasonal pattern of N fixation, which is simulated by optimal scheme. Besides, testing has shown, that plants may not use soil N for N acquisition by root uptake anymore, in case they get too much N from fixation. This issue may become more severe, when coupling mycorrhizae to fixation schemes, as high fixation rates, which are simulated by resistance scheme, are actually not plant controlled, but forced by resistance scheme (sec. 2.5).
Lacking control on N fixation is contrary to the underlying assumption that plants favor mycorrhizal support. So I decided to use only the optimal fixation scheme (and the standard scheme for comparison) for this study.

MYC model evaluation has shown, that the decomposing functionality is too implicit to be used actively by plants in order to acquire N in case of limitation, whereas saprotrophs are able to support plant N acquisition quickly, if demanded (sec. 3.4.2 and sec. 3.6). Thus, plant have stronger control on saprotrophic mycorrhizae, which may be needed to compete with N fixation as additional strategy. This is why I choose only saprotrophic mycorrhizae for the plant controlled MYFUN model in this study (in comparison with *no mycorrhizae*).

4.2.2. Observational Data

For model comparison, I use again the GFDB sites (sec. 2.2.3.1, *Luyssaert et al.* (2007)), whereby I exclude sites that are harvested after 1960. Harvest caused issues for both N fixation schemes (sec. 2.3.2.3), as well as for both mycorrhizal functionalities (sec. 3.3.2.1) by high litter input into soil and resulting high N availability in soil. Harvest is therefor likely to cause issues for MYFUN as well, which I try to avoid in this study by including only mature forest sites. The global distribution of the remaining 42 forest sites and their PFTs are shown in figure 4.4.

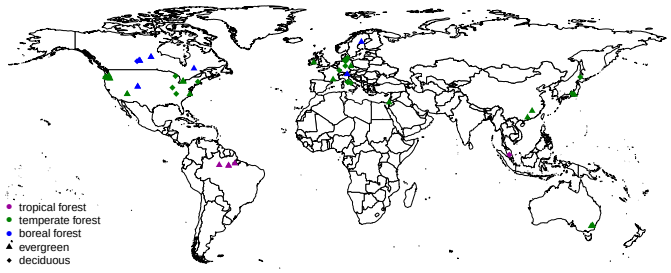

Figure 4.4.: Location and QUINCY PFT characterization of remaining GFDB sites.

4.3. Results I: MYFUN model evaluation

I evaluate QUINCY-MYFUN model (Q-MYFUN) performance in comparison to both, QUINCY (revision 1994) without any plant controlled N acquisition support (QUINCY), and to QUINCY with plant controlled N acquisition support by symbiotic fixation (Q-BNF, optimal fixation scheme, sec. 2.2.1) was well as by export from mycorrhizal fungi (Q-MYC, saprotrophic mycorrhizae, sec. 3.2.1). Table 4.2 presents an overview over the four used model variants and their plant controlled N acquisition strategies.
As the aim of this evaluation is to understand model behavior and causes for different model performance, I do not compare simulations to any observational data in this section. Besides, N acquisition data, as well as seasonal C-flux measurements are not available for the GFDB sites.

Table 4.2.: Overview over plant controlled N acquisition strategies among model variants.

	QUINCY	Q-BNF	Q-MYC	Q-MYFUN
root uptake	yes	yes	yes[a]	yes[a]
mycorrhizal support	no	no	yes[b]	yes[b]
symbiotic fixation	no[c]	yes[d]	no[c]	yes[d]

[a] modified due to the presence of mycorrhizal fungi (sec. 3.2.1)
[b] saprotrophic mycorrhizae (sec. 3.2.1)
[c] fixation scheme: standard (sec. 2.2.1)
[d] fixation scheme: optimal (sec. 2.2.1)

I start the assessment by comparing annual N acquisition rates among all GFBD sites that are not harvested after 1960 (sec. 4.2.2), before I focus on seasonal behavior of N acquisition and C investment into different strategies for specific sites. Lastly I address the question, if and how plants change N acquisition strategy in case they are N limited and how this influences ecosystem N. All runs are done with the model protocol and input data that are presented in section 2.2.2 with a 500-year spin-up period.

4.3.1. Simulated plant nitrogen acquisition among GFDB sites

Generally plant N acquisition (A_N) is increased by 26$\pm$2% with all additional plant controlled N acquisition variants (tab. 4.3) compared to QUINCY, whereby Q-BNF simulates highest annual N acquisition among GFDB sites, and Q-MYFUN lowest (tab. 4.3).
Interestingly, N acquisition in Q-BNF is mainly done by root uptake, and not by the additional possible N acquisition strategy, i.e. symbiotic fixation. Root uptake simulated by Q-BNF is 21% higher than simulated by QUINCY, and only minor supported by symbiotic fixation, which indicates higher N availability in the entire ecosystem from previous fixation. Initially fixed N that is part of plant tissues becomes part of soil organic material (SOM) after senescence or in case of death, is decomposed, and finally mineralized,

which enhances N availability for root uptake. Thus, in an evolved ecosystem, root uptake is the major part of N acquisition, and N fixation plays only a minor role (sec. 2.3.2.3). This finding implies again that present-day fixation may be limited, which is in accordance with generally low observed fixation rates (*Vitousek and Howarth* (1991), *Cleveland et al.* (1999)). But fixation may have a long-lasting effect, since N that has entered ecosystems once has a long turnover time, and is often internally recycled until it leaves the ecosystem again. Contrary to that, Q-MYC increases N acquisition mainly by the additional plant controlled N acquisition strategy, i.e. mycorrhizal support, which covers almost 80% of annual N acquisition among GFBD sites. This is close to observations, which report up to 80% of annual plant N acquisition within forest ecosystems via mycorrhizal fungi (*Van Der Heijden et al.* (2008)). Mycorrhizal support is lower in Q-MYFUN, but covers still 64% of annual N acquisition, which still meet the observed range. Root uptake covers 24%, and fixation 12% of simulated annual plant N acquisition by Q-MYFUN. Annual fixation is thereby more than twice as much as in Q-BNF, which indicates less N in ecosystem from previous fixation. This suggests that plants favor mycorrhizal support over symbiotic fixation not only during the analysis period, but throughout the entire simulation period, which is in line with H4.1. However, this behavior may also result from the hierarchical coupling approach that treats symbiotic fixation and mycorrhizal fungi differently by forcing plants to exude C to mycorrhizal fungi to avoid their extinction, whereas symbiotic fixation is entirely optional. To clarify, whether plants actually favor mycorrhizae based on an economical assessment, i.e. based on their C investment to get N in return, I analyze the MYFUN model behavior in more detail for specific sites in the following section.

Table 4.3.: Annual N acquisition rates simulated by QUINCY, Q-BNF, Q-MYC, and Q-MYFUN, presented as mean ± 1SD for the years 1986 - 2015. Values are given in gN $m^{-2}year^{-1}$.

	QUINCY	Q-BNF	Q-MYC	Q-MYFUN
N acquisition	11.15 ± 5.29	14.26 ± 7.99	14.05 ± 6.83	13.90 ± 7.84
root uptake	11.15 ± 5.29	13.50 ± 7.92	2.86 ± 1.55	3.33 ± 2.45
mycorrhizal export	NA	NA	11.20 ± 5.37	8.94 ± 4.83
symbiotic fixation	NA	0.75 ± 0.58	NA	1.64 ± 1.60

4.3.2. Simulated plant nitrogen acquisition and carbon investment at Cascade Head Experimental Forest site

In order to evaluate model performance in more detail, i.e. seasonal pattern of N acquisition, and C investment into N acquisition strategies, I run QUINCY, Q-BNF, Q-MYC, and Q-MYFUN (tab. 4.2) for the Cascade Head Experimental Forest site (CAS, sec. 2.2.3.2). I expect that symbiotic N acquisition is most sensitive to individual plant N demand, and less to other constrains such as climate, since the MYC model is not temperature or humidity sensitive at all, and symbiotic N fixation by the BNF model has been shown to

be more affected by plant N demand than by climate already (sec. 2.3). As N demand is strongly correlated to leaf habit, i.e. deciduous or evergreen, and related phenological cycles, I decided to model CAS, which provides records of both leaf habits (hereafter CAS-E to refer to evergreen stand and CAS-D to refer to the deciduous stand)

As for all GFDB sites, I find an increase of annual N acquisition among QUINCY with plant controlled N acquisition schemes compared to QUINCY without for both stands, whereby increase is strongest for Q-MYFUN (+105.1% at CAS-D, +32.2% at CAS-E), and weakest for Q-MYC at CAS-D (+45.6%), and Q-BNF at CAS-E (+8.3%, tab. 4.4).
Q-BNF increases root uptake at CAS-D by 74.7% compared to QUINCY, which covers 90.8% of annual N acquisition, but symbiotic fixation supports N acquisition throughout the entire year, and especially in winter, when soil N availability is low due to low decomposition and mineralization fluxes (fig. 4.5a). In contrast to that, root uptake is slightly decreased by 4.1% at CAS-E, but still covers 88.5% of annual N acquisition. Symbiotic fixation happens almost throughout the year, but rates are reduced to zero from February to April, indicating either that plants can meet their demand by root uptake or too high fixation costs (fig. 4.5d). By investing C into symbiotic fixation, Q-BNF is increasing biomass production (BP) by 63.5% at CAS-D and 4.9% at CAS-E, which points to strong N limitation on growth at CAS for the deciduous forest stand, and but only mild limitation for the evergreen forest stand that has a lower N demand due to their higher leaf CN ratio (*Kattge et al.* (2011)). Since C-use efficiency (CUE) is actually decreased from 0.55 (QUINCY, CAS-D) to 0.48 (Q-BNF, CAS-D), and 0.47 (QUINCY, CAS-E) to 0.46 (Q-BNF, CAS-E), higher BP is caused by increased C assimilation by photosynthesis due to higher N availability that is used for chlorophyll production and other photosynthetic active enzymes and proteins (tab. 4.4, sec. 4.4.1, fig. 4.10).
In contrast to that, Q-MYC does not support annual N nutrition in a similar way, because N availability in the entire ecosystem in lower. Consequently, internal N cycling, which is increased by mycorrhizal activity, is able to increase plant N acquisition, but not as strong as symbiotic N fixation, which accesses an ecosystem external N source (fig. 4.5b and fig. 4.5e). N limitation on plant growth is more severe at CAS-D caused by the higher N demand of deciduous trees, which lowers BP compared to Q-BNF, but increases BP compared to QUINCY. However, improved N nutrition compared to QUINCY does not influence plant biomass-production efficiency much (0.55 at CAS-D and 0.46 at CAS-E), but actually increases CUE that also includes mycorrhizal biomass (0.61 at CAS-D and 0.49 at CAS-E), which indicates again that especially CAS-D is still N limited, and CAS-E could also enhance growth in case of higher N acquisition (tab. 4.4).
Q-MYFUN enhances plant N acquisition strongest for both stands, but the enhancement is stronger at CAS-D due to higher N demand (fig. 4.5c). Compared to Q-MYC, root uptake as well as mycorrhizal support are increased by 55.7% and 18.6% respectively, indicating higher N availability in soil, which is caused by symbiotic N fixation that covers 12.8% of annual N acquisition at CAS-D and is 50.2% higher than annual fixation simulated by Q-BNF. Thereby fixation is plants' major N acquisition strategy from December

to April due to limited soil N from organic and inorganic sources, but zero the rest of the year, when mycorrhizae are able to export N. This shows the hypothesized preference for this N acquisition strategy (H4.1), but also the utilization of symbiotic N fixation in case neither roots, nor mycorrhizal fungi can meet plant N requirements (H4.2a). The seasonal pattern of fixation is similar at CAS-E (fig. 4.5f), but annual total is 11.8% lower than annual fixation simulated by Q-BNF. Annual mycorrhizal export is also lower (-12.5%) than simulated by Q-MYC, indicating that annual N nutrition at CAS-E is sufficient in Q-MYFUN simulation, or growth is limited by other sources, which is confirmed by slightly increased annual C assimilation rate compared to Q-MYC that does not lead to higher BP (BPE: 0.45, CUE: 0.48).

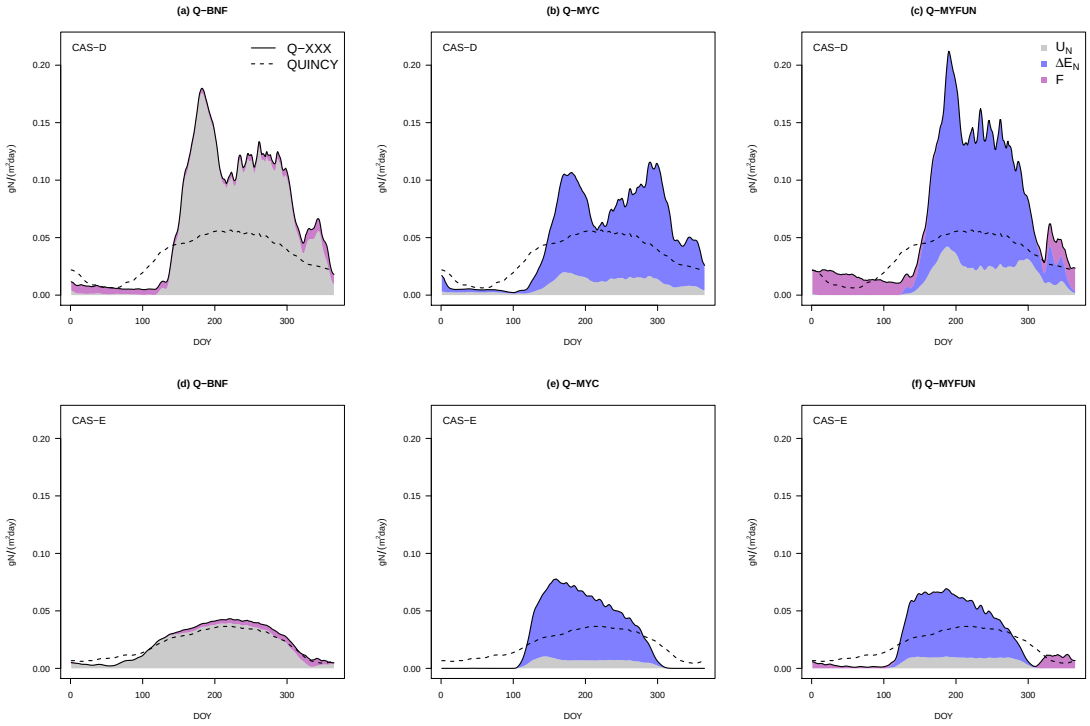

Figure 4.5.: N acquisition at CAS-D (upper row) and CAS-E (lower row), simulated by Q-BNF (left), Q-MYC (middle), and Q-MYFUN (right, always solid line), and QUINCY for comparison (dashed line). N acquisition is presented as sum of plant root uptake (U_N, grey), mycorrhizal N export (ΔE_N, blue), and symbiotic fixation (F, purple).

I find the opposite at CAS-D, where increased C assimilation in Q-MYFUN compared to QUINCY (+84.6%) or Q-MYC (+17.9%), actually lead to enhanced growth compared to all other model variants (QUINCY: +76.8%, Q-BNF: +8.1%, and Q-MYC: +12.9%). Resulting CUE (including mycorrhizal biomass[2]) is 0.59 and therefore higher than simulated by QUINCY, indicating a better simulated N nutrition by Q-MYFUN. N nutrition

[2]See section 5.1.1 for further discussions of mycorrhizal biomass inclusion to plant CUE.

by Q-MYFUN is improved due to both, mycorrhizal support and N fixation, whereby the lower annual total support by mycorrhizal fungi in Q-MYFUN compared to Q-MYC indicates a greater N availability within the entire ecosystem. Higher N availability is caused by (previous) symbiotic N fixation that generally enhanced ecosystem N (tab. 4.4 and sec. 4.3.3). However, lower fixation rates in Q-MYFUN than in Q-BNF suggest that mycorrhizal fungi actually lower (potential) rhizosphere uptake costs compared to N fixation costs, which is why plants fix less N in the presence of explicitly simulated mycorrhizal fungi.

Table 4.4.: Annual C allocation and N acquisition rates simulated by QUINCY, Q-BNF, Q-MYC, and Q-MYFUN for CAS-D and CAS-E, presented as mean for the years 1986 - 2015. Values are given in gC $m^{-2}year^{-1}$ or gN $m^{-2}year^{-1}$, respectively.

site		QUINCY	Q-BNF	Q-MYC	Q-MYFUN
CAS-D	C assimilation	1301.3	2449.5	2036.8	2401.7
	biomass production	718.0	1173.9	1124.3	1269.4
	exudation to mycorrhizae	NA	NA	115.3	138.4
	fixation respiration	NA	33.5	NA	52.7
	N acquisition	12.36	23.76	18.00	25.36
	root uptake	12.36	21.59	3.16	4.92
	mycorrhizal export	NA	NA	14.84	17.18
	symbiotic fixation	NA	2.17	NA	3.26
CAS-E	C assimilation	1652.5	1767.6	1941.5	1947.9
	biomass production	774.0	811.7	885.9	872.4
	exudation to mycorrhizae	NA	NA	61.7	58.3
	fixation respiration	NA	13.6	NA	13.4
	N acquisition	7.46	8.08	9.79	9.86
	root uptake	7.46	7.15	1.30	1.61
	mycorrhizal export	NA	NA	8.49	7.43
	symbiotic fixation	NA	0.93	NA	0.82

4.3.3. Feedback between plant nitrogen acquisition strategy and modelled ecosystem carbon and nitrogen balances and dynamics

As annual N acquisition rates indicated that soil N availability varies among N acquisition schemes, I change ecosystem N influx by varying annual N deposition rate for the stronger N-limited/more N-demanding deciduous forest CAS-D. Annual N deposition is reduced down to 10% of the original rate, and increased up 1000% of the original rate, whereby the original rate is 0.29 gN $m^{-2}year^{-1}$, which is taken from *Lamarque et al.* (2010) and *Lamarque et al.* (2011).

I find an increase in total ecosystem N (N_{Eco}) and total ecosystem C (C_{Eco}), i.e. the sum of all vegetation and soil pools, with increasing N deposition among all model versions (tab. 4.2). N_{Eco} (fig. 4.6a) increase is stronger in QUINCY (N_{Eco}: -3.3% with 10% N

deposition, and + 27% with 1000% N deposition) and Q-MYC (-4.6% with 10% N deposition, and + 45% with 1000% N deposition), whereas N_{Eco} is rather constant in variants that allow plants to fix N symbiotically to balance losses out (Q-BNF: -0.5% with 10% N deposition, and +4.1% with 1000% N deposition; and Q-MYFUN: -0.9% with 10% N deposition, and +7.7% with 1000% N deposition), which is in line with the hypothesized stabilization of N_{Eco} by additional N acquisition strategies (H4.5).
Simulated C_{Eco} responses to N deposition (fig. 4.6b) are similar to N_{Eco} responses, but much stronger in QUINCY than in all other model variants. This is linked to plant available N for growth, which is only mineral N in QUINCY that is directly increased/decreased by increasing/decreasing N deposition, whereas Q-BNF, Q-MYC, and Q-MYFUN provide additional N sources for plant growth, which result in a weaker growth limitation. Consequently, changes in ecosystem C gains by plant growth are minor.

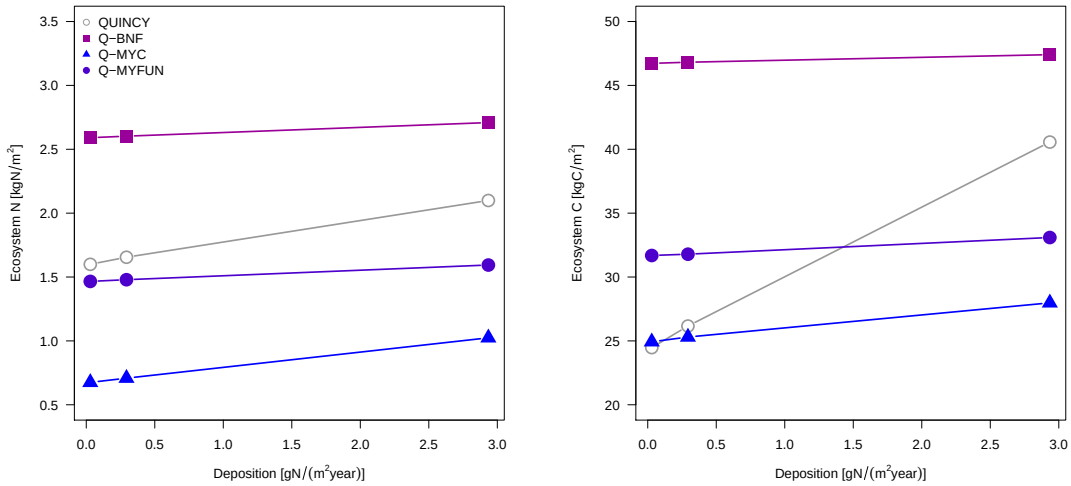

Figure 4.6.: Ecosystem N (a) and ecosystem C (b) response to de-/increasing annual N deposition, simulated by QUINCY (open grey circles), Q-BNF (filled purple squares), Q-MYC (filled blue triangles), and Q-MYFUN (filled violet circles). Values are averaged over 30 years.

Additionally N_{Eco} and C_{Eco} are significantly lower in Q-MYC than in all other QUINCY variants caused by less soil SOM that is accessed as N source (sec. 3.3), and significantly higher in Q-BNF due to higher N inflow by symbiotic fixation that enhances ecosystem ability to store C (sec. 2.3).
N_{Eco} simulated by Q-MYFUN with original annual N deposition rate is only 10% lower than N_{Eco} simulated by QUINCY, pointing to a balance between both plant controlled additional N acquisition strategies that either access ecosystem internal N sources (mycorrhizal export), or ecosystem external N sources (fixation). However, C_{Eco} in Q-MYFUN with default N deposition is 20% higher than C_{Eco} simulated by QUINCY, indicating that QUINCY vegetation growth is N limited, which is not the case for Q-MYFUN vegetation growth. N limitation on growth leads to less C_{Eco} accumulation in QUINCY, whereas the active investment of C into N acquisition in Q-MYFUN prevent plants from growth limitation without major changes in N_{Eco}. This finding is again linked to the hypothe-

sizes ecosystem stabilization by the use of different N acquisition strategies (H4.5), but confirms the active investment into fixation in case of limitation, too (H4.2b). A higher simulated ecosystem CN ratio by Q-MYFUN compared to QUINCY, also indicates a relative chance of vegetation and soil (bio)mass. As vegetation tissues have much higher CN ratios and may vary among small ranges, whereas soil CN ratios are rather low and fixed, an increase of ecosystem CN ratio in Q-MYFUN compared to QUINCY is only explainable by a higher amount of vegetation biomass compared to SOM in Q-MYFUN compared to QUINCY.

Since N_{Eco} balance is not only driven by N gain by deposition and plant controlled symbiotic fixation, but also by asymbiotic fixation, as well as losses by emission and leaching that depend on N_{Eco}, I analyze also changes in those fluxes (tab. 4.5).
As expected from N_{Eco} analysis, QUINCY responds most to deposition changes, whereby the N inflow into ecosystem responds less to deposition increase than the outflow. This is caused by asymbiotic N fixation that is switched off, after soil N exceeds a certain threshold, which limits N influx enhancement.
Q-BNF and Q-MYFUN fluxes respond less to N deposition changes that Q-MYC fluxes, which was also expected, due to minor N_{Eco} changes in response to deposition changes. Both N acquisition models that allow symbiotic fixation balance changes in total gain that are induced by deposition variations almost out, so that actual N influx changes are less than 10% of deposition changes. Minor changes in N inflow result in minor changes in N_{Eco} and in minor changes in N outflow, which stabilizes N_{Eco} against N deposition changes.
Q-MYC cannot adjust N_{Eco} inflow in response to N deposition changes, which is why total N gain responds heavily to N deposition changes. However, the response in N loss is much weaker due to both, N emission and N leaching response. This is caused by the acceleration of the internal N cycle by mycorrhizal interaction with SOM. By accessing SOM as N source, SOM is reduced, which reduces N losses, resulting in a longer turnover time of N within the entire ecosystem. Compared to Q-BNF, Q-MYFUN shows the same pattern of a reduced response of N_{Eco} losses to N deposition, but the response is weaker due to the access of external N that already stabilizes N_{Eco} (H4.2b and H4.5).
Generally, N acquisition (A_N) increases with increasing N_{Eco} that is enhanced by N deposition (fig. 4.7a and tab. 4.6). A higher N_{Eco} refers to a higher amount of N that is cycled though the ecosystem, which includes all fluxes and pools, whereby higher decomposition and mineralization fluxes due to greater SOM pools, enhance plant available N, and thus N acquisition.
QUINCY response to N deposition changes is strongest and Q-MYFUN response is lowest, indicating that QUINCY is most affected by N deposition changes, whereas Q-MYFUN is robust against changes (tab. 4.6) as I hypothesized (H4.5).

Table 4.5.: Ecosystem N balance changes in response to N deposition variations simulated by QUINCY, Q-BNF, Q-MYC, and Q-MYFUN for CAS-D, presented as mean for the years 1986 - 2015.

N flux	N deposition change	QUINCY	Q-BNF	Q-MYC	Q-MYFUN
total ecosystem N gain	10% N_{depo}	-27%	-5%	-64%	-6%
	1000% N_{depo}	+228%	+47%	+707%	+70%
total ecosystem N loss	10% N_{depo}	-21%	-5%	-13%	-6%
	1000% N_{depo}	+702%	+58%	+162%	+63%
N emission	10% N_{depo}	-12%	-3%	-9%	-4%
	1000% N_{depo}	+474%	+38%	+96%	+37%
N leaching	10% N_{depo}	-27%	-6%	-15%	-6%
	1000% N_{depo}	+843%	+66%	+193%	+70%

Table 4.6.: Plant N acquisition rate changes in response to N deposition variations simulated by QUINCY, Q-BNF, Q-MYC, and Q-MYFUN for CAS-D, presented as mean for the years 1986 - 2015.

N flux	N deposition change	QUINCY	Q-BNF	Q-MYC	Q-MYFUN
N acquisition (A_N)	10% N_{depo}	-4.9%	-1.0%	-3.1%	-0.2%
	1000% N_{depo}	+44.5%	+8.3%	+21.1%	+1.6%
root N uptake (U_N)	10% N_{depo}	-4.9%	-1.8%	-4.1%	-2.3%
	1000% N_{depo}	+44.5%	+16.0%	+43.9%	+14.6%
mycorrhizal N export (ΔE_N)	10% N_{depo}	NA	NA	-2.9%	+0.1%
	1000% N_{depo}	NA	NA	+16.3%	-0.8%
symbiotic N fixation (F)	10% N_{depo}	NA	+7.0%	NA	+1.5%
	1000% N_{depo}	NA	-67.7%	NA	-5.0%

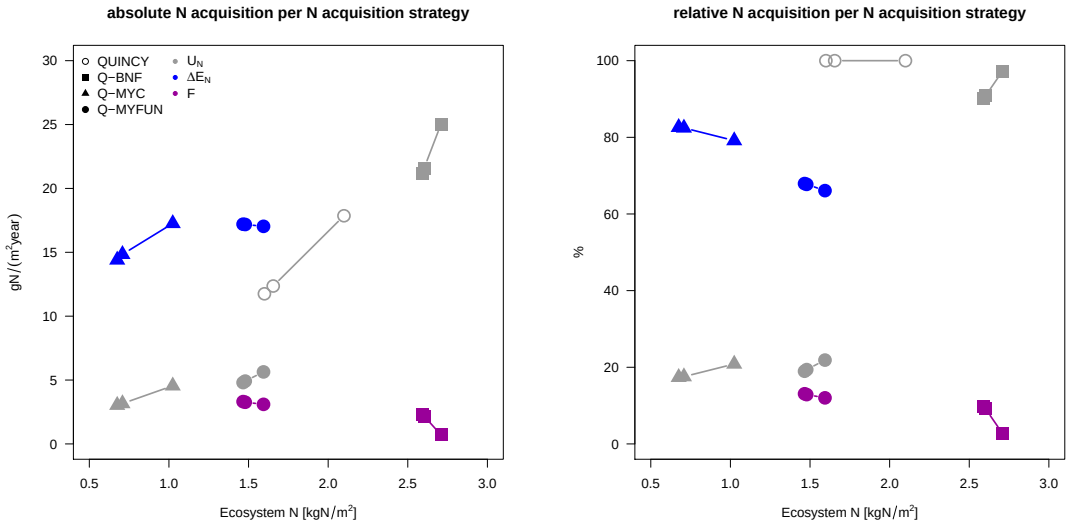

Figure 4.7.: N acquisition strategy by QUINCY (open circles), Q-BNF (filled squares), Q-MYC (filled triangles), and Q-MYFUN (filled circles) depending on ecosystem N. Root uptake (U_N) in grey, mycorrhizal N export (ΔE_N) in blue, and symbiotic N fixation (F) in purple. Values are averaged over 30 years. Left: absolute rates, right: relative rates from total N acquisition.

With increasing N deposition, all QUINCY variants increase root uptake (U_N) due to higher soil N availability, since N deposition is directly added to mineral N pools (tab. 4.6 and fig. 4.7a). Symbiotic fixation (F) is decreased with increasing deposition (Q-BNF and Q-MYFUN), since in a steady-state ecosystem, external N is only accessed as N source to balance N losses out and maintain N_{Eco}, which is in line with H4.2b. In case N input is high due to high N deposition, the need to balance N losses out is low, which reduces F. However, F response to N deposition changes is much stronger in Q-BNF, again pointing to the robustness of N_{Eco} in Q-MYFUN against external changes (H4.5), which are caused by mycorrhizal interactions with SOM that hinder major N losses by leaching by the acceleration of internal N cycling (tab. 4.6 and fig. 4.7a). Mycorrhizal export (ΔE_N) is increased in Q-MYC caused by higher N_{Eco} that provides more N internally, whereas ΔE_N slightly decreases in Q-MYFUN in response to increasing N deposition due to minor benefit by mycorrhizae for plants. Again, flux response simulated by Q-MYFUN is weak (tab. 4.6 and fig. 4.7a).
On a percentage basis, F is reduced from almost 20% of annual N acquisition to zero in Q-BNF simulations by changing N deposition over two magnitudes, whereas reduction in Q-MYFUN is only 5%. N acquisition in Q-MYC is governed by ΔE_N for all N deposition variations, but the ratio shifts from more than 80% in case of low deposition to approximately 70% in case of high deposition and resulting higher N_{Eco}. I find a similar shift in Q-MYFUN, but again changes are much weaker and only about 5% among all N deposition variations, caused by the reported rather constant N_{Eco} (fig. 4.7b).

4.4. Results II: Global assessments of plant carbon-use efficiency with different nitrogen acquisition strategies

I will now assess the importance of plant controlled N acquisition by different strategies on plant C-use efficiency (CUE) under ambient, and elevated CO_2 (eCO_2) concentrations, and analyze plant and ecosystem responses to eCO_2.
To address this, I run QUINCY (revision 1994, 500-year spin-up) without additional N acquisition strategies. i.e. only root uptake (QUINCY), with symbiotic N fixation to access ecosystem external N as N source, if needed (Q-BNF), with mycorrhizal fungi to access additional ecosystem internal N as N source, if needed (Q-MYC), and with both, symbiotic fixation and mycorrhizal fungi (Q-MYFUN; tab. 4.2) for 42 forest sites of the GFDB that are not harvested since 1960 (sec. 2.2.3.1). I conduct two rounds of simulations, one with standard model protocol and input data (sec. 2.2.2), and another one with CO_2 fertilization, where I add 200ppm CO_2 to ambient atmospheric concentrations starting 1976.

4.4.1. Plant carbon-use efficiency under ambient conditions

Simulation output by the ambient runs is averaged over 30 years, from 1986 to 2015 to avoid influence by inter-annual climate variability. Observations are taken from the GFDB (sec. 2.2.3.1, *Luyssaert et al.* (2007)).

GPP and NPP decrease from the tropics to the boreal regions due to climatic conditions, such as growing season length, temperature, and radiation, in all QUINCY simulation, as well as in observations, but since the decrease in GPP is stronger than in NPP, resulting CUE increases (fig. 4.8).
The spread among sites within the same climate zone is always smaller for simulated fluxes compared to observed fluxes due to (i) simulation output average over 30 years, (ii) less variable conditions that are described by input data, which are derived from global data, but not site specific (sec. 2.2.2), (iii) the use of generalized PFTs that may differ in their behavior from specific trees, and (iv) measurement uncertainties that enlarge the spread for observed fluxes. But the spread is again higher for QUINCY with additional N acquisition schemes due to plants' ability to invest C into N acquisition to overcome N limitation on growth. This feature enhanced C fluxes at sites that are (mildly) N limited in QUINCY, but does not change fluxes at sites that are limited by any other reason, such as temperature, water, or P.
Generally, simulated fluxes among all model variants do not differ much, since I run all model variants for mature ecosystems. Given the well constrained C-cycle of QUINCY, vegetation biomass, and thus NPP, are not intended to change much by including any symbiotic N acquisition strategy. However, there are small deviations in simulated GPP, since GPP increases due to an improved N nutrition, which is balanced by higher respiration costs for N acquisition. This results in similar NPP rates, and slightly lower CUE ratios in model variants with symbiotic N acquisition as expected.

Observed GPP is lower than simulated GPP among all climate regions, except in the boreal zone modelled by QUINCY. QUINCY simulates lowest rates among all model variants indicating strongest N limitation. GPP rates are highest in Q-MYFUN runs pointing out that the combination of N support by mycorrhizal fungi and symbiotic N fixation is most effective for plants, because N support by mycorrhizal fungi is C cost cheaper than fixation, but fixation has access to an unlimited N source. By combining both strategies, plants can always acquire N by fixation if demanded, but can also choose for the potentially cheaper N support (fig. 4.8a and fig. 4.9a).
Generally, observed NPP rates are again lower than simulated NPP rates, but not for tropical forests, where observed NPP is extremely high, but has a huge spread among the five monitored sites. NPP simulated by QUINCY is slightly lower than NPP simulated by QUINCY with additional N acquisition strategies, whereby differences are minor compared to Q-BNF simulations for tropical and temperate forests, indicating that only boreal forests suffer from N limitation in QUINCY strongly. Q-MYC forests and Q-MYFUN increase NPP stronger among all climate zones compared to QUINCY, but since NPP includes also C allocation to mycorrhizal fungi, the enhancement of plant biomass production compared to QUINCY or Q-BNF is minor (fig. 4.8b and fig. 4.9b).
CUE, as ratio between NPP and GPP (eq. 1.2, *Manzoni et al.* (2018)), increases from the tropical forest sites to the boreal forest sites, which is a usual observed and reported trend (fig. 4.8c, *Campioli et al.* (2015), *He et al.* (2019)). This trend is weaker in observations due to their large spread. Median CUE increases from 0.34 at the tropics to 0.43 at temperate forest sites, whereby deciduous forests have a significantly higher CUE (median: 0.48) than evergreen forests (median: 0.41). CUE decreases again towards the poles, since median CUE for boreal forests is 0.42. However, there is only one deciduous boreal site included, so median CUE actually increases slightly, when comparing only evergreen sites.
Simulated CUE does not differ much among N acquisition scheme variants. Simulated median CUE for tropical forest varies between 0.27 and 0.29, which about 18% lower than observed CUE. Simulated median CUE for temperate forest sites varies between 0.48 and 0.50, which is about 19% higher than observed CUE. And simulated median CUE for boreal forest sites varies between 0.54 and 0.57, which is about 32% higher than observed CUE. The higher spread in simulated CUE for boreal forest sites is linked to potential C investment into N acquisition to overcome N limitation on growth, which lowers CUE in QUINCY with symbiotic N acquisition strategies compared to QUINCY, but enhances NPP and biomass production. Generally both, observed and modelled CUE, meet the expected range of from 0.2 to 0.65 (sec. 1.2.1.1, *Amthor* (2000)).

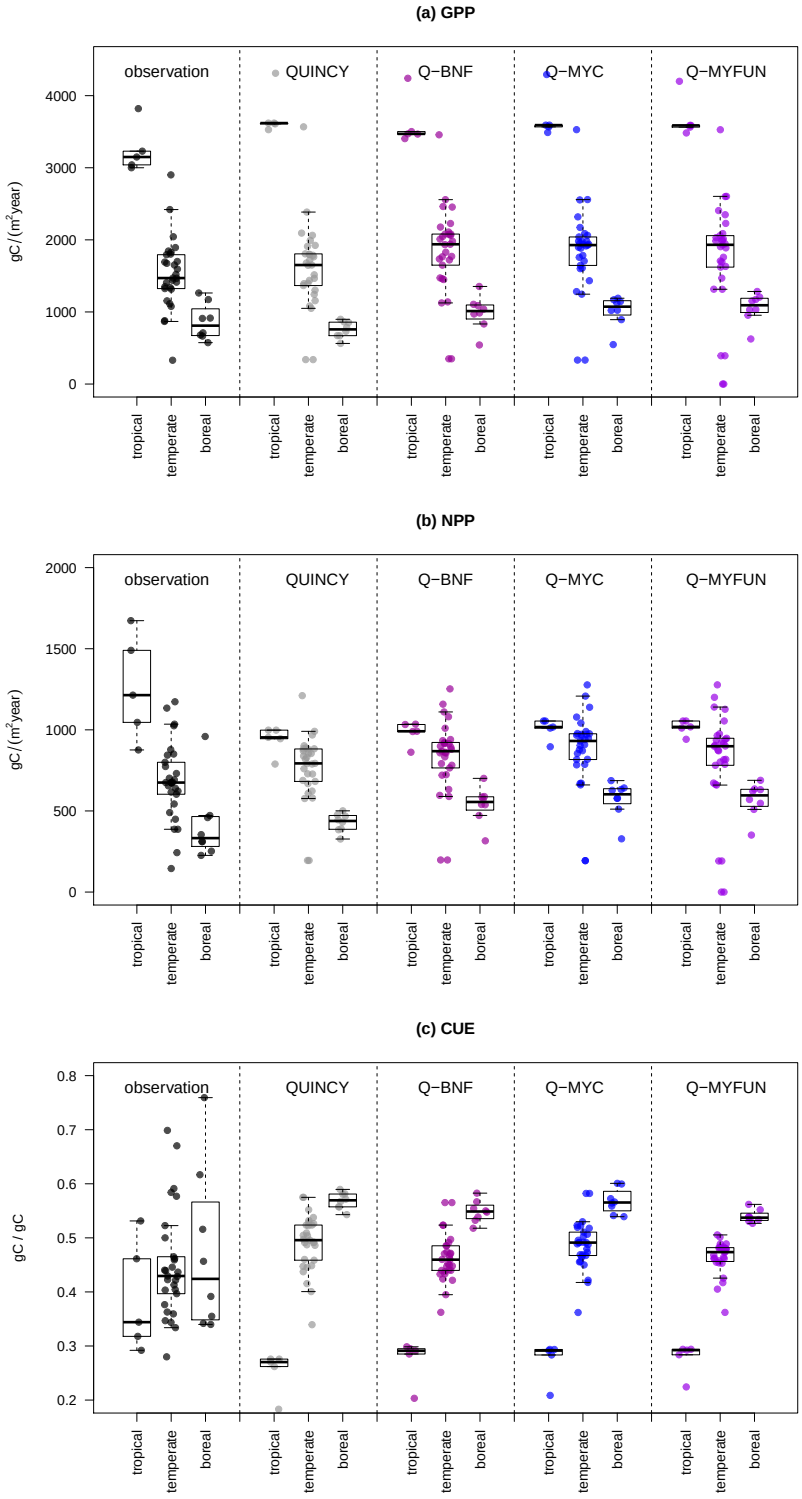

Figure 4.8.: Observed and modelled GPP, NPP, and CUE among 42 mature forest sites from GFDB (sec. 2.2.3.1). Sites are subdivided by climate zone. Observations in black, simulations, which are averaged over the years 1986-2015, by QUINCY in grey, by Q-BNF in purple, by Q-MYC in blue, and by Q-MYFUN in violet. Boxes show inner-quartile range, and are divided by median. Whisker present 10%- and 90%-quantiles.

To quantify not only general model behavior, but also model-data agreement, figure 4.9 shows the model-data comparison for GPP, NPP, and CUE for each site individually for all model variants, and table 4.7 presents calculated coefficients of determination.
Generally, model-data agreement is best for GPP, weaker for NPP, and worst for CUE. This is caused by both, model and measurement uncertainties, which are lager for NPP than for GPP, and then propagate to CUE, as reported and discussed already in section 2.4.1 and section 2.5. GPP is mainly driven by climatic conditions, such as radiation, temperature, moisture, and cCO_2, which are generally well reported and can assumed to be similar for the whole stand. This simplifies GPP simulations and improves the representativeness of measured GPP for the entire site. NPP is additionally strongly affected by soil properties, such as nutrient availability, pH, and porosity, which are less well reported due to the lack of a common protocol and general difficulties to measure below-ground and have a high spatial variability (*Vicca et al.* (2018)). This complicates NPP simulations and hampers the representativeness of measured NPP for the entire site. Weak agreements for both, NPP and GPP, then result in very low (or almost none) agreement of CUE (sec. 2.4.1 and sec. 2.5). However, there are still minor differences in model-data agreement for each flux or flux ratio among model variants.

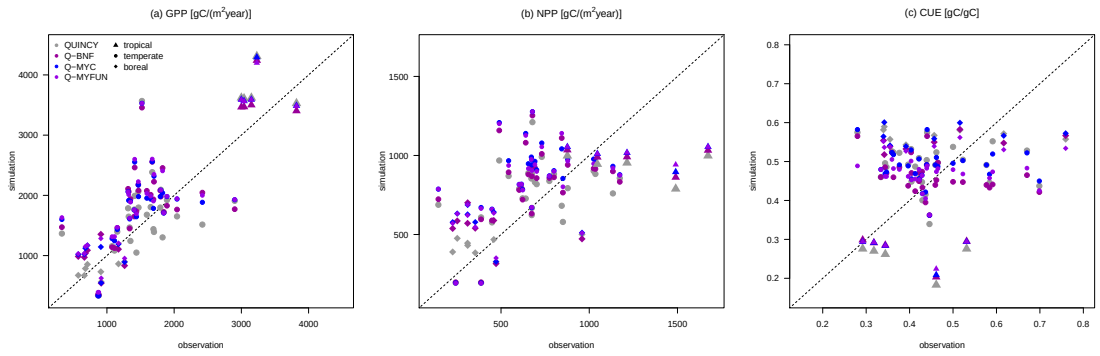

Figure 4.9.: Modelled versus observed GPP (a), NPP (b), and CUE (c) among 42 mature forest sites from GFDB (sec. 2.2.3.1). Coefficients of determination (R^2 values) can be found in table 4.7. Tropical sites are represented by triangles, temperate sites by dots, and boreal sites by diamonds. Color code refer to model variants: grey: QUINCY, purple: Q-BNF, blue: Q-MYC, and violet: Q-MYFUN.

Table 4.7.: Coefficients of determination (R^2) for each model variant compared to observations from GFDB (*Luyssaert et al.* (2007)).

	QUINCY	Q-BNF	Q-MYC	Q-MYFUN
GPP	0.55	0.51	0.52	0.46
NPP	0.29	0.23	0.21	0.20
CUE	0.02	0.03	0.02	0.03

Model-data agreement of GPP and NPP is best for QUINCY (fig. 4.9 and tab. 4.7). Consequently, the reported slight increase of GPP and NPP by applying any symbiotic N acquisition strategy lowers model-data agreement, since Q-BNF, Q-MYC, and Q-MYFUN then tend to overestimate GPP and NPP. Only agreement for tropical NPP is better for model variants that allow symbiotic N acquisition, because QUINCY underestimates tropical NPP largely.
CUE is slightly increased when considering symbiotic fixation and/or symbiotic mycorrhizal fungi at tropical sites, and reduced at temperate and boreal sites. However, this does not improve model-data agreement significantly (fig. 4.9 and tab. 4.7).

The increase in GPP and NPP by applying symbiotic N acquisition strategies (fig. 4.9), which actually lowers model-data agreement in general (tab. 4.7), indicates that QUINCY may respond too strong to an improved N nutrition, which is caused by symbiotic N fixation or the support of symbiotic mycorrhizae. This pattern is in particular observable for temperate and boreal forests, which is why I analyze GPP, NPP and CUE in dependency of leaf CN ratio of measure for N nutrition and N limitation (fig. 4.10).

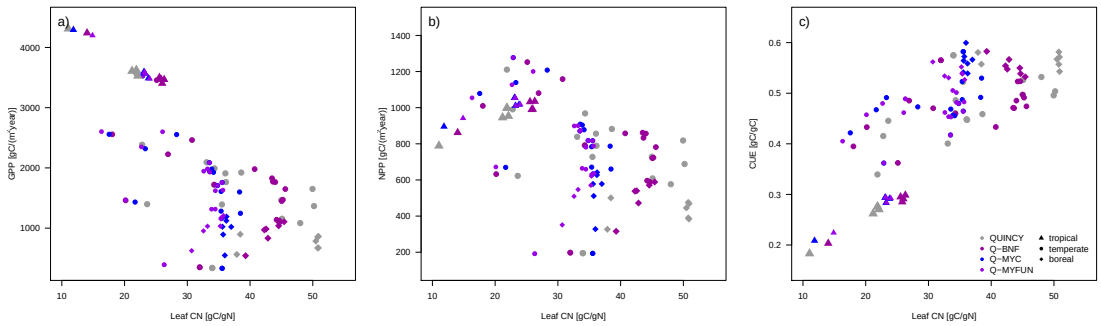

Figure 4.10.: Influence of simulated leaf CN ratios on modelled GPP (a), NPP (b), and CUE (c) among 28 mature evergreen[a] forest sites from GFDB (sec. 2.2.3.1). Tropical sites are represented by triangles, temperate sites by dots, and boreal sites by diamonds. Color code refer to model variants: grey: QUINCY, purple: Q-BNF, blue: Q-MYC, and violet: Q-MYFUN.

[a] Leaf CN ratio is presented only for evergreen forests to avoid phenological effects that also may affect comparable data from the TRY database (*Kattge et al.* (2011)). Additionally, plots that show GPP, NPP and CUE in dependency of labile CN ratio can be found in appendix D.1 to show that shifts in CN ratios are consistent among leaf habits, i.e. for evergreen forests and deciduous forests.

Generally simulated leaf CN ratios are lowered at temperate and boreal sites and increased at tropical sites by the application of symbiotic N acquisition strategies (fig. 4.10). This reduces the spread in leaf CN ratios among climate zones, which is approximately 10 gC/gN to 50 gC/gN in QUINCY simulations, and 15 gC/gN to 35 gC/gN (Q-MYC and Q-MYFUN) or to 45 gC/gN (Q-BNF).
For temperate and boreal forest sites, i.e. for coniferous trees, QUINCY simulates leaf CN ratios that are either around 50 gC/gN, or between 30 gC/gN and 40 gC/gN. The

mean of these simulated values may meet the observed mean leaf CN ratio for coniferous trees, which is approximately 42 gC/gN (*Kattge et al.* (2011)), but leaf CN ratios that are above the observed mean may indicate (mild) N limitation. This then would be the case for almost half of the QUINCY-simulated sites in the temperate and boreal regions. Contrary to that, Q-BNF simulates leaf CN ratios that meet observation-based expectations well in the mean, and also the spread among sites is low, which suggests, that there is an optimal leaf CN ratio for plants that is actually close to observed leaf CN ratios. Q-MYC and Q-MYFUN simulate even lower leaf CN ratios for temperate and boreal sites. This indicates that the support of mycorrhizal fungi may be too strong, as it is only partly controlled by plants, whereas they have full control over symbiotic fixation.
At tropical sites, leaf CN ratio is generally slightly increased by symbiotic N acquisition. This suggests, that these sites are not N limited among all model variants, but that symbiotic N acquisition may allow plants to regulate N acquisition better, as leaf CN ratios move towards expected values.
Via photosynthetic N, i.e. N that is associated with Rubisco, chlorophyll, and electron transport, leaf N content, and so leaf CN, are linked to GPP, and higher leaf CN ratios lead to higher GPP rates (*Lorimer* (1981), *Evans* (1989), *Kull and Kruijt* (1998), *Thum et al.* (2019)). Consequently, GPP is increased at temperate and boreal sites and reduced at tropical sites by Q-BNF, Q-MYC and Q-MYFUN compared to QUINCY. QUINCY already simulates slightly too high annual GPP rates compared to observations at temperate and boreal sites and rather too low rates at tropical sites (fig. 4.9). This results in a greater overestimation of GPP by model variants that include symbiotic N acquisition strategies at temperate and boreal sites and a slightly improved model-data agreement at tropical sites (fig. 4.10a).
Improved N nutrition by symbiotic N acquisition enhances NPP in Q-BNF, Q-MYC, and Q-MYFUN simulations compared to QUINCY among almost all sites (fig. 4.8b and fig. 4.9b). The enhancement is stronger at temperate and boreal forest sites, where it is supported by the shift of GPP towards higher ratios, but also observable at the tropics. Since QUINCY again has the tendency to overestimate boreal NPP, and to underestimate tropical NPP, this leads to a reduction of model-data agreement for simulations that include symbiotic fixation and/or mycorrhizal fungi again (fig. 4.9b and tab. 4.7).
CUE is not affected much by improved N nutrition that cause shifts in leaf CN, which suggests that there are other processes that drive CUE stronger than processes that are related to N nutrition. Only at tropical sites, CUE is increased significantly in combination with a increase in leaf CN, which indicates that there may be a threshold for a minimal leaf CN that is beneficial for plants, whereas ratios below, i.e. too much N, decrease productivity (4.8c and fig. 4.9c).

4.4.2. Simulated responses of vegetation carbon and nitrogen fluxes to elevated CO_2

CO_2 fertilization in elevated simulations started in 1976 with an addition of 200ppm CO_2 to ambient CO_2 concentrations.
Flux and flux ratio responses are calculated as relative changes to ambient fluxes by

$$\delta Y = \frac{Y_{ele} - Y_{amb}}{Y_{amb}} \tag{4.3}$$

where δY is the relative response to elevated CO_2 of the regarded flux or flux ratio Y. Y_{ele} depicts flux or flux ratio Y under elevated CO_2 condition, whereas Y_{amb} depicts flux or flux ratio Y under ambient CO_2 condition.

GPP, as well as NPP are initially enhanced in response to eCO_2 by 30-40% among all model variants (tab. 4.2) compared to ambient simulations, and since NPP is enhanced stronger, CUE is increased by 10-15% initially (fig. 4.11).

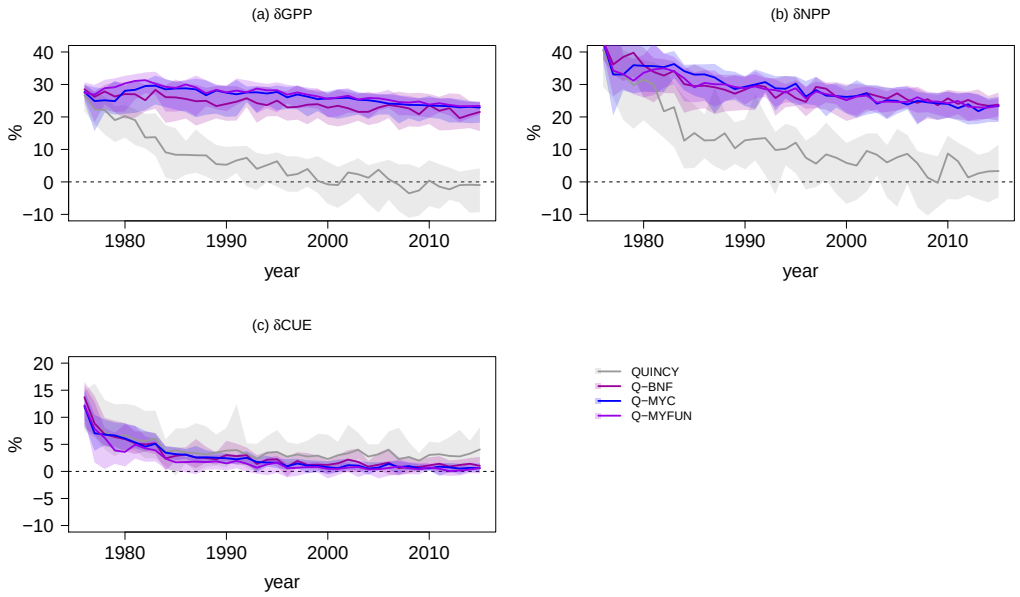

Figure 4.11.: Simulated GPP (a), NPP (b), and CUE (c) responses to eCO_2 by QUINCY (grey), Q-BNF (purple), Q-MYC (blue), and Q-MYFUN (violet) among 42 mature forest sites of the GFDB (sec. 2.2.3.1). Lines presents median, and shaded areas the inner-quartile range among sites.

However, this effect is only short-term in QUINCY due to increasing N limitation on growth, because N acquisition (A_N) is only increased by 15% due to limited N sources (fig. 4.12a). Consequently δGPP and δNPP decline quickly, and δGPP is almost zero in the long-term, whereas δNPP varies between 0% and 10%, which results in a CUE response to eCO_2 of around 5% in the long-term, but δNUE that starts with almost 20% within the first years, and is still almost 10% in the long-term (fig. 4.11 and fig. 4.12b).

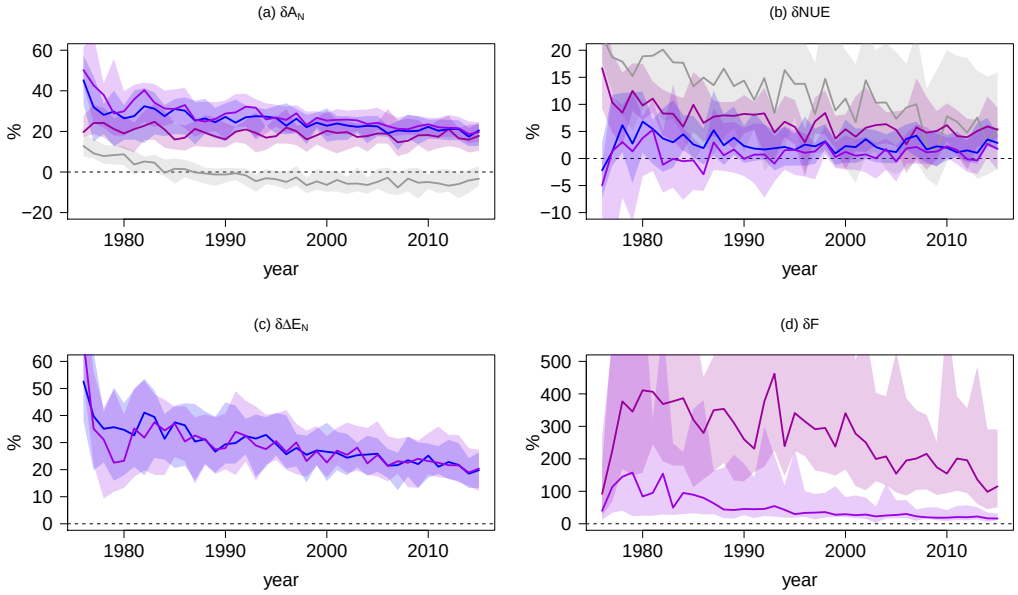

Figure 4.12.: Simulated plant N acquisition (A_N, a), N-use efficiency (NUE, b), mycorrhizal export (ΔE_N, c), and symbiotic fixation (F, d) responses to eCO_2 by QUINCY (grey), Q-BNF (purple), Q-MYC (blue), and Q-MYFUN (violet, legend can be found in fig. 4.11) among 42 mature forest sites of the GFDB (sec. 2.2.3.1). Lines presents median, and shaded areas the inner-quartile range among sites.

Q-BNF, Q-MYC, and Q-MYFUN show a persistent high response for GPP (around +30%), and only a minor decrease in NPP response to +30%, which lowers δCUE to zero and indicates a new, but rather stable plant C balance (fig. 4.11). The persistent positive response to eCO_2 is caused by the on-going positive δA_N (around +20% in the long-term, fig. 4.12a), which confirms H4.3 that plants actively invest C into N acquisition to overcome PNL. Positive δA_N is either caused by increased mycorrhizal support ($\delta \Delta E_N$, Q-MYC: +50% initially and +25% in the long-term, Q-MYFUN: +65% initially and +25% in the long-term, fig. 4.12c), or by enhanced symbiotic fixation (δF, Q-BNF: +400% after the first year and +100-200% in the long-term, Q-MYFUN: +150% after the first year and +25% in the long-term). First year δF is small in Q-BNF and Q-MYFUN simulations, because plants use their resources first to build new biomass, before they face N limitation and invest actively into symbiotic fixation, which is in line with my hypothesis that plants only invest C into fixation in case of limitation (H4.2c). In general, δF is comparably high to all other flux responses, because of low ambient F rates (fig. 4.12d).
Persistent high A_N in Q-BNF, Q-MYC and Q-MYFUN simulations lead to only minor changes of NUE (Q-BNF: +5-10%, Q-MYC and Q-MYFUN: below +5%, fig. 4.12b), which is confirmed by measurements at free-air CO_2 enrichment (FACE) sites by *Finzi et al.* (2007). Minor changes in CUE and NUE in the long-term response to eCO_2 in-

dicate that plants have an optimal status of biomass production in relation to C and N acquisition that they can hold by acquiring N actively by additional symbiotic strategies to root uptake. Initial changes are only caused by the prioritized use of previously stored resources.

4.4.3. Simulated responses of forest ecosystem carbon and nitrogen stocks to elevated CO_2

Higher C uptake by plants in response to eCO_2 does not only influence plant growth, and thus vegetation C balance, but may also affect the C balances of soil and the entire ecosystem as I hypothesized in H4.4.
I compare absolute C storage responses of vegetation C (ΔC_{Veg}), SOM C (ΔC_{SOM}), and ecosystem C (ΔC_{Eco}) among QUINCY variants with and without additional N acquisition strategies (tab to address the questions, if and how additional plant controlled N acquisition strategies influence ecosystem C and N balances under eCO_2.
Responses are calculated as following:

$$\Delta X = X_{ele} - X_{amb} \tag{4.4}$$

where ΔX is the absolute response to elevated CO_2 of the regarded pool X. X_{ele} depicts pool X under elevated CO_2 condition, whereas X_{amb} depicts pool X under ambient CO_2 condition.

C_{Veg} responds positively to eCO_2 (fig. 4.13a), because eCO_2 increases plant C uptake (GPP), and biomass production (NPP, sec. 4.4.2, fig. 4.11). ΔC_{Veg} is lower in QUINCY, and decreases during the CO_2 fertilization period of 40 years, until it is almost zero, which is caused by increasing progressive N limitation (PNL, sec. 1.2.2.2). In contrast to that, Q-BNF, Q-MYC, and Q-MYFUN are able to further increase C_{Veg} by preventing plants from PNL, as they allow plants to invest assimilated C into additional N acquisition strategies. After 40 years of CO_2 fertilization, all three model variants predict a C_{Veg} enhancement of more than 2.5 kgC m^{-2} (fig. 4.13a). Since plant pools have a rather fixed CN ratio[3], ΔN_{Veg} follows ΔC_{Veg} (fig. 4.13b). However, ΔC_{Veg} is actually driven by ΔN_{Veg}, and not the other way around. Only persistent positive N acquisition response to eCO_2 by Q-BNF, Q-MYC, and Q-MYFUN (δA_N, sec. 4.4.2, fig. 4.12a) allows plants to further increase biomass, and the negative ΔN_{Veg} in QUINCY causes the decrease in ΔC_{Veg} after around 20 years of CO_2 fertilization experiment.
C_{SOM} response to eCO_2 is slower than C_{Veg} response, since C has first to enter the ecosystem by plant uptake, before it is passed to SOM as litter. Consequently C_{SOM} response to eCO_2 is delayed, but follows ΔC_{Veg} evolution in general (fig. 4.13a and fig. 4.13c).

[3]Vegetation stock CN ratios are fixed for most tissue pools, except leaf pool, which varies within a limited range in response to plant N nutrition. Non-tissue pools, i.e. the labile and storage pools also have varying CN rations. However, non of these allowed variations does affect total plant CN ratio much due to the high amount of woody tissues with fixed CN ratio. Also allocation changes, i.e. from more CN-rich to more CN-poor tissues, influence total vegetation CN ratio only minor.

QUINCY simulates an increase of C_{SOM} in response to eCO_2 of around 1 kgC m^{-2} within 40 years, but ΔC_{SOM} starts to decrease slightly due to less litter input by less C_{Veg} (fig. 4.13c). In contrast to that, Q-BNF that allows plants to acquire additional N by fixation of atmospheric N_2 increases C_{SOM} in response to eCO_2 by more than 2 kgC m^{-2} within the 40 years of CO_2 fertilization simulation, as C_{Veg} is increased and this enhancement propagates into ΔC_{SOM} by litter fall. I.e. once C and N are fixed in the ecosystem, they have a long resident time. This is unlike to simulations that include mycorrhizal interactions (Q-MYC and Q-MYFUN). ΔC_{SOM} is very small in this simulations, because mycorrhizal fungi access SOM as N source to support plants, which enhances heterotrophic respiration, and balances additional C input by litter out. After 40 years, ΔC_{SOM} simulated by Q-MYC and Q-MYFUN is only about 0.65 kgC m^{-2} (fig. 4.13c).
Interestingly, N_{soil} responds differently to eCO_2 than C_{SOM} (fig. 4.13c and fig. 4.13d), indicating not only a change in N_{soil} in response to eCO_2, but also a shift in the relative soil N pool sizes. Q-BNF simulates the strongest positive ΔN_{soil}, which is caused by the high additional N input from N_2 by fixing in response to eCO_2 (F, sec. 4.4.2, fig. 4.12d). Over time, this additional N accumulates in the soil mainly in form of old SOM-N and mineral N, which have a low CN ratio or contain no C. In contrast to that, Q-MYC simulates even a negative response of N_{soil} to eCO_2 indicating a shift towards younger SOM-C, because litter and fast-SOM have a higher CN ratio than the older slow-SOM. This shift is also observed by *Lichter et al.* (2008) at the Duke FACE experiment (sec.3.4.2), and caused by enhanced mycorrhizal uptake of N from old SOM in order to satisfy plant N requirements by an increased N export in response to eCO_2 (ΔE_N, sec. 4.4.2, fig. 4.12c). Q-MYFUN simulates a slightly negative ΔN_{soil} initially, i.e. within the first 5 years of the CO_2 experiment, following Q-MYC, before plants invest info fixation, which enhances external N input (F, sec. 4.4.2, fig. 4.12d) and increases ΔN_{soil} until approximately 2000, i.e. from year 5 to year 30 of the experiment. Then δF is almost zero, and ΔN_{soil} is almost constant. Thus, F is only used to balance losses due to emissions and leaching out, which are comparably low in a system that contains mycorrhizal fungi, and points to the stabilization of the system against C-input changes that I hypothesized and observed against N-input changes (H4.5, sec. 4.3.3).

Caused by the development of C and N stocks of vegetation and soil, ecosystem C and N response is highest in Q-BNF, and lowest in QUINCY, whereby Q-MYC response of N_{Eco} is also low, because ΔN_{Eco} is mainly driven by ΔN_{soil}.
QUINCY-ΔC_{Eco} starts decreasing after approximately 20 years of CO_2 fertilization, which leads to a minor ΔC_{Eco} of less than 2 kgC m^{-2} after 40 years of CO_2 fertilization, and may even decrease further, given the development of ΔC_{Veg} that influences future ΔC_{SOM}. ΔC_{Eco} in Q-MYC and Q-MYFUN are mainly driven by ΔC_{Veg}, because ΔC_{SOM} is almost zero, and thus end up with additional 3 kgC m^{-2} within the entire ecosystem after 40 years of CO_2 fertilization. Q-BNF-ΔC_{Eco} is more than 4.5 kgC m^{-2} after 40 years of CO_2 fertilization, because C that has entered the ecosystem via plants persists longer in the soil, and has therefor a longer ecosystem turnover time.

Finally, I can confirm the hypothesis that the prevention from PNL by using additional plant controlled N acquisition strategies lead to a higher positive ΔC_{Eco} among all model variants compared to QUINCY as baseline version.

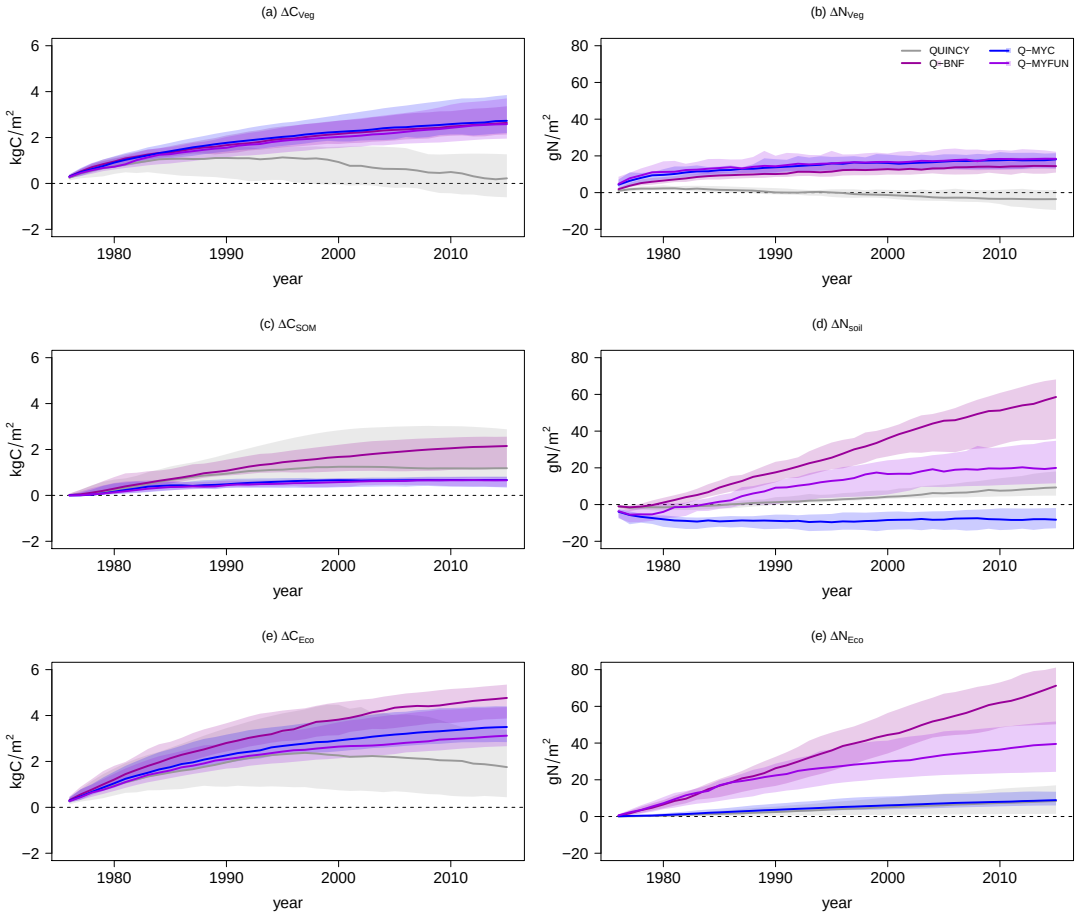

Figure 4.13.: Simulated C (a, c, e), and N (b, d, f) stock responses to eCO_2 of vegetation (a, b), total soil (c, d), including organic and inorganic pools, and ecosystem (e, f) by QUINCY (grey), Q-BNF (purple), Q-MYC (blue), and Q-MYFUN (violet) among 42 mature forest sites of the GFDB (sec. 2.2.3.1). Lines presents median, and shaded areas the inner-quartile range among sites.

4.5. Summary and Discussion

4.5.1. Discussion of hypotheses

I discuss my hypotheses (sec. 4.1.2) for the fully coupled N acquisition model MYFUN within the QUINCY framework (Q-MYFUN), either based on Q-MYFUN performance, or in comparison to QUINCY without additional N acquisition strategies (QUINCY), or to QUINCY with only one additional N acquisition strategy, namely symbiotic N fixation (Q-BNF), or mycorrhizal support (Q-MYC)[4].

H4.1: Plants favor mycorrhizal support over symbiotic fixation.
Annual plant C exudation to mycorrhizal fungi is 2.6 (CAS-D) to 4.5 (CAS-E) times higher then investment into symbiotic N fixation at Cascade Head Forest, which shows the general favor of mycorrhizal fungi of modelled plants in Q-MYFUN to support N acquisition over symbiotic fixation (sec. 4.3.2).
However, this is based not only on CN economics, but also resulting from the MYC-BNF coupling. While symbiotic fixation as an additional N acquisition strategy that is *only* used, if necessary to meet N requirements, and ended, if plants are satisfied or fixation is too C cost expensive, exudation to mycorrhizal fungi is forced to avoid mycorrhizal extinction, even in case of plant N satisfaction, or no N support (sec. 4.2.1). Another option would have been to treat all N acquisition strategies, i.e. root uptake, mycorrhizal export, and symbiotic fixation similar to *Brzostek et al.* (2014), *Shi et al.* (2016), and *Sulman et al.* (2019), but as argued in section 3.2.1 and section 4.2.1, I assume that mycorrhizal fungi are potential parasites, which will always gain a little C from their host plant, even in case the host plants do not benefit at all, either caused by too little N that turns mycorrhizal fungi into competitors, or caused by too much N that makes mycorrhizal support unnecessary. Besides, almost all terrestrial plants live in symbiosis with mycorrhizal fungi (*Read* (1991)), whereas only some host occasionally N fixing microbes (*Gutschick* (1981)). Thus, a different implementation of both symbiotic strategies may also reflect reality better.
Nevertheless, since N acquisition by mycorrhizal fungi export is 5.2 (CAS-D) to 9.2 (CAS-E) times higher than N acquisition by symbiotic fixation, mycorrhizal N support is the C cost cheaper strategy indicating that plants favor mycorrhizal support also from economical perspective (sec. 4.3.2). Globally, annual mycorrhizal support is 5.5 times higher than annual symbiotic fixation under ambient conditions pointing to a prioritization of N acquisition support by mycorrhizal fungi compared to fixation (sec. 4.3.1). Seasonal pattern of total N acquisition simulated by Q-MYFUN, as well as relative distribution among strategies over the course of a year is closed to what the 'purely' economical-based model of *Shi et al.* (2016) simulates. I.e. they report that plants majorly acquire N via associated mycorrhizal fungi (66%), and only lower via root uptake (11%) and symbiotic fixation (7%). However, their relative shares are biased, as they also include retranslo-

[4]For further information about coupled BNF and MYC schemes see tab. 4.2.

cation of N (17%) into N acquisition budget. Thus these shares tend to be lower than simulated shares by Q-MYFUN (root uptake: 24%; mycorrhizal support: 64%; symbiotic fixation: 12%) Only actual rates are higher by MYFUN, which may be due to higher N availability in soil in QUINCY in general.
Consequently, I can confirm H4.1, and modelled differences in C costs and importance for N support also may reflect differences in real-world importance of mycorrhizal fungi and N fixers for plant N acquisition based on their occurrence. However, a quantitative assessment is impossible, as it is easy to simulate ecosystems with and without mycorrhizal fungi and/or N fixers, but in reality all ecosystems contain mycorrhizal fungi and most contain N fixers facultativly. Thus, there is no chance for comparable data, and I can only argue that the fact that almost all terrestrial plants evolved symbiotic N acquisition strategies, whereby mycorrhizal fungi are much more present than N fixing microbes, suggests that the performance of Q-MYFUN is reasonable.

H4.2: Plants invest carbon into symbiotic fixation in case of nitrogen limitation, which happens (a) seasonally, (b) in nitrogen limited ecosystems, and (c) under eCO_2.
Plant N acquisition strategy changes seasonally due to N demand and availability in soil. As long as plants can meet N requirements by root uptake and mycorrhizal support, they do not acquire additional N by fixation, but in case of limitation, which happens during winter caused by slow decomposition that lowers N availability within soil, they invest C into symbiotic fixation to access atmospheric N_2 as N source (sec. 4.3.2). Thus, I can confirm H4.2a so far as that plants invest C in case of seasonal N limitation. However, the actual seasonal pattern is questionable. Cause by lower temperatures, fixation is much more C-costly in winter. So peaking fixation rates in winter are inefficient for plant C economics. But again, I do not have observations to compare my simulations quantitatively with. Comparative studies by *Shi et al.* (2016) reported similar seasonal total N acquisition patterns, which are caused by plant N demand. However, maybe caused by less soil N availability, simulated N acquisition rates were generally lower and did not meet plant N demand. In particular during the growing season, plants seemed to get much less N as they would need, which results in (i) notable fixation rates in summer, when Q-MFUN does not simulate fixation, and (ii) notable N acquisition rates in winter that are also supported by mycorrhizal fungi, which is not the case in Q-MYFUN. This leads to a much smoother seasonal cycle as simulated by Q-MYFUN. Given the lack of observational data, I cannot rate individual model performance, but both models agreed on the fact that plants need to acquire N throughout the entire year, even though, they may vary in seasonally chosen strategies. This is probably caused by there different hierarchical set-up, i.e. a clear favor of mycorrhizal support by Q-MYFUN, and the equal treatment of all strategies by the model of *Shi et al.* (2016).
I simulated ecosystem N (N_{Eco}) limitation and surplus by changing N deposition rates. Lower N deposition rates lead to higher symbiotic N fixation, whereas higher N deposition generally lowers N fixation. This pattern is more obvious for Q-BNF than for

Q-MYFUN, as Q-MYFUN stabilizes N_{Eco}. Consequently, Q-MYFUN ecosystem simulations respond less to N deposition changes, but still show a slight increase of fixation resulting from increased C investment into fixation with decreasing deposition (4.3.3). I can therefore confirm H4.2b, with the note that simulated Q-MYFUN ecosystems were hardly N limited. Again, a quantitative assessment is impossible, given the lack of observations, but generally an increase of fixation rates under N limitation is reasonable. *Batterman et al.* (2013) reported high fixation rates in early stages of (secondary) succession, which are caused by lacking N in young ecosystems, and *Cleveland et al.* (1999) estimated rather high fixation rates for ecosystems that are known to be N limited within all climate zones. However, a comparison with *Batterman et al.* (2013) is difficult, as I analyzed mature forest ecosystems, and data from *Cleveland et al.* (1999) are very broad.
Under eCO_2, which may lead to PNL (*Luo et al.* (2004)), plants invest more C into symbiotic fixation to acquire N, but again this is clearer for Q-BNF simulations that increased annual fixation rates by 200% to 400% in response to eCO_2 than for Q-MYFUN simulations, which increased fixation by only 150% initially, and about 25% in the long-term response to eCO_2. This confirms H4.2c, and is in line with global simulations of *Sulman et al.* (2019), who reported fixation rates of around 1 gN $m^{-2}year^{-1}$ under ambient conditions, and an increase of up to 1 gN $m^{-2}year^{-1}$, i.e. +100%, in response to a CO_2 enhancement of 100ppm over 20 years.
Generally, the performance of Q-MYFUN confirms H4.2, even if actual patterns are more obvious in Q-BNF simulations than in Q-MYFUN simulations caused by the hypothesized favor of mycorrhizal support over fixation (H4.1) and N_{Eco} stabilization (H4.5) that almost prevent plants from N limitation.

H4.3: The use of any additional nitrogen acquisition strategy, such as mycorrhizal support and/or symbiotic nitrogen fixation, prevent plants from progressive nitrogen limitation under elevated CO_2, and enhances growth in the short-term, as well as in the long-term response to elevated CO_2.
Short-term GPP and NPP responses to eCO_2 are positive among all tested model variants, but since QUINCY vegetation is not able to increase N acquisition accordingly, plants run into PNL within the first decade. Long-term C-flux responses to eCO_2 are therefore almost zero or even negative, which is not the case for QUINCY with any additional N acquisition strategy. With additional investment into mycorrhizal growth and/or symbiotic fixation, plants are able to increase N acquisition not only in the short-term, but also in the long-term, which prevents them from PNL on growth. Consequently, long-term growth response in Q-BNF, Q-MYC, and Q-MYFUN is positive, too, which confirms H4.3 (sec. 4.4.2). As this is close to observed responses of plant growth to eCO_2 (*Finzi et al.* (2007)), the confirmation of H4.3 indicates that the inclusion of symbiotic N acquisition strategies into TBMs may be the key to reduce uncertainty of future C uptake predictions that are caused by an inappropriate representation of plant N acquisition. Also the closeness of simulation results of Q-BNF, Q-MYC, and Q-MYFUN indicates that the inclusion of symbiotic N acquisition strategies into TBMs may reduce the disagreement of model simulations in general.

H4.4: The persistent positive response of vegetation to eCO_2 (H4.3) leads to a stronger positive ecosystem response to eCO_2 in model variants with any symbiotic N acquisition strategy than simulated with the baseline version model.
Persistent high GPP and NPP rates in response to eCO_2 lead to higher C accumulation in vegetation biomass in Q-BNF, Q-MYC, and Q-MYFUN in response to eCO_2, whereas vegetation biomass response to eCO_2 is almost zero after 40 years of fertilization experiment in QUINCY.
Minor simulated vegetation biomass increase in response to eCO_2 in QUINCY leads to only minor C accumulation within the entire ecosystem in response to eCO_2. This is mainly caused by a mild increase in soil C due to increased litter input during the first years of CO_2 fertilization experiment.
Also for Q-BNF, Q-MYC and Q-MYFUN, total ecosystem response to eCO_2 is affected by different soil C responses. N acquisition schemes that simulate mycorrhizal interaction with soil, and thus the access of SOM as N source, balance out additional C input by litter with increasing heterotrophic respiration. Consequently, the increase of soil C due to eCO_2 is low in Q-MYC and Q-MYFUN, which results in medium additional C accumulation within the entire ecosystem in response to eCO_2. Q-BNF accesses atmospheric N_2 to balance out the additional N requirements of plants, which increases N content of the entire ecosystem and increases the ability to store C in all compartments, i.e. in vegetation and soil. This results in highest ecosystem C responses to eCO_2. As all model variants with symbiotic N acquisition strategies increase C storage within the simulated ecosystem under eCO_2 compared to QUINCY, H4.4 (sec. 4.4.3) is confirmed.
Compared to *Sulman et al.* (2019), Q-MYFUN responses similar to eCO_2 than *Sulman's* dynamic N acquisition model, whereas QUINCY responses similar to *Sulman's* static model. Dynamic, plant controlled models show an increase in C_{Veg} in response to eCO_2 that drives the increase in C_{Eco}, whereas the increase in C_{SOM} is minor (Q-MYFUN) or even negative/zero (dynamic model by *Sulman et al.* (2019)) in response to eCO_2. Contrary, ΔC_{Veg} are weaker in QUINCY and the static model variant by *Sulman et al.* (2019) and show a decrease caused by PNL after an initial period, whereas ΔC_{SOM} increase initially and stay rather constant afterwards, which result in weaker positive ΔC_{Eco} in these models compared to the plant controlled ones. The similarity of model variants in response to eCO_2, which either act dynamically or statically with regard to plant N acquisition, suggests that the implementation of such processes is necessary to reduce down future C uptake uncertainty, which is caused by CN coupling and PNL in TBMs.

H4.5: Plants stabilize ecosystem nitrogen by accessing ecosystem external and internal nitrogen sources.
The access of ecosystem external N by symbiotic fixation of atmospheric N_2 stabilizes N_{Eco} in case of N stress or surplus that I simulated by decreasing or increasing N deposition (Q-BNF and Q-MYFUN). In contrast to that, N_{Eco} that is simulated by QUINCY and Q-MYC, which do not allow plants to access ecosystem external N, responds linearly to N deposition decrease/increase. This behavior is expected by H4.5 (sec. 4.3.3).

Additionally, I found that N_{Eco} is generally higher in Q-BNF then in QUINCY caused by fixation as direct N acquisition strategy, and generally lower in Q-MYC than in QUINCY due to less SOM, whereas the combination of symbiotic fixation and mycorrhizal interaction with SOM leads to an almost similar amount of N_{Eco} in Q-MYFUN compared to QUINCY. Since symbiotic fixation did not respond much to N deposition changes in Q-MYFUN, ecosystem stabilization is not only caused by the outbalance of N losses by plant controlled N inflow, i.e. symbiotic fixation, to ecosystem, but also by generally minor N_{Eco} losses in Q-MYFUN. This is caused by the acceleration of internal N cycling, which prevents leaching of organic matter (sec. 4.3.3). However, even if the similarity of Q-MYFUN-N_{Eco} to QUINCY-N_{Eco} suggests a model improvement compared to Q-BNF and Q-MYC, I cannot rate modelled N_{Eco}, because N_{Eco} is generally only weakly constrained in TBMs due to a lack of soil data. Q-BNF-N_{Eco} may be too high and Q-MYC-N_{Eco} may be too low, but actually QUINCY-N_{Eco} could also be wrong due to too high or too low soil N (N_{soil}). Caused by a lack of data, TBMs are usually constrained by C measurements that are mostly done on above-ground vegetation. Below-ground vegetation measurements as well as measurements of soil properties such as C or N pool sizes, especially mineral pool sizes, or soil C and N fluxes are difficult conduct. Additionally, there is no common observation protocol that would allow to quantify model relevant properties and fluxes such as plant available N, or N mineralization (*Vicca et al.* (2018), *Van Sundert et al.* (2019)). Consequently, despite their variance in N_{soil} and N_{Eco}, all model variants simulate reasonable vegetation C fluxes compared to observations under *ambient* conditions, but they largely differ in their response to eCO_2 (sec. 4.4.1 and sec. 4.4.2). This implies the need to better constrain our models also to *ambient* N cycle as future conditions may lead to stronger N limitation caused by eCO_2, which currently leads to a high uncertainty of future C cycle predictions in TBMs that account for N cycling (*Friedlingstein et al.* (2014)).
Finally, I observed the same stabilizing processes by Q-MYFUN in response to eCO_2 that lead to N stress by PNL as I did by stressing the ecosystem by less N gain due to a lower N deposition rate. Q-BNF simply increases N influx by fixation in response to eCO_2, and Q-MYC responds with an accelerated internal recycling of N that leads to a strong reduction in N_{soil}. Q-MYFUN uses both strategy to balance N_{soil} and following N_{Eco} in response to higher ecosystem C influx (sec. 4.4.3).

4.5.2. Plant control on nitrogen acquisition strategies

Initially, I asked the questions, where additional N may come from that was observed during free-air CO_2 enrichment (FACE) experiments by *Finzi et al.* (2007), but could not simulated by models (*Zaehle et al.* (2014)) (Q1), and how plants may control processes that supply N (Q2).
For MYFUN model development, I focused on two important N acquisition strategies that are based on symbioses, i.e. with N-fixing microbes and mycorrhizal fungi, that were previously shown to supply N on plant N demand (*Gutschick* (1981), *Read* (1991), *Marschner and Dell* (1994)), but not appropriately implemented into state-of-the-art

TBMs yet (*Brzostek et al.* (2017)). The strategies differ in the accessed N source, C investment into the strategy, and in the extend to what plants can control the symbionts. Symbiotic N fixation accesses atmospheric N_2, which is an ecosystem external, and therefore rather C cost intensive, but unlimited N source. Mycorrhizal fungi are modelled to access inorganic and organic N sources in soil, which is rather C cost extensive, but limited. Besides, plants are forced to exude C to mycorrhizal fungi to account for parasitic species and competition in case of intensive N limitation (*Franklin et al.* (2014)). Latter differs from the approach that was used by *Sulman et al.* (2019), who treats all N acquisition strategies equally and distinguishes between ectomycorrhizae (EMs) and arbuscular mycorrhizae (AMs), but is supported by observations by *Gutschick* (1981) that plants actually favor the support of mycorrhizal fungi that access ecosystem internal N sources. Besides, most terrestrial plants host mycorrhizal fungi, whereas only some host N-fixing microbes (*Gutschick* (1981), *Read* (1991)). This also indicates a favor for plant-mycorrhiza symbioses, which is represented by the hierarchical structure of MYFUN (fig. 4.3).
The simulated CO_2 elevation experiment, i.e. +200ppm CO_2 to transient climate, showed that plants use both strategies to enhance their N acquisition in response to eCO_2, but that symbiotic fixation is only strongly increased within the first years (initial response +150%, long-term response: +25%), whereas the increase in mycorrhizal support is less strong initially, but also declines less in the long-term (initial response +65%, long-term response: +25%). This is caused by both, the modelling approach that prefers mycorrhizal fungi, and the simulation set-up that is a step-increase of atmospheric CO_2. This step-increase leads to an imbalance of ecosystem dynamics. C uptake by plants via photosynthesis is strongly stimulated by eCO_2, and plants try to balance out with additional N influx into ecosystem. Consequently, they increase fixation only until the ecosystem has reached a new equilibrium regarding their C and N budgets. After outbalancing ecosystem CN, modelled plants lower external inflow, i.e. fixation, to only account for ecosystem N losses to hold ecosystem CN ratio. A gradual increase of atmospheric CO_2 instead of a step-increase would be much closer to current atmospheric changes. Gradual changes may unbalance ecosystem dynamics much less, because plants and ecosystems would have time to adjust processes and and balances to CO_2 elevation. This already may prevent modelled ecosystems from PNL without any symbiotic N acquisition strategy (*Walker et al.* (2015)).
Critics on the method of a step-increase of atmospheric CO_2 are also made by *Sulman et al.* (2019), who conducted a similar model CO_2 elevation experiment by running their model variants (dynamic N acquisition, and static N acquisition, which are similar to Q-MYFUN and QUINCY) with an atmospheric CO_2 concentration of 286ppm and a step-increase to 386ppm, and analyzed plant N acquisition and C balance changes globally after 20 years of CO_2 fertilization, and globally integrated within 100 years of fertilization. They acknowledge that the step-increase is not close to reality, because cCO_2 is increasing gradually, but they decided to use this approach anyway, since they could only evaluate their model and its behavior against two FACE experiments that used this

step-increase. To their and my knowledge, experiments that explore plant response to a gradual increase in cCO_2 are not conducted on ecosystem scale, which hinders the ability to evaluate models. *Sulman et al.* (2019) also find a stronger positive response of fixation during the initial fertilization period, and a weaker response during long-term fertilization, which they explained by increasing N stocks within ecosystems that are sufficient to meet enhanced plant N requirements for growth. Contrary, mycorrhizal activity persists high in response to eCO_2 in the dynamic model. Both findings and conclusions are in agreement to my analyses.
However, critics on the step-increase raise the question, whether PNL is actually a real problem under current atmospheric CO_2 enhancement, or just an experimental and model artefact resulting from the experimental set-up. To approach this question, one would need FACE experiments, that do not enhance atmospheric CO_2 step wise, but gradually over the entire fertilization period. That would be much closer to reality.

Now, to answer the initial questions: It is very likely that enhanced N acquisition in response to eCO_2 is mostly supported by mycorrhizal fungi that access (or interact) with SOM, but backed up with symbiotic fixation. This is underpinned by *Terrer et al.* (2018), who compared N acquisition enhancement among 20 FACE experiments at 12 sites and linked it to plants' main symbionts (ectomycorrhizae (EMs), arbuscular mycorrhizae (AMs), N fixers). They found that sites, which are known to have EMs, are most successful in increasing N acquisition in response to eCO_2, whereas sites, which are known to host N fixers, respond minor, but still positively.
Model plants control their hosted symbionts, and the resulting N acquisition strategy, by actively changing C allocation to symbionts. Besides, similar long-term enhancement of both symbiotic N acquisition fluxes in response to CO_2 elevation, i.e. at +25% to ambient fluxes, suggests an optimal N acquisition arrangement in Q-MYFUN that plants tend to reach in steady states.
However, to assess these results and quantify fluxes, I would need flux measurements that actually show an increased C flux from host plant to mycorrhizal fungi or to nodules in response to eCO_2, and an increase of the returned N flux on ecosystem scale. Also dual-labelling experiments that provide information, which N source (labelling of potential N sources) is used for N acquisition under ambient conditions, as well as under elevated CO_2 concentrations, would help to answer the question in which case plants choose which N acquisition strategy, and how they control it (plant C labelling).

4.5.3. Plant control on ecosystem carbon-nitrogen balances and dynamics

Initially, I also asked the question, to which extent plants may control ecosystem balances and soil processes (Q3), but this question will remain unanswered due to the lack of data to quantify findings.
My results suggest that the active use of symbiotic N fixation and mycorrhizal fungi to support N acquisition allows plants not only to overcome N limitation on growth, but also to control ecosystem C and N balances and dynamics to a certain extent (sec. 4.3.3 and

sec. 4.4.3) as hypothesized by *Knops et al.* (2002) and *Chapman et al.* (2006).
This control is kept by controlling (i) C influx to ecosystem entirely by photosynthesis, (ii) N influx to ecosystem partly by C investment into symbiotic fixation, and (iii) soil processes partly by C exudation to mycorrhizal fungi that interact with SOM to short-cut internal N cycling. The first two control mainly ecosystem balances, whereas latter controls rather ecosystem dynamics, but since balances and dynamics are tightly linked, one cannot separate them entirely.
However, the extent to what plants can control ecosystem N may be too high, as MYFUN is unable to respond to N fertilization, which is shown to happen in natural ecosystems (*Vitousek* (1982), *Treseder et al.* (2007), *Thomas et al.* (2010), *Wright et al.* (2018)). Nevertheless, its ability to simulate observed plant responses to C fertilization is a major improvement. Overall, I cannot confirm (or reject), or at least evaluate my findings quantitatively due to the lack of ecosystem scale data on C and N balances and dynamics. Especially soil property and soil flux information are needed to quantify plant control on ecosystem dynamics, and to potentially constrain my model accordingly.
The only experimental evidence that plants somehow control soil processes on ecosystem scale, is derived from FACE experiments, where plants are shown to increase N acquisition in response to eCO_2 to meet their enhanced growth requirements (*Finzi et al.* (2007)). *Terrer et al.* (2018) extended these findings by the inclusion of more FACE sites that are known to have different root-associated symbionts, which potentially support plant N acquisition, and by accounting for N availability. They concluded that plants benefit most from hosting EMs, indicating a strong control on EMs and resulting soil dynamics, and least from hosting AMs, indicating a weak control on AMs and resulting soil dynamics, whereby plant benefit is shown by both, increased N acquisition, and enhanced biomass production. This fits to *Chapman et al.* (2006) suggestions, who linked EMs to N-conservative plants, and AMs to N-extravagant plants, and assumed that only N-conservative plants have a strong control on ecosystem N dynamics, and i sin line with findings of *Phillips et al.* (2013), who linked EM-hosting plants to an organic nutrient economy and AM-hosting plants to an inorganic nutrient economy, which is supported by space-born observations, as *Fisher et al.* (2016) reported.
However, without soil measurements that confirm enhanced microbial or mycorrhizal activity, SOM decomposition acceleration, enhanced N uptake fluxes from different N sources, or enhanced N fixation, a quantification of plant control on ecosystem N (and C) dynamics is impossible. Consequently question to which extend plants control ecosystem C and N balances and processes remains unanswered, as I cannot assess it quantitatively, and even a proper qualitative assessment is almost impossible with current experimental evidence.

4.5.4. Assessment of model performance and model improvement

I developed a plant controlled N acquisition model (MYFUN model) by including a plant-mycorrhiza interaction model (MYC model) into a C-cost based framework for biological N fixation (BNF model). By that, I wanted to address the influence of different symbiotic plant N acquisition strategies, i.e. N fixation by symbiotic bacteria and C and N exchange with symbiotic mycorrhizal fungi, on plant N nutrition and improve the representation of plant N acquisition, plant N nutrition and plant growth in terrestrial biosphere models (TBMs).
After having discussed the general importance of symbiotic N acquisition strategies for plants and the entire ecosystem and the effect on both, in case such strategies are modelled explicitly, the question of model improvement with respect to plant growth remains. For that, I compared simulations of the original model (QUINCY) to model variants that include symbiotic N fixation (Q-BNF), plant interactions with mycorrhizal fungi (Q-MYC), or both (Q-MYFUN) among each other and to observational data from the GFDB (sec. 2.2.3.1, *Luyssaert et al.* (2007)). As I was interested in plant growth, I compared annual GPP and NPP, as well as CUE for 42 mature forest sites. Generally, the inclusion of any symbiotic N acquisition strategies increases GPP and NPP due to a better N nutrition. Since the effect is greater on GPP, CUE is slightly lower in Q-BNF, Q-MYC, and Q-MYFUN than in QUINCY. However, as QUINCY already tends to overestimate GPP and NPP of temperate and boreal forests, the inclusion of N fixation and/or mycorrhizal fungi does not improve model-data agreement. Actually, model-data agreement is lowered, when comparing each site individually (sec. 4.4.1, fig. 4.8).
Because the general shown fertilization effect, i.e. the increase of GPP and NPP, by symbiotic N fixation and/or support by mycorrhizal fungi suggests N limitation on plants in QUINCY, I also compared simulated leaf CN ratios for evergreen trees among model variants (sec. 4.4.1, fig. 4.10). I found a decrease in leaf CN ratio in Q-BNF, Q-MYC and Q-MYFUN compared to QUINCY for boreal and temperate forests, whereas leaf CN ratios are increased at tropical sites. For coniferous trees, which build the major group of evergreen trees within the boreal and temperate zone, I expect a leaf CN ratio of approximately 42 gC/gN, which is the mean of observations from the TRY database (*Kattge et al.* (2011)). QUINCY simulates leaf CN ratios below 40 gC/gN and above 50 gC/gN, which may meet observations on average, but indicate N limitation for almost half of the sites, which have very high leaf CN ratios. In combination with the observed mild overestimation of GPP and NPP by QUINCY especially for boreal forest sites, this points to a systematic bias in QUINCY concerning C assimilation and growth in dependency of N nutrition, which becomes an issue when improving N nutrition. Q-BNF simulations meet the expected leaf CN ratios best, which indicates that there is an optimal leaf CN ratio close to observations that QUINCY tries to reproduce. Since the N fixation scheme that is used for Q-BNF is based on an optimality approach, this model variant is in particular successful in reproducing optimal leaf CN ratios. Contrary to that, model variants that include support by mycorrhizal fungi, i.e. Q-MYC and Q-MYFUN, lower leaf CN ratios too strong. This suggests that mycorrhizal fungi deliver too much N to their host plant,

and plants lack control to avoid too high N acquisition rates, which points back to the question of actual plant control on symbiotic N acquisition strategies. Plants may need the entire control, or at least some mechanisms to stop N export in case they are satisfied, to achieve leaf CN ratios close to their individual optimal leaf CN ratio. Currently this is hampered by the needs of mycorrhizal fungi, and therefor needs further research to avoid general overfertilization.
Shifts of leaf CN ratios are opposite at tropical sites, meaning leaf CN ratio increases by applying symbiotic N acquisition strategies. This leads to a decrease of GPP, and to an increase of NPP that brings simulations closer to observations (sec. 4.4.1, fig. 4.8 and fig. 4.10). This points to a saturation effect of productivity with regard to N nutrition, which was also reported by *Meyerholt and Zaehle* (2015), but also suggests that tropical sites in QUINCY simulations are not N limited as N nutrition is extremely high. Enhanced productivity by model variants that include symbiotic N acquisition strategies may therefore not solely arise from changed N nutrition, but also from improved P nutrition, as effects are different for model variants with and without mycorrhizal fungi. Q-BNF, which does not include mycorrhizal support, but is based on plant optimality, increases leaf CN ratio most, and consequently lowers GPP most, as GPP is directly affected by leaf N content. This brings GPP simulations generally closest to observations. However, NPP is only slightly increased, which indicates that growth of Q-BNF simulated tropical sites is still more limited than growth in Q-MYC and Q-MYFUN simulations. These model versions include mycorrhizal support, which hampers full control over plant N nutrition, as mycorrhizal fungi deliver only their own surplus to host plants. Consequently, leaf CN ratios are not increased as much as simulated by Q-BNF, which then lowers GPP not as much. However, because mycorrhizal fungi also deliver surplus P, they improve plant P nutrition as well, which increases NPP. This indicates that tropical sites that are simulated by QUINCY are P limited and not N limited, as it needs additional P acquisition to fertilize growth[5]. P limitation at tropical forest sites is generally in line with observations (*Vitousek* (1984), *Vitousek et al.* (2010), *Gill and Finzi* (2016), *Fleischer et al.* (2019)), but the fact that Q-MYC and Q-MYFUN generally improve model-data agreement for tropical sites slightly, suggests that P limitation is too strong in QUINCY.

Even though the inclusion of symbiotic N acquisition strategies, which are (mostly) plant controlled, does not improve model-data agreement when comparing to C flux observations for most sites, it does improve the simulation of responses to atmospheric CO_2 elevation (sec. 4.4.2 and sec. 4.4.3). QUINCY, as most TBMs, is not able to reproduce the long-term positive growth response of plants that is observed at free-air CO_2 enrichment (FACE) experiments (*Finzi et al.* (2007), *Zaehle et al.* (2014)). This is caused by increasing progressive N limitation (PNL, *Luo et al.* (2004)) during the simulated experiment (fig. 4.11 and fig. 4.12). In contrast to that, the use of any symbiotic N acquisition strategy prevents plants from PNL in response to elevated CO_2 (eCO_2) and model variants are

[5]At its current state, the MYC (sub-)model is not sensitive with regard to plant P demand, i.e. C exudation to mycorrhizal fungi is not sensitive to plant P demand. But since QUINCY simulates fully coupled C, N and P cycles within ecosystems, mycorrhizal fungi also take up P from soil, as plants do, but with the higher uptake efficiency, and they deliver surplus P similarly to N to their host plants, which may improve P nutrition at severely P limited sites already.

able to reproduce the observed plant fertilization in response to eCO_2 by enhancing N acquisition (sec. 4.4.2, fig. 4.11 and fig. 4.12).
This leads to different predictions of future C storage in the simulated ecosystems (fig. 4.13). After 40 years of simulated CO_2 experiment, QUINCY simulates almost non additional C storage in vegetation and moderately increased soil C, whereas Q-BNF, Q-MYC, and Q-MYFUN simulate similarly increased vegetation C, but differ in simulated soil C responses. Due to enhanced heterotrophic respiration by mycorrhizal activity Q-MYC and Q-MYFUN simulate only a minor soil C increase, which is in line with observations of *Lichter et al.* (2008) and site-specific, as well as global simulations of *Sulman et al.* (2019). Contrary to that, Q-BNF predicts a major increase of soil C, which is caused by the strong enhancement of N influx by symbiotic N fixation into the ecosystems.
The generally improved simulation of plant responses to eCO_2 indicates a process-based model improvement, as is allows plants to respond dynamically to environmental changes, which brings simulations closer to observations. However, diverging predictions of soil responses that affect ecosystem responses largely point to still existing uncertainty due to unknown processes and/or limitations. To understand them and improve the model further by including such processes, or constrain them better, I would need further observational evidence, e.g. an answer to the question to what extend plants can increase N fixation rates.

4.5.5. Conclusion and Outlook

The presented MYFUN model, which is implemented into the TBM QUINCY, is a fully coupled dynamic plant N acquisition model. The model structure allows plants to actively invest C into different N acquisition strategies, namely mycorrhizal fungi and N fixers, concurrently and in addition to root uptake. This is a significant step forward in recent TBM development, as it connects vegetation and soil processes more tightly, which is needed to allow ecosystems to adjust persistently to environmental changes. Latter is often hindered in state-of-the-art TBMs, since vegetation and soil processes often act on different time scales and their disconnection lead to a rather static ecosystem behavior as it hampers long-term process adjustments for both, vegetation and soil.
Allowing plants to control soil processes results in quicker ecosystem responses to environmental changes such as atmospheric CO_2 elevation, since plants usually act on shorter time scales as soils do. This is necessary to improve model performance in response to elevated CO_2 and leads to a greater C storage under eCO_2 within the entire ecosystem compared to state-of-the-art TBMs.
Nevertheless, I again point out strongly the need of observational data to (i) improve process understanding, which is the basis the future model implementations, (ii) evaluate recent model development, and (iii) constrain models not only with respect to the C cycle, but also with respect to the N (or other nutrients such as P) cycle. Data should preferably come from ecosystem scale observations, since this is the scale at which most TBMs, as well as the MYFUN model act, and certainly include soil measurements that need a common protocol to ensure comparability, and an informative data basis,

which is needed to derive model relevant model parameters and constraints. However, also experiments on smaller scale, such as mesocosm experiments, possibly with ^{13}C and/or ^{15}N labelling, are highly desirable, because they provide a unique insight into plant-soil interaction processes under controlled conditions that support further model development by quantifying actual fluxes.

Prospectively, testing the other proposed mycorrhizal functionality (i.e. the decomposers, sec. 3.2.1) in combination with the N fixation scheme is reasonable, as this combination may then represent the N-extravagant strategy, where plants control microbial community only by litter quality, or, in MYFUN, by C exudation. Since *Chapman et al.* (2006) linked this strategy mostly to AM-hosting plant species, this would further support the assignment of saprotrophic behavior to EMs (organic nutrient economy, *Phillips et al.* (2013)) and decomposing functionality to AMs (inorganic nutrient economy, *Phillips et al.* (2013)), as discussed in section 3.6.
Adding P actively to the mycorrhizal framework, i.e. include P into model structures that constrain plant C exudation to mycorrhizal fungi and thus limit mycorrhizal growth (eq. 3.4 - eq. 3.6), should further improve MYFUN model behavior. Currently, plant C exudation is only driven by plant N demand, which may be too low in P limited ecosystems, such as the tropics.
This may intensify the question of actual plant control on mycorrhizal fungi, and mechanisms to avoid overfertilization, which is currently likely to happen, as simulated leaf CN ratios tend to be too low compared to observations. In case, exudation, and consequently mycorrhizal growth, is sensitive to both, N and P, and driven by the more limiting nutrient, plants need to have control mechanisms to stop export of the less limiting nutrient.
Finally, QUINCY-MYFUN should be run globally in order to assess the value of the linkage between vegetation and soil processes by plant control on N (and P) acquisition strategies. This may reduce current uncertainty of future land C uptake, which are caused by (progressive) N (and P) limitation, and may allow more accurate estimates of the impact of terrestrial ecosystems to climate change, which may be underestimated when neglecting N (and P) supporting symbioses (*Shi et al.* (2019)).
Besides such MYFUN-related steps, I would suggest to rethink the link between N nutrition and C assimilation in QUINCY, i.e. leaf CN ratio or leaf N content and GPP, as there may be a bias towards too high assimilation and productivity. This bias may be caused by the inability of ecosystems, which are modelled by QUINCY, to provide sufficient N for plants. To meet observations, parameters are adjusted accordingly.
Since most TBMs rely on similar functions, and have rather simple soil models included, this bias may also exist in other TBMs and needs generally further research.

5. Discussion and Conclusion

My thesis was guided by the question if and to what extend nitrogen (N) controls plant growth, which I quantify by analyzing both, *absolute* growth rates, i.e. net primary production (NPP), and *relative* growth rates, i.e. the carbon-use efficiency (CUE, eq. 1.2), which is defined as ratio of NPP to gross primary production (GPP). CUE therefore comprises the information, how efficient plants or ecosystems use assimilated carbon (C) for biomass production (*Manzoni et al.* (2018)), and may provide additional insights into underlying processes that are not visible by only analyzing absolute plant growth rates.
Several studies have shown that CUE is higher in fertile forests or forest ecosystems (*Vicca et al.* (2012), *Fernández-Martínez et al.* (2014)). This is caused by N being essential for both, plant photosynthesis and plant biomass production (*Wright et al.* (2018)), but also by reduced respiration rates (R) in fertile ecosystems (sec. 1.2.1.1). By implication, a poor nutrient/N availability increases R as plants are forced to invest more C into N acquisition. This happens either by enhanced root growth, or by hosting symbionts that supply N (sec. 1.2.2.1).

Lower growth rates, which are caused by an insufficient N availability, and consequently lower C sequestration rates within ecosystems become particularly important when considering currently rising atmospheric CO_2 concentrations (cCO_2). Plants are shown to increase GPP and -initially- also NPP under elevated cCO_2 (eCO_2) conditions (*Norby et al.* (2002), *Norby et al.* (2005), *Ainsworth and Rogers* (2007), *Bonan* (2008)). However, long-term CO_2 fertilization effects are uncertain, since it is unclear, whether ecosystems can persistently provide sufficient N to support enhanced plant growth. Actually initially increased biomass production may intensify N limitation, as much N is already sequestered in biomass, which is then not available for further growth. This effect, which is referred to as *progressive N limitation* (PNL, *Luo et al.* (2004)), complicates estimations of future C storage in (forest) ecosystems (sec. 1.2.2.2).
Terrestrial biosphere models (TBMs) predict that our present land C sink of atmospheric CO_2 may even turn into a C source until the end of the 21^{st} century, because occurring PNL may increase respiration rates that strong that they may even exceed C assimilation rates (*Wieder et al.* (2015)). This is caused by a rather static response of simulated vegetation to plant-available N, i.e. plants simply in- or decrease N uptake in dependency of soil N provision, whereby state-of-the-art soil models lack the complexity of state-of-the-art vegetation models, which are both part of TBMs (*Knops et al.* (2002)). Especially soil organic matter (SOM) decomposition does not or only weakly respond to higher C input into ecosystems in models. However, there is evidence from large-scale ecosystem experiments that plants actually increase their N acquisition in response to eCO_2,

which may prevent them from PNL and may lead to a long-term positive NPP-response to eCO_2 (*Finzi et al.* (2007), *Zaehle et al.* (2014)), and also that there is a strong response in soil processes that affect soil C storage (*Lichter et al.* (2008)).

Thus, the essential questions that I wanted to address with my thesis is not only to what extend N controls plant growth, but also which mechanisms and processes related to plant N nutrition are not or only poorly represented in state-of-the-art TBMs, and how the implementation of such processes affect not only vegetation responses to eCO_2, but also soil and ecosystem responses. For that, I concentrated on two symbiotic plant N acquisition strategies, which are known to be important for plant N acquisition and thus may have the power to largely impact land-atmosphere feedbacks with regard to eCO_2 (*Shi et al.* (2019)). Despite this, they are only insufficiently represented in TBMs yet in case of symbiotic N fixation (chapter 2), or not at all in case of plant-mycorrhiza symbioses (chapter 3), which is why I implemented them into the TBM QUINCY (*Thum et al.* (2019)).

In this final discussion of my thesis, I summarize and discuss key findings of N controls on plant growth from chapters 2 to 4 in the context of my research questions, i.e. what the implementation of plant controlled N acquisition by symbiotic fixation and mycorrhizal support into a TBM implies for simulated plant and ecosystem CN budgets and dynamics, and to what extend plant control on N availability/ecosystem N may be reasonable, followed by conclusions and outlook.

5.1. Summary and Discussion

5.1.1. Research question 1: What does the implementation of plant controlled N acquisition by symbiotic N fixation and/or mycorrhizal fungi into a TBM imply for simulated (i) plant N nutrition, (ii) plant CUE, and (iii) ecosystem CN budgets and dynamics?

Within chapters 2 to 4 I developed a plant controlled N acquisition model that consists of a C cost based **Biological N Fixation (BNF) model** (chapter 2), and a **plant-MYCorrhiza interaction (MYC) model** (chapter 3). Both sub-models were implemented into the TBM QUINCY (*Thum et al.* (2019)) and evaluated independently from each other, before they were coupled to build the **MYcorrhizal export, symbiotic Fixation and plant Uptake of Nitrogen (MYFUN) model** (chapter 4). The BNF and the MYC model follow different N acquisition strategies by accessing fundamentally different N sources, which affect either ecosystem N content (N_{Eco}), or N cycling within the ecosystem. The BNF model represents symbiotic N fixation as N acquisition strategy and allows plants to acquire N from atmospheric N_2, which is an ecosystem external source. Consequently, the BNF model may change N_{Eco}. The MYC model explicitly simulates mycorrhizal in-

teractions with plants and soil and thus modifies soil organic material (SOM) dynamics. This accelerates ecosystem internal recycling of N.
I start my discussion by a summary of key findings with regard to modelled N acquisition and N control on plant CUE, before I assess implications of all model variants to simulated ecosystem CN budgets and dynamics.

Implications for simulated plant N acquisition and plant CUE
Generally, the implementation of both symbionts, i.e. N-fixing bacteria and mycorrhizal fungi, into the TBM QUINCY increases simulated plant N acquisition and improves modelled plant N nutrition (fig. 5.1). Improved N nutrition increases both, GPP and NPP, whereby the positive effect on GPP via improved leaf CN ratio (fig. 5.1 ①) is stronger than the fertilization effect on plant growth (fig. 5.1 ②), i.e. on NPP. This is, because autotrophic respiration (R_a, sec. 1.2.1.1) is enhanced by (i) enhanced growth, which leads to growth respiration (R_g, fig. 5.1 ③) itself, (ii) enhanced maintenance respiration (R_m, fig. 5.1 ④) by increased biomass, (iii) enhanced N uptake respiration ($R_{N_{up}}$, fig. 5.1 ④), which are caused by a greater root biomass that increases plant N uptake, and (iv) N fixation respiration (R_F, fig. 5.1 ⑥) in case of symbiotic N fixation. The less positive effect of improved N nutrition by symbiotic N acquisition on NPP compared to GPP decreases modelled CUE in general, but details differ among symbionts and among their function, i.e. the optimal and resistance scheme in case of N fixation, and saprotrophic and decomposing mycorrhizae. To account for such differences, I review key findings of implications for simulated plant N nutrition and growth for each chapter individually.

The inclusion of two C cost based BNF models into QUINCY (chapter 2), i.e. the *optimal scheme*, following the idea of *Rastetter et al.* (2001), and the *resistance scheme*, based on the FUN model by *Fisher et al.* (2010) and *Brzostek et al.* (2014), enhances plant N acquisition and improves plant N nutrition compared to the *standard scheme*, which is part of QUINCY (sec. 2.2.1). Improved N nutrition has a strong positive effect on modelled GPP, but C investment into symbiotic N fixation also enhances autotrophic respiration (R_a) by N fixation respiration (R_F). Consequently, modelled *absolute* growth rates, i.e. NPP, do not differ significantly among model variants with and without symbiotic N fixation, but *relative* growth rates, i.e. CUE, are lowered by simulating symbiotic N fixation (sec. 2.4.1).
This pattern does not change under eCO_2 conditions, because modelled plants avoid PNL by investing additional C into symbiotic N fixation, which lowers CUE further, but increases NPP even in the long-term compared to the basic model variant that has no adaptive N fixation scheme (sec. 2.4.2).

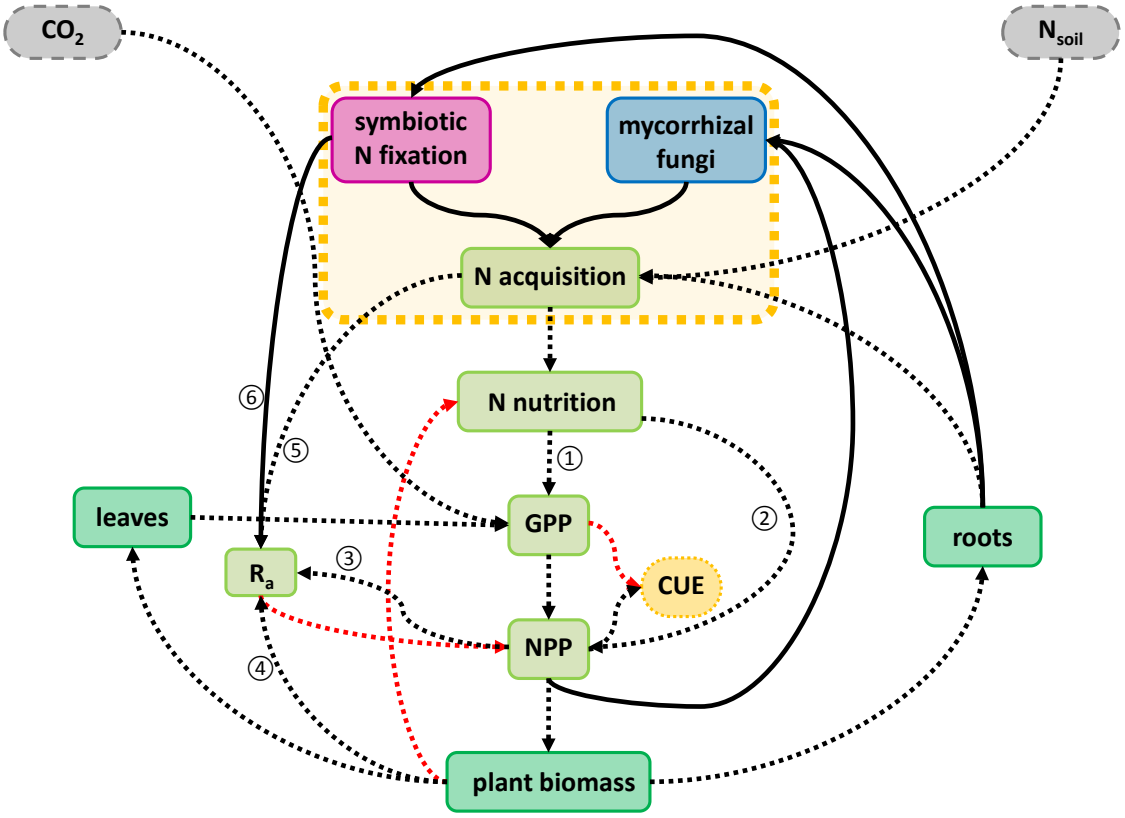

Figure 5.1.: Schematic representation of implications of the implementation of symbiotic N fixation (pink box) and mycorrhizal fungi (blue box) into a TBM on simulated plant growth.
Light green boxes refer to plant fluxes and characteristics, and dark green boxes refer to plant biomass pools. Grey ovals represent environmental conditions. Orange oval shows plant CUE, and orange box highlights plant N acquisition by supportive symbionts as main focus of the thesis.
Arrows show direction of dependency, whereas black arrows represent positive dependencies and red arrows represent negative dependencies. Solid arrows depict dependencies of new model structure by BNF and/or MYC sub-models, dashed arrows depict dependencies within the QUINCY model framework.
Numbers refer to main dependencies, i.e. fluxes and ratios, that shape plant CUE with regard to N acquisition: ① leaf N content, ② plant CN ratios, ③ growth respiration (R_g), ④ maintenance respiration (R_m), ⑤ N uptake respiration ($R_{N_{up}}$), ⑥ N fixation respiration (R_F).

The inclusion of plant-mycorrhiza interactions into QUINCY (chapter 3) complicates the definition of *plant* CUE, since CUE includes exudation to mycorrhizal fungi as part of NPP by the used definition by *Manzoni et al.* (2018), but mycorrhizal biomass does not belong to plant biomass (BP). So for the analysis I had to decide, whether I still use NPP for calculating CUE (including exudation), or if I define plant BP efficiency (BPE; excluding exudation; sec. 1.2.1.1) as *plant* CUE[1].
From modelling perspective, it is easy to distinguish between BP and NPP, because the exudation flux is explicitly calculated, and it is also easy to separate fine root biomass from mycorrhizal biomass, but both separations are (almost) impossible from measurement perspective. Below-ground measurements are generally difficult, and especially for natural ecosystems. Thus, a discrimination between (fine) root biomass and mycorrhizal biomass is almost impossible, and below-ground C and/or N fluxes between plants and mycorrhizae are unfeasible on ecosystem scale. Recent lab studies show first exchange rates between plants and mycorrhizae, but they are still highly uncertain, and the transferability of such lab-measured fluxes to ecosystem fluxes is questionable. They only provide evidence that plants and mycorrhizae exchange C and N, and that rates are positively correlated, i.e. high C exudation is linked to high N provision (*Gorka et al.* (2019)). The impossibility to distinguish between BP and NPP from observational perspective (*Vicca et al.* (2012)), and the fact that NPP is often derived from GPP and R_a measurements (sec. 2.2.3.1, *Luyssaert et al.* (2007)), which then explicitly includes exudation into NPP, led me to the decision to use the more general definition of CUE as ratio of NPP to GPP. Besides, I assume that mycorrhizal fungi were implicitly simulated in previous TBMs and thus part of their modelled NPP as well, which I then cannot distinguish from BP. Consequently, using BP for CUE calculations would treat models with and without mycorrhizal fungi differently.
Simulated CUE is higher in QUINCY with mycorrhizal fungi compared to QUINCY without mycorrhizal fungi at Duke, i.e. more C is incorporated into (plant and mycorrhizal) biomass per unit assimilated C, since N acquisition meets growth requirements (sec. 3.3, tab. 3.3). This is caused by both, a decrease of simulated GPP and an increase of simulated NPP in model variants with mycorrhizal fungi. Decreased GPP results from higher C allocation to below-ground tissues in the presence of mycorrhizal fungi, which lowers the amount of leaves that assimilate C. This effect is stronger in the presence of decomposing mycorrhizae, because they entirely depend on plant C exudation, whereas saprotrophic mycorrhizae gain some C by taking up organic N, which is why they need less supply from their host plants. NPP is increased by mycorrhizal biomass itself, but also by an improved N nutrition, which allows plants to grow better, i.e. BP is increased in the presence of mycorrhizal fungi, too (sec. 3.3). In combination, this may suggest a too strong parasitic behavior of modelled mycorrhizal fungi, as plants are forced to exude C to hosted mycorrhizae, even in case they do not benefit from them.

[1] An assessment of differences between using CUE and BPE for quantifying plant growth can be found in *Collalti et al.* (preprint).

However, decreased GPP and increased NPP that lead to increased CUE by simulating mycorrhizal fungi as N acquisition strategy are rather unexpected, as I assumed a stronger fertilization effect on GPP than on NPP, which decreases CUE in the presence of mycorrhizal fungi. Further analyses of GPP, NPP and CUE in model variants the include mycorrhizal fungi in chapter 4 show, that the model behavior at Duke in chapter 3 is only site specific and caused by stand age. During succession C allocation pattern shifts from growth of new tissues towards maintenance of existing tissues, which is why young forests have generally higher growth rates, and use more freshly assimilated C for biomass production, whereas mature forests do not grow much anymore, as they need most freshly assimilated C for maintenance processes (*Amthor* (2000), *Fernández-Martínez et al.* (2014), *Campioli et al.* (2015), *Collalti et al.* (2018), *Collalti et al.* (2019)). As Duke forest is rather young and still growing (sec. 3.4.2), its growth rate, i.e. NPP, benefits stronger from improved N nutrition than NPP of mature forests[2]. This causes the unexpected increase in CUE in the presence of mycorrhizal fungi, which I do not find in simulations of 42 mature forest sites of the GFDB (sec. 4.4.1). They show the expected stronger enhancement of GPP in the presence of mycorrhizal fungi, and only minor fertilization effects on NPP, which decreases modelled CUE compared to QUINCY without mycorrhizal fungi. Nevertheless, the unexpected model behavior at Duke suggests that parasitic mycorrhizae may be a problem for simulating young forests in general (sec. 3.3.2.1), which has to be explored further.

Finally, I included the MYC model into the BNF framework (chapter 4) and analyzed the results for one BNF model and one MYC model, i.e. the optimal BNF scheme that performed better on my sub-annual time steps (sec. 2.5), and the saprotrophic mycorrhizae that allow plants a stronger control on soil processes (sec. 3.6).
As analyzed in section 4.4.1, I found the expected increase in GPP in all model variants that included additional plant controlled N acquisition strategies, i.e. optimal BNF (Q-BNF), saprotrophic mycorrhizae (Q-MYC), or the fully coupled MYFUN model (Q-MYFUN), compared to the basic QUINCY model (QUINCY) at mature temperate and boreal sites. This is caused by an improved N nutrition that allows plants to assimilate more C (fig. 5.1). The effect is strongest for Q-BNF, because C investment into N fixation allows plants best to balance out their N demand, and lowest for Q-MYC, because plants allocate more C below-ground, which lowers the amount of leaves that assimilate C. GPP at tropical sites did not change much, or even decreased by applying symbiotic N acquisition strategies, indicating that N is not the most limiting nutrient, but P.
P limitation at tropical sites leads to almost no change in NPP fluxes by applying any symbiotic N acquisition strategy, whereby NPP is mildly increased at temperate forest sites, and strongly increased at boreal forest sites. Increased NPP generally indicates an improved N nutrition that allows plants to grow better. Since boreal sites usually suffer most from N limitation (*Vitousek* (1984), *Vitousek et al.* (2010), *Gill and Finzi* (2016)),

[2]Model simulations of forest succession with and without symbiotic N fixation, i.e. symbiotic N acquisition, also showed the strong fertilization effect on plant growth especially during the first years of evolution, which is reduced and vanishes after around 30 years. This also indicates that one has to distinguish between growing and mature forests, when comparing effects of symbiotic N acquisition on plant growth (sec. 2.3.2.3).

the effect of symbiotic N acquisition strategies is strongest in this area.
As result form the absolute fluxes, CUE is generally rather decreased by applying additional plant controlled N acquisition strategies as expected (fig. 5.1). The effect is strongest for Q-BNF (median: 0.46; -7.6% on average compared to QUINCY, which has a median-CUE of 0.50), weakest for Q-MYC (median: 0.49; -1.8%), and moderate for Q-MYFUN (median: 0.47; -4.8%), which combines the effects of the BNF and the MYC sub-models . And generally all simulated values for CUE meet the expected range of *Amthor and Baldocchi* (2001), i.e. 0.2 to 0.65 for mature forests. CUE-decrease is rather caused by the strong effect of improved N nutrition by symbiotically supported N acquisition on GPP (Q-BNF: +19.0%, Q-MYC: +20.6%, Q-MYFUN: +20.0% on average compared to QUINCY) than due to the effect on NPP (Q-BNF: +8.9%, Q-MYC: +14.0%, Q-MYFUN: +10.6% on average compared to QUINCY), as symbiotic N acquisition also increases respiration rates. Only at boreal sites, CUE is increased by symbiotic N acquisition, because these heavily N limited sites benefit strongest from additional N and growth is strongly fertilized, i.e. the effect on NPP is stronger than on GPP. Generally, the induced change of simulated plant CUE by symbiotic N acquisition strategies is depending on the original N availability/limitation simulated by QUINCY. In case of minor N limitation, CUE decreases due to a stronger increase in GPP than in NPP. In case of strong N limitation on plant growth, CUE increases due to an improved N nutrition that causes a higher NPP increase than GPP increase (sec. 4.4.1).
However, a site-to-site comparison with observations showed that model-data agreement with respect to C fluxes, i.e. GPP and NPP, is better for QUINCY than for Q-BNF, Q-MYC, and Q-MYFUN, and also CUE model-data agreement is not improved by the application of any symbiotic N acquisition strategy. Latter suggests to rethink the meaning of CUE for plant growth quantification in relation to N nutrition, as model-data agreement is almost zero for all model variants. Thus, CUE may be too strongly affected by other environmental parameters such as temperature and water availability (*DeLucia et al.* (2007), *He et al.* (2019), *Collalti et al.* (preprint)). Leaf CN ratio or leaf N content may be better to quantify effects of symbiotic N acquisition on plant nutrition, and their link to GPP and NPP may better show a dependency of N availability and plant growth. Nevertheless, I also reported a potential bias of the link between GPP and leaf N content, which hinders a quantitative assessment of N control on plant growth currently (sec. 4.4.1 and sec. 4.5.4).

Besides, as discussed previously, I only analyzed model performance at mature forest sites to avoid affects of simulated harvest on soil N availability and soil dynamics (sec. 2.3.2.3 and sec. 3.3.2.1). This also excludes potentially strong(er) fertilization effects of symbiotic N acquisition on plant growth, which may change relative increases of GPP and NPP by improved N nutrition in a manner that CUE may actually increase (*Granier et al.* (2000), *DeLucia et al.* (2007), *Drake et al.* (2011), *Campioli et al.* (2015), *Fernández-Martínez et al.* (2014), *Collalti et al.* (2019)). Also this issue has to explored further by comparing young and mature forest behavior in models, by using not only GPP, NPP and CUE as quantification parameters, but also leaf CN ratio as measure for N nutrition.

Under eCO_2 all model variants with symbiotic N acquisition responded similarly with a persistent increase in GPP and NPP, whereas GPP and NPP were only increased initially in QUINCY simulations (sec. 4.4.2). All model variants agree in an initial increase in CUE that is lowered in the long-term until it is almost zero, which indicates an optimal CUE for plants in a steady-state. The agreement of Q-BNF, Q-MYC, and Q-MYFUN suggests that the inclusion of plant controlled symbionts that support plant N acquisition is necessary to reduce current uncertainty of future C flux predictions as it explains persistent positive plant growth responses that are observed (*Finzi et al.* (2007), *Zaehle et al.* (2014)).

Implications for simulated ecosystem CN budgets and dynamics

The implementation of symbiotic N fixation and/or mycorrhizal fungi as plant controlled strategy to enhance N acquisition does not only influence plant CN budgets by changing CUE and increasing N acquisition (fig. 5.1), but feedbacks to ecosystem CN budgets and dynamics (fig. 5.2), which I analyzed in section 4.3.3.

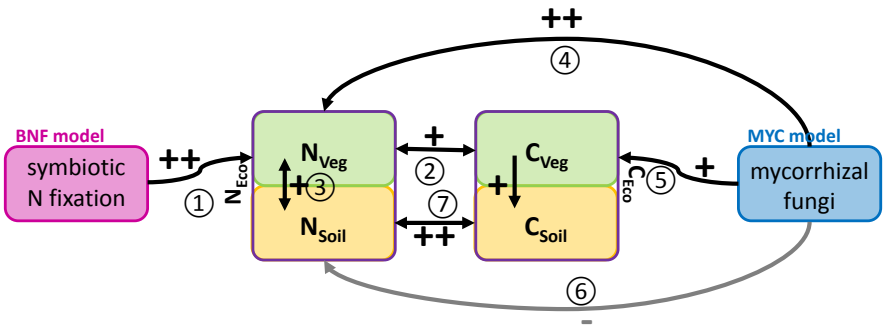

Figure 5.2.: Schematic representation of implications of the implementation of symbiotic N fixation by the BNF model (pink box) and mycorrhizal fungi by the MYC model (blue box) into a TBM on modelled ecosystem C and N budgets.
Green boxes refer to plant pools, orange boxes refer to soil/SOM pools, the violet frame represents the common ecosystem. Arrows show direction of dependency, whereas black arrows represent positive (+) or very strong positive (++) dependencies and grey arrows represent negative (-) dependencies.
Numbers refer to processes/ratios that underlay the dependency: ① symbiotic N fixation, ② plant CN ratios, ③ recycling of N, ④ mycorrhizal N export, ⑤ mycorrhizal biomass as part of vegetation biomass, ⑥ uptake of SOM-N, ⑦ tight and fixed SOM-CN ratios.

Generally, model variants that apply the BNF sub-model, i.e. Q-BNF and Q-MYFUN, increase C_{Eco} and N_{Eco} compared to QUINCY, whereas model variants that apply the MYC sub-model, i.e. Q-MYC and Q-MYFUN, tend to decrease C_{Eco} and N_{Eco}. This is, because the BNF sub-model allows plants to symbiotically fix N from atmosphere, i.e. to acquire ecosystem external N in case of limitation. This increases primarily N_{Veg} (fig. 5.2 ①) and consequently C_{Veg} due to plant CN ratios (fig. 5.2 ②). But it has a long-lasting effect on C_{Eco} and N_{Eco}, as previously fixed N and C have a long turnover time within the ecosystem by internal recycling (fig. 5.2 ③). This increases C_{Eco} and N_{Eco} compared to QUINCY.

Contrary to that, model variants that apply the MYC model, i.e. Q-MYC and Q-MYFUN, tend to decrease C_{Eco} and N_{Eco}. This is caused by a shift in allocation, since mycorrhizal fungi increase N_{Veg} and C_{Veg}, as consequence from improved plant N nutrition (fig. 5.2 ④ and ②), but also by mycorrhizal biomass itself (fig. 5.2 ⑤), but decrease N_{Soil} by accelerating the ecosystem internal N cycle to liberate N from soil organic material (SOM, fig. 5.2 ⑥). Because of fixed SOM-CN ratios (fig. 5.2 ⑦), C_{Soil} is also reduced by applying the MYC model. This decreases total C_{Eco} and N_{Eco} compared to QUINCY.
By applying both sub-models concurrently, the C and N allocation shift towards vegetation, which is caused by the MYC model, remains, but the decrease of soil pools is balanced out by additional N input to the ecosystem by the BNF model. This leads to an almost similar amount of N_{Eco} in Q-MYFUN compared to QUINCY, in combination with increased C_{Eco}, since more C and N are stored in vegetation with higher and more flexible CN ratios than in soil, which has low and fixed CN ratios.

Changes in ecosystem CN balances caused by symbiotic N acquisition strategies, i.e. the de- or increase of C_{Eco} and N_{Eco} simulated by Q-BNF, Q-MYC and Q-MYFUN compared to QUINCY, are rather robust against external perturbations, such as a de- or increase in N deposition (sec. 4.3.3), or an increase in cCO_2 (sec. 4.4.3), whereas such perturbations strongly affect CN balances simulated by QUINCY.
N_{Eco} simulated by QUINCY responds almost linearly to N deposition. This strong fertilization effect of N deposition indicates N limitation at the evaluation site. Model variants that include symbiotic N fixation, i.e. Q-BNF and Q-MYFUN, balance a de- or increase of N deposition out by an in- or decrease of fixation, which is why also C_{Eco} does not respond much to N deposition. Missing effects of N deposition variations indicate that the BNF sub-model creates an almost non-limiting environment with respect to N. Interestingly, Q-MYC responds to N deposition changes similar to QUINCY with regard to N_{Eco}, but much less with regard to C_{Eco}. This implies a N fertilization effect for vegetation, but mycorrhizal acceleration of soil decomposition lead to less C accumulation in the soil compared to QUINCY.

The fertilization effect of eCO_2 is similar to the fertilization effect from N deposition among all model variants. Due to the inability of QUINCY to fix enough N in ecosystems, positive responses to eCO_2 are only short-term effects. In the longer term, ecosystems run into PNL in QUINCY simulations, which limits the CO_2 fertilization effect on vegetation first, and then on soil. In contrast to that, all simulations with additional symbiotic N acquisition strategies show a positive vegetation response to eCO_2 in the short- and long-term, but ecosystem responses differ due to different responses of soil C and N. Q-BNF balances an increasing N demand to avoid PNL by strongly increased N fixation, which increases N_{Eco} (and C_{Eco}) strongly. Q-MYC accelerates the internal cycling of N (and C), which leads to only minor changes in soil C due to enhanced heterotrophic respiration, and even a negative response of soil N, since more N is sequestered in vegetation. Thus, especially N_{Eco} response is weak, whereas C_{Eco} response is indeed weaker than simu-

lated by Q-BNF due to soil C responses, but stronger than simulated by QUINCY due to vegetation responses. Q-MYFUN does increase N fixation in response to eCO_2, too, but less than Q-BNF, since the acceleration of internal N cycling by mycorrhizal fungi almost provides enough N to meet vegetation N demand. Nevertheless, soil N is increased, which increases N_{Eco} similar to Q-BNF. However, the mycorrhizal-induced acceleration of soil cycling leads to a very weak soil C response to eCO_2 similar to Q-MYC simulations, which explains the similar C_{Eco} responses to eCO_2, which are simulated by Q-MYC and Q-MYFUN.

Taken this together, C responses of Q-MYFUN to C and N perturbations rather follow Q-MYC responses due to the acceleration of the soil C (and N) cycles, but N responses rather follow Q-BNF responses, even though effects are weaker in both cases due to counteracting effects from the other sub-model. This indicates a strong impact (or even control) of plants on ecosystem CN dynamics by applying symbiotic N acquisition strategies and therefore links to research question 2.

5.1.2. Research question 2: What drives ecosystem dynamics? Does N availability control plant growth, or do plants control N availability by investing C into N acquisition?

Limited N availability forces plants to invest C into N acquisition strategies to avoid growth limitation (*Gutschick* (1981), *Marschner and Dell* (1994)). This obviously affects plant CUE, because freshly assimilated C, i.e. GPP, that is invested into N acquisition lowers C, which is available for biomass production, i.e. NPP (*Gutschick* (1981), *Zerihun et al.* (1998), *Marschner and Dell* (1994), *Fisher et al.* (2010), *Meyer et al.* (2010), *Gorka et al.* (2019)). However, the force to use N acquisition strategies besides root uptake differs in Q-MYFUN, since symbiotic fixation is implemented as optional strategy, whereas mycorrhizal fungi are implemented as potential parasites and competitors that oblige plants to exude C, which is contrary to *Sulman et al.* (2019) (sec. 4.2.1.2). This is necessary to avoid mycorrhizal extinction, but also to ensure sufficient plant N nutrition, because plants rely on mycorrhizal N support, as mycorrhizae coincidentally build a physical barrier between plant roots and soil (*Read* (1991)), and thus hinder direct root uptake (sec. 3.2.1 and sec. 4.2.1). Besides, the obligation for plants to feed hosted mycorrhizae, takes into account that almost all plants are in symbiosis with mycorrhizal fungi (*Read* (1991)), whereas only some host N-fixing microbes (*Gutschick* (1981)). And it follows the CUE-definition from *Manzoni et al.* (2018), which includes exudation to mycorrhizal fungi to NPP. Additionally, N fixation changes N_{Eco} by accessing an ecosystem external source. In case this is modelled symbiotically, i.e. by the BNF sub-model in Q-MYFUN, this allows plants to directly influence N_{Eco}, which may be unintended and raise the question, to what extent plants may be able to actively affect N_{Eco}.
Total N_{Eco} in Q-MYFUN simulations is almost similar to simulated N_{Eco} by QUINCY, but plant N acquisition is enhanced, and so simulated N_{Veg}, which induces an allocation shift

of N from soil to vegetation in Q-MYFUN compared to QUINCY. As C and N in vegetation biomass and soil compartments are tightly linked, the shift in N allocation causes a shift in C allocation within the simulated ecosystem in Q-MYFUN, i.e. C_{Veg} is increased and C_{Soil} reduced. Since CN ratios of plant tissues are mostly higher than soil CN ratios (*Manzoni et al.* (2008), *Kattge et al.* (2011)), this results in an enhancement of C_{Eco} in Q-MYFUN compared to QUINCY. Consequently, simulated C storage by Q-MYFUN is higher than simulated C storage by QUINCY, without affecting N_{Eco} much, as Q-MYFUN creates a system, where plants control N availability to such an extent that they avoid any potential N limitation that may occur in QUINCY. This is caused by a combination of mycorrhizal induced acceleration of soil decomposition, which speeds up ecosystem N cycling, and N-fixation induced outbalancing of ecosystem N losses.
Especially this self-balancing characteristic of Q-MYFUN becomes more obvious when varying ecosystem N input externally, i.e. by varying N deposition. This disturbance strongly affects QUINCY simulations, as a decrease of N deposition increases growth limitation, and an increase fertilizes growth, but creates only minor responses within Q-MYFUN simulations. Growth fertilization by increased N deposition in QUINCY indicates N limitation on modelled plants even under unchanged conditions, i.e. ambient CO_2 and standard N deposition rates. Missing responses to both variations, i.e. a de- and increase in annual N deposition, in Q-MYFUN indicate a potentially too strong plant control on ecosystem dynamics, since real-world plants and ecosystems are shown to respond positively to N fertilization (*von Liebig* (1863), *Vitousek* (1982), *Treseder et al.* (2007), *Thomas et al.* (2010), *Vicca et al.* (2012), *Fernández-Martínez et al.* (2014), *Campioli et al.* (2015), *Wright et al.* (2018)).

The self-balancing characteristic of Q-MYFUN with regard to N_{Eco} and the relative C shift from soil to vegetation, which enhances C_{Eco} compared to QUINCY, are of special interest, when taking the effects of elevated atmospheric CO_2 concentrations (eCO_2) and the theory of progressive N limitation (PNL, *Luo et al.* (2004)) into account. Classically, simulated growth responses to eCO_2 are decreasing in long-term predictions, because modelled ecosystems run into PNL (*Luo et al.* (2004), *Zaehle et al.* (2014), *Wieder et al.* (2015)).
Q-MYFUN simulates only a minor increase of N_{Eco} compared to QUINCY, but predicts a persistent positive plant growth response to eCO_2, i.e. avoiding PNL by C investment into symbiotic N acquisition strategies. This doubles C storage within the ecosystems in response to eCO_2 within 40 years in Q-MYFUN (ΔC_{Eco}: $\approx$3 kgC/m^2, and still increasing) compared to QUINCY (ΔC_{Eco}: $\approx$1.5 kgC/m^2, but decreasing). As PNL is shown to be much weaker in reality than predicted by TBMs, plant controlled N acquisition may be the missing link in state-of-the-art TBMs (*Finzi et al.* (2007), *Zaehle et al.* (2014)) and neglecting N-supportive symbioses may largely underestimate simulated impacts of the terrestrial biosphere to climate change (*Shi et al.* (2019)). However, to support (or reject) such reported modelling features as the plant control on ecosystem C and N budgets, and the self-balancing characteristic of Q-MYFUN with regard to N_{Eco}, ecosystem scale

measurements are needed. Especially soil measurements are scarce, but necessary to understand processes and feedbacks to constrain Q-MYFUN further (*Van Sundert et al.* (2019)).
Additionally stored C in response to eCO_2 modelled by Q-MYFUN is mainly caused by an enhancement of vegetation biomass, whereas C increase in soil is minor. Measurements at the Duke FACE experiment point in a similar direction, even though these measurements cover less than 10 years (*Lichter et al.* (2008)). However, *Lichter et al.* (2008) also reported a slight increase in SOM-CN ratio under eCO_2, which indicates further C accumulation in soils that is neither represented by QUINCY, nor by Q-MYFUN due to fixed SOM-CN ratios (sec. 1.2.4.3 and sec. 3.6). This indicates again the need of data to constrain C and N cycle dynamics and links in TBMs. In particular, measurements to constrain the terrestrial N cycle and its influence on the C cycle are needed (*Vicca et al.* (2018)).

The terrestrial C cycle is known to have strong influence on C cycle-climate feedbacks (*Arneth et al.* (2010), *Arora et al.* (2013), *Bonan* (2015), *Friedlingstein et al.* (2019)). Thus C fluxes are monitored in-situ or derived from space-born observations, and/or aboveground biomass is estimated from forest inventory data or space-born observations, to derive the land C reservoir (*Ayres et al.* (1994), *Falkowski et al.* (2000), *Dlugokencky and Tans* (2019), *Friedlingstein et al.* (2019)). But N fluxes, as well as N stocks are highly uncertain due to difficulties to measure fluxes, since the background concentration of atmospheric N_2 is too high, and generally missing studies that focus on N stocks, N dynamics, and/or N cycling on ecosystem scale (*Gutschick* (1981), *Galloway et al.* (2004), *Vitousek et al.* (2013), *Wieder et al.* (2015)). The lack of studies that report soil (or ecosystem) N in any form and estimate total stocks in combination with the lack of a common measurement protocol, hampers quantitative and comparable statements about most important processes that shape the ecosystem N cycle, and inhibit proper constrains for TBM-N cycles (*Vicca et al.* (2018)).
Thus, a *quantitative* assessment of plant control on ecosystem CN dynamics and/or N availability is impossible, and also a *qualitative* answer to the question **What drives ecosystem dynamics?** is difficult with current experimental evidence on ecosystem N fluxes and stocks.

Nevertheless, observed responses to C and N fertilization indicate (i) existing plant control on N availability, since plants are shown to be able to increase N acquisition (*Finzi et al.* (2007)), and (ii) N limitation that hinders plant growth even under ambient conditions, i.e. present cCO_2 and present (plant) available N in soils (*Vicca et al.* (2012), *Fernández-Martínez et al.* (2014)).

The response to CO_2 fertilization is better represented by Q-MYFUN than by QUINCY, suggesting that plant controlled symbiotic N acquisition strategies may be the missing link in state-of-the-art TBMs to explain also positive long-term plant responses to eCO_2. This may reduce uncertainties within future C-cycling predictions. But the response to N fertilization is better represented by QUINCY, indicating a too strong control on ecosystem CN dynamics and budgets by plants simulated by Q-MYFUN. However, the simulated N fertilization response is only tested by changing N deposition and analyzed for the steady-state ecosystems, i.e. for mature forests. This may cause *missing* effects, because both sub-models, i.e. the BNF model and the MYC model, are shown to respond differently within forest succession. Symbiotic fixation fertilized growth of young forests and led to higher growth rates (sec. 2.3.2.3), and simulated NPP rates were higher at the young forest at Duke in the presence of mycorrhizal fungi mycorrhizal fungi (sec. 3.4.1), compared to mature forest sites by applying the MYC model (sec. 4.4.1 and sec. 5.1.1). Thus, there may be differences in ecosystem response to N fertilization between young and mature forests (*Desai et al.* (2005)), since latter already achieved an internal CN balance, which plants are able to keep by using symbiotic N acquisition strategies, whereas former may respond stronger by enhanced growth to reach a mature CN equilibrium. However, the performance of Q-MYFUN at young forest simulations has not been tested within this study and has to be assessed primarily without additional fertilization before addressing N fertilization (again).
In any case, the extent to what plants control ecosystem CN budgets and dynamics may be overestimated in Q-MYFUN at its current state and needs further research, as well as potential co-drivers of ecosystem dynamics, e.g. P limitation, and general plant survival strategy, such as a conservative/organic nutrient economy or extravagant/inorganic nutrient economy strategy (*Chapman et al.* (2006), *Phillips et al.* (2013)).

5.2. Conclusion

Plants have evolved several strategies to increase N acquisition by symbiotic support (e.g. *Gutschick* (1981), *Read* (1991), *Marschner and Dell* (1994), *Vitousek et al.* (2013)). The implementation of two of such strategies, i.e. symbiotic N fixation and mycorrhizal fungi, into the terrestrial biosphere model (TBM) QUINCY (*Thum et al.* (2019)) is shown to influence not only plant C and N budgets by an improved N nutrition that enhances growth (slightly), but also plant C allocation by investing C into symbiotic N acquisition. This is, because I chose active C investment into N acquisition strategies as plant control mechanism. Consequently, plant growth is affected by either lowering CUE and/or enhancing below-ground C allocation, which includes C exudation to mycorrhizal fungi. However, absolute growth rates, i.e. NPP, are changed minor in QUINCY simulations with symbiotic N acquisition strategies (Q-MYFUN) simulations compared to QUINCY without symbiotic N acquisition strategies (QUINCY). Only sites that are severely N limited are shown to respond with a strong growth enhancement to symbiotic N acquisition support (sec. 4.4.2 and sec. 5.1).
Missing fertilization effects on plant growth rates are reasonable, since Q-MYFUN was tested at mature forest sites. Mature forests have generally low growth rates, and QUINCY itself is well constrained with regard to above-ground vegetation C stocks, and related fluxes by a wide range of observations that reach in-situ measurements, forest inventory data, and retrievals from space-born observations. Even thought, most sites are shown to be mildly N limited, a significant effect on simulated NPP rates by Q-MYFUN compared to QUINCY would be unintended. This may be contradictory at first sight to studies based on observations, such as *Vicca et al.* (2012) and *Fernández-Martínez et al.* (2014), that point out that nutrient/N availability is a key regulator for growth, but it may not. As reported by *Fernández-Martínez et al.* (2014), growth rates, i.e. NPP or net ecosystem production (NEP), are determined by C input, i.e. GPP, and respiration rates, i.e. autotrophic respiration (R_a) and heterotrophic respiration (R_h), which all respond to nutrient availability. This is also the main assumption underlying MYFUN. But in contrast to observational studies that compare *different* ecosystems with similar GPP rates and/or similar nutrient availability based on nutrient content measurements, QUINCY and Q-MYFUN simulate the *same* ecosystems, which have equal soil information that lead to similar nutrient contents (sec. 2.2.2), but nutrient availability changes by applying symbiotic N support, which is proven by leaf CN ratio analyses. This increases GPP, as well as R_a and R_h in Q-MYFUN compared to QUINCY, but does not change NPP significantly, since the ecosystem itself is still the same. Consequently, the almost *missing* fertilization effect on plant growth under ambient conditions by Q-MYFUN compared to QUINCY is not only intended, but also in line with observational studies.
Actually, even minor GPP and NPP enhancements, which are simulated by Q-MYFUN, lower model-data agreement compared to QUINCY, when comparing site-to-site. This is caused by (i) a general tendency of QUINCY to overestimate GPP and NPP, which is intensified by improved N nutrition in Q-MYFUN, and (ii) a potential bias within the link between plant N nutrition and modelled C fluxes, since simulated leaf CN ratios by QUINCY tend to be too high, and are lowered by Q-MYFUN, which actually indicates N

limitation in QUINCY and fertilization by MYFUN (sec. 4.4.1, sec. 4.5.4 and sec. 5.1). Consequently, one should also ask, whether C fluxes (or flux ratios), i.e. GPP, NPP and CUE, are the best indicators to quantify fertilization, particularly when modelling mature forest sites. Actually leaf CN ratio, or plant tissue CN ratios, may show a fertilization effect as improvement of plant fitness better.
Apart from that, Q-MYFUN simulates the intended effect under changed conditions, such as eCO_2, which increases GPP. By using symbiotic N acquisition support that increases N availability compared to QUINCY, Q-MYFUN simulates enhanced growth rates not only in the short-term, but also in the long-term (sec. 4.4.2 and sec. 4.5.4. This suggests an improved process representation that allows plants to dynamically respond correctly to environmental changes and disturbances.
Thus, I conclude that my model developments presented in this thesis are a necessary step forward in TBM development (*Davies-Barnard et al.* (2020)), as Q-MYFUN is able to simulate observed responses to eCO_2 better than QUINCY. The implementation of a dynamic plant N acquisition model, such as MYFUN, which includes plant interactions with symbiotic N fixers and mycorrhizal fungi, provides process-based pathways to simulate plants that actively react to environmental changes in short-term, but also persistently in long-term simulations. This may improve model predictions and reduce recent model uncertainties with respect to a changing climate and rising cCO_2, which are caused by a too rigid system with regard to N availability/accessibility that impede observed plant responses.

However, the understanding of below-ground processes and ecosystem N cycling is still limited due to the lack of data, as well as exact knowledge of plant processes that link N nutrition to plant growth. This hinders a proper assessment of the implemented model structure, and leads to the reported inability to constrain the model properly. In consequence, modellers need observational data that (i) track C and N fluxes within the *entire* ecosystem, e.g. by using tracers such as ^{13}C or ^{15}N, especially with respect to the questions

- Where does plant-acquired N come from?
- How is this source approached, i.e. directly or via symbionts?
- How do plants allocate C and N?
- How flexible are plant CN ratios for each tissue, especially how flexible are leaf CN ratios and how does this link to plant C assimilation and allocation?

and (ii) measure below-ground C and N stocks to derive fine root and mycorrhizal biomass, SOM-CN ratios, plant available N, and understand plant-soil interactions and controls, and the influence of symbionts, as well as C accumulation processes that may increase soil C storage potential. Measurements should therefore follow a common protocol to be comparable and include soil properties that may influence stocks and fluxes, such as soil texture and pH (*Vicca et al.* (2018)).

Fundamental scientific questions, which rose (again) from my analysis are, how ecosystems operate, and which functionality each organism is taking care of, and how theses functionalities support each other, e.g. which nutrient acquisition strategy a specific plant evolves and why, how this strategy is utilized, which symbionts or microbes are involved, what this means for plant nutrient nutrition and ecosystem nutrient cycling. This builds on suggestions by *Chapman et al.* (2006) and *Phillips et al.* (2013) that emphasized the necessity to understand plant nutrient economics in order to understand their nutrient acquisition strategy and nutrient cycling within ecosystems. Understanding the economics behind different nutrient acquisition strategies would help to formulate dependencies and implement them into TBMs, which may improve future C-cycle predictions by a better process representation.
As TBMs simulate C and nutrient pools and fluxes on ecosystem scale, ecosystem observations would be most desirable, but also most expensive, complicated to set-up and to replicate, and time-consuming. Besides, it may be difficult to disentangle mechanisms and processes, as environmental conditions cannot be entirely controlled. Thus, also cheaper and potentially shorter greenhouse/mesocosm experiments could provide needed data, which one could scale up, and/or help to understand key processes that need to be implemented into TBMs to improve their prediction ability with respect to environmental changes.
Besides, it is necessary to rethink approaches to simulate future environmental conditions from experimental, as well as from modelling perspective. For example, free-air CO_2 enrichment (FACE) experiments and their simulations use a step-increase of cCO_2 to directly simulate possible conditions in the end of the 21^{st} century, while in nature cCO_2 is increasing gradually. The step-increase neglects potential adaptation processes from both, plants and soil, that could prevent plants from PNL.
However, transient (field) experiments often loose their statistical power, because they are hard to repeat and may be too short to provide evidence on ecosystem responses. Additionally, they are hardly comparable to other studies, since they do not exists. The combination of these difficulties make transient field or lab experiments extremely hard to fund, even though the modelling would be easy.
Thus, both experimental set-ups have their disadvantages, but also benefits that one could likely use best by combining both approaches. FACE experimental studies should always be set-up in close cooperation with modelling groups that may run their models in advance to (i) predict potential outcomes and (ii) ask for important quantities to measure to get the most out of the experiments. Transient field experiments may be too complicated and expensive to fund in general, but running models with such set-ups may still allow to get a deeper insight into adaptation processes, especially when comparing them to step-increase simulations.
In any case, model development and experimental research have to go hand-in-hand and support each other in order to finally understand ecosystem processes and implications for estimating the future development of ecosystems (*Medlyn et al.* (2015)). Models can only simulate processes that scientists have understood by observing them, and operate as good as the data are that modellers use to constrain such processes, whereas measurements are needed to be set-up to answer specific questions on a prescribed scale of interest.

5.3. Outlook

The reported lack of experimental evidence on ecosystem scale processes with regard to C-nutrient cycling limits my ability to develop the model further. However, there are some prospective steps that can be done on the current knowledge basis:

1. Investigating the influence of forest/ecosystem succession/age on MYFUN behavior, which was not done within this study. Forest age has been shown to affect real-world forest growth (*Campioli et al.* (2015), *He et al.* (2019)) and the performance of both sub-models, i.e. the BNF model and the MYC model, and is therefore likely to also influence MYFUN. This may also rise the question of competition, i.e. between plants that can host N-fixers, which may have assets in early stages, and those that cannot, which may succeed in mature ecosystems (*Fisher et al.* (2010)).

2. Investigating competition may be also on interest within the plant-mycorrhiza symbiosis, exploring the question to what extend plants can control hosted mycorrhizae, and when they may be rather competitors, or even parasites (*Franklin et al.* (2014)), or how plants may avoid overfertilization by mycorrhizal fungi, which causes currently too low simulated leaf CN ratios.

3. Running Q-MYFUN globally. As sub-model of a TBM, MYFUN is developed with the aim to run it globally to analyze, if the model is able to capture current C flux and stock pattern, if there are spatial patterns with respect to the chosen N acquisition strategy, how patterns may change under rising atmospheric CO_2 concentrations, and what this implies for future C land sink and climate change.

4. Linking mycorrhizal functionalities (or plant nutrient economics/strategies) to mycorrhizal types, i.e. ectomycorrhizae (EMs) and arbuscular mycorrhizae (AMs). EMs are usually found in temperate and boreal forests that are known to be rather N limited, and would therefore potentially act rather nutrient conservative/follow an organic nutrient strategy (*Chapman et al.* (2006), *Phillips et al.* (2013)), whereas AMs are usually hosted by grasses and tropical forests that are either shown to be less N limited, and/or have to ability to fix N symbiotically. This would then point to a rather nutrient extensive behavior/inorganic nutrient strategy.
   The coupling and analysis of decomposing mycorrhizal fungi to the symbiotic N fixation scheme may be a reasonable step for that, as both strategies are rather C-cost intensive and target for inorganic nutrients, whereas saprotrophic mycorrhizae target organic nutrients. This may then link decomposing mycorrhizae to AM-ecosystems with facultative N-fixers, and saprotrophic mycorrhizae to EM-ecosystems (sec. 4.2.1.2 and sec. 4.5).

5. Linking the N and P cycle by including P acquisition into MYFUN to extend the current N acquisition model to a plant controlled nutrient acquisition model. The general principles of P cycling are already implemented in QUINCY. Besides, P is known to be limiting in many ecosystems that are not N limited, such as the tropics

(*Vitousek* (1984), *Vitousek et al.* (2010), *Gill and Finzi* (2016), *Yang* (2014), *Fleischer et al.* (2019)), and mycorrhizal fungi are know to support plant P acquisition as well (*Read* (1991), *Hodge et al.* (2001)).
This may improve our understanding of co-limitations, and of plant nutrient acquisition strategies under different kinds of limitation. E. g. there is no similar strategy to approach ecosystem-external P, as N fixation to access ecosystem-external N. Consequently, plants rely much more on soil processes, in case they are P limited, and may invest more C into symbiotic or free-living soil microbes by exudation that liberate P from SOM or mineral/not plant available sources. This may influence plant nutrient acquisition strategy (see also 1.), and consequently needs to be taken into account, when implementing into TBMs (sec. 3.6 and sec. 4.5).

6. Revising of inflexible soil CN (or CNP) ratios that inhibit soil C accumulation in the presence of mycorrhizal fungi. Both tested functionalities lower soil C, either by accessing SOM as nutrient source directly, or by accelerating SOM decomposition. This generally lowers ecosystem C stocks significantly and the ability of simulated ecosystems to store additional C under eCO_2 (sec. 3.6). This would require a more advanced soil model, which allows soil C accumulation not only in organic forms, but potentially also in mineral forms, and may protect soil C.

7. Revising functions that link simulated GPP to plant leaf N content, as they may be biased towards too high C assimilation (sec. 4.5). This bias may be caused by parameterizations, which allow state-of-the-art TBMs to simulate C fluxes that meet observations, even though they tend to be N limited, as their simulated ecosystems do not provide sufficient N for plants. This bias becomes then an issue when improving plant N nutrition and thus enhancing leaf N content.

8. Conducting further eCO_2 simulations, and comparing simulated plant responses to a single major step-increase of cCO_2 to gradually increasing CO_2 concentrations, not only with the fully coupled N acquisition model, but also with the basic model.
This could help to understand (i) plant adaptation processes by providing insights into underlying mechanisms and their feedbacks, and (ii) plant control on ecosystem C and N dynamics and especially the level of control. And, by that, potentially revise the idea of PNL in response to eCO_2 (sec. 4.5).
Besides, further eCO_2 studies will help to estimate the importance of plant controlled symbiotic nutrient acquisition strategies with regard to future climate change predictions.

Thinking further, and combining above mentioned ideas, one could scale up MYFUN to plant functional types (PFTs) that take different nutrient economics into account. Currently, PFTs include information about climate (tropical, temperate, or boreal climate), plant type (broad-leaved trees, needle-leaved trees, shrubs, grasses), and leaf-habit and/or C assimilation strategy (deciduous, evergreen, C3 photosynthesis, C4 photosynthesis), e.g. temperate broad-leaved deciduous trees or tropical broad-leaved evergreen trees. This is reasonable, because PFTs were established for C-cycle models given a specific climate.

The recent inclusion of other nutrient cycles necessitates to also include different nutrient acquisition strategies, e.g. an inorganic and an organic strategy, which would lead to new PFTs, such as temperate broad-leaved deciduous organic nutrient acquiring trees or tropical broad-leaved evergreen inorganic nutrient acquiring trees. Running TBMs which those *new* PFTs may improve simulations significantly on ecosystem as well as on global scale and simulated responses to environmental changes.

A. QUINCY model appendix

Table A.1.: QUINCY model parameter

symbol	description	value	unit	reference
$f_{resp,growth}$	growth respiration fraction per unit new biomass	0.25	molC/molC	*Sprugel et al.* (1995)
$f_{resp,maint}^{non-woody}$	maintenance respiration rate for fine roots and leaves	1.0	mmolCO_2/(molN s)	*Sprugel et al.* (1995)
$f_{resp,maint}^{woody}$	maintenance respiration rate for wood	0.25	mmolCO_2/(molN s)	*Sprugel et al.* (1995)
K_{m1,NH_4}	low affinity half-saturation parameter for NH_4 uptake	0.0416	m^3/mol	*Kronzucker et al.* (1996)
K_{m1,NO_3}	low affinity half-saturation parameter for NO_3 uptake	0.0416	m^3/mol	*Kronzucker et al.* (1995)
K_{m2,NH_4}	high affinity half-saturation parameter for NH_4 uptake	1.0	m^3/mol	*Kronzucker et al.* (1996)
K_{m2,NO_3}	high affinity half-saturation parameter for NO_3 uptake	1.0	m^3/mol	*Kronzucker et al.* (1995)
N_{limit}^{F}	max. sum of NH_4 and NO_3 at which aBNF occurs	0.05	molN/m^2	*Zaehle and Friend* (2010)
r_{NH_4}	uptake respiration per unit NH_4	1.8	gC/gN	*Zerihun et al.* (1998)
r_{NO_3}	uptake respiration per unit NO_3	2.3	gC/gN	*Zerihun et al.* (1998)
τ_{labile}	turnover time of plant labile pool (as average period)	7	days	*Thum et al.* (2019)
$\tau_{lit_{met}}$	turnover time of metabolic litter pool	0.033	years	*Parton et al.* (1993)
$\tau_{lit_{str}}$	turnover time of structural litter pool	0.124	years	*Parton et al.* (1993)
$\tau_{lit_{wd}}$	turnover time of woody litter pool	2.5	years	*Thum et al.* (2019)
$\tau_{SOM_{fast}}$	turnover time of fast SOM pool	2.0	years	*Thum et al.* (2019)
$\tau_{SOM_{slow}}$	turnover time of slow SOM pool	100	years	*Thum et al.* (2019)
v_{max,F^a}	max. rate of asymbiotic fixation	0.005	molN/(m^2s)	*Zaehle and Friend* (2010)
$v_{max,j}$	max. N_j uptake capacity per unit biomass	0.42	μmolN/(molC s)	*Zaehle et al.* (2010)
χ_{CN}^{labile}	target CN ratio of plant labile pool	PFT dep.	gC/gN	*Thum et al.* (2019)
$\chi_{CN}^{lit_{met}}$	CN ratio of metabolic litter pool	PFT dep.	gC/gN	*Thum et al.* (2019)
$\chi_{CN}^{lit_{str}}$	CN ratio of structural litter pool	PFT dep.	gC/gN	*Thum et al.* (2019)
$\chi_{CN}^{lit_{wd}}$	CN ratio of woody litter pool	PFT dep.	gC/gN	*Thum et al.* (2019)
$\chi_{CN}^{SOM_{fast,max}}$	max. CN ratio of fast SOM pool	13.0	gC/gN	*Manzoni et al.* (2008)
$\chi_{CN}^{SOM_{fast,min}}$	min. CN ratio of fast SOM pool	5.0	gC/gN	*Manzoni et al.* (2008)
$\chi_{CN}^{SOM_{slow}}$	CN ratio of SOM	9.0	gC/gN	*Parton et al.* (1993)

B. BNF model appendix

B.1. Model modification assessments

As I adjusted some formulations within the BNF calculations from *Rastetter et al.* (2001) and *Fisher et al.* (2010), I assess the effect of these modifications in the first part of this appendix. I show how the changes effect resulting functions and fluxes theoretically, as well as in QUINCY simulations. For latter, I use QUINCY (revision 1878, 300-year spin-up, as in chapter 2) with the affected BNF scheme for specific sites with the previously described modeling protocol (sec. 2.2.2). Sites are described in section 2.2.3.2.

B.1.1. Minimal and maximal C costs for N fixation

In general maximal and minimal C costs for N fixation ($r_{F,max}$ and $r_{F,min}$) are based on measurements by *Gutschick* (1981). However, those measurements are done under controlled lab conditions, which may not cover the entire natural temperature range. Thus I decided to enlarge the C cost range by increasing $r_{F,max}$ up to 17.5 gC/gN, which is only reached under very hot or cold conditions, to meet Gutschick's measurements under reasonable lab temperatures, i.e. approximately between 15°C and 30°C. I did not change $r_{F,min}$, which represents C costs that corresponds to the optimal temperature (T_0, 25.15°C; *Houlton et al.* (2008)), because this temperature is usual for lab conditions. Figure B.1 shows how the enlargement of the C cost range fits the C-cost curve to the measurements by *Gutschick* (1981) under typical lab temperatures.

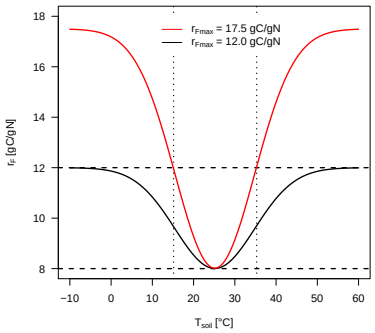

Figure B.1.: Carbon costs for symbiotic N fixation with adjusted $r_{F,max}$ (red) and measured $r_{F,max}$ (black). Dashed horizontal lines show measured C-cost range by *Gutschick* (1981). Dotted vertical lines show assumed lab temperature range.

B.1.2. Adjustment of optimal scheme

I modified the N fixation rate (F_{opt}) calculation by *Rastetter et al.* (2001) (eq. 2.10a), which is used for the *optimal approach*, by modifying both, the maximum fixation capacity per unit root biomass ($v_{max,F}$), and the half-saturation parameter (k_F).
$v_{max,F}$ defines the maximum fixation rate (here: in dependency of root biomass). Here, I multiply it with the scaling factor f_{ϕ_F} (eq. 2.10c) to account for more efficient fixation under optimal conditions, i.e. optimal temperatures, and less efficient fixation under very hot or cold conditions. Figure B.2a shows the effect of this modification to the normalized maximum fixation capacity per unit root biomass. I.e. fixation becomes less efficient under cold/hot conditions, and more efficient the closer the temperature is to the optimal temperature, which is shown by the temperature-sensitive maximum fixation capacity (purple curve), whereas the original maximum fixation capacity is not temperature sensitive (grey, fig. B.2a).
k_F is the half-saturation parameter, which shapes the curve of the saturation function. Thus, it has to be in the range of the independent variable (here: Δr). Δr in QUINCY simulations with optimal scheme usually range between 0 gC/gN and 10 gC/gN (fig. B.2b, dotted line, cf. sec. 2.3, fig. 2.9), which is why I adjusted k_F accordingly from 50 gC/gN (k_F^{org}, *Rastetter et al.* (2001), *Meyerholt et al.* (2016)) to 5 gC/gN (k_F). This modification allows a significant increase in the resulting fixation rate, and reaching high fixation rates within a reasonable range of Δr, if demanded (fig. B.2b, solid line). Contrary to that, using the original k_F (dashed line) leads to an almost linear increase of fixation, and fixation rates do only reach about 20% of their potential maximum within usually simulated Δr.
Actual effects on symbiotic fixation rates at CAS, and THO, which have different temperature ranges, as CAS is a temperate forest site and THO is a boreal forest site, and a clear seasonal cycle, are shown in figure B.2c and figure B.2d. The temperature-dependency of $v_{max,F}$ shifts fixation from mainly during winter, which is unreasonable due to the enzymatic activity of nitrogenase, to (late) summer. k_F modification leads to higher fixation rates in general, which are suppressed by the higher original k_F.

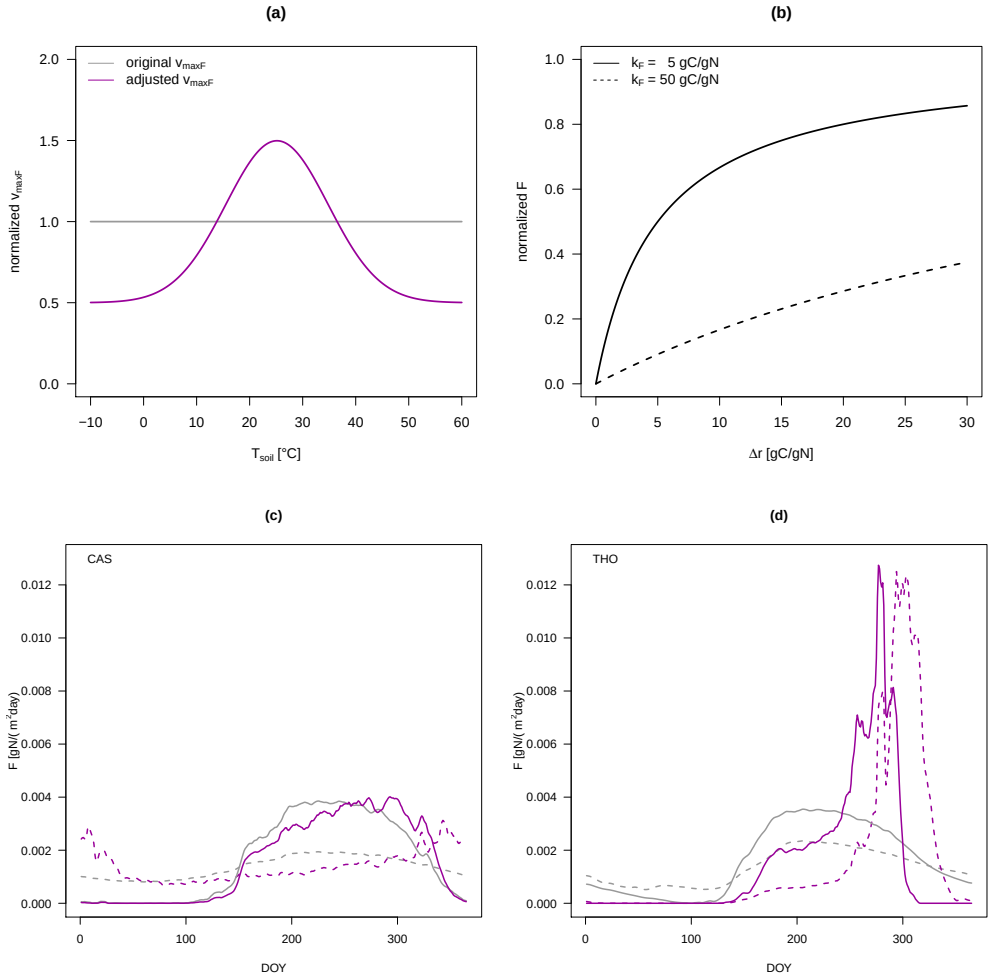

Figure B.2.: Effects of optimal scheme modifications on normalized maximum fixation rate by scaling $v_{max,F}$ with am temperature function based on *Houlton et al.* (2008) (a; grey: temperature insensitive $v_{max,F}$, purple: temperature sensitive $v_{max,F}$) and total fixation rate by adjusting the half-saturation parameter k_F in accordance to QUINCY ranges of Δr (b; solid line: adjusted k_F, dashed line: original k_F). Figures c and d show effects on actual fixation rates for CAS (c), and (d) THO (sec. 2.3.2). Colors refer to $v_{max,F}$ accordingly to (a) and line types refer to k_F accordingly to (b).

B.1.3. Offset parameter for resistance scheme

I modified the N fixation rate (F_{res}) calculation by *Fisher et al.* (2010), which is used for the *resistance approach* by introducing the offset parameter α_0. This modification is needed, because QUINCY accounts for transformation costs for mineral N uptake by roots (r_j; *Zerihun et al.* (1998)), which is not considered in the original N fixation calculation by *Fisher et al.* (2010). Without considering r_j, root uptake costs (r_{U_N}, eq. 2.4a) are zero, if opportunity costs (r_{opp}, eq. 2.4b) are zero. This is possible, in case meet their N requirements by already existing roots, i.e. gain N (g_N, eq. 2.5) is zero. By adding r_j to r_{U_N}, r_{U_N} is never zero (fig. B.3a; red line), since plants have at least to invest C for transforming mineral N into amino acids. Thus, F_{res} is never zero, even in case plants could meet their N requirements without fixation (fig. B.3a; black curves). To set this off, α_0 is introduced (fig. B.3a; green curves), which is calculated based on costs for NH_4 uptake and NO_3 uptake and likely resulting uptake rates, given different costs (r_{NH_4} and r_{NO_3}; *Zerihun et al.* (1998)). Figures B.3b and B.3c show how the offset parameter affects actual fixation rates at CAS for the evergreen and the deciduous stand. Generally, fixation rates are reduced by introducing α_0, which makes resulting rates more reasonable, and also the sharp peaks in spring at both stands are smoothed, which results from increasing demand due to the begin of the growing season.

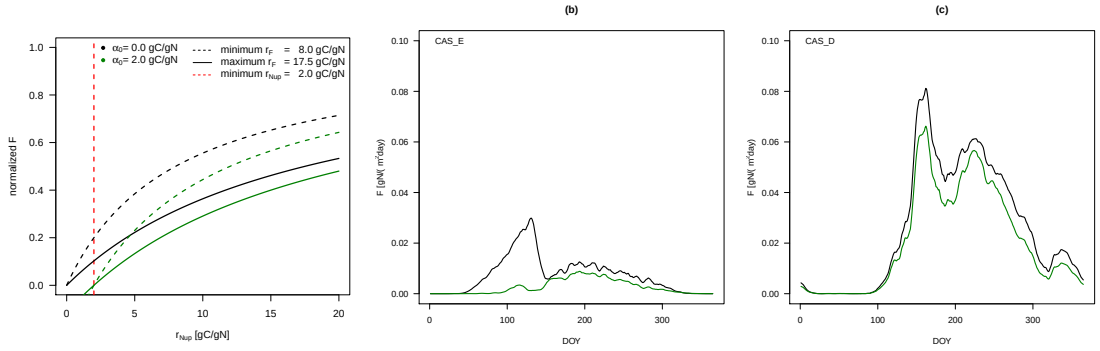

Figure B.3.: Effects of resistance scheme modification by the offset parameter α_0 (eq. 2.11b) on normalized fixation rates (a), as well as actual fixation rates at CAS_E (b) and CAS_D (c). Colors refer to the offset parameter: green: used parameter, i.e. $\alpha_0 = 2.0$ gC/gN, black: no offset, i.e. $\alpha_0 = 0.0$ gC/gN. Line type in (a) refer to minimal and maximal possible normalized fixation rates, which are estimated using by $r_{F,min}$ (dashed) and $r_{F,max}$ (solid) in combination with $r_N up$, and the red, dashed line represents minimal N uptake costs by average transformation costs per unit N.

B.2. Comparison of sites to related climate zones

I use the same runs as in chapter 2, section 2.3.2.1, to address the question, if the chosen sites represent their assigned climate zone well.

I find a good agreement of simulated N fixation by the standard scheme for TAP and THO (<10% variation between average forests and representative sites; representative sites within 1 SD). N fixation at CAS is slightly out of the bounds of 1 SD.
Site specific annual N fixation rates simulated by the resistance scheme have a poor agreement with mean rates over all sites within the related climate zone. Only CAS meet the limits of 1 SD. Poor agreement is caused by the high variability within N fixation rates by resistance scheme, which I find in high standard deviation ranges compared to mean values for both, climate zone mean and representative sites, too. At TAP and THO, resistance scheme fixes more N then on average for tropical or boreal forests. It simulates less fixation at CAS compared to average over temperate forests, which is caused by CAS being an evergreen forest, whereas almost a half of all temperate forest sites are deciduous, which have generally higher N fixation rates (fig. 2.5).
Agreement between averaged N fixation rates over all forest sites within climate zones and representative sites for each climate zone is even poorer for optimal scheme. This is caused by three boreal sites, six temperate sites, and one tropical sites that do not fix symbiotically with optimal scheme, whereas only two boreal sites, two temperate sites, and one tropical sites do not fix symbiotically with resistance scheme. Non-simulated symbiotic N fixation shifts mean values over climate zones during the analyzed period towards lower rates, whereas TAP, CAS, and THO are sites that simulate symbiotic fixation additionally to asymbiotic fixation.

Table B.1.: Annual BNF rates across climate zones and representative sites

climate		standard	resistance	optimal
tropical	average [gN/(year m^2)]	1.07 ± 0.18	1.04 ± 0.43	0.48 ± 0.17
	TAP [gN/(year m^2)]	1.03 ± 0.22	1.92 ± 2.23	0.80 ± 0.31
temperate	average [gN/(year m^2)]	0.44 ± 0.22	1.59 ± 1.82	0.47 ± 0.44
	CAS [gN/(year m^2)]	0.68 ± 0.02	1.36 ± 0.31	1.21 ± 0.33
boreal	average [gN/(year m^2)]	0.36 ± 0.09	0.46 ± 0.36	0.30 ± 0.32
	THO [gN/(year m^2)]	0.39 ± 0.02	1.39 ± 0.47	1.28 ± 0.44

C. MYC model appendix

C.1. Latin Hypercube Sampling

In order to test the sensitivity of the new model structures within QUINCY, which are presented in the following chapters, I conduct a Latin Hypercube Sampling (LHS) after *Saltelli et al.* (2000) to vary chosen parameters.
LHS generates a near-random sample of N parameter values statistically within M sets of parameters, where M is predefined. The parameter intervals of all N parameters are divided into M equally probable intervals and organized in a square (two dimensions/parameters) or cube (three dimensions/parameters) or hypercube design (more than three dimensions/parameters). Then the method picks randomly combinations of parameters, from which each combination covers a specific row and column of the square (or cube/hypercube, respectively). Figure C.1 shows the a LHS for two parameters (x_1 and x_2; N=2) that are represented by four parameter sets (p_1 to p_4; M=4). The ranges of x_1 and x_2 are equally divided into four intervals and combinations are selected to cover the full space (Coverage of p_2 is shown by grey area; coverage of p_1, p_3, and p_4, respectively).
Thus, LHS ensures that the parameter space is represented with an approximately full coverage by the previously defined M sets of parameters, which reduces the amount of combinations that are needed to get statistically usable results.
Note: LHS is only working, if parameters are independent. If there are any cross-correlations, the method is not applicable.

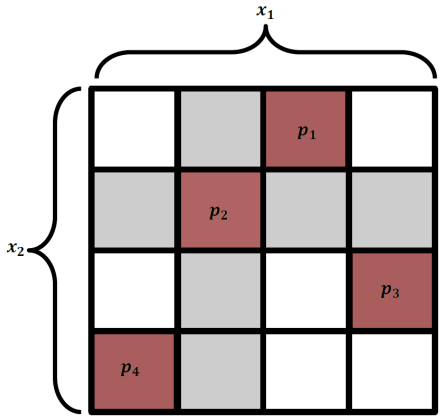

Figure C.1.: Two dimensional LHS.

C.2. 1^{st} LHS round

In order to test model sensitivity to all parameters that directly shape C and N fluxes between plant and mycorrhizae, mycorrhizae and soil, or plant and soil at the same time, I conduct a Latin Hypercube Sampling (LHS, *Saltelli et al.* (2000)) with 500 runs for each mycorrhizal type with QUINCY (revision 1878, 500 year-spin up, protocol as described in section 2.2.2), where I vary parameters within ranges that are presented in table 3.1. I normalize the LHS results by results of reference runs using the standard parameterization, whereby both, LHS runs and reference runs, were averaged for 1971 to 1980 to eliminate climate variability.

I find the inner-quartile range of model output for both, QUINCY with decomposers and QUINCY with saprotrophs, well centered around the results of the standard parameterization (fig. C.2 and fig. C.3).
In general QUINCY related fluxes and pools differ less then fluxes of MYC model. Especially plant C exudation to mycorrhizal fungi varies caused by $f_{m2r,min}$, CUE^m, and τ_{myc}, which determine the necessity to export C to avoid mycorrhizal extinction. Caused by the high efficiency of mycorrhizal fungi, plants try to exude the minimum that is possible, which is already enough to fulfill plant N demands by mycorrhizal N export in return. N return differs much less, because plants can control how much N they get by refusing export, which stops the entire MYC model.
Pools on ecosystem scale are less affected by parameter variations within the MYC model, because the ecosystem reaches an equilibrium in the presence of mycorrhizal fungi that is robust against parameter changes. In case of saprotrophic mycorrhizae, SOM-C shows a slightly higher variation, but still the inner-quartile range lies within $\pm$20% of the standard run.

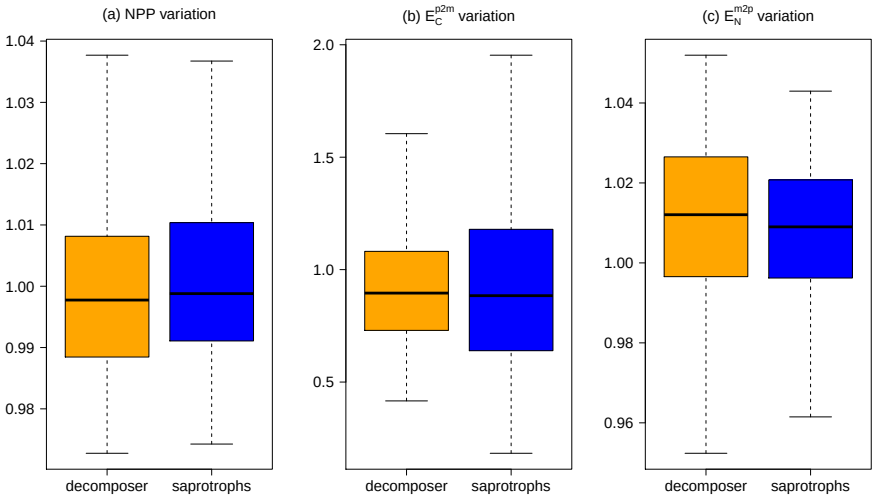

Figure C.2.: Sensitivity of fluxes due to parameter uncertainty.
(a) NPP variations, (b) C exudation (E_C^{p2m}) variations, and (c) N export (E_N^{m2p}) variations caused by parameter uncertainty relative to standard parameterization.

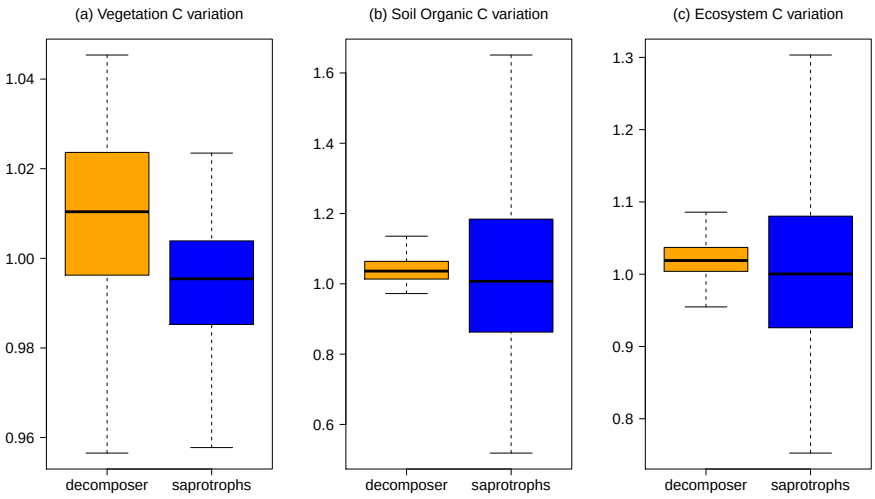

Figure C.3.: Sensitivity of ecosystem C pools due to parameter uncertainty.
(a) Vegetation C variations, (b) soil organic C variations, and (c) total ecosystem C variations caused by parameter uncertainty relative to standard parameterization.

C.3. Comparison of plant below-ground and fine-root C allocation response to eCO_2

Terrer et al. (2018) assume a constant ratio between plant C allocation into fine root growth and into C transfer to mycorrhizal fungi (and N fixers). Based on this assumption, the derive that the response of below-ground C allocation, which includes root growth and C transfer, to eCO_2 is similar to plant C allocation response to only fine root growth (*Terrer et al.* (2018), eq. 4), and use latter as proxy for their estimations of plant *return on investment* (Ψ_N^{-1}, eq. 3.21) response amongst FACE sites.
Compared to my results from QUINCY simulations (revision 1878, 500 year-spin up, protocol as described in section 2.2.2) without and with both mycorrhizal types, they get 1.5 times higher *return on investment* ratios, especially for ectomycorrhizae (EMs), which I found to show an almost similar support of plant N acquisition as saprotrophic mycorrhizae.
This mismatch is mainly caused by the mentioned assumption, as modelled response of below-ground C allocation that includes transfer to mycorrhizae, is 1.5 times higher than only fine-root C allocation response to eCO_2 (fig. C.4).

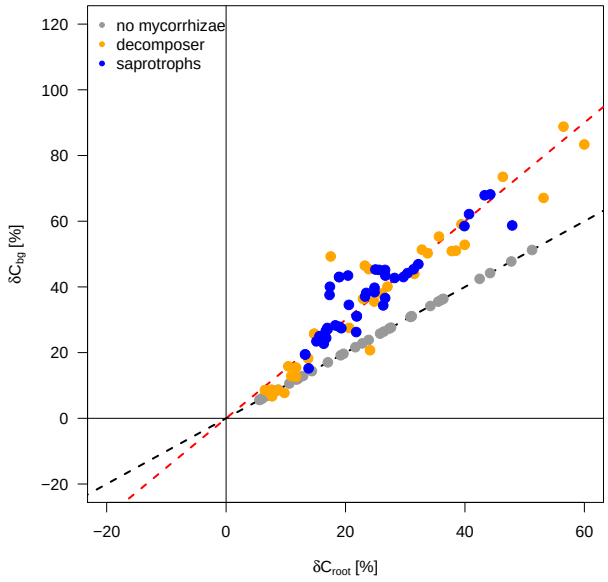

Figure C.4.: Comparison of plant below-ground and fine root C allocation response to eCO_2 amongst 42 mature forest sites from GFDB. Grey: QUINCY without mycorrhizal fungi, orange: QUINCY with decomposers, blue: QUINCY with saprotrophs. Black dashed line show 1:1 line, red dashed line show 1.5:1 line.

D. MYFUN model appendix

D.1. Consistency of simulated N nutrition improvement

In addition to figure 4.10, which represents only shifts in simulated leaf CN ratio for 28 evergreen forest sites (QUINCY revision 1994, 500-year spin-up, protocol as described in sec. 2.2.2), figure D.1 shows shifts in simulated labile CN ratio for all 42 mature forest sites from the same simulation round and links them to simulated GPP, NPP, and CUE. Shifts, that are caused by symbiotic N acquisition schemes, i.e. BNF and/or MYC sub-models, are similar for leaf habits, i.e. for deciduous and evergreen forests.
Simulated labile CN ratios for temperate and boreal forest sites are decreased by Q-BNF, Q-MYC and Q-MYFUN, indicating an improved N nutrition by symbiotic N acquisition compared to labile CN ratio simulated by QUINCY. Simulated labile CN ratios for tropical forests increase slightly. Both patterns are consistent with findings for simulated leaf CN ratio shifts in section 4.4.1. However, leaf CN ratios were analyzed, owing to the availability of observations, whereas no observations of labile CN ratios exists as this pool is artificial.

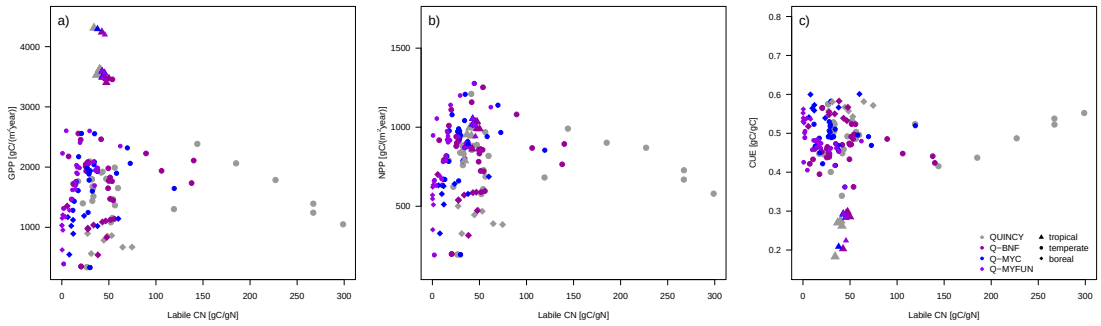

Figure D.1.: Influence of simulated labile CN ratios on modelled GPP (a), NPP (b), and CUE (c) among 42 mature forest sites from GFDB (sec. 2.2.3.1). Tropical sites are represented by triangles, temperate sites by dots, and boreal sites by diamonds. Color code refer to model variants: grey: QUINCY, purple: Q-BNF, blue: Q-MYC, and violet: Q-MYFUN.

Glossary

acronym/ symbol		description
A_N	plant N acquisition	model flux
aBNF	asymbiotic BNF	BNF by free-living bacteria
aCO_2	ambient cCO_2	
AM	arbuscular mycorrhizae	mycorrhizal fungi type
BEM	Behavioral Ecological Model	model type that simulates dynamical behaviour of ecosystem communities. Part of DGVMs
BNF	(symbiotic) biological N fixation	process that fixes N_2
BP	plant biomass-production	
BPE	BP efficiency	individual plant CUE: ratio between BP and GPP
C	carbon	
CAS	Cascade Head Experimental Forest	temperate forest site that has evergreen and deciduous stands
cCO_2	atmospheric CO_2 concentration	
CENTURY	soil model	state-of-the-art in DGVMs
CMPI	Coupled Model Intercomparison Project	
CO_2	carbon dioxide	
CRUNCEP		atmospheric forcing dataset
CSE	C-storage efficiency	ecosystem CUE: ratio between NEE and GPP
CUE	C-use efficiency	ratio between NPP and GPP
D^m_{SOM}	mycorrhizal exudation to SOM	MYC model flux
DGVM	Dynamical Global Vegetation Model	model typ that presents the land component of ESMs
DOM	dissolved organic matter	soluble part of SOM
DOY	day of year	
dt	time-step	
E_{FF}	fossil fuel emissions	
E_{LUC}	(increased) emissions by land-use change	
E_X	exchange fluxes between plants and mycorrhizae	MYC model flux
eCO_2	elevated cCO_2	
EM	ectomycorrhizal fungi	mycorrhizal type
ESM	Earth System Model	models that are used to explore global climatic and environmental evolution
ET	evapotranspiration	water flux from land to atmosphere: sum of evaporation from soil and transpiration from plants

acronym/ symbol		**description**
F	symbiotic N fixation flux	BNF model flux
F^{asym}	asymbiotic N fixation flux	BNF model flux
F^{tot}	total biological N fixation flux	BNF model flux: sum of F and F^{asym}
FACE	free-air CO_2 enrichment	experimental set-up
FUN	Fixation and Uptake of Nitrogen	model
G_{ATM}	gain of atmospheric C	
G_X	growth rate	QUINCY model flux
g_X	gain of X	
GCM	General Circulation Model	model type that atmospheric and ocean component of ESMs
GFDB	Global Forest Database	data set
GHG	greenhouse gas	clima-relevant gases in the atmosphere
GPP	gross primary production	gross plant C assimilation via photosynthesis
L_i	loss rate	QUINCY model flux
LHS	Latin Hypercube Sampling	a method to vary parameters
MET	Metolius Forest	temperate forest site that has different stand ages
MYC	plant-MYCorrhizal interaction	model
MYFUN	MYcorrhizal export, Fixation and Uptake of Nitrogen	model
N	nitrogen	
N_2	atmospheric dinitrogen	main component of atmosphere
NEE	net ecosystem exchange	net C exchange between atmosphere and biosphere: GPP - R_a - R_h
NH_3	ammonia	N-form ins soils
NH_4	ammonium	plant-available N in soils
NO	nitrogen oxide	gaseous form of N
NO_2	nitrogen dioxide	gaseous form of N
NO_3	nitrate	plant-available N in soils
NO_X	nitrogen oxides	sum of NO and NO_2
NPP	net primary production	net C exchange between atmosphere and vegetation: GPP - R_a
NUE	N-use efficiency	ratio between NPP and A_N
P	phosphorus	
PFT	plant functional type	model classification of plants
PNL	progressive N limitation	N limitation on plant growth in (long-term) response to eCO_2
QUINCY	QUantifying Interactions between terrestrial Nutrient CYcles and the climate system	TBM
Q-BNF		QUINCY with BNF model
Q-MYC		QUINCY with MYC model
Q-MYFUN		QUINCY with BNF and MYC models

acronym/ symbol		description
r	C costs	
R_a	autotrophic respiration	plant respiration: sum of R_g, R_m, and R_X
R_F	N fixation respiration	C/energy investment into BNF
R_g	growth respiration	respiration that is associated to (plant) biomass production
R_h	heterotrophic respiration	soil respiration
R_m	maintenance respiration	respiration that is associated to maintenance processes
R_{U_N}	N uptake respiration	respiration that is associated to N uptake
R_X	nutrient acquisition respiration	respiration that is associated to nutrient acquisition, e.g. R_F or R_{U_N}
RCP	Representative Concentration Pathway	GHG concentration trajectory
S_{LAND}	land C sink	
S_{OCEAN}	ocean C sink	
S_X	storage flux	QUINCY model flux
SD	standard deviation	
SE	standard error	
SOM	soil organic matter	organic material in soil that contains C, N, P
SVA	Soil-Vegetation-Atmosphere	model type that presents the (bio)physical core of DGVMs, i. e. the exchange of mass, momentum and energy between atmosphere and land
T	temperature	
T_0	optimal temperature	optimal operation temperature for enzymatic processes
T_s	soil temperature	
T_X	turnover rate	model flux
TAP	Tapajos National Forest	tropical forest site
TBM	Terrestrial Biosphere Model	model type that presents the biogeochemical core of DGVMs, i. e. C and nutrient exchange between atmosphere and biosphere, and C and nutrient cycling within the biosphere
THO	Thompson Forest	boreal forest site
U_X	uptake rate	model flux
X	chemical element or model pool/stock	C, N or P
X_{Eco}	total ecosystem stock	model pool; contains C, N, and P
X_{fr}	plant fine-root pool	model pool; contains C, N, and P
X_{labile}	plant labile pool	pool to de-couple acquisition and allocation fluxes model pool; contains C, N, and P
X_{leaf}	plant leaf pool	model pool; contains C, N, and P
X^m	mycorrhizal pool	model pool; contains C, N, and P
X_{Veg}	total vegetation stock	model pool; contains C, N, and P
X_{soil}	soil stock	sum of mineral pools (N and P) in soil and X_{SOM} model pool; contains C, N, and P
X_{SOM}	SOM stock	model pool; contains C, N, and P
Y	flux	

acronym/ symbol		**description**
Δ	absolute difference	net fluxes or absolute responses to eCO_2, e.g. ΔE_X as net exchange flux between host plant and mycorrhizal fungi, or ΔX_{Veg} as difference between X_{Veg} (simulated) under aCO_2 and eCO_2 conditions
δ	relative difference	relative flux, e.g. NPP, (or flux-ratio, e.g. CUE) changes in response to eCO_2 in relation to fluxes (or flux-ratios) under aCO_2 conditions
ζ_X	demand of X	requirements for biomass production
η_X	(mycorrhizal) support	
τ	turnover time	(average) time period that a certain material remains within a particular system
Φ	flux or pool for process memory	
ϕ_F	nitrogenase activity	activity of nitrogenase, which is the enzyme that drives BNF
χ^{CN}	CN ratio	
Ψ_N^{-1}	return-on-investment ratio	
ω	memory weight	

Bibliography

Aerts, R., and F. S. Chapin III, The mineral nutrition of wild plants revisited: a re-evaluation of processes and patterns, in *Advances in ecological research*, vol. 30, Elsevier, 1999.

Ahrens, B., et al., Contribution of sorption, DOC transport and microbial interactions to the 14C age of a soil organic carbon profile: Insights from a calibrated process model, *Soil Biology and Biochemistry*, *88*(C), 2015.

Ainsworth, E. A., Rice production in a changing climate: a meta-analysis of responses to elevated carbon dioxide and elevated ozone concentration, *Global Change Biology*, *14*(7), 2008.

Ainsworth, E. A., and A. Rogers, The response of photosynthesis and stomatal conductance to rising [CO_2]: mechanisms and environmental interactions, *Plant, cell & environment*, *30*(3), 2007.

Allen, M. F., et al., Ecology of mycorrhizae: a conceptual framework for complex interactions among plants and fungi, *Annual Review of Phytopathology*, *41*(1), 2003.

Ames, R. N., et al., Hyphal uptake and transport of nitrogen from two 15N-labelled sources by glomus mosseae, a vesicular-arbuscular mycorrhizal fungus, *New Phytologist*, *95*(3), 1983.

Ammann, C., et al., The carbon budget of newly established temperate grassland depends on management intensity, *Agriculture, Ecosystems & Environment*, *121*(1), 2007.

Amthor, J. S., Respiration and carbon assimilate use, *Physiology and determination of crop yield*, 1994.

Amthor, J. S., Higher plant respiration and its relationships to photosynthesis, in *Ecophysiology of photosynthesis*, Springer, 1995.

Amthor, J. S., The McCree–de Wit–Penning de Vries–Thornley respiration paradigms: 30 years later, *Annals of botany*, *86*(1), 2000.

Amthor, J. S., and D. D. Baldocchi, Terrestrial higher plant respiration and net primary production, *Terrestrial global productivity*, 2001.

Arneth, A., et al., Terrestrial biogeochemical feedbacks in the climate system, *Nature Geoscience*, *3*, 2010.

Arora, V., Modeling vegetation as a dynamic component in soil-vegetation-atmosphere transfer schemes and hydrological models, *Reviews of Geophysics*, *40*(2), 2002.

Arora, V. K., et al., Carbon–concentration and carbon–climate feedbacks in CMIP5 earth system models, *Journal of Climate*, *26*(15), 2013.

Averill, C., et al., Mycorrhiza-mediated competition between plants and decomposers drives soil carbon storage, *Nature*, *505*(7484), 2014.

Ayres, R. U., et al., Human impacts on the carbon and nitrogen cycles, *Industrial ecology and global change*, 1994.

Batterman, S. A., et al., Key role of symbiotic dinitrogen fixation in tropical forest secondary succession, *Nature*, *502*(7470), 2013.

Beringer, J., et al., Patterns and processes of carbon, water and energy cycles across northern australian landscapes: From point to region, *Agricultural and Forest Meteorology*, *151*(11), 2011.

Bonan, G. B., Forests and Climate Change: Forcings, Feedbacks, and the Climate Benefits of Forests, *Science*, *320*(5882), 2008.

Bonan, G. B., *Ecological Climatology: Concepts and Applications*, 3 ed., Cambridge University Press, 2015.

Bonan, G. B., and S. C. Doney, Climate, ecosystems, and planetary futures: The challenge to predict life in earth system models, *Science*, *359*(6375), 2018.

Bond-Lamberty, B., et al., Net primary production and net ecosystem production of a boreal black spruce wildfire chronosequence, *Global Change Biology*, *10*(4), 2004.

Bradford, M. A., et al., Managing uncertainty in soil carbon feedbacks to climate change, *Nature Climate Change*, *6*(751), 2016.

Brzostek, E. R., et al., Modeling the carbon cost of plant nitrogen acquisition: Mycorrhizal trade-offs and multipath resistance uptake improve predictions of retranslocation, *Journal of Geophysical Research: Biogeosciences*, *119*(8), 2014.

Brzostek, E. R., et al., Mycorrhizal type determines the magnitude and direction of root-induced changes in decomposition in a temperate forest, *New Phytologist*, *206*(4), 2015.

Brzostek, E. R., et al., Integrating mycorrhizas into global scale models: A journey toward relevance in the earth's climate system, in *Mycorrhizal mediation of soil*, Elsevier, 2017.

Caldararu, S., et al., Whole-plant optimality predicts changes in leaf nitrogen under variable CO_2 and nutrient availability, *New Phytologist*, *225*(6), 2020.

Campioli, M., et al., Biomass production efficiency controlled by management in temperate and boreal ecosystems, *Nature Geoscience*, *8*(11), 2015.

Chapin III, F. S., New cog in the nitrogen cycle, *Nature*, *377*(6546), 1995.

Chapman, S. K., et al., Plants actively control nitrogen cycling: uncorking the microbial bottleneck, *New Phytologist*, *169*(1), 2006.

Cheng, L., et al., Arbuscular mycorrhizal fungi increase organic carbon decomposition under elevated CO_2, *Science*, *337*(6098), 2012.

Cheng, W., et al., Synthesis and modeling perspectives of rhizosphere priming, *New Phytologist*, *201*(1), 2014.

Ciais, P., et al., Carbon and other biogeochemical cycles, in *Climate change 2013: the physical science basis. Contribution of Working Group I to the Fifth Assessment Report of the Intergovernmental Panel on Climate Change*, Cambridge University Press, 2014.

Cleveland, C. C., et al., Global patterns of terrestrial biological nitrogen (N_2) fixation in natural ecosystems, *Global biogeochemical cycles*, *13*(2), 1999.

Collalti, A., and I. Prentice, Is NPP proportional to GPP? Waring's hypothesis 20 years on, *Tree physiology*, *39*(8), 2019.

Collalti, A., et al., Thinning can reduce losses in carbon use efficiency and carbon stocks in managed forests under warmer climate, *Journal of advances in modeling earth systems*, *10*(10), 2018.

Collalti, A., et al., The sensitivity of the forest carbon budget shifts across processes along with stand development and climate change, *Ecological Applications*, *29*(2), 2019.

Collalti, A., et al., Forest production efficiency increases with growth temperature, *bioRixv*, preprint.

Comins, H. N., and R. E. McMurtrie, Long-term response of nutrient-limited forests to CO_2 enrichment; equilibrium behavior of plant-soil models, *Ecological Applications*, *3*(4), 1993.

Cornelissen, J., et al., Carbon cycling traits of plant species are linked with mycorrhizal strategy, *Oecologia*, *129*(4), 2001.

D'Antonio, C. M., and P. M. Vitousek, Biological invasions by exotic grasses, the grass/fire cycle, and global change, *Annual review of ecology and systematics*, *23*(1), 1992.

Davidson, E. A., et al., The Dual Arrhenius and Michaelis-Menten kinetics model for decomposition of soil organic matter at hourly to seasonal time scales, *Global Change Biology*, *18*(1), 2012.

Davies-Barnard, T., et al., Nitrogen cycling in CMIP6 land surface models: Progress and limitations, *Biogeosciences Discussions*, 2020.

De Mazancourt, C., et al., Grazing optimization and nutrient cycling: when do herbivores enhance plant production?, *Ecology*, *79*(7), 1998.

Deckmyn, G., et al., ANAFORE: a stand-scale process-based forest model that includes wood tissue development and labile carbon storage in trees, *Ecological Modelling*, *215*(4), 2008.

Deckmyn, G., et al., Simulating C cycles in forest soils: Including the active role of microorganisms in the ANAFORE forest model, *Ecological modelling*, *222*(12), 2011.

DeLucia, E. H., et al., Forest carbon use efficiency: is respiration a constant fraction of gross primary production?, *Global Change Biology*, *13*(6), 2007.

Desai, A. R., et al., Comparing net ecosystem exchange of carbon dioxide between an old-growth and mature forest in the upper midwest, USA, *Agricultural and Forest Meteorology*, *128*(1), 2005.

DeVries, F. W. T. P., Respiration and growth, in *Crop processes in controlled environments*, 2, Academic Press, 1972.

Dlugokencky, E., and P. Tans, NOAA/ESRL: Globally averaged marine surface monthly mean data, 2019.

Drake, J. E., et al., Mechanisms of age-related changes in forest production: the influence of physiological and successional changes, *Global Change Biology*, *17*(4), 2011.

Ek, H., et al., Carbon and nitrogen flow in silver birch and norway spruce connected by a common mycorrhizal mycelium, *Mycorrhiza*, *6*(6), 1997.

Evans, J. R., Photosynthesis and nitrogen relationships in leaves of C3 plants, *Oecologia*, *78*(1), 1989.

Falkowski, P., et al., The global carbon cycle: a test of our knowledge of earth as a system, *science*, *290*(5490), 2000.

Farquhar, G. D., et al., On the Relationship Between Carbon Isotope Discrimination and the Intercellular Carbon Dioxide Concentration in Leaves, *Functional Plant Biology*, *9*(2), 1982.

Fernández-Martínez, M., et al., Nutrient availability as the key regulator of global forest carbon balance, *Nature Climate Change*, *4*(6), 2014.

Field, C. B., Diverse controls on carbon storage under elevated CO_2: toward a synthesis, in *Carbon dioxide and environmental stress*, Elsevier, 1999.

Finlay, R. D., Ecological aspects of mycorrhizal symbiosis: with special emphasis on the functional diversity of interactions involving the extraradical mycelium, *Journal of experimental botany*, *59*(5), 2008.

Finzi, A. C., et al., Progressive nitrogen limitation of ecosystem processes under elevated CO_2 in a warm-temperate forest, *Ecology*, *87*(1), 2006.

Finzi, A. C., et al., Increases in nitrogen uptake rather than nitrogen-use efficiency support higher rates of temperate forest productivity under elevated CO_2, *Proceedings of the National Academy of Sciences*, *104*(35), 2007.

Finzi, A. C., et al., Rhizosphere processes are quantitatively important components of terrestrial carbon and nutrient cycles, *Global Change Biology*, *21*(5), 2015.

Fisher, J. B., et al., Carbon cost of plant nitrogen acquisition: A mechanistic, globally applicable model of plant nitrogen uptake, retranslocation, and fixation, *Global Biogeochemical Cycles*, *24*(1), 2010.

Fisher, J. B., et al., Global nutrient limitation in terrestrial vegetation, *Global Biogeochemical Cycles*, *26*(3), 2012.

Fisher, J. B., et al., Modeling the terrestrial biosphere, *Annual Review of Environment and Resources*, *39*, 2014.

Fisher, J. B., et al., Tree-mycorrhizal associations detected remotely from canopy spectral properties, *Global Change Biology*, *22*(7), 2016.

Fleischer, K., et al., Amazon forest response to CO_2 fertilization dependent on plant phosphorus acquisition, *Nature Geoscience*, *12*(9), 2019.

Fowler, D., et al., Effects of global change during the 21st century on the nitrogen cycle, *Atmospheric Chemistry and Physics*, *15*(24), 2015.

Franklin, O., et al., Forests trapped in nitrogen limitation–an ecological market perspective on ectomycorrhizal symbiosis, *New Phytologist*, *203*(2), 2014.

Frey, S. D., Mycorrhizal fungi as mediators of soil organic matter dynamics, *Annual Review of Ecology, Evolution, and Systematics*, *50*, 2019.

Friedlingstein, P., et al., Uncertainties in CMIP5 Climate Projections due to Carbon Cycle Feedbacks, *Journal of Climate*, *27*(2), 2014.

Friedlingstein, P., et al., Global carbon budget 2019, *Earth System Science Data*, *11*(4), 2019.

Friend, A. D., et al., Photosynthesis in Global-Scale Models, in *Photosynthesis in silico: Understanding complexity from molecules to ecosystems*, Springer, 2009.

Friends of the Metolius (web presence), Metolius basin, `https://metoliusfriends.org/metolius-basin/`, last accessed on 2019-10-20, 2019.

Galbraith, D. R., and B. O. Christoffersen, Modelling climate impact on forest ecosystems, in *Routledge Handbook of Forest Ecology*, Routledge, 2015.

Galloway, J. N., et al., Nitrogen cycles: past, present, and future, *Biogeochemistry*, *70*(2), 2004.

Galloway, J. N., et al., Transformation of the nitrogen cycle: recent trends, questions, and potential solutions, *Science*, *320*(5878), 2008.

Gerber, S., et al., Nitrogen cycling and feedbacks in a global dynamic land model, *Global Biogeochemical Cycles*, *24*(1), 2010.

Gill, A. L., and A. C. Finzi, Belowground carbon flux links biogeochemical cycles and resource-use efficiency at the global scale, *Ecology letters*, *19*(12), 2016.

Godbold, D. L., et al., Mycorrhizal hyphal turnover as a dominant process for carbon input into soil organic matter, *Plant and Soil*, *281*(1-2), 2006.

Goll, D. S., et al., Nutrient limitation reduces land carbon uptake in simulations with a model of combined carbon, nitrogen and phosphorus cycling, *Biogeosciences*, *9*, 2012.

Göransson, H., et al., Estimating the relative nutrient uptake from different soil depths in quercus robur, fagus sylvatica and picea abies, *Plant and Soil*, *286*(1-2), 2006.

Gorham, E., et al., The regulation of chemical budgets over the course of terrestrial ecosystem succession, *Annual Review of Ecology and Systematics*, *10*(1), 1979.

Gorka, S., et al., Rapid transfer of plant photosynthates to soil bacteria via ectomycorrhizal hyphae and its interaction with nitrogen availability, *Frontiers in microbiology*, *10*, 168, 2019.

Goulden, M. L., et al., Dial and seasonal patterns of tropical forest CO_2 exchange, *Ecological Applications*, *14*(4), 2004.

Government of Canada (web presence), Environment and natural resources - historical climate data, `https://climate.weather.gc.ca/`, last accessed on 2019-10-20, 2019.

Granier, A., et al., The carbon balance of a young beech forest, *Functional Ecology*, *14*(3), 2000.

Grote, R., et al., A new modular biosphere simulation framework, 2008.

Grote, R., et al., Modelling and observation of biosphere–atmosphere interactions in natural savannah in burkina faso, west africa, *Physics and Chemistry of the Earth, Parts A/B/C*, *34*(4-5), 2009.

Gruber, N., and J. N. Galloway, An earth-system perspective of the global nitrogen cycle, *Nature*, *451*(7176), 2008.

Gu, B., et al., The role of industrial nitrogen in the global nitrogen biogeochemical cycle, *Scientific Reports*, *3*, 2013.

Gutschick, V. P., Evolved strategies in nitrogen acquisition by plants, *The American Naturalist*, *118*(5), 1981.

Gutschick, V. P., Energetics of microbial fixation of dinitrogen, in *Microbes and engineering aspects*, Springer, 1982.

Hartmann, D. L., et al., Observations: atmosphere and surface, in *Climate change 2013 the physical science basis: Working group I contribution to the fifth assessment report of the intergovernmental panel on climate change*, Cambridge University Press, 2013.

Harvard University (web presence), Large scale biosphere-atmosphere experiment in Amazonia, `http://atmos.seas.harvard.edu/lab/brazil/lbasite.html`, last accessed on 2019-10-20, 2002.

Hauptmann, S., *Organische Chemie*, Deutscher Verlag für Grundstoffindustrie, 1985.

He, H., et al., Simulating ectomycorrhiza in boreal forests: implementing ectomycorrhizal fungi model MYCOFON in CoupModel (v5), *Geoscientific Model Development*, *11*(2), 2018.

He, Y., et al., Global vegetation biomass production efficiency constrained by models and observations, *Global change biology*, 2019.

Hobbie, E. A., Carbon allocation to ectomycorrhizal fungi correlates with belowground allocation in culture studies, *Ecology*, *87*(3), 2006.

Hodge, A., and K. Storer, Arbuscular mycorrhiza and nitrogen: implications for individual plants through to ecosystems, *Plant and soil*, *386*(1-2), 2015.

Hodge, A., et al., An arbuscular mycorrhizal fungus accelerates decomposition and acquires nitrogen directly from organic material, *Nature*, *413*(6853), 2001.

Hoosbeek, M., M. Lukac, E. Velthorst, and D. Godbold, Free atmospheric CO_2 enrichment did not affect symbiotic N_2-fixation and soil carbon dynamics in a mixed deciduous stand in wales., *Biogeosciences Discussions*, *7*(3), 2010.

Hou, E., et al., Effects of climate on soil phosphorus cycle and availability in natural terrestrial ecosystems, *Global Change Biology*, *24*(8), 2018.

Houlton, B. Z., et al., A unifying framework for dinitrogen fixation in the terrestrial biosphere, *Nature*, *454*(7202), 2008.

Hungate, B. A., et al., Nitrogen and climate change, *Science*, *302*(5650), 2003.

IPCC, *The Intergovernmental Panel on Climate Change Report: Climate change 2013*, Cambridge University Press Cambridge, 2013.

Jakobsen, I., and L. Rosendahl, Carbon flow into soil and external hyphae from roots of mycorrhizal cucumber plants, *New Phytologist*, *115*(1), 1990.

Jansson, P.-E., CoupModel: model use, calibration, and validation, *Transactions of the ASABE*, *55*(4), 2012.

Johnson, N. C., et al., From Lilliput to Brobdingnag: extending models of mycorrhizal function across scales, *BioScience*, *56*(11), 2006.

Jordy, M. N., et al., Cytolocalization of glycogen, starch, and other insoluble polysaccharides during ontogeny of paxillus involutus–betula pendula ectomycorrhizas, *The New Phytologist*, *140*(2), 1998.

Kattge, J., et al., TRY - a global database of plant traits, *Global Change Biology*, *17*(9), 2011.

Keenan, T. F., and C. A. Williams, The terrestrial carbon sink, *Annual Review of Environment and Resources*, *43*, 2018.

King, J., et al., Fine-root biomass and fluxes of soil carbon in young stands of paper birch and trembling aspen as affected by elevated atmospheric CO_2 and tropospheric O_3, *Oecologia*, *128*(2), 2001.

Knops, J. M. H., et al., Mechanisms of plant species impacts on ecosystem nitrogen cycling, *Ecology Letters*, *5*(3), 2002.

Kronzucker, H. J., et al., Kinetics Of NO_3- influx In Spruce, *Plant Physiology*, *109*(1), 1995.

Kronzucker, H. J., et al., Kinetics of NH_4+ influx in spruce, *Plant Physiology*, *110*(3), 1996.

Kull, O., and B. Kruijt, Leaf photosynthetic light response: a mechanistic model for scaling photosynthesis to leaves and canopies, *Functional Ecology*, *12*(5), 1998.

Laczko, E., et al., Lipids in roots of pinus sylvestris seedlings and in mycelia of pisolithus tinctorius during ectomycorrhiza formation: changes in fatty acid and sterol composition, *Plant, Cell & Environment*, *27*(1), 2004.

Lam, S. K., et al., Effect of elevated carbon dioxide on growth and nitrogen fixation of two soybean cultivars in northern china, *Biology and Fertility of Soils*, *48*(5), 2012.

Lamarque, J. F., et al., Historical (1850–2000) gridded anthropogenic and biomass burning emissions of reactive gases and aerosols: methodology and application, *Atmospheric Chemistry and Physics*, *10*(15), 2010.

Lamarque, J. F., et al., Global and regional evolution of short-lived radiatively-active gases and aerosols in the representative concentration pathways, *Climatic Change*, *109*(1), 2011.

Law, B. E., et al., Carbon storage and fluxes in ponderosa pine forests at different developmental stages, *Global Change Biology*, *7*(7), 2001.

Law, B. E., et al., Disturbance and climate effects on carbon stocks and fluxes across western oregon USA, *Global Change Biology*, *10*(9), 2004.

Lawrence, D. M., et al., Parameterization improvements and functional and structural advances in version 4 of the community land model, *Journal of Advances in Modeling Earth Systems*, *3*(1), 2011.

LeBauer, D. S., and K. K. Treseder, Nitrogen limitation of net primary productivity in terrestrial ecosystems is globally distributed, *Ecology*, *89*(2), 2008.

LeQuéré, C., et al., Global carbon budget 2017, *Earth System Science Data*, *10*(1), 2018.

Lichter, J., et al., Soil carbon sequestration in a pine forest after 9 years of atmospheric CO_2 enrichment, *Global Change Biology*, *14*(12), 2008.

Lindahl, B. D., and A. Tunlid, Ectomycorrhizal fungi–potential organic matter decomposers, yet not saprotrophs, *New Phytologist*, *205*(4), 2015.

Lloyd, J., and J. A. Taylor, On the temperature dependence of soil respiration, *Functional ecology*, 1994.

Lorimer, G. H., The carboxylation and oxygenation of ribulose 1, 5-bisphosphate: the primary events in photosynthesis and photorespiration, *Annual Review of Plant Physiology*, *32*(1), 1981.

Lovett, G. M., and S. E. Lindberg, Atmospheric deposition and canopy interactions of nitrogen in forests, *Canadian Journal of Forest Research*, *23*(8), 1993.

Luo, Y., et al., Progressive nitrogen limitation of ecosystem responses to rising atmospheric carbon dioxide, *Bioscience*, *54*(8), 2004.

Luyssaert, S., et al., CO_2 balance of boreal, temperate, and tropical forests derived from a global database, *Global Change Biology*, *13*(12), 2007.

Magill, A. H., et al., Ecosystem response to 15 years of chronic nitrogen additions at the harvard forest LTER, massachusetts, USA, *Forest ecology and management*, *196*(1), 2004.

Mäkelä, A., et al., Optimal co-allocation of carbon and nitrogen in a forest stand at steady state, *New Phytologist*, *180*(1), 2008.

Malcolm, G. M., et al., Acclimation to temperature and temperature sensitivity of metabolism by ectomycorrhizal fungi, *Global Change Biology*, *14*(5), 2008.

Manzoni, S., et al., Soil heterogeneity in lumped mineralization–immobilization models, *Soil Biology and Biochemistry*, *40*(5), 2008.

Manzoni, S., et al., Reviews and syntheses: Carbon use efficiency from organisms to ecosystems-definitions, theories, and empirical evidence, *Biogeosciences*, *15*(19), 2018.

Marschner, H., and B. Dell, Nutrient uptake in mycorrhizal symbiosis, *Plant and soil*, *159*(1), 1994.

Matamala, R., and W. H. Schlesinger, Effects of elevated atmospheric CO_2 on fine root production and activity in an intact temperate forest ecosystem, *Global Change Biology*, *6*(8), 2000.

McCarthy, H. R., et al., Temporal dynamics and spatial variability in the enhancement of canopy leaf area under elevated atmospheric CO_2, *Global Change Biology*, *13*(12), 2007.

Medlyn, B. E., et al., Using ecosystem experiments to improve vegetation models, *Nature Climate Change*, *5*(6), 2015.

Meyer, A., et al., Simulating mycorrhiza contribution to forest C-and N cycling-the MYCOFON model, *Plant and soil*, *327*(1-2), 2010.

Meyer, A., et al., Integrating mycorrhiza in a complex model system: effects on ecosystem C and N fluxes, *European journal of forest research*, *131*(6), 2012.

Meyerholt, J., and S. Zaehle, The role of stoichiometric flexibility in modelling forest ecosystem responses to nitrogen fertilization, *New Phytologist*, 2015.

Meyerholt, J., and S. Zaehle, Controls of terrestrial ecosystem nitrogen loss on simulated productivity responses to elevated CO_2, *Biogeosciences*, *15*(18), 2018.

Meyerholt, J., et al., Variability of projected terrestrial biosphere responses to elevated levels of atmospheric co_2 due to uncertainty in biological nitrogen fixation, *Biogeosciences*, *13*(5), 2016.

Moorcroft, P. R., How close are we to a predictive science of the biosphere?, *Trends in Ecology & Evolution*, *21*(7), 2006.

Nasto, M. K., et al., Nutrient acquisition strategies augment growth in tropical N_2-fixing trees in nutrient-poor soil and under elevated CO_2, *Ecology*, *100*(4), 2019.

Nehls, U., Mastering ectomycorrhizal symbiosis: the impact of carbohydrates, *Journal of experimental botany*, *59*(5), 2008.

Norby, R. J., et al., Net primary productivity of a CO_2-Enriched deciduous forest and the implications for carbon storage, *Ecological applications: a publication of the Ecological Society of America*, *12*(5), 2002.

Norby, R. J., et al., Forest response to elevated CO_2 is conserved across a broad range of productivity, *Proceedings of the National Academy of Sciences*, *102*(50), 2005.

Norby, R. J. o., CO_2 enhancement of forest productivity constrained by limited nitrogen availability, *Proceedings of the National Academy of Sciences*, *107*(45), 2010.

Oren, R., et al., Soil fertility limits carbon sequestration by forest ecosystems in a CO_2 enriched atmosphere, *Nature*, *411*(6836), 2001.

Orwin, K. H., et al., Organic nutrient uptake by mycorrhizal fungi enhances ecosystem carbon storage: a model-based assessment, *Ecology Letters*, *14*(5), 2011.

Parton, W. J., The century model, in *Evaluation of soil organic matter models*, Springer, 1996.

Parton, W. J., et al., Observations and modelling of biomass and soil organic matter dynamics for the grassland biome worldwide, *Global Biogeochemical Cycles*, *7*(4), 1993.

Paterson, E., et al., Arbuscular mycorrhizal hyphae promote priming of native soil organic matter mineralisation, *Plant and Soil*, *408*(1-2), 2016.

Pérez-Tienda, J. o., Kinetics of NH_4+ uptake by the arbuscular mycorrhizal fungus rhizophagus irregularis, *Mycorrhiza*, *22*(6), 2012.

Peñuelas, J., et al., Human-induced nitrogen–phosphorus imbalances alter natural and managed ecosystems across the globe, *Nature Communications*, *4*(2934), 2013.

Phillips, R. P., et al., Roots and fungi accelerate carbon and nitrogen cycling in forests exposed to elevated CO_2, *Ecology Letters*, *15*(9), 2012.

Phillips, R. P., et al., The mycorrhizal-associated nutrient economy: a new framework for predicting carbon–nutrient couplings in temperate forests, *New Phytologist*, *199*(1), 2013.

Pongratz, J., et al., Radiative forcing from anthropogenic land cover change since AD 800, *Geophysical Research Letters*, *36*(2), 2009.

Prentice, I. C., and S. A. Cowling, Dynamic global vegetation models, in *Encyclopedia of biodiversity*, Elsevier, 2013.

Prentice, I. C., et al., Dynamic global vegetation modeling: quantifying terrestrial ecosystem responses to large-scale environmental change, in *Terrestrial ecosystems in a changing world*, Springer, 2007.

Pritsch, K., et al., A rapid and highly sensitive method for measuring enzyme activities in single mycorrhizal tips using 4-methylumbelliferone-labelled fluorogenic substrates in a microplate system, *Journal of microbiological methods*, *58*(2), 2004.

Rastetter, E. B., et al., Resource optimization and symbiotic nitrogen fixation, *Ecosystems*, *4*(4), 2001.

Raupach, M. R., et al., Terrestrial biosphere models and forest-atmosphere interactions, 2005.

Read, D. J., Mycorrhizas in ecosystems, *Experientia*, *47*(4), 1991.

Read, D. J., and J. Perez-Moreno, Mycorrhizas and nutrient cycling in ecosystems–a journey towards relevance?, *New Phytologist*, *157*(3), 2003.

Reed, S. C., et al., Phosphorus cycling in tropical forests growing on highly weathered soils, in *Phosphorus in Action Biological Processes in Soil Phosphorus Cycling*, Springer Berlin Heidelberg, 2011.

Reich, P. B., et al., Nitrogen limitation constrains sustainability of ecosystem response to CO_2, *Nature*, *440*(7086), 2006.

Rhein, M., et al., Observations: ocean, in *Climate change 2013 the physical science basis: Working group I contribution to the fifth assessment report of the intergovernmental panel on climate change*, Cambridge University Press, 2013.

Saltelli, A., et al., *Sensitivity Analysis*, John Wiley & Sons, ltd., Chichester, New York, 2000.

Scheffer, F., and P. Schachtschnabel, *Lehbruch der Bodenkunde*, 14. ed., Enke, 1998.

Schimel, D., et al., Effect of increasing CO_2 on the terrestrial carbon cycle, *Proceedings of the National Academy of Sciences*, *112*(2), 2015.

Schlesinger, W. H., and E. S. Bernhardt, *Biogeochemistry: an analysis of global change*, Academic press, 2013.

Schmidt, I. K., et al., Effects of labile soil carbon on nutrient partitioning between an arctic graminoid and microbes, *Oecologia*, *112*(4), 1997.

Scott, E. E., and D. E. Rothstein, The dynamic exchange of dissolved organic matter percolating through six diverse soils, *Soil Biology and Biochemistry*, *69*, 2014.

Shevliakova, E., et al., Carbon cycling under 300 years of land use change: Importance of the secondary vegetation sink, *Global Biogeochemical Cycles*, *23*(2), 2009.

Shi, M., et al., Carbon cost of plant nitrogen acquisition: global carbon cycle impact from an improved plant nitrogen cycle in the community land model, *Global Change Biology*, *22*(3), 2016.

Shi, M., et al., Neglecting plant–microbe symbioses leads to underestimation of modeled climate impacts., *Biogeosciences*, *16*(2), 2019.

Six, J., et al., Stabilization mechanisms of soil organic matter: implications for C-saturation of soils, *Plant and soil*, *241*(2), 2002.

Smith, S. E., and D. J. Read, *Mycorrhizal symbiosis*, Academic press, 2010.

Sokolov, A. P., et al., Consequences of considering carbon–nitrogen interactions on the feedbacks between climate and the terrestrial carbon cycle, *Journal of Climate*, *21*(15), 2008.

Sprent, J. I., *The ecology of the nitrogen cycle*, Cambridge University Press, 1987.

Sprugel, D. G., et al., Respiration from the organ level to the stand, in *Resource Physiology of Conifers*, Academic Press, 1995.

Staddon, P. L., et al., Rapid turnover of hyphae of mycorrhizal fungi determined by AMS microanalysis of 14C, *Science*, *300*(5622), 2003.

Stock, W. D., et al., Impacts of invading N_2-fixing acacia species on patterns of nutrient cycling in two cape ecosystems: evidence from soil incubation studies and 15N natural abundance values, *Oecologia*, *101*(3), 1995.

Sulman, B. N., et al., Microbe-driven turnover offsets mineral-mediated storage of soil carbon under elevated CO_2, *Nature Climate Change*, *4*(12), 2014.

Sulman, B. N., et al., Feedbacks between plant N demand and rhizosphere priming depend on type of mycorrhizal association, *Ecology letters*, *20*(8), 2017.

Sulman, B. N., et al., Diverse mycorrhizal associations enhance terrestrial C storage in a global model, *Global Biogeochemical Cycles*, *33*(4), 2019.

Tang, G., and P. J. Bartlein, Simulating the climatic effects on vegetation: approaches, issues and challenges, *Progress in Physical Geography*, *32*(5), 2008.

Tedeschi, V. o., Soil respiration in a mediterranean oak forest at different developmental stages after coppicing, *Global Change Biology*, *12*(1), 2006.

Terrer, C., et al., Mycorrhizal association as a primary control of the CO_2 fertilization effect, *Science*, *353*(6294), 2016.

Terrer, C., et al., Ecosystem responses to elevated CO_2 governed by plant–soil interactions and the cost of nitrogen acquisition, *New Phytologist*, *217*(2), 2018.

Thomas, R. Q., and M. Williams, A model using marginal efficiency of investment to analyze carbon and nitrogen interactions in terrestrial ecosystems, 2014.

Thomas, R. Q., et al., Increased tree carbon storage in response to nitrogen deposition in the US, *Nature Geoscience*, *3*(1), 2010.

Thomas, R. Q., et al., Global patterns of nitrogen limitation: confronting two global biogeochemical models with observations, *Global Change Biology*, *19*(10), 2013.

Thornley, J. H. M., and M. G. R. Cannell, Modelling the components of plant respiration: representation and realism, *Annals of Botany*, *85*(1), 2000.

Thornton, P. E., et al., Influence of carbon-nitrogen cycle coupling on land model response to CO_2 fertilization and climate variability, *Global biogeochemical cycles*, *21*(4), 2007.

Thornton, P. E., et al., Carbon-nitrogen interactions regulate climate-carbon cycle feedbacks: results from an atmosphere-ocean general circulation model, *Biogeosciences*, *6*(10), 2009.

Thum, T., et al., A new terrestrial biosphere model with coupled carbon, nitrogen, and phosphorus cycles (QUINCY v1.0; revision 1772), *Geoscientific Model Development*, *12*, 2019.

Treseder, K. K., et al., Mycorrhizal responses to nitrogen fertilization in boreal ecosystems: potential consequences for soil carbon storage, *Global Change Biology*, *13*(1), 2007.

Trumbore, S. E., Potential responses of soil organic carbon to global environmental change, *Proceedings of the National Academy of Sciences*, *94*(16), 1997.

Trumbore, S. E., Age of soil organic matter and soil respiration: radiocarbon constraints on belowground C dynamics, *Ecological Applications*, *10*(2), 2000.

Trumbore, S. E., and C. I. Czimczik, An uncertain future for soil carbon, *science*, *321*(5895), 2008.

U.S. Forest Service (web presence), Pacific northwest research station - Cascade Head Experimental Forest, `https://www.fs.usda.gov/pnw/experimental-forests-and-ranges/cascade-head-experimental-forest`, last accessed on 2019-10-20, 2019.

Van Der Heijden, M. G. A., et al., The unseen majority: soil microbes as drivers of plant diversity and productivity in terrestrial ecosystems, *Ecology letters*, *11*(3), 2008.

Van Sundert, K., et al., Towards comparable assessment of the soil nutrient status across scales–review and development of nutrient metrics, *Global change biology*, 2019.

Vicca, S., et al., Fertile forests produce biomass more efficiently, *Ecology Letters*, *15*(6), 2012.

Vicca, S., et al., Using research networks to create the comprehensive datasets needed to assess nutrient availability as a key determinant of terrestrial carbon cycling, *Environmental Research Letters*, *13*(12), 2018.

Viovy, N., CRUNCEP version 7 - atmospheric forcing data for the community land model, doi: 10.5065/PZ8F-F017, 2016.

Vitousek, P. M., Nutrient cycling and nutrient use efficiency, *The American Naturalist*, *119*(4), 1982.

Vitousek, P. M., Litterfall, nutrient cycling, and nutrient limitation in tropical forests, *Ecology*, *65*(1), 285–298, 1984.

Vitousek, P. M., and R. W. Howarth, Nitrogen limitation on land and in the sea - how it can occur, *Biogeochemistry*, *13*, 1991.

Vitousek, P. M., et al., Biological invasion by myrica faya alters ecosystem development in hawaii, *Science*, *238*(4828), 1987.

Vitousek, P. M., et al., Terrestrial phosphorus limitation: mechanisms, implications, and nitrogen–phosphorus interactions, *Ecological Applications*, *20*(1), 2010.

Vitousek, P. M., et al., Biological nitrogen fixation: rates, patterns and ecological controls in terrestrial ecosystems, *Philosophical Transactions of the Royal Society B: Biological Sciences*, *368*(1621), 2013.

von Liebig, J., *The natural laws of husbandry*, D Appleton, 1863.

von Lützow, M., et al., Stabilization of organic matter in temperate soils: mechanisms and their relevance under different soil conditions–a review, *European journal of soil science*, *57*(4), 2006.

Walker, A. P., et al., Comprehensive ecosystem model-data synthesis using multiple data sets at two temperate forest free-air CO_2 enrichment experiments: Model performance at ambient CO_2 concentration, *Journal of Geophysical Research: Biogeosciences*, *119*, 2014.

Walker, A. P., et al., Predicting long-term carbon sequestration in response to CO_2 enrichment: How and why do current ecosystem models differ?, *Global Biogeochemical Cycles*, *29*(4), 2015.

Walker, T. W., and J. K. Syers, The fate of phosphorus during pedogenesis, *Geoderma*, *15*(1), 1976.

Wallander, H., et al., Direct estimates of C:N ratios of ectomycorrhizal mycelia collected from norway spruce forest soils, *Soil Biology and Biochemistry*, *35*(7), 2003.

Waring, R. H., et al., Net primary production of forests: a constant fraction of gross primary production?, *Tree physiology*, *18*(2), 1998.

Wedin, D. A., and D. Tilman, Species effects on nitrogen cycling: a test with perennial grasses, *Oecologia*, *84*(4), 1990.

White, M. A., et al., Parameterization and Sensitivity Analysis of the BIOME-BGC Terrestrial Ecosystem Model: Net Primary Production Controls, *Earth Interactions*, *4*, 2000.

White, R. E., *Principles and Practice of Soil Science: The soil as a Natural Resource*, vol. 32, 4th ed., Blackwell Publishing, Malden, 2006.

Whittaker, R. H., et al., The Hubbard Brook ecosystem study: forest nutrient cycling and element behavior, *Ecology*, *60*(1), 203–220, 1979.

Wieder, W. R., et al., Effects of model structural uncertainty on carbon cycle projections: biological nitrogen fixation as a case study, *Environmental Research Letters*, *10*(4), 2015.

Wright, S. J., et al., Plant responses to fertilization experiments in lowland, species-rich, tropical forests, *Ecology*, *99*(5), 2018.

Wu, T., et al., A possible role for saprotrophic microfungi in the N nutrition of ectomycorrhizal pinus resinosa, *Soil Biology and Biochemistry*, *37*(5), 2005.

Yang, X. o., The role of phosphorus dynamics in tropical forests – a modeling study using CLM-CNP, *Biogeosciences*, *11*(6), 2014.

Zaehle, S., and D. Dalmonech, Carbon–nitrogen interactions on land at global scales: current understanding in modelling climate biosphere feedbacks, *Current Opinion in Environmental Sustainability*, *3*(5), 2011.

Zaehle, S., and A. D. Friend, Carbon and nitrogen cycle dynamics in the O-CN land surface model: 1 Model description, site-scale evaluation, and sensitivity to parameter estimates, *Global Biogeochemical Cycles*, *24*(1), 2010.

Zaehle, S., et al., Terrestrial nitrogen feedbacks may accelerate future climate change, *Geophysical Research Letters*, *37*(1), 2010.

Zaehle, S., et al., Evaluation of 11 terrestrial carbon–nitrogen cycle models against observations from two temperate Free-Air CO_2 Enrichment studies, *New Phytologist*, *202*(3), 2014.

Zanetti, S., and U. A. Hartwig, Symbiotic n2 fixation increases under elevated atmospheric pco2 in the field, *Acta Oecologica*, *18*(3), 1997.

Zerihun, A., et al., Photosynthate costs associated with the utilization of different nitrogen–forms: influence on the carbon balance of plants and shoot–root biomass partitioning, *The New Phytologist*, *138*(1), 1998.

Acknowledgments

Since a PhD is a perennial journey, I would like to gratefully thank all the people that guided me on my way, joint my path, and were there, whenever I faced (apparently) insurmountable hurdles, unforeseen gorges, or simply lost my track by taking circuitous routes. Thank you for calming me down, whenever I got occasionally mad...

(a) Usual mood. **(b)** Occasional madness.

Moods and look-alikes during my PhD journey.
The way back from (b) to (a) was sometimes just an open door, a sympathetic ear, or a cup of tea...
THANK YOU!!!

Firstly, I would like to thank my supervisors, mentors, and hosts that always had an eye on me, when I tried to find my way through this wild jungle of biogeochemical cycles and terrestrial biosphere models, and friendly opened their office doors, whenever I knocked.

- My biggest thanks goes to Sönke Zaehle, who offered me the travel ticket to this unique journey and guided me all the way long. Thank you for the countless discussions and advice and your (almost?) infinite mental paper library. As (former?) meteorologist I would have been lost somewhere between vegetation and soils without you.
- Thank you, Anja Rammig, for your guidance from the minute on that you joined my PhD-journey team, for your interest, your hundreds of comments to all my reports and drafts, and your always open door, whenever my travel led me to Freising. Your outside-of-Jena perspective was an immeasurable help to keep on track.

- Thanks to Sara Vicca and her group at PLECO, and to Oskar Franklin and his colleagues at IIASA for hosting me during parts of my PhD. Thank you for all the open discussions, for your interest and for sharing your offices, ideas and points of view, which showed me potential junctions that I may have overseen without taking your perspectives. And, of course, thanks for all the cake, chocolate and coffee that seems to be part of the hosting-service everywhere.

- And finally, thank you, Silvia Caldararu, for keeping the closest eye on me, in particular on the final very steep and slippery meters.

Secondly, I would like to thank all the people that joined my way in Jena and made this PhD journey an unforgettable experience.

- Thanks to the TBM group for all the deep discussions, fresh ideas, and helpful advice during the past 4.5 years. And for all the (really bad) Mensa lunches, and the (certainly better) potlucks/cakes/drinks/... Special thanks to Silvia and Tea for reading my drafts. I know that not all of it was merit a literature prize... Thanks to Jan for all the IT/code/programming support and your gentle mediation between the cluster, my computer and me. I guess, without your help at least one of us would not have survived. And thanks to Martina and Johannes for all the (not always scientific) discussions and hints. It was good to have someone that has gone through it all before.
  I couldn't have done it without all of your help.

- Thanks to the whole BGI department for having me and making me feel home from the beginning on. Thank you for all the open discussions, ideas, and in-front-of-the-coffee-machine talks. Special thanks to Uli, René, and all the people that contributed to my coffee/chocolate/fruits treatments. A sufficient caffeine/sugar/vitamin nutrition is obviously mandatory for that sometimes stony and exhausting way. Thanks to Kerstin, Corinne, and Linda for always taking care and asking for needs, work-related or personal.

- Biggest thanks and 1000 hugs to Tina, Maria, Lucia, Sandra, Neele, and Juliane (and all the others that were always here for a coffee and a talk) for your company on my way and taking care of my work-life balance ;)
  Without any of you, I would have been lost at some point. And majorly because of you, this PhD journey became a unique and wonderful experience. Knowing that I'm not alone in this jungle, but that I have friends around that joint this path and that always have a hand or an ear free for me, was probably the most important support that let me (mostly) smile even facing the next canyon right in front of me.

And finally, I would like to thank all the people all over the world that supported me in various ways conducting this journey.

- Thanks to my friends in Bonn that always made me feel home, when I find my way back to Western Germany. Thank you, Joe, for always awaiting me with a cosy sofa and a big cup of aromatic tea (or two or three). And thanks to André for your advice, support and time, since I was a annoying little bachelor student ;-P
- Deepest thanks to my family. Thank you for your on-going support not only during the last 4.5 years of my PhD, but during the last almost 3 decades, for your believe in me, and your always open doors. Thanks for your interest in my work, and for letting me go my way, even (or especially) when the outcome was not as clear as you had wished, or when I took another circuitous route.
- And last, but not least... Thanks to Martin for your unintended support since 2016 and your encouragement during the last year. Thank you for accepting my sometimes incomprehensible ways to climb the next hill in my own pace, and for bringing me back to Earth, when I lost the ground under my feet.

I was lucky to meet you all, and thank you all for your support in all the different ways.
And I apologize for all the un-named supporters and companions that I had to skip for reasons of space. Or simply, because my memory is like a sieve, now, right after writing this journey report. Sorry. And thank you anyway!

Besides, I gratefully thank the European Research Council (ERC) that funded the *Quantifying the effects of interacting nutrient cycles on terrestrial biosphere dynamics and their climate feedbacks* (QUINCY) project, which I was working in, under the grant agreement No 647204 within its European Union's Horizon 2020 research and innovation program, and the European Cooperation in Science & Technology (COST) Action ES1308 - Climate Change Manipulation Experiments in Terrestrial Ecosystems - Networking and Outreach (ClimMani) that also supported my research under grant No ES1308 - 39449.
I further acknowledge the support of the *International Max Planck Research School for global Biogeochemical Cycles* (IMPRS-gBGC) in Jena and the *Graduate Center Weihenstephan* (Graduiertenzentrum Weihenstephan, GZW) as part of the *TUM Graduate School* (TUM-GS) in Freising.